L'intégration du confort thermique des occupants dans la conception des bâtiments performants

Abed Al Waheed Hawila

Thèse
de doctorat
de l'UTT

Abed Al Waheed HAWILA

Integrating Occupants' Thermal Comfort in the Design of Energy-efficient Buildings

Champ disciplinaire :
Sciences pour l'Ingénieur

2019TROY0009 **Année 2019**

utt
UNIVERSITÉ DE TECHNOLOGIE
TROYES

THESE

pour l'obtention du grade de

DOCTEUR
de l'UNIVERSITE DE TECHNOLOGIE DE TROYES

EN SCIENCES POUR L'INGENIEUR

Spécialité : SYSTEMES SOCIOTECHNIQUES

présentée et soutenue par

Abed Al Waheed HAWILA

le 13 mars 2019

Integrating Occupants' Thermal Comfort in the Design of Energy-efficient Buildings

JURY

M. R. BENNACER	PROFESSEUR DES UNIVERSITES	Président
M. C. INARD	PROFESSEUR DES UNIVERSITES	Rapporteur
M. B. YANNOU	PROFESSEUR DES UNIVERSITES	Rapporteur
M. S. ATTIA	PROFESSEUR	Examinateur
M. A. MERABTINE	ENSEIGNANT CHERCHEUR	Directeur de thèse
Mme N. TROUSSIER	PROFESSEURE DES UNIVERSITES	Directrice de thèse

Acknowledgements

Completing my Ph.D. has been one of the most significant academic challenges that I ever had to face, but provided me a remarkable experience! Accomplishing this academic challenge would not have been possible without many people, not only for their contributions to scientific knowledge, but also for my personal benefit from the privilege of working alongside them during this journey. These lines are dedicated to all of you.

First of all, I would like to express my deepest appreciation to my thesis supervisors, *Abdelatif MERABTINE* and *Nadège TROUSSIER*. I am fully indebted to you for creating me a new chance, welcoming me as a Ph.D. student. I have always felt privileged to be working with you. I thank *Abdelatif* for his continuous support, advice, encouragement, patience, enthusiasm, and for being always beside me, teaching me the importance of critical thinking and inspiring me to work multi-disciplinary. I am grateful to *Nadège* for here guidance, encouragement and critical appraisal of my thesis. This thesis would not have been possible without your unwavering support either on academic or personal issues, critiques, questions and remarkable patience.

I would like to thank my lab mates for their continued support. I would like also to offer my special gratitude to the EPF's (école d'ingénieur-e-s, Troyes) members and students for providing me the required objective and subjective data to accomplish my research work. This thesis would not be accomplished without your valuable help.

I would like to express my deepest gratitude to all my co-authors: *Abdelhamid KHEIRI, Salim MOKRAOUI, Rachid BENNACER, Mahdi CHEMKHI, Chadi MAALOUF, Nadia MARTAJ* and *Guillaume POLIDORI*. Thank you all for your valuable advices and valued discussions.

I would like to offer my special thanks to *Bernard YANNOU* and *Christian INARD* for accepting to review this dissertation. I would like to thank also the other members of the jury: *Rachid BENNACER* and *Shady ATTIA* for their interest in my research work.

Thanks are also due to the Conseil régional de Champagne-Ardenne (CRCA) and the Fonds européen de développement économique et régional (FEDER) for their financial support that I otherwise would not have been able to develop my scientific discoveries.

Last but not least, I would like to express my deepest gratitude to my family and friends. This journey would not have been possible without their warm love, continued patience, and endless support.

Abstract

The building sector is one of the largest energy end-use sectors in the world and reducing energy consumption has been the foundation of numerous research works. However, the primary objective of buildings must be to provide a comfortable environment for its occupants, because inappropriate indoor thermal comfort leads to lower work efficiency, higher possibility of personal errors, and an indirect effect on the energy consumption of the buildings. Thus, it is necessary to design energy-efficient buildings so that a trade-off between energy-savings and occupants' thermal comfort is fulfilled. Recently, glass façades and extensive glazing areas have gained popularity due to their aesthetic appearance as well as because of users' requirements of higher light transmittance and better view. However, they often cause occupants thermal discomfort, in addition to consuming considerable amounts of energy.

The main purpose of this thesis is to understand and formulate the relationship between building design parameters, occupants' thermal comfort and heating energy, in order to integrate occupants' thermal comfort in the design of energy efficient buildings. The combined use of numerical simulations, the Design of Experiments (DoE) technique and an optimization approach are thus adopted for this aim. Numerical simulations help in extending the investigations with low additional costs and less time. In addition, it facilitates the assessment of new control strategies since no additional costs are added for the installations and experimentations. Moreover, the combined use of numerical simulations and DoE technique allows the development of meta-modeling relationships between response variable, here thermal comfort and heating energy, and design parameters. These meta-models could be used, first, to perform a sensitivity analysis, and second, to integrate thermal comfort in the process of building design. The desirability function approach is then considered in order to simultaneously optimize both thermal comfort and heating energy. This trade-off helps in developing an optimal design of buildings at both energy consumption and thermal comfort levels. The proposed method is applied in a real case study after subjectively assessing the real occupants' perception of the thermal environmental conditions using survey questionnaires. The obtained results indicated that integrating occupants' thermal comfort in the design of energy efficient buildings leads to a trade-off between energy-savings and thermal comfort.

In order to evaluate the added value of the proposed approach, a comparative study with another approach that integrates occupant thermal comfort in the control of the indoor environment, such as thermal comfort based control, is then performed. The obtained results indicated that, thermal comfort based control represents a good approach to neutralize the trade-off between energy-saving and thermal comfort in the presence of extensive glazing areas, integrating occupants' thermal comfort in the design of energy efficient buildings leads to optimized building design for both thermal comfort and heating energy consumption, and it represents also a significant step towards achieving a trade-off between energy-saving and thermal comfort without the need of advanced and complicated control strategies. In addition, the proposed approach represents a simple and fast method to integrate occupants' thermal comfort in the design of energy-efficient buildings.

Keywords: design of experiments, numerical simulation, Sensitivity analysis, Energy consumption, thermal comfort.

Résumé

Le secteur du bâtiment est l'un des plus grands consommateurs d'énergie parmi les secteurs économiques. Il est important alors de promouvoir la conception selon les critères de la basse consommation et du bien-être afin qu'un compromis entre le confort thermique et la performance énergétique puisse être trouvé. L'amélioration de l'efficacité énergétique des bâtiments a fait l'objet de nombreux travaux de recherche. Il est donc nécessaire de concevoir des bâtiments à faible consommation d'énergie afin de réaliser un compromis entre les économies d'énergie et le confort des occupants. Récemment, les systèmes des façades hautement vitrées ont suscité un grand intérêt de par leur aspect esthétique. Cependant, si elles ne sont bien conçues, elles induisent un inconfort thermique et à une surconsommation énergétique.

L'objectif de ces travaux de thèse est de comprendre et formaliser la corrélation entre les paramètres de conception, le confort thermique et la consommation d'énergie, pour une meilleure intégration du confort thermique dans la conception des bâtiments. En conséquence, nous adoptons une approche basée sur l'utilisation des plans d'expérience (DoE) reposée sur des simulations numériques. Ces dernières permettent de réaliser des investigations avec un faible coût et moins de temps. Elles facilitent l'évaluation de nouvelles stratégies de contrôle. Par ailleurs, l'utilisation combinée de simulations numériques et de la DoE a permis le développement des méta-modèles afin d'évaluer le confort thermique et la consommation énergétique des bâtiments. Ces modèles ont ensuite été déployés, d'une part, pour effectuer une analyse de sensibilité et, d'autre part, pour intégrer le confort thermique dans le processus d'optimisation de la conception des bâtiments. Une fonction de désirabilité a été considérée pour optimiser aussi bien le confort thermique et la consommation énergétique. La méthode proposée a été appliquée sur un bâtiment réel. Les résultats obtenus montrent que l'intégration du confort thermique des occupants dans la conception de bâtiments performants satisfait le compromis entre économies d'énergie et confort thermique.

Afin d'évaluer la valeur ajoutée de l'approche proposée, une étude comparative avec une autre approche qui intègre le confort thermique des occupants dans le contrôle de l'environnement intérieur, comme le contrôle du confort basé sur les PMV, a été réalisée. Les résultats obtenus indiquent que: (1) l'intégration du confort thermique des occupants dans la conception de bâtiments performants permet d'améliorer l'efficacité énergétique des bâtiments; (2) la méta-modélisation de la relation entre le confort thermique, la consommation énergétique et les paramètres de conception représente un processus simple et rapide pour intégrer le confort thermique des occupants dans la conception de bâtiments performants ; et (3) dans le cas d'une grande surface vitrée, la régulation basés sur le PMV représente une bonne approche pour une meilleure performance énergétique.

Mots clés : Plans d'expérience ; Simulation numérique ; Analyse de sensibilité ; Consommation d'énergie ; confort thermique

Table of contents

List of Figures

List of Tables

List of symbols

Abbreviations

ADEME	Agence De l'Environnement et de la Maîtrise de l'Energie (French Environment and Energy Management Agency)
AHU	Air Handler Unit
ANOVA	Analysis Of Variance
ANSI	American National Standards Institute
ASHRAE	American Society of Heating, Refrigerating and Air-Conditioning Engineers
AV	Air velocity
BMS	Building Management System
CEN	European Committee for Standardization
CFD	Computational Fluid Dynamics
CI	Clothing Insulation
CVRMSE	Coefficient of Variation of the Root Mean Square Error
DoE	Design of Experiments
Dymola	Dynamic Modeling Laboratory
EN	European Norm
EQI	Environmental Quality Index
FBS	Function-Behavior-Structure
GDP	Gross Domestic Product
GHG	Greenhouse Gas
GSA	Global Sensitivity Analysis
HVAC	Heating, Ventilation and Air Conditioning
IEA	International Energy Agency
IEQ	Indoor Environment Quality
IES	l'Institut d'Electronique et des Systèmes Institute of Electronics and Systems
ISO	International Organization for Standardization
LSA	Local Sensitivity Analysis

LULUCF	Land Use, Land Use Change and Forestry
MBE	Mean Bias Error
MBPC	Model Based Predictive Control
MR	Metabolic Rate
MRT	Mean Radiant Temperature
Mtoe	Million Tons of Oil Equivalent
NMBE	Normalized Mean Bias Error
OFAT	One-Factor-At-a-Time
PMV	Predicted Mean Vote
PPD	Percentage of Persons Dissatisfied
PRESS	Prediction Error Sum of Squares
RH	Relative Humidity
RT	Réglementation Thermique (Thermal Regulation)
SA	Sensitivity Analysis
SHGC	Solar Heat Gain Coefficient
TBS	Thermal Building Simulation
TMY	Typical Meteorological Year
TPES	Total Primary Energy Supply
TSV	Thermal Sensation Vote
UNFCCC	United Nations Framework Convention on Climate Change
WFR	Window-to-Floor Ratio
WWR	Window-to-Wall Ratio

Nomenclature

A_{pf}	Projected area of fenestration (m^2)
C	Convective heat loss ($W.m^{-2}$)
C_i, C_{ij}	Regression coefficients
C_{res}	Sensible heat loss due to respiration ($W.m^{-2}$)
D	Global desirability function
d_i	Individual desirability function

e	Residual
E	Evaporative heat loss ($W.m^{-2}$)
f	Occurrence frequency
F_{cl}	Clothing area factor
G	Incident total irradiance ($W.m^{-2}$)
h	Heat transfer coefficient ($W.K^{-1}.m^{-2}$)
I_{cl}	Thermal resistance of clothing ($m^2.K.W^{-1}$)
I_h	Global horizontal solar irradiance ($W.m^{-2}$)
m	Measured data
M	Metabolic heat production ($W.m^{-2}$)
p	Pressure (kPa)
q	Heat flow ($W.m^{-2}$)
Q	Total heat flow (W)
r	Weighting parameter
R	Radiative heat loss ($W.m^{-2}$)
R^2	Coefficient of determination
s	Simulated data
S	Heat storage ($W.m^{-2}$)
S_i	Area of surface i
T	Temperature (K or °C)
U	Heat transfer ($W.K^{-1}.m^{-2}$)
v_a	Air velocity ($m.s^{-1}$)
W	External work ($W.m^{-2}$)
X_i	Coded factors
Y	Predicted response variable

Greek letters

α	Coefficient determined as a function of the relative air velocity
β	Solar radiation absorptivity of the surface exposed to solar radiation
ε	Constant effectiveness
ϵ	Error

Subscripts

a	Air
avg	Average
c	Convective
cl	Clothing
cr	Core compartment
db	Dry-bulb
ex	External
in	Internal
max	Maximum
min	Minimum
mr	Mean radiant
op	Operative
opt	Optimum
pf	Projected area of fenestration
r	Radiative
res	Respiration
sk	Skin compartment
sol-air	Sol-air temperature

Résumé étendu (extended summary in French)

Le secteur du bâtiment combiné est responsable de 35% de la consommation finale globale d'énergie devant le transport et l'industrie [1]. Le secteur du bâtiment représente 44,5% de la consommation totale d'énergie en France [2], 40% en Europe [3,4] et aux Etats-Unis [4]. Les progrès vers des bâtiments durables progressent, mais les améliorations ne suivent toujours pas la croissance du secteur du bâtiment et la demande croissante de services énergétiques. En outre, le secteur du bâtiment est également responsable de 19 % des émissions de gaz à effet de serre dans le monde [5]. Elle se classe devant le secteur des transports (14 %), le secteur de l'énergie (11 %) et le secteur du traitement des déchets (3 %). L'industrie demeure le secteur le plus émetteur de gaz à effet de serre (29 %), suivi du secteur d'UTCF (Utilisation des Terres, leurs Changements et la Foret) qui est responsable de 24 %.

Cette préoccupation a conduit à l'élaboration de différentes stratégies, concepts, politiques, normes et réglementations visant à promouvoir le développement durable dans les bâtiments, tels que les bâtiments à faible consommation d'énergie et les bâtiments à énergie nulle [6]. A l'instar d'autres pays développés, les autorités françaises ont mis en place la Réglementation Thermique 2012 (RT 2012), qui définit les normes de performance des bâtiments. Ce règlement constitue une étape ambitieuse vers la promotion des bâtiments écologiques puisqu'il prévoit de diviser par trois la consommation énergétique des nouveaux bâtiments à partir de la fin de l'année 2012 [7]. Pour atteindre les niveaux de performance énergétique indiqués dans la RT 2012, une attention particulière est requise dans le choix des "éléments" constituant le bâtiment, tels que la réduction des pertes de chaleur en améliorant l'isolation thermique de l'enveloppe [8,9], la réduction des ponts thermiques, le choix d'un système de ventilation qui limite les pertes de chaleur, etc.

D'autre part, l'objectif premier des bâtiments doit être d'offrir un environnement confortable aux occupants, qui passent 80 à 90 % de leur temps à l'intérieur [10]. De plus, un confort thermique intérieur inadéquat entraîne une baisse de l'efficacité au travail, une plus grande possibilité d'erreurs personnelles et un effet indirect sur la consommation d'énergie des bâtiments [11]. Il est donc nécessaire de concevoir des bâtiments à faible consommation d'énergie afin de réaliser un compromis entre les économies d'énergie et le confort des occupants[12]. Le confort thermique a été défini par Givoni comme "*l'absence d'irritation et d'inconfort dus à la chaleur ou au froid, et comme un état de plaisir*" [13]. Hensen le définit comme "*un état dans lequel il n'y a pas d'impulsions motrices pour corriger l'environnement par le comportement"* [14]. Il y a un concept que toutes ces définitions et d'autres du confort thermique confirment: le confort thermique est la condition que l'individu ne

ressente ni trop froid ni trop chaud lorsqu'il porte une des vêtures adaptés à la tâche qu'il doit accomplir [15].

L'interaction complexe entre l'homme et son environnement a donné lieu à de nombreuses recherches dans différentes disciplines: physiologistes, psychologues, chercheurs en sciences sociales, ingénieurs en environnement et physiciens [16]. Chaque discipline a sa propre approche pour définir le confort thermique. Ainsi, le confort thermique humain peut être perçu comme un contexte global, puisqu'il est basé sur la perception subjective humaine d'un certain nombre de facteurs physiologiques, psychologiques et physiques. Les facteurs physiques sont considérés comme les facteurs les plus importants du confort thermique humain. Ces facteurs sont les plus étudiés dans le domaine. On peut les classer en trois groupes : bilan thermique du corps, paramètres personnels et paramètres environnementaux ambiants. Le *bilan thermique du corps humain* commence avec deux conditions initiales essentielles pour maintenir le confort thermique : 1) une sensation thermique neutre doit être obtenue par la combinaison de la température de la peau et du corps entier, et 2) dans un bilan énergétique corporel complet, la quantité de chaleur produite par le métabolisme doit être égale à celle perdue dans l'atmosphère (état stable). Les *paramètres personnels* représentent les caractéristiques des occupants. Ces paramètres sont l'isolation des vêtements et le taux de chaleur métabolique. Le premier est la résistance thermique des vêtements que porte l'occupant, elle est exprimée en unités de *clo* (1 *clo* = 155 $m^2.K.W^{-1}$). La dernière est la production nette de chaleur du corps humain, ou le taux de transformation de l'énergie chimique en chaleur et en travail mécanique par les activités à l'intérieur du corps. Elle est exprimée en unités *met* (1 met = 58,2 $W.m^{-2}$). La valeur du taux métabolique est toujours positive puisque le corps produit toujours de la chaleur. Les *paramètres environnementaux et ambiants* représentent les caractéristiques de l'environnement intérieur du bâtiment, comme la vitesse de l'air, l'humidité relative et plusieurs paramètres de température. La *vitesse de l'air* est la vitesse à laquelle l'air se déplace sur une distance donnée au fil du temps. La vitesse de l'air affecte la perte de chaleur par convection du corps. L'*humidité relative* est le rapport entre la pression de vapeur réelle (mesurée) et la pression de vapeur saturée à la même température [17]. La *température de l'air* est la température de l'air intérieur entourant le corps. Elle est mesurée à l'aide d'un thermomètre à bulbe sec. C'est un facteur important dans la détermination du confort thermique des occupants, puisque la convection est responsable des deux cinquièmes de la perte de chaleur du corps. L'intervalle de température recommandée est comprise entre 18 °C et 23 °C, et la différence de température ne peut pas dépasser 1 °C dans les espaces occupés [18]. La *Température Radiante Moyenne (MRT)* est définie par la norme ANSI/ASHRAE 55-2010 comme *" la température d'une enceinte uniforme et noire qui échange la même quantité de rayonnement thermique avec l'occupant que l'enceinte avec elle-même "* [19]. En ce qui concerne le corps humain, l'ISO l'a défini comme *"la température uniforme d'une enceinte imaginaire dans laquelle le transfert de chaleur radiatif du corps humain est égal au transfert de chaleur radiatif dans l'enceinte réelle non uniforme"* [20]. La MRT est exprimée

comme la moyenne pondérée des températures des surfaces environnantes à l'état d'équilibre. La *température de fonctionnement* est définie comme "*la température uniforme d'une enceinte noire imaginaire dans laquelle un occupant échangerait la même quantité de chaleur par rayonnement et convection par rapport à un environnement non uniforme* " [21]. Les normes ASHRAE 55 et CEN EN 15251 utilisent la température opérative pour prédire la température de confort. Il ne s'agit pas d'une mesure empirique, mais d'une mesure théorique, exprimée par la moyenne de la température radiante moyenne et de la température de l'air pondérée, respectivement, par les coefficients de transfert thermique radiatif et convectif [22].

Parmi tous les indices de confort thermique, plus de 80 indices ont été adoptées dans la littérature [23], l'indice PMV (Predicted Mean Vote) et l'indice PPD (Percentage of Persons Dissatisfied) proposés par Fanger sont les indices les plus étudiées afin d'évaluer le confort thermique dans un espace confiné [18]. Le PMV est défini comme " *l'indice qui prédit le vote moyen de sensation thermique sur une échelle standard pour un échantillon représentatif de personnes en mettant en jeu une combinaison donnée de variables thermiques environnementales, d'activité et de la vêture* " [15]. Fanger [24] a développé une relation empirique qui permet de calculer la PMV en fonction de deux paramètres liés aux occupants comme l'isolation des vêtements et le taux métabolique ainsi que quatre paramètres environnementaux qui sont la température de l'air, la température radiante moyenne, l'humidité relative et la vitesse d'air. Cette corrélation a été établie grâce à des études en laboratoire et en chambre climatique à l'aide de l'échelle de sensation thermique ASHRAE en sept points [19]. Cette échelle représente les votes d'un groupe de personnes exprimant la sensation thermique qu'elles ressentent dans un environnement donné. Les votes sont définis par le vote dit de la sensation thermique (TSV : Thermal Sensation Vote) [19]. PMV représente le vote moyen déterminé à partir de la moyenne des valeurs de la TSV [25]. Il a été adopté par diverses normes nationaux et internationaux, directives et chercheurs, tels que ISO 7730 [20], ASHRAE 55 [16,19,26], et CEN CR 1752 [27]. ISO 7730 recommande de maintenir le PMV à 0 avec une tolérance de 0.5 afin d'assurer un climat intérieur confortable [20]. Cette recommandation entraîne une insatisfaction maximale de 10 % dans l'environnement intérieur [20]. La sensation thermique des occupants est meilleure si le PMV est plus proche de zéro [18]. Humphreys [28] a également abordé la tolérance de 0.5 en confirmant qu'en ambiance légèrement froide on pourrait préférer une sensation légèrement plus chaude que neutre, et vice versa. En plus du modèle PMV, Fanger a introduit le modèle PPD pour calculer le pourcentage de personnes qui sont insatisfaites dans leur environnement thermique Cet indice est corrélé à la valeur du PMV de manière symétrique par rapport à la neutralité thermique (PMV = 0).

Malgré son importance, le confort thermique n'a jamais été pris en compte dans le contrôle de la température de consigne des systèmes CVC (Chauffage, Ventilation et Climatisation) jusqu'à

récemment. En effet, la majorité des normes de construction recommandent une température statique de l'air intérieur, ce qui amène les concepteurs à concevoir les bâtiments et à évaluer leur comportement thermique en fonction d'une température intérieure fixe, alors que dans la plupart des cas, l'environnement intérieur est supposé uniforme, ce qui signifie que la température radiante moyenne est égale à la température ambiante. Cette hypothèse pourrait conduire à une mauvaise estimation du confort thermique des occupants, principalement dans les bâtiments à grandes surfaces vitrées. C'est pourquoi de nombreux groupes de recherche ont orienté leurs travaux vers l'élaboration de stratégies avancées de contrôle des bâtiments [29]. Au cours des deux dernières décennies, des approches de contrôle basées sur le confort thermique ont été proposées et étudiées dans la littérature.

Dans une étude antérieure, Hamdi et Lachiver [30] ont proposé une nouvelle méthode de contrôle des systèmes CVC basée sur la sensation de confort thermique. Une telle stratégie vise à maintenir un confort thermique intérieur constant, mais pas une température constante de l'air intérieur. Kolokotsa et al. [11] ont présenté et évalué trois stratégies de contrôle, soit le Fuzzy PID, fuzzy PD et une adaptive fuzzy PD, pour l'ajustement et la préservation de la qualité de l'air intérieur et du confort visuel et thermique tout en s’assurant de la performance énergétique. Kolokotsa [31] a appliqué et comparé la performance de cinq contrôleurs flous (fuzzy P, fuzzy PID, fuzzy PI, fuzzy PD et adaptive fuzzy PD) selon l'indice PMV et d'autres paramètres de qualité de l'air intérieur. Calvino et al. [32] ont étudié la performance d'un contrôleur adaptive fuzzy-PID basé sur le PMV comme indice de conduite pour la procédure de contrôle. Liang et Du [33] ont développé un contrôleur de réseau neuronal direct avec l'adoption de l'indice PMV comme objectif de contrôle. Donaisky et al. [34] ont étudié deux algorithmes de contrôle prédictif basés sur des modèles et sur l'indice PMV. Le premier utilise PMV pour générer le signal de la température de consigne, et le dernier utilise PMV pour composer le modèle de prédiction. Freire et al. [35] ont analysé cinq algorithmes de contrôle prédictif pour optimiser les conditions de l'air intérieur en mettant l'accent sur le confort thermique et/ou les économies d'énergie. Certains des algorithmes proposés sont basés sur la détermination de l'indice PMV et d'autres sont basés sur une approche par zone de confort. Castilla et al. [36] ont effectué une comparaison entre plusieurs approches de contrôle prédictif. Ferreira et al. [37] ont formulé une contrôle prédictif basé sur un modèle en utilisant la méthode branch and bound pour contrôler les systèmes CVC en utilisant l'indice PMV. Ruano et al. [38] ont proposé un contrôle prédictif basé sur un modèle amélioré, basé sur l'indice PMV, pour des systèmes CVC existant. Xu et al. [39] ont testé une nouvelle approche d'optimisation opérationnelle des bâtiments basée sur l'indice PMV. Kang et al. [40] ont proposé le calcul inverse de l'indice PMV en utilisant directement les paramètres mesurés et la formulation de l'indice PMV pour ajuster la température de consigne. Les auteurs ont étudié l'effet d'une telle approche sur la consommation d'énergie et le confort thermique dans un espace doté d'une grande surface vitrée. Ils ont réalisé une étude comparative entre le contrôle basé sur le confort thermique proposé et le contrôle thermostatique conventionnel. Leur étude a conclu que le contrôle du

confort thermique pourrait être plus efficace que le contrôle thermostatique. Par la suite, Hwang et Shu [41] ont étudié le potentiel d'économie d'énergie du contrôle basé sur le confort thermique sous différentes réglementations d'enveloppe. Les résultats de l'étude ont démontré l'avantage de l'utilisation d'un contrôle basé sur le confort thermique, qui pourrait permettre de réduire environ 20 % l'énergie issue du refroidissement par rapport au contrôle thermostatique traditionnel. Erakovic et Evans [42] ont évalué le contrôle basé sur le confort thermique en effectuant une étude comparative avec le contrôle basé sur la température de l'air en utilisant un modèle CFD d'un espace de bureau avec une enveloppe vitrée. Les résultats montrent que le régulateur étudié a amélioré les niveaux de confort thermique, tout en évitant le sur-refroidissement. Les économies d'énergie résultant de l'utilisation du contrôle du confort thermique pouvaient atteindre jusqu'à 48,6 % en fonction de plusieurs facteurs.

Bien que ces études ont montré que la stratégie de régulation basée sur le confort thermique proposée offre un effet d'économie d'énergie ainsi qu'un confort thermique constant, certaines études ont conclu que, si l'enveloppe est mal conçue, une régulation basé sur le PMV pourrait consommer énergétiquement autant que la régulation thermostatique pour atteindre un niveau de confort satisfaisant [41]. En revanche, si l'enveloppe est bien conçue, une régulation de confort basée sur le PMV permet de réaliser des économies d'énergie. Cette constatation nous amène donc à nouveau au problème de conception. Les façades vitrées ont gagné en popularité ces dernières années en raison de leur aspect esthétique ainsi que de l'exigence des utilisateurs d'une meilleure transmission de la lumière et d'une meilleure visibilité [43]. Les menuiseries, particulièrement les fenêtres, permettent à de profiter au mieux de la lumière naturelle, ce qui procure aux occupants un confort visuel et des avantages biologiques [44,45]. Cependant, les façades vitrées qui sont mal conçues affectent considérablement le confort thermique des occupants, en raison des grandes surfaces chaudes résultant de la dissipation du rayonnement solaire [40]. Ainsi, la conception de façades vitrées dans les bâtiments économes en énergie nécessite une planification adéquate afin de répondre à sa nature d'éclairage naturel et de vue extérieure tout en maintenant un équilibre entre le confort thermique et la performance énergétique du bâtiment.

De nombreuses études ont été menées pour étudier l'influence de la conception des façades vitrées sur la consommation énergétique des bâtiments [46–50] et le confort thermique [51–54]. Poirazis et al. [47] ont réalisé des simulations énergétiques des bâtiments pour un grand nombre de scénarios combinant différents types de vitrages et des solutions d'ombrage pour un immeuble de bureaux avec façades entièrement vitrées. Les principaux résultats de l'étude indiquent que les bâtiments avec des façades entièrement vitrées sont susceptibles d'avoir une consommation d'énergie plus élevée que les bâtiments avec des façades conventionnelles ; la faible transmission thermique des fenêtres diminue la charge de chauffage et influence à peine la demande de refroidissement, tandis que la transmisivité a un impact important sur la demande de refroidissement. De plus, tant que la

superficie de la fenêtre augmente, l'impact de la température de consigne sur la consommation d'énergie diminue. Tzempelikos et al. [51] ont étudié l'effet du changement de type de vitrage et de dispositif d'ombrage sur le confort thermique intérieur et la consommation d'énergie dans un immeuble de bureaux à grande surface vitrée. Les auteurs ont utilisé un modèle thermique dynamique basé sur la méthode des différences finies [55]. Il a été conclu que la résistance thermique et la transmission solaire du vitrage ont un effet important sur le confort thermique. Une faible valeur d'isolation avec un facteur de transmission élevé révèle une grande hétérogénéité de l'environnement thermique intérieur. Inversement, les fenêtres à haute résistance thermique et à faible facteur de transmission offrent des conditions plus confortables et moins sensibles au climat extérieur. Cependant, une faible transmission peut entraîner une augmentation de la demande de chauffage en raison de la réduction des gains solaires. Dans une étude réalisée sur un immeuble de bureaux à paroi hautement vitrée, situé au Danemark, (Winther et al. [56]) il a été constaté que la demande totale d'énergie d'un immeuble de bureaux pourrait être réduite de 96 $kWh.m^{-2}$ par an à 73 $kWh.m^{-2}$ par an si une combinaison était faite entre un coefficient de transfert thermique le plus bas possible, un faible coefficient de gain solaire et un contrôle automatisé de l'éclairage. Et la demande varie entre ces deux valeurs si différentes combinaisons sont appliquées. Stavrakakis et al. [53] ont présenté une nouvelle méthode de calcul pour optimiser la conception des fenêtres pour le confort thermique dans les bâtiments ventilés naturellement. La méthodologie proposée associe les indices de confort thermique à des variables de conception architecturale et à une technique spéciale d'optimisation. L'étude a montré qu'à mesure que la hauteur de l'une des ouvertures augmente, la sensation thermique s'améliore. Anderson et Luther [52] ont conçu plusieurs systèmes de vitrage à l'aide de deux outils logiciels et ont étudié leur effet sur l'amélioration de l'environnement thermique intérieur dans un immeuble de bureaux commercial. Les systèmes proposés ont également été fabriqués et les résultats de la modélisation ont été validés expérimentalement. Les principales conclusions de l'étude indiquent que l'utilisation d'un écran d'ombrage pourrait améliorer le confort thermique et l'efficacité énergétique pendant la période de refroidissement. Cependant, il n'est pas efficace pour prévenir les pertes de chaleur pendant les périodes de refroidissement, ce qui entraîne un inconfort pour les occupants. De plus, l'utilisation de fenêtres à triple vitrage offre de meilleures caractéristiques d'isolation et conduirait à une plus grande stabilité dans l'environnement thermique intérieur. Ainsi, il est possible d'obtenir une plus grande satisfaction grâce à la réduction des hétérogéinété thermiques dans l'ambiance. Thalfeldt et al. [46] ont étudié de nombreuses conceptions de façades, y compris la configuration des fenêtres, le rapport fenêtre/mur (window-to-wall ratio (WWR)), l'isolation des murs et protection solaire, dans des bâtiments à zéro énergie. L'étude indique que la demande de chauffage domine la consommation d'énergie du bâtiment si l'on utiliserait des fenêtres conventionnelles. Cependant, la performance s'est considérablement améliorée lorsque les propriétés thermiques de la fenêtre ont été améliorées par l'application de quadruple (quatre vitrages) et quintuple (cinq vitrages) vitrages. En outre, l'étude a conclu que, d'un point de vue énergétique, l'utilisation d'un quintuple vitrage combiné à une isolation

extérieure des murs de 390 mm et d'un WWR de 60 % pour toutes les façades offre le potentiel d'économie d'énergie le plus élevé. Cependant, d'un point de vue économique, sur la base d'un calcul de la valeur actuelle nette sur 20 ans, les résultats indiquent que la meilleure performance énergétique a été obtenue avec des fenêtres à triple vitrage combinées à une isolation des murs extérieurs de 200 mm et un WWR de 37,5% pour la façade orientée nord et 23,9% pour les façades orientées sud, est et ouest. Lee et al. [49] ont étudié l'effet des systèmes de fenêtres sur la consommation d'énergie des bâtiments pour cinq climats asiatiques typiques en utilisant une analyse de régression. Les auteurs ont fait varier la surface vitrée de 0% à 100% WWR. La principale conclusion de l'étude, en ce qui concerne la zone de vitrage, est que le WWR doit être réduit au minimum, sauf pour la paroi opaque orientée nord de deux des climats étudiés. En ce qui concerne l'emplacement des fenêtres, il a observé que l'emplacement d'une fenêtre dépend amplement des conditions climatiques ; par exemple, une fenêtre orientée vers le nord offre le plus grand avantage pour les économies totales d'énergie dans deux des climats étudiés, mais pas dans les autres où l'orientation sud a le plus grand avantage. Jin et Overend [48] ont réalisé une étude comparative sur 13 types de vitrages sur la façade d'un bureau cellulaire typique. L'étude indique que les technologies de vitrage à haute performance, comme le vitrage photovoltaïque intégré, offrent des améliorations significatives par rapport aux murs isolés opaques et aux vitrages isolants conventionnels, même pour les grandes enveloppes vitrées, en termes de consommation énergétique et de qualité environnementale intérieure. Zomorodian et Tahsildoost [54] ont évalué l'effet de la conception des fenêtres sur le confort thermique et visuel en utilisant des simulations dynamiques dans un bâtiment éducatif. Les résultats de l'étude suggèrent que les vitrages enduits de contrôle solaire à faible coefficient de gain de chaleur solaire et à transmission visuelle élevée pourraient être une solution alternative aux pare-soleil. Le rôle que jouent les porte-à-faux et les persiennes dans la correction du mécanisme des ouvertures surdimensionnées permet au spécialiste du bâtiment de choisir une plus large gamme de dimensions de fenêtres. Même dans un faible WWR, une fenêtre avec un faible coefficient de transfert de chaleur peut conduire à un phénomène de surchauffe dans les climats chauds.

L'objectif principal de ces travaux de thèse est de formuler la relation entre le confort thermique des occupants, la consommation d'énergie de chauffage et les paramètres de conception des bâtiments performant hautement vitrée en climat européen, pour une meilleure intégration du confort thermique dans la conception des bâtiments. Les objectifs visés par son de : (1) comprendre la relation entre la performance énergétique, le confort thermique et les facteurs de conception, (2) fournir des prévisions réalistes et précises de la consommation d'énergie et du confort thermique tout au long du processus de conception, (3) identifier les paramètres et les interactions entre les paramètres qui affectent considérablement les objectifs de conception pour des fins d'optimisation

A la lumière de cela, nous identifions les limites suivantes associées aux approches trouvées dans la littérature :

Bien que la stratégie de contrôle basée sur le confort thermique proposée offre un effet d'économie d'énergie ainsi qu'un confort thermique constant, la plupart des schémas proposés sont basés sur des méthodes d'intelligence artificielle, qui peuvent donner des prévisions très précises, mais ils nécessitent suffisamment de données historiques de performance et sont extrêmement complexes à utiliser dans le processus de conception. De plus, la mise en œuvre de ces approches de contrôle nécessite une surveillance et des calculs continus pour fixer la température de consigne. Cela pourrait entraîner des coûts supplémentaires, tels que les coûts d'investissement et la consommation d'énergie pour le fonctionnement des équipements. De plus, des valeurs d'entrée inappropriées de l'habillement et du taux métabolique peuvent entraîner une discordance avec le confort thermique intérieur dès lors qu'ils ne peuvent pas être mesurés par des capteurs.

Bien que de nombreux travaux étudient l'effet de la conception des façades vitrées sur la consommation d'énergie [47–49], le confort thermique [51,52,54], et le confort visuel [57] en utilisant plusieurs paramètres. Cependant, peu d'études ont évalué simultanément l'effet de la conception des façades vitrées sur le confort thermique et la consommation d'énergie [48,51], même s'il est confirmé que le confort thermique est en concurrence avec les économies d'énergie dans un espace thermostatique contrôlé [40]. Il est donc essentiel de tenir compte à la fois de la consommation d'énergie et du confort thermique dans la conception des bâtiments afin d'obtenir un compromis. De plus, la grande majorité des études mentionnées ont été réalisées à l'aide d'outils de simulation de bâtiments, puisque, d'une part, les études réalisées exigent un grand nombre de scénarios pour obtenir des résultats robustes et que l'expérimentation pourrait être longue et complexe, et que, d'autre part, les outils de simulation de bâtiments ont été reconnus comme une méthode largement approuvée pour évaluer la qualité de l'air intérieur et la consommation énergétique. En outre, plusieurs études ont utilisé des études paramétriques pour étudier les scénarios proposés. Bien que les études paramétriques fournissent des résultats solides en ce qui concerne les paramètres influents affectant la réponse étudiée, elles sont d'une précision limitée en termes d'obtention de solutions optimales car elle n'est pas continue et il est difficile d'identifier les interactions entre paramètres à moins qu'un grand nombre de simulations soient effectuées. Afin de surmonter cette limitation, les résultats numériques pourraient être utilisés pour former une base de données allouée au processus de méta-modélisation [53,58]. Les méta-modèles mathématiques peuvent convertir le domaine discrétisé en un domaine continu, servant ainsi d'outil pratique, qui pourrait améliorer la précision de la solution quasi optimale sans avoir besoin d'une puissance excessive de calcul [53].

Ainsi, une question de recherche majeure (Q.1) et deux questions mineures (Q.1.1 et Q.1.2) émanent de l'état de l'art :

Q.1 : Est-il possible de concevoir des bâtiments performants assurant un compromis entre les économies d'énergie et le confort des occupants ?

Hypothèse : l'intégration du confort thermique des occupants dans la conception de bâtiments performants peut représenter une étape importante vers un compromis entre les économies d'énergie et le confort thermique.

Q.1.1 : Comment intégrer le confort thermique des occupants dans la conception de bâtiments économes en énergie ?

Q.1.2 : Quels sont les avantages d'intégrer le confort thermique des occupants dès la conception de bâtiments performants ?

Il est difficile de formuler et de résoudre un problème de conception d'un bâtiment performant ; les solutions doivent répondre à un grand nombre d'objectifs. L'intégration du confort thermique des occupants dans le processus de conception entraîne une complexité supplémentaire Nous avons utilisé la sFBS (situated Function-Behavior-Structure) comme un pont pour relier les caractéristiques de conception et les objectifs souhaités tout au long du processus de conception. Le modèle sFBS exprime la conception comme une activité qui vise à transformer un ensemble d'exigences et de fonctions en un ensemble de descriptions de conception [59]. Ceci est obtenu en transformant la fonction en comportement, puis en structure. Le sFBS comprend huit processus fondamentaux pour la conception. Ces processus sont la formulation, la synthèse, l'analyse, l'évaluation, la documentation, la reformulation de structure, la reformulation de comportement et la reformulation de fonction. Le mappage de la conception du bâtiment dans le sFBS nous permet d'identifier les étapes critiques qui nécessitent l'intervention de l'agent de conception. Cela facilite ensuite le choix d'outils et d'approches adéquats pour réduire la complexité de l'intégration du confort thermique des occupants dans les phases de conception du bâtiment.

Dans ce travail de recherche, nous nous concentrerons sur l'analyse et l'évaluation du comportement thermique du bâtiment, et nous reformulerons sa structure pour obtenir des résultats satisfaisants. En effet, le processus d'analyse nécessite une approche appropriée et adéquate pour prédire le comportement thermique réel. Ce dernier est influencé par de nombreux facteurs à côté de la structure du bâtiment, tels que les conditions météorologiques, le fonctionnement de l'éclairage et des systèmes CVC, l'occupation et leur comportement. Ainsi, la prédiction de la performance thermique d'un bâtiment nécessite des modèles qui décrivent avec précision les phénomènes physiques. De nombreux modèles ont été développés dans la littérature pour prédire la performance des bâtiments, y compris des méthodes de simulation dynamique [60], des méthodes statistiques [61] et des méthodes d'intelligence artificielle [62]. Chaque approche a ses avantages et ses inconvénients. La simulation dynamique est un modèle élaboré et complet qui permet d'obtenir des prédictions précises, mais il est

difficile de la mettre en pratique en raison de sa grande complexité et du manque d'information d'entrée [63]. Le modèle statistique est relativement facile à développer mais ses inconvénients sont l'imprécision et le manque de flexibilité [63]. Les méthodes d'intelligence artificielle sont appropriées pour résoudre des problèmes non linéaires, comme la prédiction de l'énergie dans les bâtiments ; elles peuvent donner une prédiction très précise tant que la sélection du modèle et l'établissement des paramètres sont bien effectués. Les inconvénients de ces modèles sont qu'ils exigent des données historiques suffisantes sur le rendement et qu'ils sont extrêmement complexes [63].

C'est pourquoi, dans le cadre de ces travaux de recherche, l'utilisation combinée de modèles de simulation de bâtiments et de modèles statistiques est adoptée. En effet, d'une part, les simulations de performance des bâtiments ont suscité beaucoup d'intérêt dans ce domaine comme alternative à l'approche empirique en raison de leur capacité à fournir des conclusions adéquates avec moins de temps et de coût, et d'autre part, elles permettent au concepteur ou à l'ingénieur d'analyser différents scénarios pendant la phase de conception sans avoir recours au bâtiment existant. D'autre part, le modèle statistique combine la vitesse de modèles simples et la précision de simulations dynamiques s'il est développé adéquatement [64]. Les modèles statistiques sont développés par des techniques de régression à partir de données historiques ou de modèles dynamiques, ce qui signifie qu'avant d'obtenir le modèle, nous devons recueillir suffisamment de données. Le principe des modèles statistiques est de proposer une fonction qui relie la variable étudiée, telle que le confort thermique, aux paramètres environnementaux (par exemple les températures, MRT) et aux paramètres de conception (par exemple le type et la surface de vitrage) et d'identifier les coefficients de cette fonction par une méthode de régression. La fonction obtenue permet au concepteur ou à l'ingénieur d'évaluer la sensibilité des variables étudiées aux paramètres présumés. De plus, la fonction développée, ou formulation mathématique, facilite le processus d'optimisation pour obtenir la conception souhaitée. L'analyse de sensibilité représente une approche intéressante car elle permet de comprendre la relation entre la variable étudiée et les paramètres de conception.

La modélisation numérique et les simulations ont été effectuées à l'aide de Modelica [65], un langage de modélisation basé sur des équations orientées objet de source ouverte. Modelica permet la simulation et la modélisation combinées de systèmes multi-physiques. Il diffère des autres environnements de programmation largement utilisés en utilisant une modélisation non causale. La modélisation à l'aide de Modelica peut se faire soit par une interface graphique, soit par des équations. La fonction basée sur les équations permet de s’affranchir des erreurs par rapport à la modélisation basée sur les assignations (par ex. TRNSYS, Matlab Simulink) [66]. Une comparaison fonctionnelle a été effectuée dans [67] indiquant que Modelica est plus approprié que TRNSYS® et Matlab Simulink® en termes de modularité, de modélisation multi-domaines, de comportement de contrôle réaliste et de flexibilité.

Dans cette étude, l'utilisation d'une approche de méta-modélisation basée sur la technique des plans d'expérience (DoE, Design of Experiments) est adoptée. La technique du DoE est une méthode statistique utilisée pour estimer la relation mathématique entre différents facteurs affectant plusieurs variables de réponse, et le plus souvent une variable de réponse. Elle pourrait être utilisée pour simplifier les études paramétriques en réduisant considérablement le nombre d'expériences ou de simulations nécessaires [58]. Les méta-modèles obtenus pourraient être utilisés à la place d'outils de simulation numérique pour simplifier et accélérer les études paramétriques afin de trouver des solutions optimales et d'analyser l'effet de chaque facteur sur la variable réponse et l'interaction entre facteurs. Les méta-modèles les plus courants sont le modèle linéaire du premier ordre, le modèle linéaire avec termes d'interaction, le modèle quadratique pur et le modèle quadratique complet. L'adéquation du modèle, et par conséquent l'adéquation de l'analyse effectuée, peut être facilement réalisée par une analyse graphique des résidus [68]. Si le modèle est exact, les résidus doivent être sans structure et distribués normalement.

En effet, la dernière étape consistera à mettre en œuvre une approche d'optimisation qui optimise à la fois la conception des bâtiments en termes de confort thermique et de consommation d'énergie. C'est pourquoi l'approche de la fonction de désirabilité est utilisée. L'approche de la fonction de désirabilité vise à optimiser simultanément plusieurs équations. Son idée de base est de convertir un problème à réponses multiples en un seul en convertissant chaque réponse en une fonction de désirabilité individuelle qui varie dans l'intervalle [0, 1]. Les fonctions de désirabilité individuelles ont différentes formulations en fonction de l'objectif souhaité (maximiser, minimiser ou valeur cible). Ensuite, les fonctions de désirabilité individuelles sont combinées dans la fonction de désirabilité globale (D). Enfin, l'algorithme devrait rechercher l'ensemble des facteurs d'entrée pour maximiser la fonction de désirabilité globale D [69]. Figure 1 montrer la représentation graphique de la méthodologie de recherche proposée.

Pour tester notre proposition, une étude de cas de référence est nécessaire pour la modélisation et les investigations. Une étude de cas réel, en particulier un bâtiment à faible consommation d'énergie, est préférable, car elle permettra d'obtenir des résultats plus réalistes et plus fiables de l'enquête. Le bâtiment envisagé pour cette étude est une école d'ingénieurs existante située à Troyes, France, où le système de chauffage représente une part importante de la consommation totale d'énergie. Le bâtiment a été conçu pour répondre aux normes de construction à basse consommation d'énergie et aux nouvelles normes françaises [7]. Les étudiants qui occupent l'espace qui comprend les cafés et l'espace, appelé le foyer (Figure 2), ont signalé une différence importante de température par rapport à d'autres parties du bâtiment et ont indiqué leur insatisfaction à l'égard des conditions thermiques. Le foyer, situé dans la partie sud-est du rez-de-chaussée, est un lieu de vie communautaire où les étudiants se réunissent tous les jours pour prendre le repas, se reposer et faire des activités. Le foyer a

une surface au sol de 58m^2 et des façades vitrées orientées sud et est d'environ 31m^2, dont 13m^2 pour le premier et 18m^2 pour le second. Bien que ces façades vitrées puissent améliorer le confort visuel et réduire la consommation d'énergie pour l'éclairage et le chauffage, elles peuvent produire de grandes surfaces chaudes lorsqu'elles sont exposées à un rayonnement solaire intense, ce qui affecte les conditions thermiques environnementales et par conséquent le confort thermique.

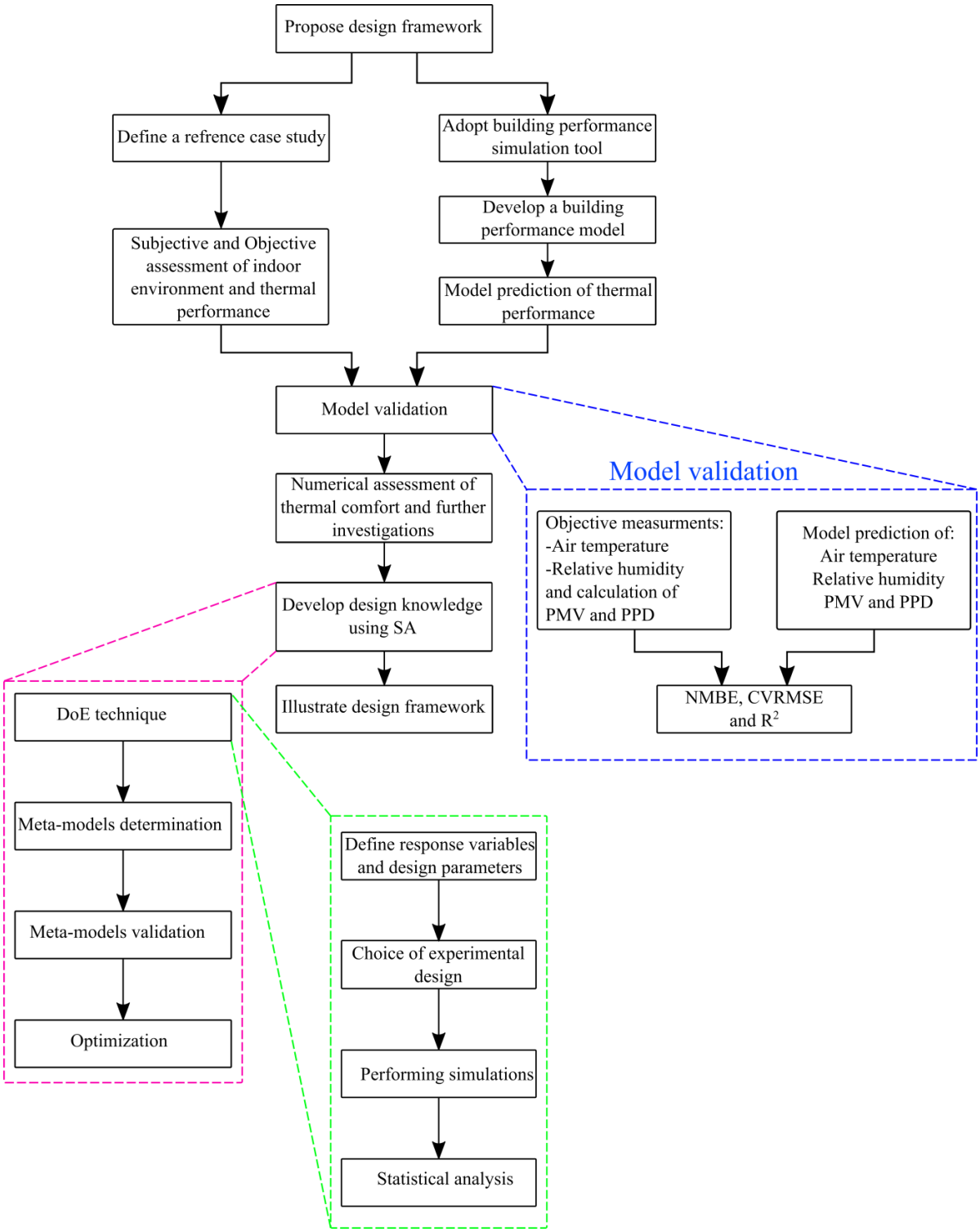

Figure 1 : Méthodologie de recherche.

La première étape de notre enquête est d'analyser et d'évaluer le comportement réel du foyer. Pour se faire, les sensations subjectives des élèves sont déterminées par un questionnaire d'enquête mesurant le vote par sensation thermique (TSV, thermal sensation vote), la préférence thermique, le niveau d'activité, etc. La TSV a été évaluée selon l'échelle à sept niveaux de l'ISO (Froid, frais, légèrement frais , Neutre, légèrement tiède, tiède, chaud) [20,22]. La préférence thermique a été évaluée à l'aide d'une échelle de sept points : ‘j’ai très froid, ‘j’ai froid’, ‘j’ai légèrement froid ’, ‘pas de changement’, ‘j’ai légèrement chaud, ‘j’ai chaud’ et ‘j’ai très chaud, ce qui signifie que le sujet exige des conditions thermiques en fonction de sa préférence. De plus, le taux de satisfaction thermique est évalué à l'aide d'une question indépendante selon une échelle à deux points : " satisfait " et " insatisfait ". Par ailleurs, le niveau d'activité des élèves a été évalué à l'aide d'une échelle en cinq points : " assis", " debout ", " activité légère ", " activité moyenne " et " activité élevée ".

Figure 2: Le Foyer : (a) vue sud-est ; (b) plan du rez-de-chaussée et emplacement des foyers ; (c) vue intérieure.

Le questionnaire d'enquête, intitulé "Confort thermique dans le Foyer", est construit à partir du site web de *surveyplant* [70]. Au total, 54 questionnaires ont été recueillis et analysés auprès d'élèves âgés de 17 à 22 ans en décembre 2016 (du 1er au 12 décembre). Les réponses recueillies montrent que les élèves ressentaient une ambiance chaude et que 37 % des répondants étaient insatisfaits des conditions thermiques environnementales (Figure 3). Cela est dû au fait que 60 % du niveau d'activité

des élèves était supérieur à celui supposé lors de la phase de conception. De plus, les sensations thermiques neutres n'étaient pas préférées par la majorité des élèves, alors qu'ils avaient tendance à être plus réceptifs à des conditions " légèrement chaudes ". Cela a été confirmé lorsque les élèves ont exprimé le moins d'insatisfaction lorsqu'ils se sentaient un peu chauds.

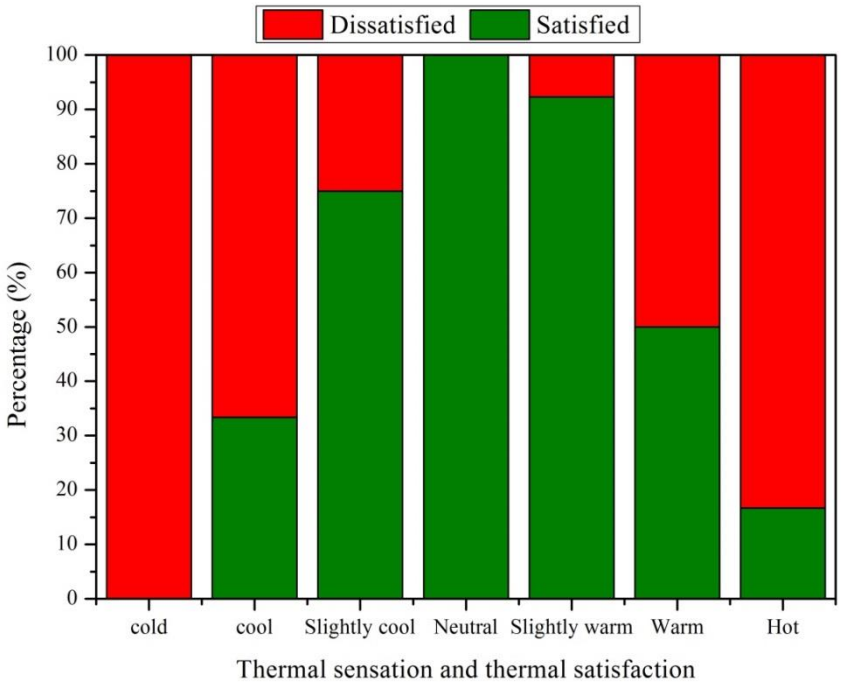

Figure 3: Relation entre la sensation thermique et la satisfaction thermique.

Dymola® est ensuite utilisé pour développer le modèle d'étude de cas et réaliser les simulations (Figure 4). Le composant `MixedAir` de `Rooms package` [71] est utilisé pour illustrer une seule pièce avec un nombre illimité de constructions opaques. Les propriétés thermiques des murs intérieurs, des plafonds, des planchers et des façades vitrées sont définies à l'aide des composants `OpaqueConstructions` et `GlazingSystems` de `HeatTransfer package`. Le système de ventilation mécanique du foyer est implémenté dans le modèle en utilisant `FlowControlled_m_flow` de `Fluid package` [72]. Le système de chauffage est modélisé à l'aide du `radiateurEN442_2` du `Fluid package`, qui représente un radiateur pouvant être utilisé comme modèle dynamique ou en régime permanent. De plus, `DaySchedule` est utilisé pour représenter le profil d'occupation dans le foyer et est relié au raccord d'entrée `qGai` du modèle `MixedAir` pour ajouter les gains de chaleur radiative, convective et latente internes. Le composant `ReaderTMY3` du `BoundaryConditions package` [73] est utilisé pour représenter les conditions météorologiques extérieures. Le composant `Fanger` du `Utilities package` de la `Modelica Buildings`

`library` est ensuite implémenté dans le modèle pour calculer les valeurs PMV et PPD pendant le temps de simulation.

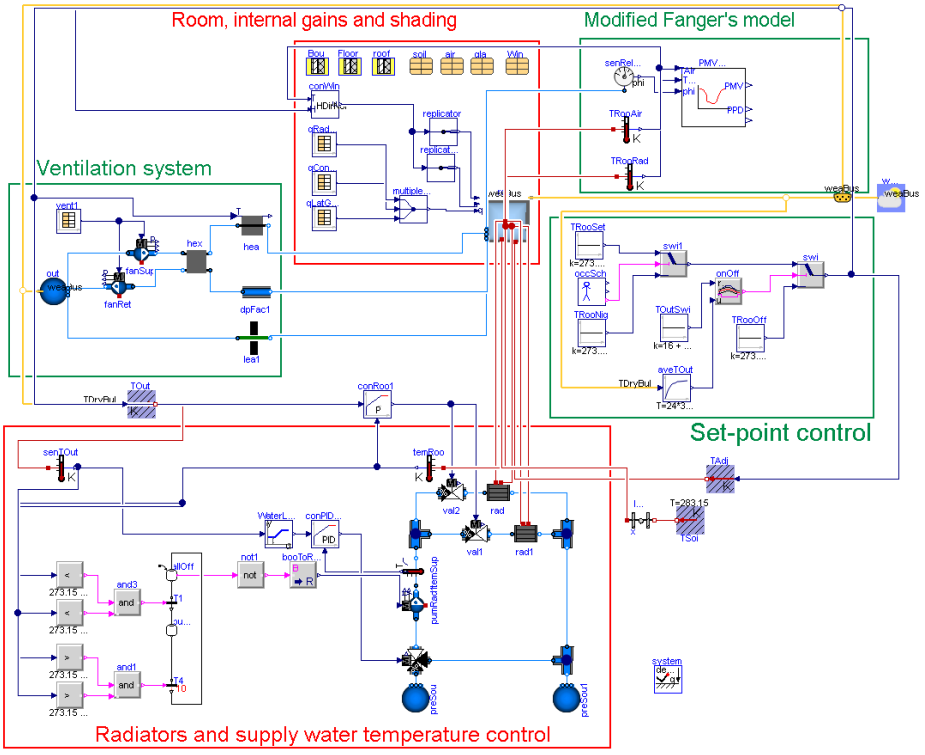

Figure 4: Modèle Global du Foyer.

Le modèle est ensuite validé en comparant ses prédictions avec des mesures objectives de la température de l'air et de l'humidité relative. NMBE (normalized mean bias error), CVRMSE (coefficient of variation of the root mean square error) et le coefficient de détermination (R^2) permettent de quantifier les écarts entre les valeurs prévues et les valeurs mesurées. Les valeurs obtenues pour le NMBE et le CVRMSE se situent dans les limites acceptables de ± 10 et $\pm 30\%$ [74], respectivement, (Table 1). De plus, le coefficient de détermination qui peut donner une indication de la façon dont les valeurs prédites correspondent aux données mesurées est obtenu en traçant les courbessur un graphique de dispersion en fonction des valeurs mesurées. Une bonne corrélation est observée montrant une valeur R^2 de 0,9751 et 0,9083 pour la température ambiante et l'humidité relative, respectivement, ce qui signifie que 97,51 % et 90,83 % de la variance s'explique par le modèle. De plus, les valeurs moyennes de PMV et de PPD obtenues à partir du modèle expérimental et du modèle Modelica pour les cinq cycles expérimentaux sont comparées (Figure 5). Les résultats montrent une bonne concordance entre la simulation et les résultats calculés à partir des données mesurées. En général, toutes les valeurs moyennes obtenues de PMV sont négatives et se situent en dehors de l'intervalle de confort acceptable [-0,5, +0,5]. Par conséquent, toutes les valeurs moyennes obtenues de PPD sont supérieures à l'intervalle de confort recommandé qui est de 10 %. Ces résultats

indiquent que l'environnement thermique intérieur du Foyer est froid. Nous constatons que les températures extérieures moyennes ont diminué progressivement du 12 au 14 novembre. Ces données sont cohérentes avec les valeurs mesurées de PMV qui indiquent que l'environnement intérieur du Foyer est devenu plus froid. Enfin, tous les résultats obtenus indiquent que la prédiction du modèle est en accord avec les données mesurées. Par conséquent, le modèle est considéré comme validé et pourrait être utilisé pour des fins d'évaluations et d'enquêtes ultérieures.

Table 1 : NMBE et CVRMSE de la température ambiante et de l'humidité relative pour les cinq cycles.

NMBE (%)	Cycle 1	Cycle 2	Cycle 3	Cycle 4	Cycle 5
Room Temperature	-2.12	-2.60	-0.29	-1.25	-4.68
Relative humidity	-2.21	1.55	-1.13	1.85	-3.10
CVRMSE (%)					
Room Temperature	2.20	5.00	6.38	2.40	4.73
Relative humidity	2.23	3.09	3.43	2.56	2.89

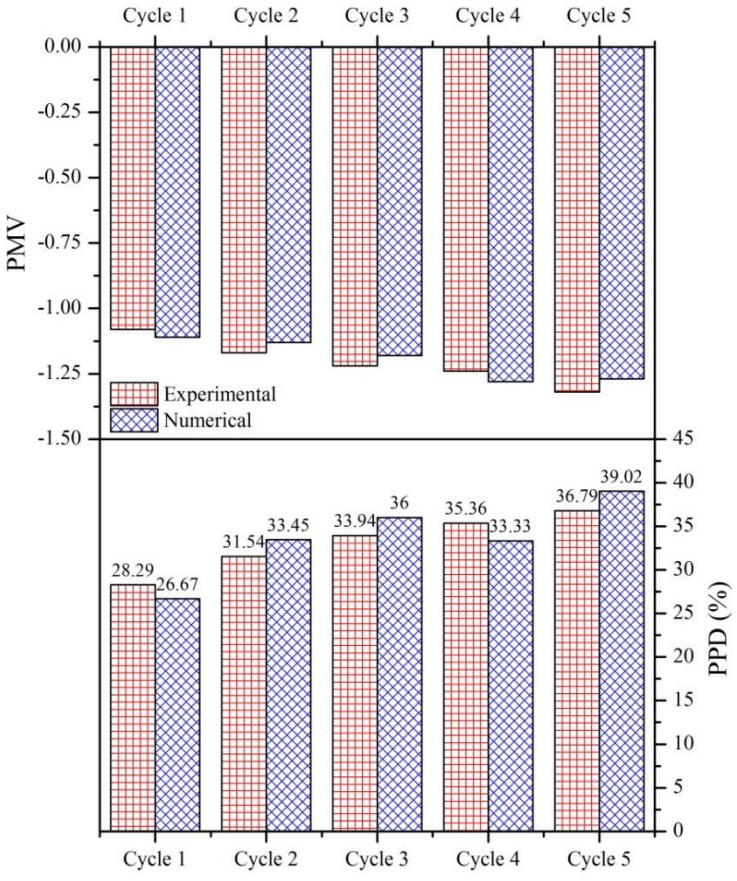

Figure 5: Valeurs moyennes de la PMV et de la PPD correspondante pour les différents cycles.

Le modèle développé est ensuite utilisé pour effectuer des simulations tout au long de journées d'hiver représentatives et de toute la saison hivernale afin d'évaluer et d'analyser les caractéristiques de

confort thermique du foyer. L'utilisation d'une échelle de temps différente est importante dans l'évaluation du comportement d'un bâtiment, car un bâtiment peut avoir un comportement satisfaisant sur une base annuelle ou saisonnière, alors que les problèmes se produisent sur une base mensuelle ou quotidienne. Les simulations de performances thermiques ont mis en évidence l'évolution de l'indice PMV et la température radiante moyenne sur quatre jours d'hiver correspondant à des journées ordinaires, partiellement nuageuses, nuageuses et ensoleillées. Les résultats montrent que l'indice PMV a suivi la même tendance que MRT, qui a suivi la même tendance que le rayonnement solaire en raison de la présence d'une enveloppe fortement vitrée. Ces résultats indiquent que l'indice PMV dans un espace avec façades vitrées est fortement influencé par les changements des conditions climatiques extérieures. De plus, l'effet du niveau d'activité sur l'indice PMV est ensuite évalué en simulant plusieurs scénarios pour différents niveaux d'activité. Les résultats montrent que, lors d'une journée où la température extérieure est basse et le rayonnement solaire est faible, l'indice PMV est inférieur aux limites de confort acceptables pour un élève ayant un niveau d'activité assis ou debout. Toutefois, l'indice PMV a été maintenu à l'intérieur de l'intervalle de confort acceptable pour un niveau d'activité léger ou moyen, et autour de la limite supérieure de confort pour un niveau d'activité élevé. De plus, le jour où le rayonnement solaire est intense, les résultats montrent que dans tous les cas étudiés, l'indice PMV dépasse la limite supérieure de confort lors de la présence du rayonnement solaire. Ces résultats expliquent l'apparition de différents votes et confirment la grande variabilité de la sensation thermique des élèves durant la même période.

Le modèle développé est ensuite utilisé pour effectuer des simulations tout au long de la période de chauffage. La température de l'air soufflé dans le foyer était généralement réglée à 20 °C pendant la saison de chauffage. Toutefois, les nouvelles normes françaises recommandent que la consigne de température ambiante soit fixée à 19 °C. Ainsi, deux cas avec des températures ambiantes de consigne de 19 °C et 20 °C ont été étudiés. Les valeurs de l'indice PMV pour les deux consignes variaient entre -1,5 et +3,0 et -0,7 et +3,0, respectivement. Les résultats indiquent que 79,5 % et 67,8 % des indices PMV pour les consignes de 19 °C et 20 °C, respectivement, se situaient en dehors de l'intervalle de confort acceptable de [-0,5, +0,5] ; par conséquent, le PPD recommandée de 10 % n'a pas été atteinte. Les résultats ont montré que l'on s'attend à ce que les occupants ressentent des sensations thermiques à la fois chaudes et froides. De plus, l'indice PMV est sensible aux conditions climatiques extérieures, au niveau d'activité des sujets et à la température de consigne. Cependant, l'indice PMV est influencé par d'autres facteurs principaux tels que l'isolation des vêtements qui affectent directement la sensation thermique des occupants et la surface vitrée qui affecte la valeur PMV à travers la température radiante moyenne. Il est donc essentiel d'étudier la sensibilité de l'indice PMV à certains de ces facteurs afin d'évaluer l'effet de chaque facteur sur le confort thermique et de déterminer les facteurs les plus critiques influençant la valeur PMV.

À cette fin, la technique du DoE est utilisée pour élaborer les plans d'expérience requis. Afin de la mettre en œuvre, la procédure suivante est recommandée [68] : (1) Reconnaissance et énoncé du problème, (2) Choix de la variable réponse, (3) Choix des facteurs, des niveaux et des intervalles, (4) Choix de la conception expérimentale, (5) Réalisation de l'expérience, (6) Analyse statistique des données, et (7) Conclusions et recommandations. Les variables de réponse prises en compte sont : les valeurs moyennes quotidiennes, maximales et minimales de PMV, car il n'est pas logique d'avoir une valeur hebdomadaire, mensuelle ou annuelle de PMV puisqu'elle peut changer fréquemment pendant la journée ; en outre la moyenne peut être considérée comme une valeur représentative pour remplacer les valeurs horaires. Cependant, les valeurs moyennes seules, dans le cas du ressenti des occupants, ne sont pas significatives si elles ne sont pas complétées par les valeurs maximales et minimales, qui permettent d'évaluer si la valeur PMV dépasse la limite supérieure ou inférieure de confort acceptable. Les paramètres étudiés sont la température ambiante, le taux métabolique, l'isolation des vêtements, le WFR, le type de vitrage et la température sol-air. Cette dernière est définie comme " *la température de l'air extérieur qui, en l'absence de rayonnement solaire, donnerait la même distribution de température et le même taux de transfert de chaleur à travers un mur (ou un toit) qu'en présence des effets combinés de la distribution réelle de la température extérieure plus le rayonnement solaire incident* " [75]. L'humidité relative et la vitesse de l'air ont été exclues de l'étude de sensibilité, car l'indice PMV s'est révélé moins sensible pour les deux paramètres que pour les quatre autres paramètres [76,77]. Chaque paramètre considéré à un niveau inférieur (-1) et supérieur (+1). Le niveau élevé du WFR et du type de vitrage représente l'étude de base, et le niveau bas a été choisi par rapport aux valeurs recommandées par les normes des bâtiments à faible consommation d'énergie [78]. La température sol-air moyenne quotidienne a été calculée et les valeurs minimale et maximale ont été choisies pour représenter les niveaux inférieur et supérieur. Alors que les niveaux supérieurs et inférieurs des facteurs restants sont basés sur les résultats du questionnaire, pour le taux métabolique, et les valeurs recommandées par les normes européennes et les bâtiments à faible consommation énergétique [78,79]. Le DoE a été réalisé à l'aide d'un plan factoriel complet à deux niveaux. Cette conception tient compte de toutes les combinaisons possibles de facteurs. Le plan factoriel complet vise à identifier les variables significatives qui influencent la variable réponse. De plus, il aide à analyser l'interaction entre ces facteurs [80], et offre des résultats plus précis que le plan factoriel fractionnaire et évite les conclusions erronées [81]. Le nombre d'expériences est de 2^k, où k est le nombre de facteurs. Ce plan a donné lieu à 64 expériences visant à étudier l'effet principal des facteurs et leurs interactions. Chaque expérience représente une combinaison unique de niveaux de facteurs et de variables de réponse. Le logiciel Minitab® a été utilisé pour le posttraitement statistique des données de simulation.

L'analyse de variance (ANOVA) a été utilisée pour identifier les facteurs significatifs. La signification d'un facteur ou de son effet est déterminée par rapport à sa valeur P, qui est un paramètre

important utilisé pour identifier les facteurs statistiquement significatifs influençant la variable réponse. Si la valeur P d'un facteur ou de son effet est inférieure à 0,05, elle est considérée comme significative [82]. Les résultats montrent que le taux métabolique a l'effet le plus important sur les valeurs quotidiennes moyennes, maximales et minimales de la PMV. De plus, les valeurs moyennes et maximales quotidiennes ont été influencées de façon significative par la température sol-air moyenne quotidienne, l'isolation des vêtements, l'interaction entre la température sol-air et WFR, la température de consigne et WFR. Cependant, la valeur minimale de la PMV a été influencée de façon significative par l'isolation des vêtements, la température de consigne, l'interaction entre l'isolation des vêtements et le taux métabolique et le WFR, respectivement. Les effets d'autres facteurs et leurs interactions sont présentés par ordre décroissant, comme le montrent les diagrammes de Pareto. Ces résultats sont en accord avec les résultats discutés précédemment concernant l'effet du niveau d'activité et des climats extérieurs sur la sensation thermique des occupants de la pièce à l'étude. Les résultats de l'étude de sensibilité confirment que dans le foyer étudié, le confort thermique des élèves est fortement influencé par leur comportement (activité et niveau vestimentaire). De plus, dans la conception actuelle, les valeurs moyennes et maximales quotidiennes de la PMV sont plus sensibles aux conditions climatiques extérieures et aux paramètres de l'enveloppe qu'à la température ambiante de consigne. De plus, les résultats montrent que l'interaction entre la température sol-air et le WFR a l'impact le plus significatif sur la valeur quotidienne moyenne et maximale des PMV. Cet effet d'interaction indique que la relation entre la valeur PMV et les conditions climatiques extérieures dépende de la surface vitrée extérieure. Cette constatation indique qu'à mesure que la surface vitrée extérieure augmente ou diminue, l'effet des conditions climatiques extérieures devient plus ou moins important par rapport à la valeur moyenne quotidienne et maximale des PMV. De plus, les valeurs de PMV sont très sensibles aux paramètres liés aux occupants (niveau d'activité et isolation des vêtements) et toute sous-estimation des valeurs du taux métabolique et de l'isolation des vêtements dans la phase de conception peut entraîner des incertitudes dans les résultats.

L'utilisation de la technique du DoE nous permet de développer une relation de méta-modélisation entre la variable réponse et les paramètres étudiés. En effet, la validité de ces méta-modèles est cruciale pour confirmer la pertinence de l'analyse effectuée. Les résultats de l'analyse de variance indiquent une bonne performance avec R^2 (> 0,98) et R^2 ajusté (0,97). Le R^2 ajusté est une forme d'expression du degré d'ajustement et il est plus fiable que R^2 pour comparer des modèles avec différents nombres de variables indépendantes [69]. La valeur de R^2 ajustée indique que plus de 97 % du total des facteurs associés à la PMV sont attribués aux paramètres choisis du modèle. Le R^2 prédit est en accord raisonnable avec le R^2 ajusté, c'est-à-dire que la différence est inférieure à 0,2. De plus, les courbes de réponse résiduelles par rapport aux courbes de réponse prévues montrent des formes moins structurées, et les courbes de probabilité normales indiquent que les résidus ont suivi une ligne droite, ce qui confirme la validité des modèles. Les méta-modèles obtenus sont ensuite utilisés pour

optimiser la conception du bâtiment en termes de confort thermique. A cet effet, l'approche de la fonction de désirabilité est utilisée. L'objectif est de maintenir les valeurs PMV dans l'intervalle de confort thermique acceptable de [-0,5 ; +0,5]. Selon les résultats obtenus, la valeur maximale D (fonction de désirabilité globale), D=1, est fournie lorsque la température de consigne, le coefficient de transmission thermique du vitrage U et le WFR sont respectivement de 20,8 °C, 2,8 $W.m^{-2}.K^{-1}$ et 16%. Les résultats montrent que l'utilisation de cette combinaison de paramètres donnera des valeurs moyennes, minimales et maximales de PMV de -0,381, -0,5 et 0,107, respectivement. Le modèle Dymola validé est utilisé pour simuler le scénario optimisé afin de valider l'adéquation des résultats obtenus. La moyenne, le minimum et le maximum obtenus sont respectivement de -0,284, -0,41 et 0,124. Ces résultats sont en accord avec les résultats prévus par l'optimisation des méta-modèles, confirmant ainsi la validité des résultats obtenus.

Le cas optimisé permet de réduire les valeurs élevées de PMV et d'améliorer les valeurs basses de PMV pour qu'elles se situent toutes dans l'intervalle de confort thermique acceptable (Figure 6). Ces résultats montrent que l'optimisation de la conception permet d'obtenir de meilleures conditions de confort thermique dans la pièce étudiée. De plus, bien que le boîtier optimisé permette une augmentation de la température de consigne pour maintenir des conditions acceptables de confort thermique, il permet de réduire la consommation d'énergie de chauffage. La consommation totale d'énergie de chauffage du scénario de base était de 3034 kWh par année (scénario de base à une température de consigne de 20 °C), tandis que celle du scénario optimisé est de 2566 kWh par année. Ces résultats sont corrélés à la diminution de la surface vitrée, ce qui se traduit par une meilleure résistance thermique des parois extérieures, ce qui permet de réduire la perte de chaleur de transmission à basse température sol-air, en améliorant ainsi la consommation d'énergie de chauffage. Les résultats obtenus indiquent que l'intégration du confort thermique des occupants dans la conception de bâtiments performants entraîne un compromis entre les économies d'énergie et le confort thermique.

Afin d'évaluer la valeur ajoutée de l'approche proposée, une étude comparative avec une autre approche qui intègre le confort thermique des occupants dans le contrôle de l'environnement intérieur, comme le contrôle du confort basé sur les PMV, est réalisée. Le concept d'une telle approche est basé sur le calcul inverse de l'indice PMV [40]. Il vise à maintenir le PMV défini par l'utilisateur en ajustant la température ambiante par rapport aux changements d'autres paramètres affectant le confort thermique intérieur, principalement la température radiante moyenne. La température ambiante est calculée par calcul itératif de la racine des fonctions non linéaires et un signal de commande est envoyé au régulateur de consigne du système de chauffage pour maintenir la température ambiante déterminée. La Figure 7 illustre le diagramme du régulateur implémenté dans le modèle précédemment développé. Une étude comparative entre le contrôle de confort à base de PMV et le

contrôle thermostatique conventionnel est réalisée. Les critères de comparaison comprennent la consommation d'énergie de chauffage et l'indice de qualité environnementale (EQI, Environmental Quality Index) [83]. Ce dernier est un indice utilisé pour l'évaluation à long terme de la qualité thermique environnementale basée sur les quatre catégories de qualité (I, II, III et IV) définies par les normes européennes EN 15251 [79]. Pour les simulations, la consigne de température ambiante du thermostat a été réglée sur 19 °C, 20 °C et 21 °C et l'indice PMV sur -0,5 dans le régulateur de confort thermique basé sur PMV. Cette valeur représente le minimum dans les limites de la catégorie II, la catégorie recommandée pour les bâtiments neufs et rénovés [79], ce qui permet d'utiliser le moins d'énergie pour le chauffage.

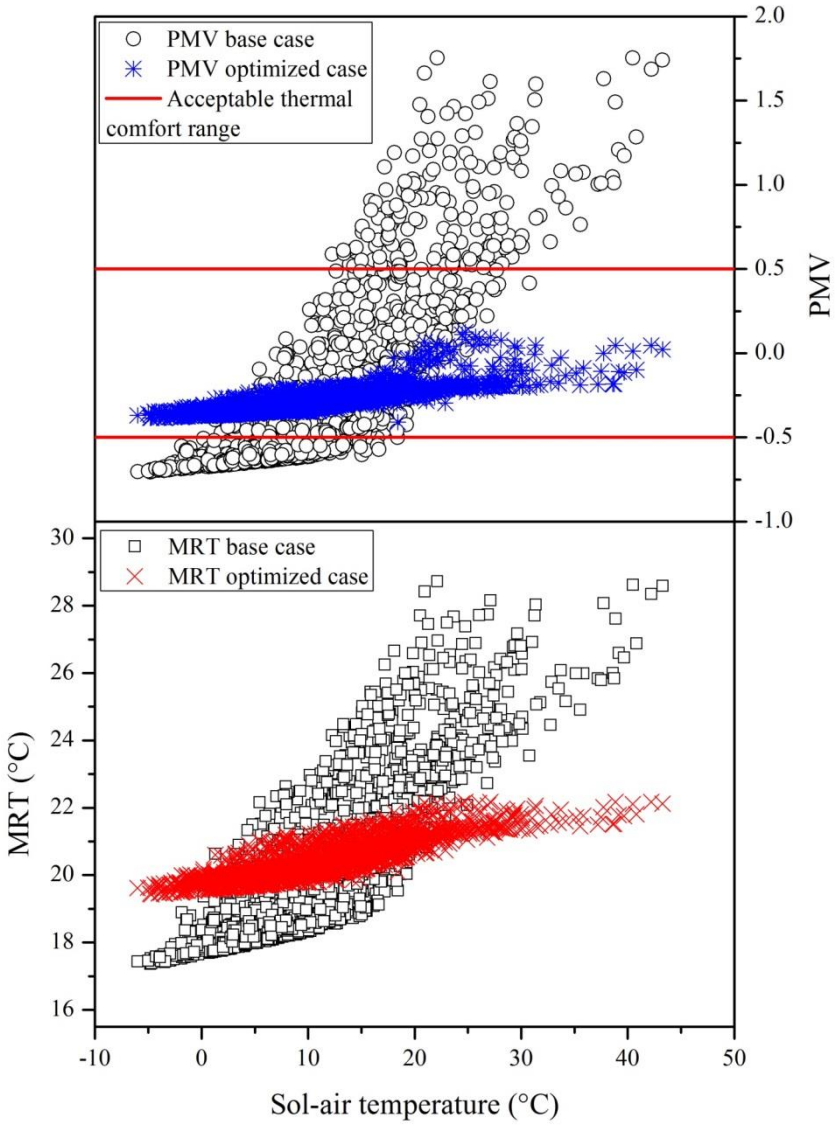

Figure 6: Valeurs horaires numériques de (a) l'indice PMV et (b) MRT obtenues à partir du modèle Dymola® validé pour les deux cas étudiés.

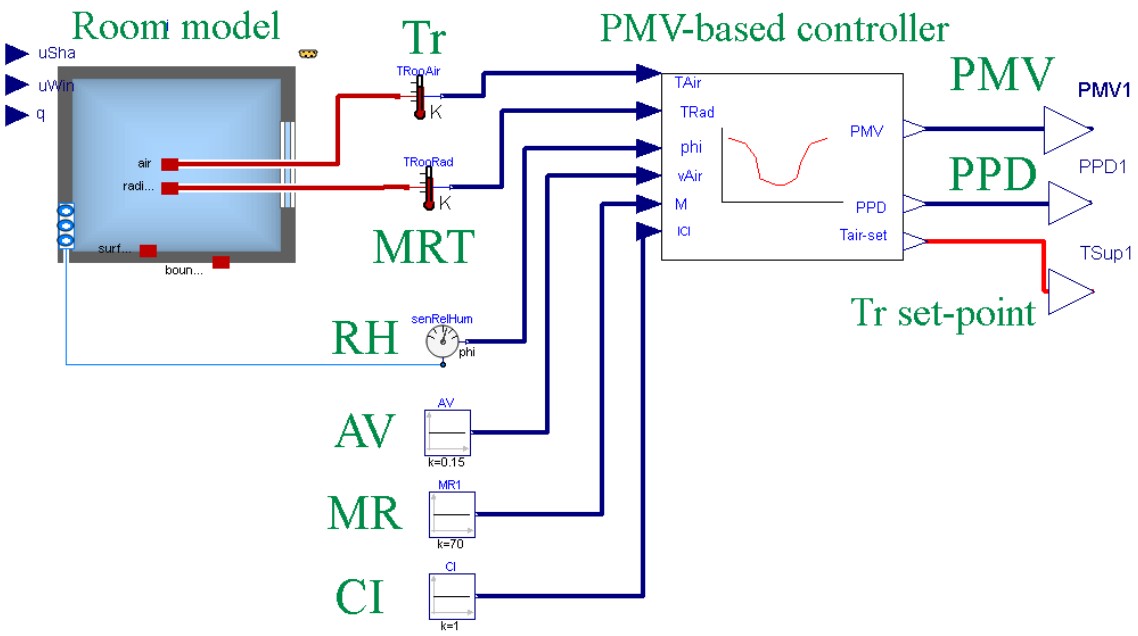

Figure 7: Schéma de régulation du confort thermique basé sur les PMV, implémenté sur le modèle Dymola®.

Les résultats obtenus sont présentés dans Table 2. Les résultats montrent que le confort thermique dans un espace thermostatique est en concurrence avec l'économie d'énergie, en raison de la présence d'une grande surface vitrée. A basse température sol-air, une température de consigne plus élevée (21°C) est nécessaire pour maintenir un confort thermique acceptable, donc une plus grande consommation d'énergie de chauffage. Cependant, une température sol-air élevée entraine une augmentation des températures radiantes moyennes, donc des valeurs PMV plus élevées, puisque le contrôle thermostatique conventionnel ne prend pas en compte les changements dans les autres paramètres environnementaux Cela pourrait être dû au fait que la température ambiante dans un espace à confort contrôlé est principalement déterminée en fonction de la température radiante moyenne pour maintenir la valeur PMV prédéfinie. De plus, en cas de basse température sol-air, le potentiel d'économie d'énergie est réduit grâce au contrôle de confort thermique, mais le confort thermique est maintenu. De plus, les résultats indiquent que la consommation d'énergie avec un contrôle de confort est plus sensible aux climats extérieurs qu'avec un contrôle thermostatique, ce qui permet de réaliser plus d'économies d'énergie à haute température sol-air, tout en maintenant un meilleur confort thermique.

La régulation basée sur l'indice de confort PMV est ensuite comparée avec celui basé sur la température de consigne (régulation thermostatique). L'objectif est d'évaluer l'effet de l'intégration du confort thermique dans la phase de conception du bâtiment. Les résultats (Figure 8) montrent que l'intégration du confort thermique dans la conception des bâtiments permet d'obtenir un meilleur état

de confort thermique que son intégration dans la commande du système de chauffage. De plus, il permet une réduction d'environ 16,5 % de la consommation d'énergie de chauffage par rapport au cas de confort contrôlé. Ces résultats montrent que l'intégration du confort thermique au stade de la conception des bâtiments supprime la nécessité d'une stratégie de contrôle avancée, ce qui pourrait nécessiter l'installation de dispositifs supplémentaires afin de maintenir une surveillance continue de l'environnement intérieur, entraînant ainsi des coûts d'installation et de fonctionnement supplémentaires.

Table 2: Fréquence (heures) de l'indice PMV pour les boîtiers thermostatiques et pour le boîtier thermique pendant la période de chauffage.

PMV index	Thermostatic control			Comfort control
	19 °C	20 °C	21 °C	PMV -0.5
-1.0 to -0.7	1442	0	0	0
-0.7 to -0.5	306	1427	0	0
-0.5 to -0.2	187	441	1721	1900
-0.2 to +0.2	199	214	299	305
+0.2 to +0.5	98	105	133	84
+0.5 to +0.7	49	68	67	37
+0.7 to +1.0	44	52	66	30
+1.0 to +1.5	34	49	63	10
+1.5 to +3.0	7	10	17	0
% outside category A, B, C and resultant comfort class				
A	91.58	90.95	87.36	87.10
B	79.54	67.87	9.00	3.25
C	64.53	4.69	6.17	1.69
Class	IV	IV	IV	III
Energy consumption (kWh)				
	2710	3034	3377	3078

Dans la dernière étape de ces travaux de recherche, la sensibilité de la consommation d'énergie de chauffage dans un cas de confort contrôlé est étudiée à l'aide de DoE. On considère comme variable de réponse la consommation d'énergie du système de chauffage pendant une semaine d'hiver représentative. Les paramètres étudiés sont la température radiante moyenne, l'humidité relative, la vitesse de l'air, le taux métabolique et l'isolation des vêtements. Chaque facteur à deux niveaux notés comme élevé (+1) et faible (-1). Les niveaux supérieurs et inférieurs de chaque facteur sont basés sur les valeurs maximales et minimales recommandées par les normes européennes [79]. Le PMV a été fixé à une valeur fixe de -0,5. Le plan factoriel complet tenant compte de cinq facteurs, chacun à deux niveaux, donne 32 passes. L'étude de sensibilité réalisée indique que la température radiante moyenne et les paramètres personnels tels que le taux métabolique et l'habillement ont le plus d'impact sur la consommation d'énergie dans une pièce hautement vitrée confort contrôlé. Ainsi, pour améliorer la performance énergétique, les paramètres personnels doivent être définis de manière adéquate plutôt que de les considérer comme des valeurs par défaut. En ce qui concerne le taux métabolique, des dispositifs portables pourraient être utilisés pour fournir une rétroaction continue sur la valeur

métabolique moyenne des occupants du bâtiment, comme nous l'avons mentionné dans [76]. Toutefois, d'autres études sont nécessaires pour confirmer si une telle solution est faisable en terme d'acceptabilité par les occupants du bâtiment. De plus, au cours des dernières années, de nombreux modèles ont été mis au point pour prédire la vêture et le changement d'isolation des vêtements intérieurs en fonction de la température extérieure, à partir de différentes fonctions de régression [84–86]. Selon ces modèles, un pourcentage important de la variance de l'isolation des vêtements s'explique par les variations d'un indice climatique extérieur, comme la température extérieure, la température extérieure moyenne quotidienne, la température extérieure moyenne mensuelle et la température extérieure pondérée. Ces modèles peuvent être appliqués aux bâtiments équipés de systèmes intelligents de gestion d'énergie du bâtiment pour les espaces thermostatiques et à confort contrôlé afin de prédire l'isolation des vêtements des occupants en fonction des changements des conditions climatiques extérieures.

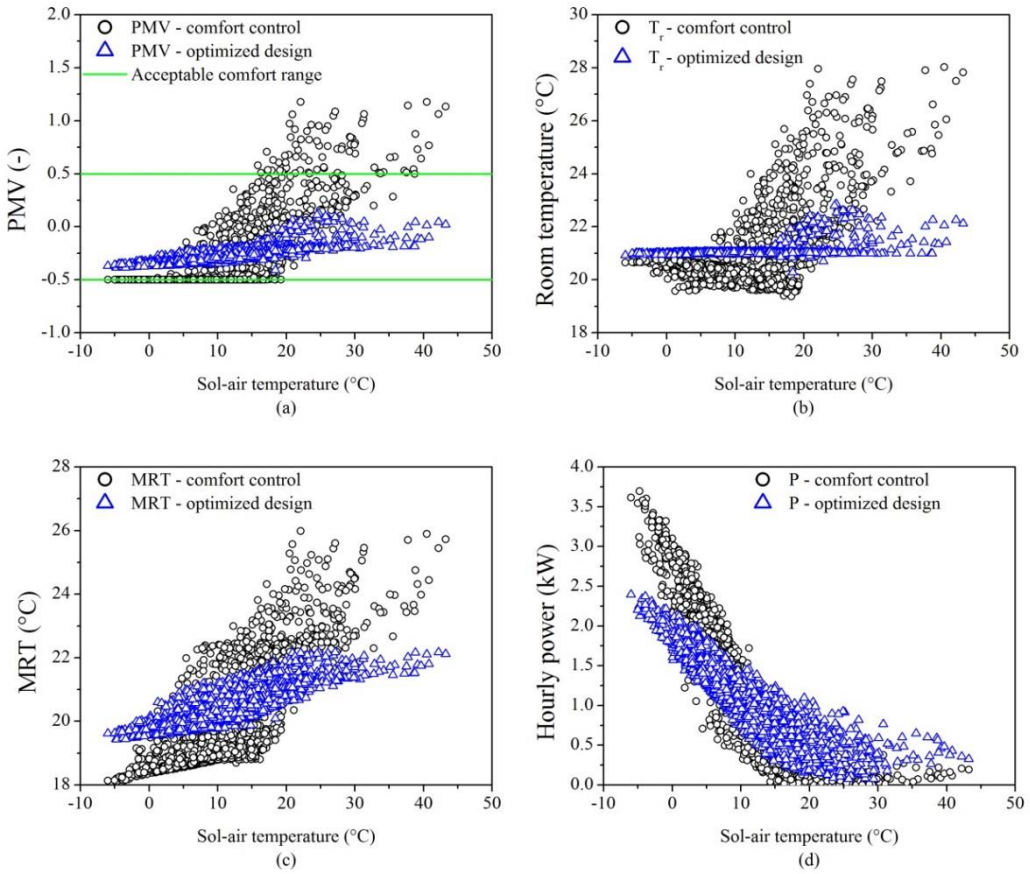

Figure 8 : Valeurs horaires numériques de (a) l'indice PMV, (b) la température ambiante, (c) la MRT et (d) la puissance horaire de l'énergie de chauffage obtenue du modèle Dymola® validé pour les deux cas.

Ces résultats indiquent que les principaux problèmes ciblant le confort thermique dans l'espace étudié sont le risque d'environnement chaud et le phénomène de surchauffe. Sur la base des résultats

déjà discutés, le risque d'environnement chaud et de phénomène de surchauffe peut être réduit en baissant la température radiante moyenne. Ainsi, un traitement soigné et approprié de la configuration des façades vitrées pourrait offrir un meilleur confort thermique et une meilleure consommation d'énergie. A cet effet, la sensibilité du MRT aux paramètres de conception, principalement les façades vitrées est examinée, dans le but d'obtenir une conception optimale permettant d'atteindre un compromis entre économie d'énergie et confort thermique. Les paramètres pris en compte dans les études sont l'orientation des façades vitrées, l'ombrage intérieur, le type de vitrage, le WFR et la température sol-air. Le DoE était basé sur un plan factoriel complet tenant compte de cinq paramètres à deux niveaux chacun, générant ainsi32 simulations. Les niveaux supérieurs et inférieurs de l'orientation et de l'ombrage sont basés sur les résultats de la simulation qui donne les valeurs minimale et maximale du MRT. Par exemple, si la pièce est orientée nord-est, il en résultera une plus faible exposition au rayonnement solaire et donc une diminution des valeurs MRT, de sorte que l'orientation nord-est soit fixée au niveau -1 ; inversement, l'orientation sud-ouest est fixée au niveau +1. De plus, le niveau élevé de la surface vitrée et du type de vitrage représente la conception de base, et le niveau bas a été choisi par rapport aux valeurs recommandées par les normes françaises selon les critères de la basse consommation [7,78]. Les valeurs moyennes, maximale et minimale du MRT sont considérées comme les variables de réponse implémentées dans le DoE.

Les résultats des simulations ont montré que les paramètres clés affectant le MRT sont la température sol-air, l'orientation WFR et les façades vitrées, l'influence des conditions climatiques est fortement corrélée à la surface et à l'orientation des façades vitrées. Par exemple, la variation du MRT en fonction de la température sol-air a diminué avec la diminution WFR. D'autre part, le type de vitrage peut avoir un impact significatif lorsque la surface vitrée devient plus importante ou lorsque la température sol-air est basse, car l'amélioration de la valeur U du vitrage peut réduire la perte de chaleur à travers l'enveloppe vitrée, et peut donc empêcher la baisse de la température de surface des façades vitrées. Ces résultats indiquent que les variations des valeurs MRT sont fortement corrélées aux orientations des WFR et aux façades vitrées, ce qui, avec un traitement adéquat, pourrait compenser significativement les effets d'ombrage, de type de vitrage et de conditions extérieures.

L'étude de sensibilité réalisée permet de développer des méta-modèles pour la consommation d'énergie de chauffage et des MRT. Ces méta-modèles sont ensuite validés à l'aide des deux approches graphiques résiduelles. Les courbes de réponse résiduelle en fonction des réponses théoriques montrent des structures moins structurées, et les courbes de probabilité normales que les erreurs résiduelles ont un caractère linéaire, ce qui confirme la validité des modèles. Enfin, une optimisation basée sur l'approche de la fonction de désirabilité est réalisée en utilisant le méta-modèle obtenu pour trouver une conception optimale qui compense simultanément les valeurs élevées de PMV et permet de réaliser des économies d'énergie. Dans un premier temps, l'objectif de l'optimisation est de

minimiser la consommation d'énergie tout en maintenant les valeurs PMV dans l'intervalle de confort acceptable de [-0,5 ; +0,5]. L'étude d'optimisation a montré que, pour réaliser un compromis entre les économies d'énergie et le confort thermique, l'humidité relative et la vitesse de l'air doivent varier dans les intervalles [40 %, 55 %] et [0,15 $m.s^{-1}$, 0,235 $m.s^{-1}$] respectivement. En outre, la configuration de l'enveloppe de la pièce doit garantir que le MRT se situe dans l'intervalle [17.3 °C, 21.1 °C]. Le méta-modèle du MRT est également optimisé afin de maintenir les valeurs dans l'intervalle souhaité Les résultats indiquent que la valeur D maximale de 0,995 est fournie lorsque la pièce est orientée vers le sud-est, équipée d'un système d'ombrage interne, le système de vitrage est triple à faible émissivité et le WFR est réduit au minimum (16 %). Les résultats obtenus suggèrent que l'application de ces paramètres à l'étude de cas permettra d'obtenir des valeurs de MRT dans l'intervalle [19.1 °C, 21 °C].

Après avoir identifié les paramètres critiques affectant le MRT et la consommation d'énergie dans l'étude de cas présumé et avoir trouvé les meilleures solutions pour parvenir à un compromis entre économie d'énergie et confort thermique, une étude comparative est réalisée entre le cas optimisé à confort thermique contrôlé, le cas de base à confort contrôlé et le cas conventionnel contrôlé. Les résultats ont indiqué que les deux cas optimisés offrent un confort thermique équivalent, avec un léger avantage de la régulation thermostatique, les valeurs de PMV tendant plus vers zéro (Figure 9). Cependant, la régulation basé sur l'indice PMV a permis de réduire d'environ 10 % la consommation d'énergie de chauffage par rapport à la régulation thermostatique. En somme, la régulation basé sur le PMV exige : (1) une surveillance continue pour calculer la température de consigne, (2) un coût supplémentaire pour les appareils, et (3) elle doit être soumise à des incertitudes de mesure et à des erreurs de paramètres définies par l'utilisateur. Nous pouvons donc conclure que l'intégration du confort thermique des occupants dans la phase de conception des bâtiments économes en énergie dans le cas de la commande classique représente un pas important vers la réalisation de compromis entre économie d'énergie et confort thermique sans avoir recours à des stratégies avancées et complexes de régulation.

Les principales conclusions de ce travail de thèse sont les suivantes : (1) l'intégration du confort thermique des occupants dans la conception de bâtiments performants permet d'optimiser la conception des bâtiments pour le confort thermique et la consommation d'énergie de chauffage ; (2) la méta-modélisation de la relation entre confort thermique, consommation énergétique et paramètres de conception représente une processus simple et rapide pour intégrer le confort thermique des occupants dans la conception de bâtiments performants ; (3) l'intégration du confort thermique des occupants dans la conception de bâtiments à faible consommation énergétique pour une régulation thermostatique classique constitue une étape importante vers un compromis entre économie d'énergie et confort thermique sans pour autant mettre en place des stratégies avancées et complexes ; et (4) dans

le cas d'une grande surface vitrée, la régulation basés sur le PMV représente une bonne approche pour une meilleure performance énergétique.

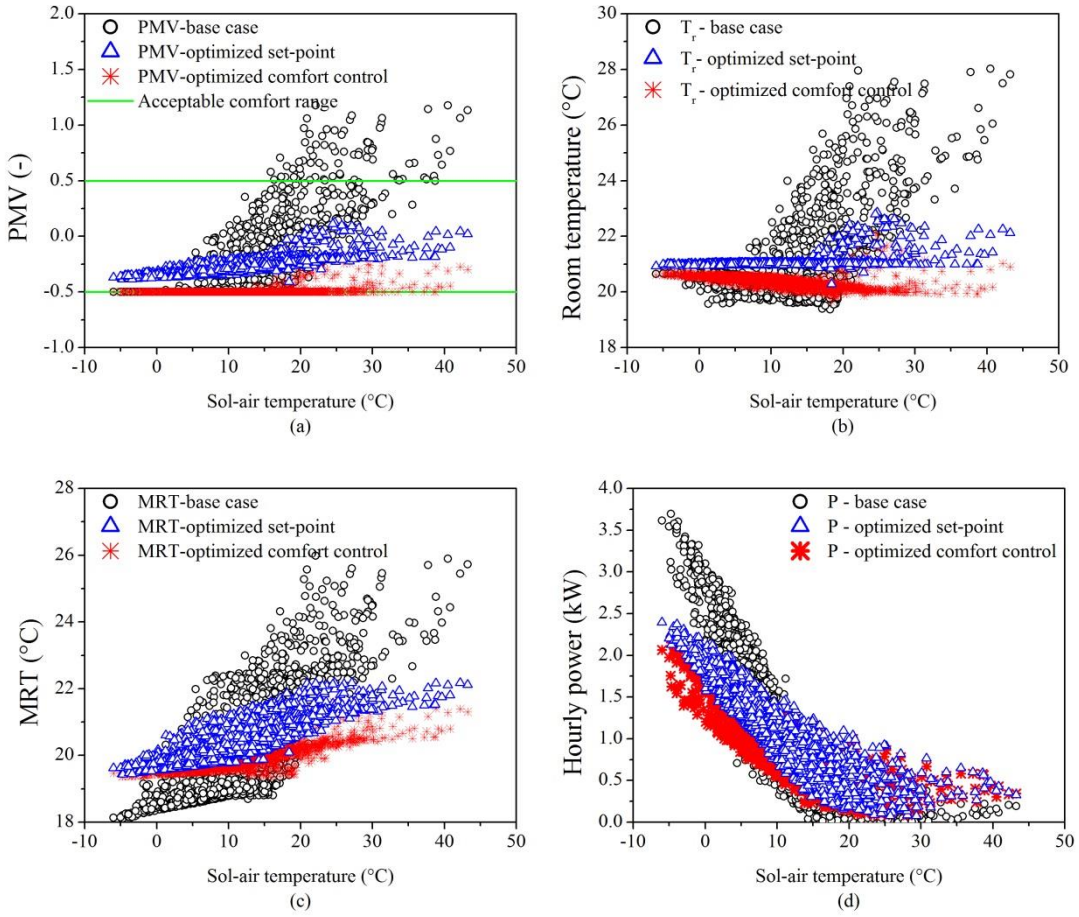

Figure 9 : Valeurs horaires numériques de (a) l'indice PMV, (b) la température ambiante, (c) MRT et (d) la puissance horaire de l'énergie de chauffage obtenue à partir du modèle Dymola® validé pour les trois cas.

L'approche proposée a été appliquée à une seule étude de cas avec une mise en jeu de peu de paramètres et de variables de réponse. Cela représente une des limites de ce travail de thèse. Par conséquent, les travaux futurs auront pour objectif d'augmenter le nombre de paramètres et de variables de réponse en considérant simultanément plusieurs cas d'étude et en appliquant l'approche proposée à d'autres typologies de bâtiments. La technique du DoE pourrait aider à réduire considérablement le nombre de simulations en appliquant différents types de plans expérimentaux tels que le plan factoriel fractionnaire. De plus, en raison de son impact sur la consommation d'énergie et le confort thermique, l'élaboration d'un modèle qui prédit le niveau d'habillement en fonction des conditions climatiques extérieures (plutôt qu'en supposant une valeur fixe) permettrait l'intégration du niveau d'activité des occupants dans le processus de conception des bâtiments. Enfin, la mise en place de cette méthodologie permettant l'utilisation combinée de la simulation dynamique, du DoE et de

l'approche par fonction de désirabilité pourrait être un outil d’aide à la décision à destination des ingénieurs du bâtiment.

Introduction

Motivation and Background

The building sector is one of the largest energy end-use sectors, accounting for 44.5% of the total energy consumption in France [2], 40% in Europe [3,4] and the USA [4]. This concern has led to the development of different strategies, concepts, policies, standards and regulations that aim to promote sustainable development in the building, such as low energy consumption buildings and zero energy buildings [6]. These concepts are based on improving the building envelope and using high-efficiency equipment as well as renewable energy resources [58,87]. Similarly to other developed countries, French authorities have established the so-called Thermal Regulation 2012 (i.e. Réglementation Thermique 2012), which defines performance standards of buildings. This regulation is an ambitious step towards promoting green buildings since it plans to divide by three the energy consumption of new buildings starting from the end of the year 2012 [7]. To achieve the energy performance levels stated in the RT 2012, a special attention is required in the selection of the "elements" constituting the building, such as reducing heat loss by improving the thermal insulation of the envelope [8,9], minimize thermal bridges, choose ventilation system that limits heat loss through air exchange, etc.

On the other hand, the primary objective of buildings must be to provide a comfortable environment for the people, since they spend 80-90% of the day indoors [10]. In addition, inappropriate indoor thermal comfort leads to lower work efficiency, higher possibility of personal errors, and an indirect effect on the energy consumption of the buildings [11]. Therefore, it is necessary to design low energy buildings in order to fulfill a tradeoff between energy-saving and occupants' comfort [12]. Thermal comfort is defined as "that condition of mind which expresses satisfaction with the thermal environment" [20,26]. Among all the standard thermal comfort indices [23], Fanger's [15] Predicted Mean Vote (PMV) and Percentage of Persons Dissatisfied (PPD) are the most applicable indices that can be used to evaluate the thermal comfort within an air-conditioned space and to quantify its value [18].

In spite of its importance, thermal comfort has not been considered in the control of the HVAC system set-point until recently. In fact, the majority of building standards recommend a static indoor air temperature, leading building designer and experts to design buildings and evaluate their thermal behavior based on a fixed indoor air temperature, while in most cases the indoor environment is assumed uniform, which means that the mean radiant temperature is equal to the air temperature. This assumption could lead to a false estimation of occupants' thermal comfort, mainly in buildings with extensive glazed areas.

In recent years, glass façades and extensive glazing areas are becoming more popular for office, public and educational buildings due to their aesthetic appearance as well as because of users' requirements of higher light transmittance and better view [43]. However, poorly designed glass façades hugely affect occupants' thermal comfort, because of the large hot surfaces resulting from dissipated solar radiation [40]. For instance, high intensity solar radiation leads to an increase in the interior surface temperature of the glass façade, which leads to an increase in the mean radiant temperature (MRT) and ultimately occupants' thermal comfort [40]. Thus, glass façade design in energy-efficient buildings needs proper planning in order to fulfill its nature of providing natural lighting and external view while keeping a balance between thermal comfort and energy performance of the building.

For this reason, researchers in building domain are tending toward integrating new control strategies that take into consideration the changes in environmental conditions to regulate the indoor temperature for thermal comfort. This shift towards integrating occupants' thermal comfort in the control of the indoor environment, leads to further requirements of adequate monitoring devices and calculations to determine the required temperature. In addition, the majority of the proposed approaches are based on artificial intelligence, thus implementing them in the early stage of building design leads to more complexity in the design process. Therefore, better comprehension and integration of occupants' thermal comfort into the design of buildings, especially in the very early phases, could be an essential step towards achieving a trade-off between energy-savings and thermal comfort.

Objectives and research questions

The objective of this research work is to formulate the relationship between occupants' thermal comfort, heating energy consumption and building design parameters, in order to integrate occupants' thermal comfort in the design of energy-efficient buildings. The aims intended through this formulation are:

- First, to understand the relationship between energy performance, thermal comfort, and design factors.
- Second, to provide realistic and accurate predictions of energy consumption and thermal comfort throughout the design process.
- Third, to be able to identify the parameters and interactions between parameters those considerably affect the design objectives in order to achieve an optimal design.

The review of the literature at the beginning of the thesis allowed us to formulate one major (Q.1) and two minor (Q.1.1 and Q.1.2) research questions that are outlined below:

Q.1: Is it possible to design energy-efficient buildings so that a tradeoff between energy-saving and occupants' comfort is fulfilled?

In the aim of reducing energy consumption, most standards and regulations tend toward decreasing and increasing heating and cooling set-points, respectively. This act could encourage the efficient use of energy and reduce environmental risks that result from excessive energy consumption. However, thermal comfort, which represents the primary objective of a building, is not a function of room temperature only. On the other hand, advanced control strategies are complex to investigate in the early stages of building design; also it requires continuous monitoring of the environment, which could lead to additional costs. Thus, integrating occupants' thermal comfort in the design of energy-efficient buildings may represent an important step towards achieving a trade-off between energy-savings and thermal comfort.

Q.1.1: How to integrate occupants' thermal comfort in the design of energy efficient buildings?

Thermal comfort can vary dramatically between different building types. This variation is due to the difference in occupants' related parameters, as well as building design which leads to variations in the environmental parameters, namely radiant temperature. Formulating the relationship between thermal comfort, energy consumption, and related design parameters is thus an important step towards integrating occupant thermal comfort in the design of energy efficient buildings.

Q.1.2: What are the advantages of integrating occupants' thermal comfort in the early design stage of energy efficient buildings?

Advanced control strategies are complex to integrate into the design stage of the building. They are also subject to measurements and user-defined parameters errors. Integrating occupants' comfort in the design phase of building with adequate analysis of the effects of significantly contributing factors, such as climatic conditions, could lead to optimized design for both thermal comfort and energy consumption. As a result, it may lead to suppressing the need for advanced and complicated control strategies.

Research outcomes

In this work, we adopt a research methodology to formulate the relationship between occupants' thermal comfort, energy consumption, and design parameters, in order to integrate occupants' thermal comfort in the design of energy-efficient buildings. The methodology is based on the combined use of numerical simulations, the Design of Experiments (DoE) technique and the desirability function approach. Numerical simulations help in extending the investigations with low additional costs and less time. In addition, it facilitates the assessment of new control strategies since no additional costs

are added for the installations and experimentations. Moreover, the combined use of numerical simulations and DoE leads to the development of meta-models for the prediction of thermal comfort conditions and heating energy consumption. These meta-models are then used to perform a sensitivity analysis in order to identify the critical parameters affecting thermal comfort and energy consumption. Finally, the obtained meta-models are used to determine a set of optimal solutions using the desirability function approach.

The proposed method is applied to a real case study, particularly a part of low energy consumption building located in Troyes, France, after subjectively assessing occupants' thermal comfort using a survey questionnaire [88]. First, a numerical model using an object-oriented modeling tool based on the *Modelica* approach is developed. The numerical model is then validated via a comparative study between simulation results and objective measurements regarding room temperature and relative humidity [89]. The validated model is then used to assess occupants' thermal comfort in the deemed case study [90]. In addition, the case study was considered to investigate and analyze the effect of integrating occupants' thermal comfort in the design of energy-efficient buildings. For the analysis, the developed and validated numerical model is used. DoE technique is then employed to determine the critical parameters affecting thermal comfort, as well as to develop meta-modeling relationships between design factors and occupants' thermal comfort. The developed meta-models are then used to determine a set of optimal solutions by performing a simultaneous optimization of building design based on the desirability function approach [88]. Furthermore, a thermal comfort based control approach is implemented in the developed model to investigate the energy saving potential of integrating occupants' thermal comfort in the control scheme of the indoor environment [91,92]. The sensitivity of heating energy consumption in comfort controlled space is then evaluated using the DoE approach. A comparative study among all the investigated cases is then performed. This enables highlighting the advantage of integrating thermal comfort in the design of energy-efficient buildings. A generalized framework for integrating occupant thermal comfort into the design process of energy-efficient buildings is proposed.

Thesis structure

In order to achieve the overall purpose of this research study, the thesis comprises five chapters as well as an introduction and general conclusions and perspectives, described as follow:

- **Introduction** summaries the motivation and background of this research work, the objective, and the outcomes.

- **Chapter 1** demonstrates a comprehensive literature review followed by identifying some research gaps.

- **Chapter 2** details the design framework and the adopted research methodology after presenting its theoretical basis.

- **Chapter 3** justifies and describes the case study used in this research work as well as the subjective assessment of thermal comfort. In addition, the chapter designates the development of building simulation model and its validation criteria. The validated model is then used to extend the investigations.

- **Chapter 4** presents a sensitivity study based on the DoE technique; the aim is to build knowledge on the relationship between design parameters and thermal comfort. This permits identifying the main parameters affecting thermal comfort within the studied case as well as to develop meta-modeling relationships between thermal comfort index and design parameters. These meta-models are then used to integrate occupants' thermal comfort in the design process of building.

- **Chapter 5** experiments the employment of thermal comfort based control strategy in the developed model. The aim is to evaluate the added value of integrating occupants' thermal comfort in the design process by comparing the proposed approach with another method that integrates occupants' thermal comfort in the control of the indoor environment. For this, an analysis of the impact of using the last on energy consumption and thermal comfort is carried out. Finally, the chapter presents a sensitivity study to identify the key parameters affecting heating energy consumption in a comfort controlled space in order to optimize building design for a trade-off between energy-savings and thermal comfort.

- **General conclusions and perspectives** summarize the main findings of the present research work demonstrated in this thesis and outline the potential for future investigations in this field.

Chapter 1: Literature review

1.1 Energy, Economy and environment context

According to the International Energy Agency (IEA) organization [93], world total primary energy supply (TPES) increased by almost 2.5 times between 1971 and 2016 from nearly 5489 Mtoe (Million Tons of Oil Equivalent) in 1971 to about 13760 Mtoe in 2016 (Figure 1-1). In 2016, fossil fuels (coal, natural gas, and oil) accounted for 81% of the global TPES. Oil remains the largest energy source at a global level, accounting for 31.9 % of global needs, followed by coal (27.11 %) and natural gas (22.06 %). Nuclear power and renewable energies meet about 4.94 % and 4.18 %, respectively, of the total demand. Between 1971 and 2016, the share of oil has fallen by 12.5%, in favor of natural gas (+5.7 %), nuclear power (+4.94 %) and renewable energies (+2.29 %). These statistics show the strong global dependence on fossil fuels even though they are responsible for a dangerous climatic change for the planet. Furthermore, the supply of these resources is subject to high uncertainties and can be disturbed very quickly by natural events (the exhaustion of oil in 50 years) or technical (industrial disaster), but also geopolitics (political instability in the Middle East region for example).

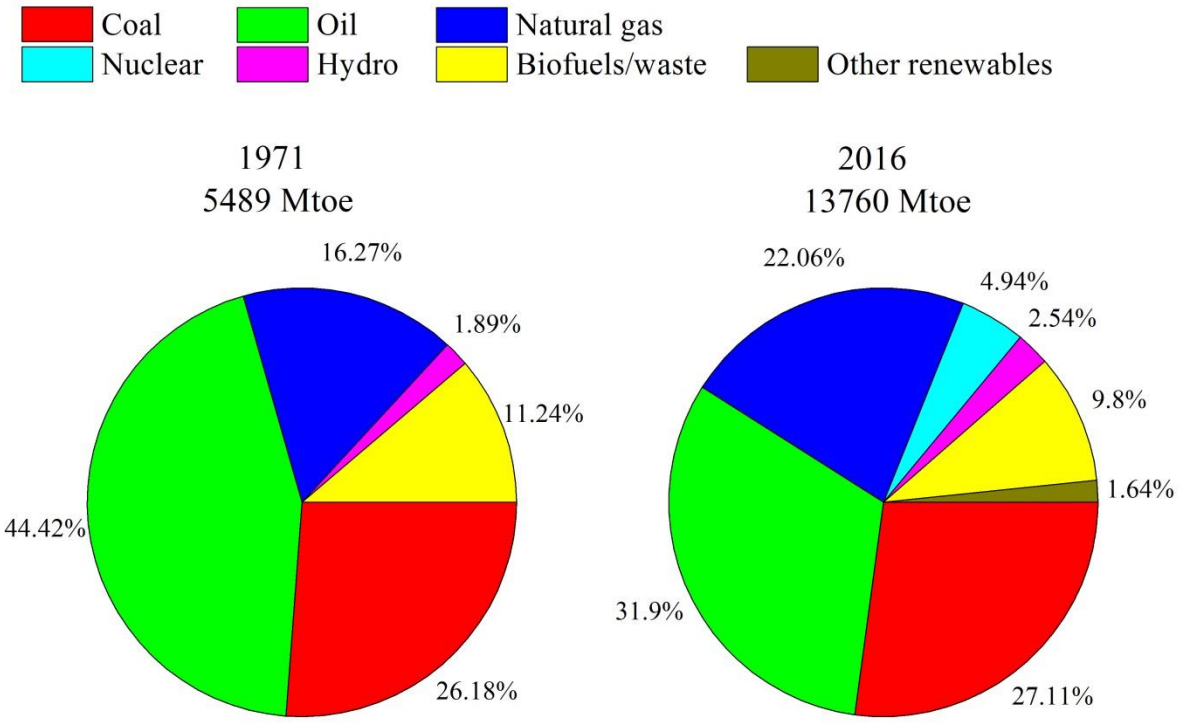

Figure 1-1: World total primary energy supply (TPES) between 1971 and 2016 [93].

Regarding the economic growth, according to the statistics of the World Bank [94], the Gross Domestic Product (GDP) has always increased or stagnated over the years since 1960, except during the financial crisis in 2009 and 2015. In these years, the GDP worldwide dropped by 5.28 % and 5.41 %, respectively, compared to the previous year. These delays were quickly caught up in 2010 and 2017, correspondingly, as shown in Figure 1-2. The global GDP growth has been accompanied by carbon dioxide (CO_2) emissions. These emissions increased by almost 2.3 times from nearly 15.3 billion tons CO_2 in 1971 to about 36.1 billion tons CO_2 in 2014 [94]. The increasing trend of CO_2 emissions related to energy leads to a 6 °C rise in the average temperature by 2100 [95], thus causing very dangerous climatic phenomena (flood, drought, etc.). Indeed, it is urgently necessary to take measures to adjust the energy and environmental balance to the configuration for each economic sector.

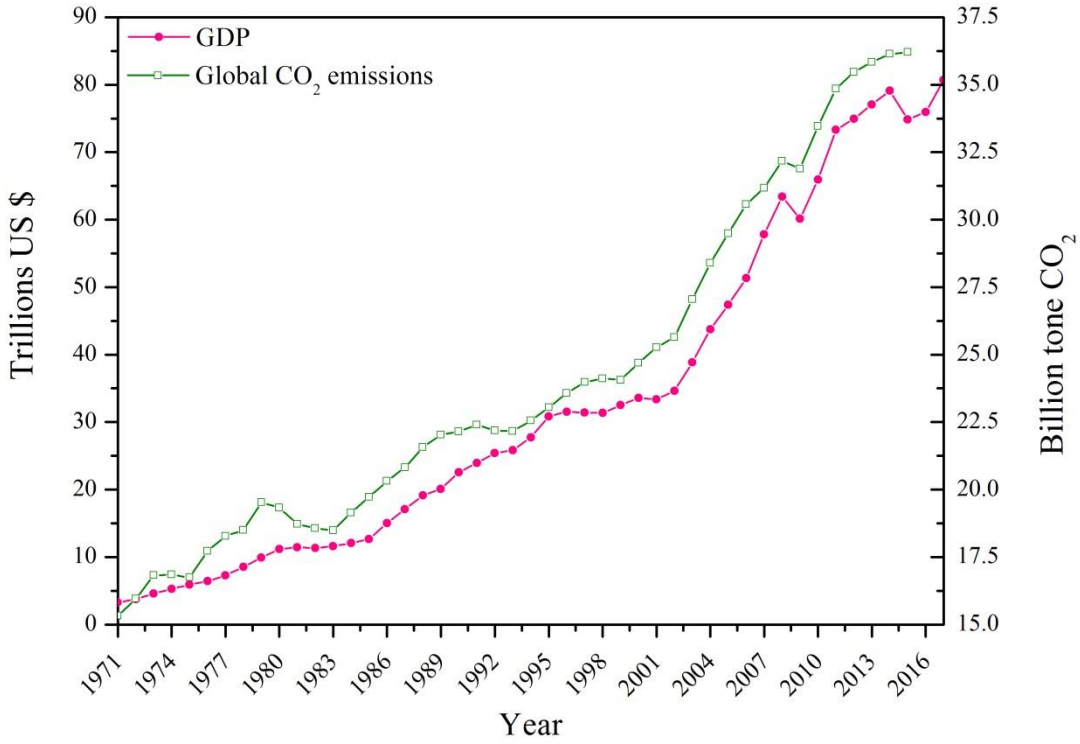

Figure 1-2: Global GDP growth and CO_2 emissions in trillion dollars and billion tone CO_2 equivalent [94].

In this regard, the United Nations Framework Convention on Climate Change (UNFCCC), the first international treaty aiming at preventing dangerous human interference with the climate system, was adopted in 1992 in Rio de Janeiro [96]. Then, the Kyoto Protocol was agreed in 1997, the first outcome of international negotiations on climate, and entered into force in 2005. This Protocol aims to reduce greenhouse gas (GHG) emissions by almost 5% between 2008 and 2012 compared to 1990

levels. In 2011, at COP17 in South Africa, Parties, representing 13% of global emissions in 2010, agreed to continue the Protocol for a second period of commitment from 2013 to 2020 [96]. Later, in December 2015 at COP21 in Paris, the Paris Agreement was approved by the UNFCCC and entered into force on November 2016. The Agreement sets a global objective of long-term GHG emissions reductions but gives countries flexibility in determining their own climate commitments [96].

1.2 Building sector

The sectorial break-down of global energy consumption is shown in Figure 1-3 [1]. The buildings sector, residential and commercial, is responsible for 35% of global final energy consumption in front of transport and industry that consume respectively 33% and 29% [1]. Progress towards sustainable buildings is advancing, but improvements are still not keeping up with a growing buildings sector and rising demand for energy services. In addition, the buildings sector is also responsible for 19 % of greenhouse gas emissions worldwide [5]. It is ranked ahead of the transport sector (14%), the energy sector (11%) and the waste treatment sector (3%). The industry remains the most emitting sector of greenhouse gas (29%) followed by the Land Use, Land Use Change and Forestry (LULUCF) sector which is responsible for 24% (Figure 1-4).

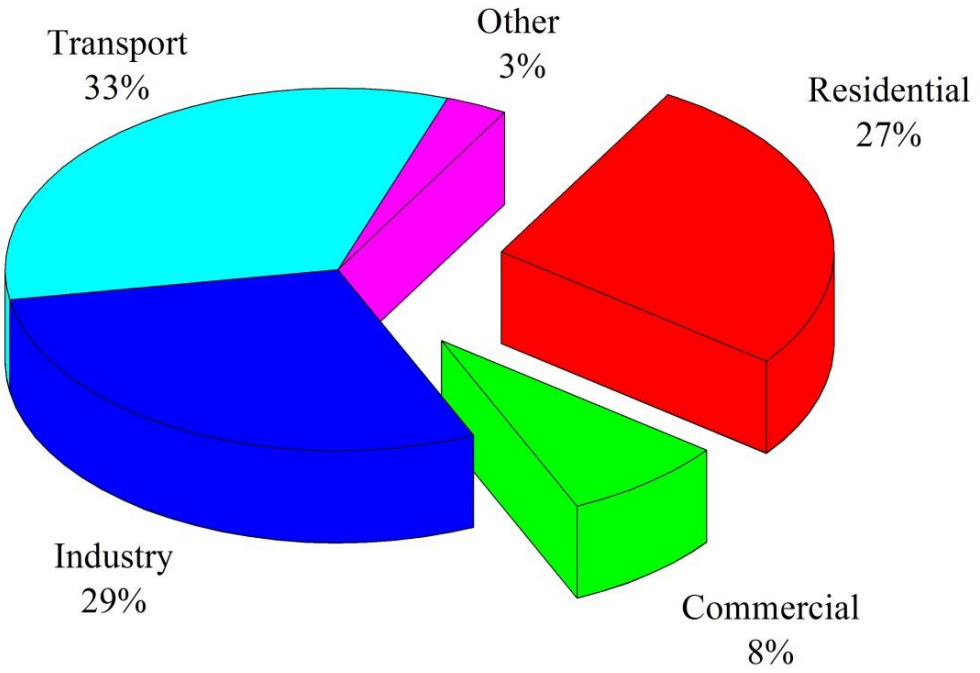

Figure 1-3 : Global energy consumption by sector in 2015 [1].

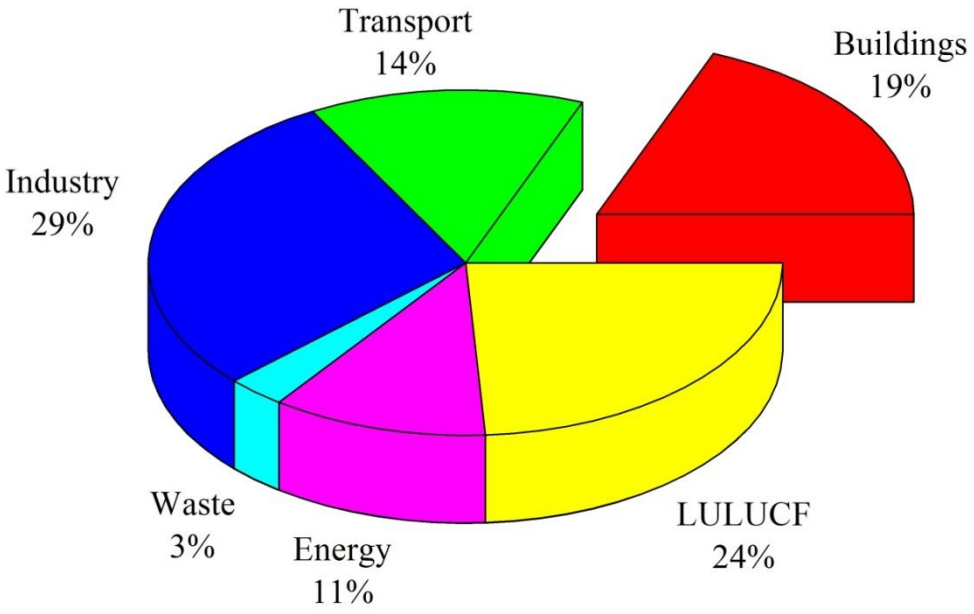

Figure 1-4 : Breakdown of global GHG emissions by sector in 2010 [5].

The break-down of final energy consumption by end-use in the building sector is demonstrated in Figure 1-5. HVAC systems account for about 34% to 40% of the total energy use in buildings (in residential and commercial buildings, respectively) [97]. Domestic hot water denotes 24% in residential buildings and 12% in commercial buildings and the remaining total energy use is distributed among all other end-uses. However, these percentages may hugely differ from one region to another, for example in EU-28 energy use in the residential sector is mainly consumed by space heating (68.4%) followed by lighting and appliances (14.1%) [98].

In recent years, a number of standards and regulations that aim to promote sustainable development in the building sector have been established worldwide. For instance, French authorities have established the so-called Thermal Regulation 2012 (i.e. Réglementation Thermique 2012), which defines performance standards of buildings. This regulation is an ambitious step towards promoting green buildings since it plans to divide by three the energy consumption of new buildings starting from the end of the year 2012. The regulation provides a better understanding of the steps taken by French authorities through the knowledge of the elements concerned by their requirements. To achieve the energy performance levels stated in the RT 2012, a special attention is required in the selection of the "elements" constituting the building, such as reducing heat loss by improving the thermal insulation of the envelope [8,9], minimize thermal bridges, choose a system of ventilation that limits heat loss through air exchange, etc.

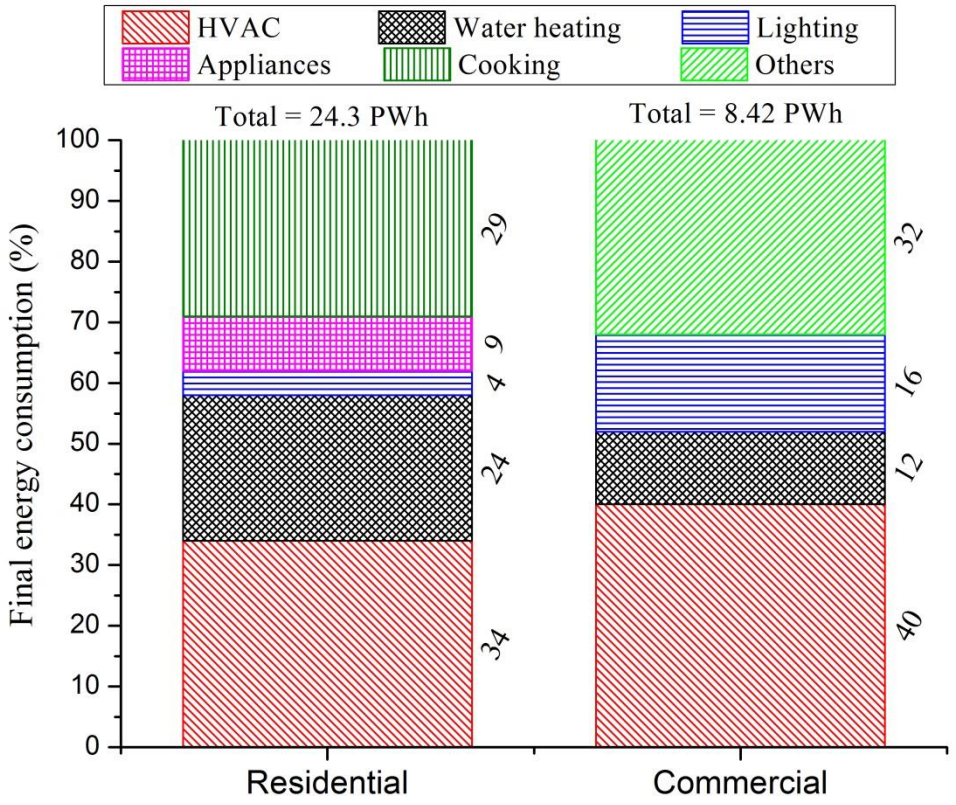

Figure 1-5: Final building energy consumption in the world by end-use in 2010 [97].

In addition, energy-savings could also be achieved by substituting conventional energy equipment systems with energy efficient equipment. Such as the use of condensation boilers for heating [99], solar thermal panels for the production of the domestic hot water [100,101], dual flow ventilation systems with high-efficiency heat recovery system [102] or using the Canadian wells. These choices represent promising alternatives that aim at helping designers and engineers to attain energy-efficient buildings. Therefore, promoting energy-efficient buildings requires the integration of improved building elements as well as energy efficient systems.

On the other hand, the primary objective of buildings must be to provide a comfortable environment for the people, since they spend 80-90% of the day indoors [10]. Moreover, inappropriate indoor thermal comfort leads to lower work efficiency, higher possibility of personal errors, and an indirect effect on the energy consumption of the buildings [11]. Therefore, the improvement of the energy performance of buildings must take into account thermal comfort alongside energy-savings measures, and as a result, it is necessary to design energy-efficient buildings so that a trade-off between energy-savings and occupants' thermal comfort is fulfilled. The following section presents the theory of thermal comfort and the widely used indices to evaluate thermal comfort in air-conditioned buildings.

1.3 Thermal comfort definition and its concept

Over the last decades, the terminology of thermal comfort has evolved. Initially, it was limited to physiological factors. It evolved then to include physical and psychological aspects. Thermal comfort has been defined by Givoni as "*the absence of irritation and discomfort due to heat or cold, and as a state involving pleasantness*" [13]. Hensen defined it as "*a state in which there are no driving impulses to correct the environment by the behavior"* [14]. The American Society of Heating, Refrigerating and Air-Conditioning Engineers (ASHRAE) defined it as "*the condition of the mind in which satisfaction is expressed with the thermal environment*" [16].

The complex interaction between humans and their environment has led to numerous research studies from different disciplines; physiologists, psychologists, social scientists, environmental engineers and physicists [103]. Each discipline has its own approach to defining thermal comfort. Thus, human thermal comfort can be perceived as a comprehensive context, since it is based on the human subjective perception of a number of physiological, psychological, and physical factors.

1.3.1 Physiological factors

Physiological factors represent the first thermal perception of a human due to the nervous sensors. They affect the thermal sensation of the human and are considered the first reaction to restore the human body preferred thermal conditions. These factors are the human thermoregulation system, state of health, metabolic rate, gender, age, and food intake. Human thermoregulation differs from one person to another and depends on other physiological factors. The thermoregulatory center keeps the body temperature in its normal range (37 °C +/- 1°C). Once the body temperature changes, the thermoregulatory center reacts to restore the heat balance. Regarding the age effect on thermal comfort, studies indicated that the thermal preference of older people does not significantly differ from the thermal preference of younger people since the lower metabolic rate of older people was found to be compensated by lower evaporative loss [104]. While in practice, elderly people prefer a higher indoor temperature level due to the lower activity level [104]. The effect of gender difference was also studied in the literature, but diverse results were obtained. Some studies revealed that the effect of gender difference is small and insignificant in terms of thermal sensations [104–106]. On the other hand, several laboratories and field studies have found that females express more dissatisfaction than males in the same thermal environments [107–109]. Very few studies have found males to be more dissatisfied than females [110]. However, most studies found no significant difference in neutral temperatures between the genders [111]. It is indicated that females have a greater need for adaptive actions than males, and should primarily be used as subjects when examining indoor thermal comfort requirements [111].

1.3.2 Psychological factors

Psychology is the scientific study of the human mind and its behavior. The impact of Psychological factors on thermal comfort has been studied by a number of researchers in the last few decades [105,112]. The main results show that occupants tend to interact with their environment or change their behavior when they feel cold or hot. These behaviors include, but not limited to, changing their clothing or activity level, opening windows, adjusting shading devices, moving to different rooms, and consuming cold or hot drinks and food [112]. In addition, Psycho-social and Psychophysical factors influence the thermal sensation of occupants. People in different countries have developed several techniques for adapting to the climate; each technique could be unsuitable to other countries because of climatic and socio-cultural factors. In this regard, Fountain et al. [113] mentioned that people's sensations and thermal preferences could be influenced by the culture and climate associated with expectation and thermal adaptation.

1.3.3 Physical factors

Physical factors are considered the most important factors in human thermal comfort. These factors are the most studied in the field. They can be categorized into three groups; heat balance of the body, personal parameters, and environmental ambient parameters. Knowing that the heat balance of the body is affected mainly by the personal and ambient parameters [18].

- The ***heat balance of the human body*** starts with two essential initial conditions to maintain the thermal comfort: 1) a neutral thermal sensation must be obtained from the combination of skin temperature and full body and 2) in a full body energy balance, the amount of heat produced by metabolism must be equal to that lost to the atmosphere (steady state). The thermal interaction between the human body and the surrounding environment is illustrated in Figure 1-6.

The human body produces energy by metabolism. This energy is the so-called metabolic rate (M). It comprises both the metabolic rate required for the person's activity and the metabolic rate required for shivering. The external work (W) done by muscles may consume a portion of this energy. Then the net heat production (M-W) in the human body is either stored (S), or dissipated to the surrounding environment through skin surface (q_{sk}) and respiratory tract (q_{res}). Therefore, the heat balance for a human body is [114]:

$$M - W = q_{sk} + q_{res} + S = (C + R + E_{sk}) + (C_{res} + E_{res}) + (S_{sk} + S_{cr}) \quad (1.1)$$

where, C $(W.m^{-2})$ and R $(W.m^{-2})$ are respectively, the convective and the radiative heat losses from the clothed body, $E_{sk}(W.m^{-2})$ is the evaporative heat loss from the skin, C_{res} $(W.m^{-2})$ is the convective heat loss from respiration, E_{res} $(W.m^{-2})$ is the evaporative heat loss from respiration, and S_{sk} $(W.m^{-2})$ and $S_{cr}(W.m^{-2})$ are successively the rate of heat storage in the skin and core compartments. The detailed mathematical formulation of each parameter is discussed in [14].

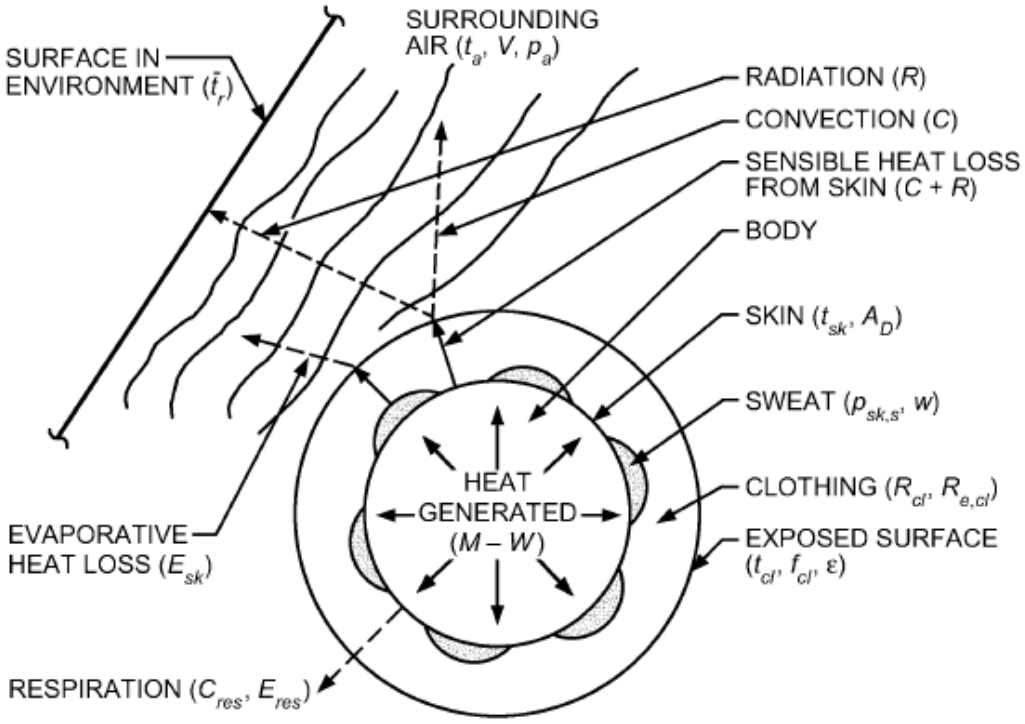

Figure 1-6: The thermal interaction between a human body and its environment [114].

In addition, quantitative information on calculating the heat exchange between the human body and its surrounding environment is provided in [15]. A detailed description of the mathematical formulation of the energy balance equation and several terms of the heat exchange are presented in the ASHRAE Handbook of Fundamentals [115].

- ***Personal parameters*** represent the characteristics of the occupants. These parameters are defined as follow:
  - **Clothing insulation** (I_{cl})**,** that is the thermal resistance of clothing the occupant is wearing, it is expressed in *clo* units (1 *clo* = 155 $m^2.K.W^{-1}$). It is also defined as "the thermal resistance layer that controls the level of heat loss from the body to the surrounding environment [18].
  - **Metabolic heat rate, or activity level** (M), that is the net heat output from the human body, or the rate of transformation of chemical energy into heat and mechanical work by activities within the body. It is expressed in *met* units (1 met = 58.2 $W.m^{-2}$). The

value of the metabolic rate is always positive since the body always produces heat; it is ranged between 45 $W.m^{-2}$, representing a sleeping person, and 500 $W.m^{-2}$, representing a running person.

- ***Environmental/Ambient parameters*** represent the characteristics of the building indoor environment such as air velocity, relative humidity, and several temperature parameters. These parameters are defined as follows:

  - ***Air velocity*** (v_a) [$m.s^{-1}$] is the rate of air movement to a given distance over time. Air velocity affects the convective heat loss from the body. Air velocity within indoor environments is recommended to be less than 0.2 $m.s^{-1}$ [18].

  - ***Relative humidity*** (*RH)* [%] is the ratio of actual (measured) vapor pressure to saturated vapor pressure at the same temperature [17]. A detailed description of the mathematical formulation used to calculate the relative humidity is provided in references [17,18]. Different organizations suggested that RH must be in the range of [30 % – 70 %] to ensure occupant thermal comfort [79]. Numerous studies show that relative humidity is considered to affect the perception of indoor air quality [116], thermal comfort [15,117], and energy consumption [18]. In addition, it is indicated that the RH has a big influence on the thermal balance of the body at high metabolic rates, in hot environments, and under transient conditions [118].

  - ***Air (Dry bulb) temperature*** (T_a) is the temperature of the indoor air surrounding the body. It is measured using a dry bulb thermometer. It is an important factor in determining occupant thermal comfort since convection is responsible for two-fifths of the heat loss from the body. The recommended range of temperature is between 18 °C and 23 °C, and the temperature difference cannot exceed 1 °C in the occupied spaces [18].

  - ***Mean radiant temperature (MRT or T_{mr})*** is defined by ANSI/ASHRAE Standard 55-2010 as *"the temperature of a uniform, black enclosure that exchanges the same amount of thermal radiation with the occupant as the actual enclosure"* [19]. Regarding the human body, ISO defined it as *"the uniform temperature of an imaginary enclosure in which radiant heat transfer from the human body is equal to the radiant heat transfer in the actual non-uniform enclosure"* [20].

MRT is expressed as the weighted average of the surrounding surfaces temperatures in steady-state conditions as illustrated in Equation (1.2).

$$T_{mr} = \frac{\sum_i^n T_i \times S_i}{\sum_i^n S_i} \quad (1.2)$$

where T_{mr} is the mean radiant temperature, T_i is the temperature of surface i, S_i is the area of surface i, and n is the number of surrounding surfaces.

- ***Operative temperature (T_{op}):*** de Dear [21] defined the operative temperature as "*the uniform temperature of an imaginary black enclosure in which an occupant would exchange the same amount of heat by radiation and convection as in the actual non-uniform environment*". ASHRAE 55 and CEN EN 15251 standards use the operative temperature in the adaptive section to predict comfort temperature. It is not an empirical but a theoretical measure. It is expressed as the average of the mean radiant temperature and the air temperature weighted, respectively, by the radiative and the convective heat transfer coefficients [22]. The expression of the operative temperature is:

$$T_{op} = \frac{(T_{mr} \times h_r + T_a \times h_c)}{(h_r + h_c)} \quad (1.3)$$

where h_r (W.K^{-1}.m^{-2}) and h_c (W.K^{-1}.m^{-2}) are respectively the radiative and the convective heat transfer coefficients.

For an accurate evaluation, operative temperature has to be evaluated using Equation (1.3). However, ISO 7726 [119] suggests two simplified equations. The first equation is based on a weighted average of the mean radiant temperature and air temperature:

$$T_{op} = \alpha . T_a + (1 - \alpha) . T_{mr} \quad (1.4)$$

so that α is a coefficient determined as a function of the relative air velocity and equals to 0.5, 0.6 or 0.7 if the relative air velocity is respectively less than 0.2 m.s^{-1}, between 0.2 m.s^{-1} and 0.6 m.s^{-1}, or between 0.6 m.s^{-1}and 1.0 m.s^{-1}. Equation (1.4) is also reported in the standard ASHRAE 55 [16], but with the further restriction that the metabolic rate is in the range from 1 to 1.3 met, in addition to the absence of solar radiation.

The second equation is the arithmetic average between T_{mr} and T_a values (Equation (1.5)). It is recommended when the air velocity is less than 0.2 m.s^{-1} and the absolute difference between the MRT and air temperature is less than 4 °C ($v_a < 0.2\ m.s^{-1}$ and $|T_{mr} - T_a| < 4\ °C$) [120].

$$T_{op} = \frac{T_{mr} + T_a}{2} \quad (1.5)$$

Table 1-1 shows the optimum operative temperature, defined as *"the operative temperature that satisfies the greatest possible number of people at a given clothing and activity level"* [121], for the occupants engaged in light, sedentary activity (1.2 *met*) at 0.15 $m.s^{-1}$ air velocity and 50% relative humidity, and the ranges of the operative temperature values accepted by 80% and 90% of the occupants in buildings with central HVAC systems [121].

Table 1-1: Operative temperature for occupants in buildings with central HVAC systems [121].

Period	Clothing insulation $I_{cl}\ (clo)$	Optimum temperature $T_{opt}\ (°C)$	Operative temperature $T_{op}\ (°C)$ 80% accepted	90% accepted
winter	1.05	22.5	20.5 −24.5	21.3 −23.7
summer	0.65	23.5	21.5 −25.5	22.3 −24.7

1.3.4 PMV and PPD indices

The thermal comfort models have been categorized by the researchers into "static" and "adaptive" models [23,122]. The static model is an analytical model built on physical and physiological bases, by analyzing the balance between the produced and dissipated heat from the human body, under steady-state conditions occurring in uniform thermal environment, such as climate chambers [23]. The adaptive model is an empirical model that takes into consideration the psychological and behavioral responses of occupants under transient conditions in a non-uniform thermal environment using statistical analysis from field studies [123].

Among all the standard thermal comfort indices, more than 80 indices have been proposed [23], Fanger's Predicted Mean Vote (PMV) and Percentage of Persons Dissatisfied (PPD) are the most applicable indices that can be used to evaluate the thermal comfort within an air-conditioned space and to quantify its value [18]. PMV is used to evaluate the thermal comfort and is defined as "*the index that predicts the mean thermal sensation vote on a standard scale for a large group of persons for any given combination of the thermal environmental variables, activity and clothing levels*" [15].

Fanger [24] developed an empirical equation, based on the Fanger comfort equation for human body heat exchange [24], which makes it possible to calculate the PMV as a function of two occupants related parameters described as clothing insulation and metabolic rate and four environmental parameters noted as air temperature, mean radiant temperature (MRT), relative humidity, and air velocity. The model was developed through laboratory and climate chamber studies using the seven-point ASHRAE thermal sensation scale [19]. This scale represents the votes of a group of persons expressing the thermal sensation they feel in a given environment. The votes are defined by the so-

called Thermal Sensation Vote (TSV) [19]. The PMV represents the mean vote determined from the average of the TSV values [25]. The mathematical formulation used to calculate the PMV index is:

$$\begin{aligned}\mathrm{PMV} = {} & (0.303e^{-0.036M} + 0.028) \times [(\mathrm{M} - \mathrm{W}) - 3.05 \times 10^{-3}\{5733 - 6.99(\mathrm{M} - \\ & \mathrm{W}) - \mathrm{P_a}\} - 0.42\{(\mathrm{M} - \mathrm{W}) - 58.15\} - 1.7 \times 10^{-5}\mathrm{M}(5867 - \mathrm{P_a}) - 0.0014\mathrm{M}(34 - \\ & \mathrm{T_a}) - 3.96 \times 10^{-8}\mathrm{f_{cl}} \times \{(T_{cl})^4 - (T_{mr})^4\} - \mathrm{f_{cl}h_c}(\mathrm{T_{cl}} - \mathrm{T_a})]\end{aligned} \quad (1.6)$$

where M, W and P_a are the metabolic rate (W.m^{-2}), the external work (W.m^{-2}) and the partial vapor pressure (Pa), respectively, T_a, T_{cl} and T_{mr} represent the air temperature (K), the surface temperature of clothing (K) and the MRT (K), respectively, f_{cl} is the ratio of surface area of the body with clothes to the surface area of the naked body, and h_c is the convective heat transfer coefficient (W.m^{-2}.K^{-1}). The clothing surface temperature $\mathrm{T_{cl}}$ can be obtained by solving iteratively the following equation:

$$\mathrm{T_{cl}} = 35.7 - 0.028(\mathrm{M} - \mathrm{W}) - 0.155\mathrm{I_{cl}}\left[3.96 \times 10^{-8}\mathrm{f_{cl}}\left(\mathrm{T_{cl}^4} - \mathrm{T_{mr}^4}\right) + \mathrm{f_{cl}h_c}(\mathrm{T_{cl}} - \mathrm{T_a})\right] \quad (1.7)$$

The convective heat transfer coefficient is given by:

$$h_c = \begin{cases} 2.38(\mathrm{T_{cl}} - \mathrm{T_a})^{0.25} & \text{for } 2.38(\mathrm{T_{cl}} - \mathrm{T_a})^{0.25} > 12.1\sqrt{\mathrm{v_a}} \\ 12.1\sqrt{\mathrm{v_a}} & \text{for } 2.38(\mathrm{T_{cl}} - \mathrm{T_a})^{0.25} < 12.1\sqrt{\mathrm{v_a}} \end{cases} \quad (1.8)$$

The ratio of clothed surface area f_{cl} is expressed by:

$$\begin{cases} f_{cl} = 1.00 + 0.2I_{cl} & if\ I_{cl} \le 0.5clo \\ f_{cl} = 1.05 + 0.1I_{cl} & if\ I_{cl} > 0.5clo \end{cases} \quad (1.9)$$

PMV index has been adopted by various national and international standards, guidelines and researchers, such as, ISO 7730 [20], ASHRAE 55 [16,19,26], and CEN CR 1752 [27]. ISO 7730 recommends maintaining the PMV at 0 with a tolerance of 0.5 in order to ensure a comfortable indoor climate [20]. This recommendation leads to a maximum of 10% dissatisfaction in an indoor environment [20]. Occupants' thermal sensation is better if the PMV is closer to zero [18]. Humphreys [28] also addressed the 0.5 tolerance by confirming that the occupants in cold climates might prefer a sensation slightly warmer than neutral, while the people in hot climates might prefer a sensation slightly cooler than neutral. According to the Standard ISO 7730 [94], it is recommended to use the PMV index only for values between -2 and +2 and when the six main parameters are inside the intervals presented in Table 1-2 [20].

Table 1-2 : recommended ranges of the six main parameters in calculating the PMV index [20].

Parameter	M ($W.m^{-2}$)	I_{cl} (clo)	T_a (°C)	T_{mr} (°C)	v_a ($m.s^{-1}$)	Pa (Pa)
Min	46	0	10	10	0	0
Max	232	2	30	40	1	2700

Through the years, various studies have been conducted to investigate the validity of the PMV index. Some studies confirmed the validity and proved the strength of the model, while others criticized it [27]. The PMV model suggests that the optimal thermal sensation is neutral; however, Humphrey and Hancock [124] in their study concluded that the thermal neutrality does not necessarily correspond to the preferred thermal sensation. In addition, PMV accurately predicts occupants' thermal sensation in laboratory studies under sedentary activities and light clothing, while many discrepancies observed for higher activity levels and heavier clothing [125]. In addition, field studies suggested that the PMV model does not always accurately predict occupants' actual thermal sensation. This discrepancy is primarily due to measurement errors related to occupants' activity level and clothing insulation [126]. Van Hoof stated that the PMV index applies to healthy adults but not for children or elderly and disabled persons [27].

At the same time, there are many studies that confirm the validity of PMV for air-conditioned offices. Tse et al. [127] confirmed that the PMV model accurately represented the average thermal sensation of occupants of air-conditioned offices and that it was not affected by other human factors. Nasrollahi et al. [128] concluded that PMV is a valid index for use in Iranian air-conditioned buildings. Brager and de Dear [112] and Oseland [129] also justified the validity of the PMV model in air-conditioned environments. Whereas in the case of non-air-conditioned buildings, Han et al. [130] and Hong et al. [131] show that there is a difference between the PMV model and the actual thermal sensation declared by the occupants. In addition, Yang et al. [132] noted that the PMV model is not recommended for predicting the overall thermal comfort of the occupants in naturally ventilated buildings. Gilani et al. [133] show that for naturally ventilated buildings the PMV equation underestimates the thermal sensation by 13% in the summer season, and overestimates it by 35% in the winter season. It appears that the PMV model is more appropriate for predicting the thermal sensation of occupants in certain contexts.

Besides the PMV model, Fanger's introduced the so-called Predicted Percentage of Dissatisfied (PPD) model to compute the percentage of persons that are dissatisfied within their surrounding thermal environment. This index depends on the PMV value and its mathematical formulation is expressed in terms of the PMV index using the following equation:

$$PPD = 1 - 0.95\exp(-0.03353PMV^4 - 0.2179PMV^2). \quad (1.10)$$

It can be seen (Figure 1-7) that, even when the PMV index is 0, there are some individual cases of dissatisfaction with the level of temperature, although all are dressed in a similar way and that the level of activity is the same. This is due to some differences of approach in the evaluation of thermal comfort from one person to another. It is shown that at PMV = 0, a minimum rate of dissatisfied of 5% exists [134]. Recommended PMV-PPD criteria for the thermal well-being for mechanically heated and cooled buildings are illustrated in Table 1-3 and their applicability is described in

Table 1-4. The recommended steps for the assessment of the thermal environment are presented and discussed in [135]. Further, a brief summary of some thermal comfort standards is provided in Appendix A: Thermal comfort standards.

Table 1-3: Recommended categories and PPD-PMV for mechanically conditioned buildings [20,79].

Category	Thermal state of the body as a whole	
	PPD %	Predicted mean vote
I	<6	-0.2 < PMV < +0.2
II	<10	-0.5 < PMV < +0.5
III	<15	-0.7 < PMV < +0.7
IV	>15	PMV < -0.7; or PMV > +0.7

Table 1-4: Description of the applicability of thermal comfort categories [20,79].

Category	Explanation
I	High level of expectation and is recommended for spaces occupied by very sensitive and fragile persons with special requirements like handicapped, sick, very young children and elderly persons
II	Normal level of expectation and should be used for new buildings and renovations
III	An acceptable, moderate level of expectation and may be used for existing buildings
IV	Values outside the criteria for the above categories. This category should only be accepted for a limited part of the year

After presenting an extensive summary about the theory of thermal comfort and the widely used indices, PMV and PPD, to evaluate thermal comfort in air-conditioned buildings, one can observe that occupants' thermal comfort is more than just air temperature. However, most standards and regulations set up a fixed set-point temperature for the control of indoor air temperature. For instance, the thermal regulation in France has recommended that the set-point room temperature should be 19°C during the heating period [7]. This act was established to encourage efficient use of energy and to reduce environmental risks that result from excessive energy consumption. Although this represents good progress towards reducing heating energy use in buildings, it is still not accounting sufficiently for occupants' thermal comfort. This is because in reality, mainly in buildings with extensive glazing areas, this could lead to fluctuations in occupants' thermal comfort.

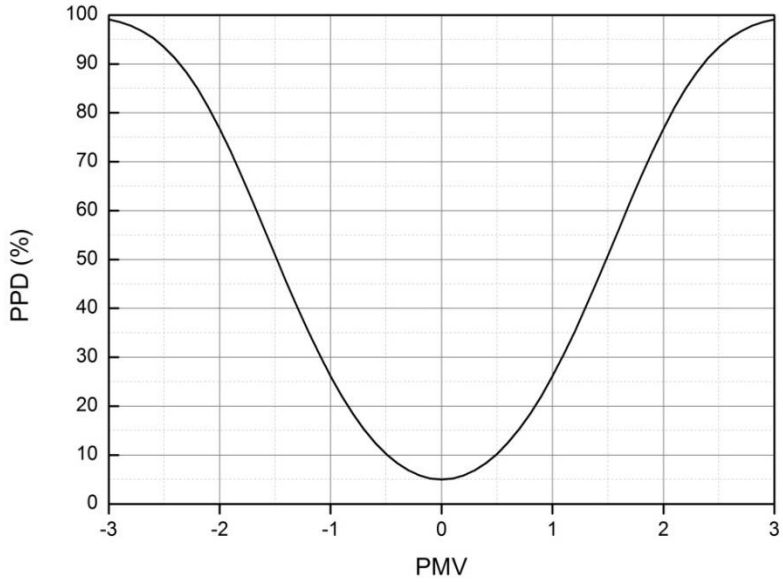

Figure 1-7 : Relationship PMV versus PPD.

For this reason, many research groups oriented their work towards the development of advanced building control strategies. This approach aims at maximizing energy savings with minimal retrofitting [29]. In the last two decades, two thermal comfort based control approaches have been proposed and investigated in the literature. One approach is based on PMV determination, where an advanced control scheme is used to adjust the controlled variable, such as room temperature and relative humidity, so that the user-defined PMV is maintained [11,35–39,136]. The other approach proposed by Kang et al. [40] is based on the inverse calculation of the PMV index and was rarely addressed in the literature [40,41,137]. This approach adjusts the set-point room temperature according to a user-defined PMV and changes in the indoor environmental parameters [40]. These approaches aim at maintaining consistent indoor thermal comfort, rather than static indoor air temperature. The following section presents a state of the art of PMV-based thermal comfort control approaches proposed and investigated in the literature.

1.4 PMV-based thermal comfort control

In an early study, Hamdi and Lachiver [30] proposed a new fuzzy-based HVAC control method that is based on the human thermal comfort sensation. Such a strategy aims at maintaining constant indoor thermal comfort, but not indoor air temperature. Kolokotsa et al. [11] presented and evaluated three control strategies, Fuzzy PID, fuzzy PD, and an adaptive fuzzy PD, for the adjustment and preservation of indoor air quality, visual and thermal comfort while, simultaneously, achieving energy-saving. Kolokotsa [31] applied and compared the performance of five fuzzy controllers (fuzzy P, fuzzy PID, fuzzy PI, fuzzy PD, and adaptive fuzzy PD) based on PMV index and other indoor air

quality parameters. Calvino et al. [32] investigated the performance of an adaptive fuzzy-PID controller based on the PMV as the driving index for the control procedure. Liang and Du [33] developed a direct neural network controller with the adoption of the PMV index as the control objective. Donaisky et al. [34] investigated two model-based predictive control algorithms based on the PMV index. The first uses PMV to generate a set-point signal, and the last uses PMV to compose the prediction model. Freire et al. [35] analyzed five model predictive control algorithms to optimize indoor air conditions with the focus on thermal comfort and/or energy savings. Some of the proposed algorithms were based on PMV index determination and the others were based on a comfort zone approach. Castilla et al. [36] carried out a comparison between several predictive control approaches. Ferreira et al. [37] formulated a model-based predictive control (MBPC) using the branch and bound method to control HVAC systems using the PMV index. Ruano et al. [38] proposed an improved-MBPC, based on the PMV index, for an existing HVAC system. Xu et al. [39] tested a novel building operational optimization approach based on the PMV index. Kang et al. [40] proposed the inverse calculation of the PMV index by using directly the measured parameters and PMV index formulation to adjust the set-point. The authors investigated the effect of such an approach on energy consumption and thermal comfort in a space with an extensive area of glass façades. They carried out a comparative study between the proposed thermal comfort-based control and conventional thermostatic control. Their study concluded that thermal comfort control could be more efficient than traditional thermostatic control. In addition, Hwang and Shu [41] investigated the energy saving potential of thermal comfort-based control under different envelope regulations. The results of the study demonstrated the advantage of using thermal comfort-based control, which could possibly achieve a reduction of about 20% of the cooling energy compared to conventional thermostatic control. Erakovic and Evans [42] assessed the thermal comfort-based control by conducting a comparative study with air temperature-based control using a CFD model of office space with an extensively glazed envelope. The results show that the investigated controller improved the thermal comfort levels, as well as prevents over-cooling. Energy savings resulted from the use of thermal comfort control could reach up to 48.6% depending on several factors. Although these studies show that the proposed thermal comfort-based control strategy provides the energy-saving effect as well as consistent thermal comfort, some investigations conclude that a PMV-based comfort control consumes energy as the thermostatic control to achieve an acceptable comfort range if the space is poorly designed [41]. On the contrary, if the space is well designed a PMV-based comfort control leads to energy savings. Thus, this finding leads us again toward the design problem.

One of the main issues in building design is the design of a glazed envelope [138], an adequate design is essential to ensure the occurrence of a uniform environment. This last is important because glass façades and extensive glassing areas have gained popularity in recent years due to their aesthetic appearance as well as because of users' requirements of higher light transmittance and better view

[43]. Building fenestration, particularly the window, allows the natural light to penetrate into the building, which provides occupants' visual comfort as well as biological benefits [44,45]. Thus, fenestration design needs proper planning in order to fulfill its nature of providing natural lighting and external view while keeping a balanced energy performance of the building.

In the last decade, some research works have revealed that highly glazed façades can offer a better behavior than conventional envelope fenestration, if designed carefully [139–141]. Contrarily, poorly designed glass façades vastly affect the occupants' thermal comfort, because of the large hot surfaces resulting from dissipated solar radiation. In addition, it leads to an increase in building energy consumption [41]. We hereafter present some of the studies that have been conducted to investigate the influence of glass façade design on building energy consumption [46–50] and thermal comfort [51–54], the proposed solution to achieve optimal design of glass façades and the resulting conclusions of each study.

1.5 Influence of glass façade design on energy consumption and thermal comfort

Poirazis et al. [47] carried out building energy simulations for an extensive amount of scenarios combining different glazing types and shading solutions for an office building with fully glazed facades. The main results of the study indicated that the buildings with fully glazed facades are likely to have higher energy consumption than buildings with conventional facades; low thermal transmittance of windows decreases the heating load and barely influences the cooling demand, while the g-value has a great impact on the cooling demand. In addition as the area of window increases as the impact of temperature set-points on the energy use decreases. Tzempelikos et al. [51] investigated the effect of changing glazing type and shading device on indoor thermal comfort and energy consumption in an office building with an extensive glazing area. The authors used a validated explicit finite-difference dynamic building thermal model that was previously developed by them [55]. The study concluded that both the thermal resistance and the solar transmittance of glazing have a profound effect on thermal comfort. Low insulating value with high transmittance reveals a great fluctuation in the indoor thermal environment. Conversely, windows with a high insulating value and low transmittance offer more comfortable conditions and less sensitivity to the outdoor climate. However, the low transmission may lead to higher heating demand due to the reduced solar gains. Thus it is noticeable that the appropriate fenestration represents a trade-off between energy consumption, thermal comfort, and daylighting needs. In a study carried out on an office building having highly glazed wall, located in Denmark, Winther et al. [56] found that the total energy demand of an office building could be reduced from 96 $kWh.m^{-2}$ per year to 73 $kWh.m^{-2}$ per year if a combination is done between a lowest possible glazing heat transfer coefficient, low solar heat gain coefficient, and automated lighting control. Besides, the demand varies between these two values if

different combinations are applied. Stavrakakis et al. [53] presented a novel computational method to optimize window design for thermal comfort in naturally ventilated buildings. The proposed methodology connects thermal comfort indices with architectural-design variables and a special optimization technique. The study found that as one of the openings' height increases, the thermal sensation is improved. Anderson and Luther [52] designed several glazing systems using two software tools and investigated their effect on improving the indoor thermal environment in a commercial office building. The proposed systems were also fabricated and the modeling results were validated experimentally. The main findings of the study indicated that shading screens could lead to improvements in thermal comfort and energy efficiency during the cooling period. However, it is not effective in preventing heat losses during cooling periods, thus leading to occupants' discomfort. In addition, the use of a triple-glazed window offers better insulating characteristics and would lead to greater stability in the indoor thermal environment. Thus increased satisfaction may be possibly achieved due to the reduced fluctuation in the thermal environment. Thalfeldt et al. [46] investigated numerous façade designs, including window configuration, window-to-wall ratio (WWR), wall insulation, and external shading, in nearly zero energy building. The study indicated that heating demand dominated the energy consumption of the building if conventional windows are applied. However, the performance improved significantly when improving the thermal properties of the window by applying quadruple (four glazing panes) and quintuple (five glazing panes) windows. Further, the study concluded that, from an energy point of view, the use of a quintuple window combined with external wall insulation of 390 mm and WWR of 60% for all facades yields the most energy-saving potential. However from an economic point of view, based on 20 years net present value calculation, the results indicated that the best energy performance was achieved with triple glazed windows combined with 200 mm of external wall insulation and a WWR of 37.5% for the north oriented facade and 23.9 % for the south, east and west oriented facades. Lee et al. [49] investigated the effect of window systems on the energy consumption of buildings in five typical Asian climates using regression analysis. The authors varied the glazing area from 0% to 100% WWR. The main finding of the study, concerning the glazing area, is that the WWR must be minimized except for the north facing opaque wall for two of the studied climates. Regarding the windows positioning, it was found that the placement of a window depends hugely on the climatic conditions; for example, the north-oriented window offers the highest advantage for total energy-savings in two of the studied climates but not in the others where the south-oriented has the greatest advantage. Jin and Overend [48] carried out a comparative study on 13 glazing types on the facade of a typical cellular office. The study indicated that high-performance glazing technologies, such as photovoltaic integrated glazing, offer significant improvements over opaque insulated walls and conventional insulated glazing windows, even for an extensively glazed envelope, in terms of both energy consumption and indoor environmental quality. Zomorodian and Tahsildoost [54] assessed the effect of window design on thermal and visual comfort using dynamic simulations in an educational

building. The results of the study suggested that solar-control coated glazing with low solar heat gain coefficient and high visual transmission could be an alternative solution to solar shadings. The role that the overhangs and louvers play in correcting the mechanism of over-dimensioned openings allows the building specialist to choose a wider range of windows dimensions. Even in low WWR, a window with a low heat transfer coefficient could lead to an overheating phenomenon in hot climates. In addition, some studies were performed in the residential sector [50,142]. Cheong et al. [142] evaluated the effect of changing the glazing system type on both thermal comfort and daylighting. The results indicated that improving the glazing type resulted in a 43% to 61% reduction in the cooling load, and electricity cost was reduced by a maximum of 24%, noting that the electricity consumption of the lighting system and all electric equipment was included in the electricity consumption.

1.6 Discussion and research gaps

We recall that the main objective of this research work is to formulate the relationship between occupants' thermal comfort, heating energy consumption and building design parameters, in order to integrate occupant thermal comfort in the design of energy-efficient buildings. The aims intended through this formulation are:

- First, to understand the relationship between energy performance, thermal comfort, and design factors.
- Second, to provide realistic and accurate predictions of energy consumption and thermal comfort throughout the design process.
- Third, to be able to identify the parameters and interactions between parameters those considerably affect the design objectives in order to achieve an optimal design.

Specifying these research perspectives, we identify the following limitations associated with approaches found in literature:

Although the proposed thermal comfort-based control strategy provides the energy-saving effect as well as consistent thermal comfort, some investigations conclude that a PMV-based comfort control consumes energy as the thermostatic control to achieve an acceptable comfort range if the building is poorly designed [41]. On the contrary, if the building is well designed a PMV-based comfort control leads to energy savings. In addition, Most of the proposed schemes are based on Artificial intelligence methods, which can give a highly accurate prediction, but they require sufficient historical performance data and are extremely complex to use in the design process. In addition, implementing these control approaches requires continuous monitoring and calculations to fix the set-point temperature. This could lead to additional costs, such as costs of devices, and energy consumption for the function of installed devices. Besides, inappropriate input values of the clothing and metabolic rate

might cause discordance with indoor thermal comfort because these values cannot be measured by sensors.

Moreover, it is clear that numerous works investigate the effect of glass façade design on energy consumption [47–49], thermal comfort [51,52,54], and visual comfort [57] using several parameters. However, few studies evaluated simultaneously the effect of glass façade design on both thermal comfort and energy consumption [48,51], even though it is confirmed that thermal comfort competes with energy-savings in thermostatic controlled space [40]. Thus, simultaneous consideration of both energy consumption and thermal comfort is essential to design buildings so that a trade-off is achieved. Furthermore, the overwhelming majority of the aforementioned studies were performed using building simulation tools, since on one hand, the performed investigations require extensive amount of scenarios to outcome robust results and experimentation could be extensive and time-consuming, and on the other hand, building simulation tools have been recognized as a broadly approved method for assessing indoor air quality and energy consumption. Additionally, parametric studies are used to investigate the proposed scenarios. Although the parametric study provides solid outcomes regarding the influential parameters affecting the studied response, it is of limited accuracy in terms of achieving optimal solutions because it is not continuous and it is hard to identify the interactions between parameters unless a huge number of simulations are performed. In order to overcome this limitation, the numerical results could be used to form a database allocated for the meta-modeling process [53,58]. Mathematical meta-models can convert the discretized domain into a continuous one, thus serving as a practical tool, which improves the accuracy of the near-optimal solution without the need for excessive computational power [53].

The literature review conducted in this second chapter, and the above analysis of research gaps, were used as a basis for constructing our research approach. The latter is to be presented in the next chapter in detail.

Chapter 2: Design framework and research methodology

2.1 Introduction

Energy-efficient building design taking account of occupants' thermal comfort is highly valued in achieving a trade-off between energy-savings and thermal comfort during building use. Unfortunately, the energy-efficient building design problem is difficult to formulate and to solve; solutions must deal with a large number of objectives (energy efficiency, thermal comfort, environmental impact, etc.). To tackle this challenge, the Function-Behavior-Structure (FBS) ontology could be used as a bridge to link design features and desired objectives throughout the design process. The robustness of this design model is that it adds an intermediate state between the functional requirement and design parameters, called behavior, unlike other approaches that transform design information from an abstract form into concrete form during the design process [143]. Nowadays, the FBS is considered as a '*reference model to describe the design processes and tasks*' [144].

2.2 Design framework for energy-efficient buildings

2.2.1 Background of the FBS model

The FBS model of designing, also known as FBS design ontology or FBS conceptual framework, has been first introduced by John Gero in 1990 [145]. It represents a schema to support '*the initiation and continuation of the act of designing*'. The FBS model expresses design as, an activity that aims to transform a set of requirements and functions into a set of design descriptions [59]. It consists of six design issues and eight fundamental processes linking the design issues in a generic design process (Figure 2-1). The six design issues are defined in Table 2-1, and the fundamental design processes are described in Table 2-2.

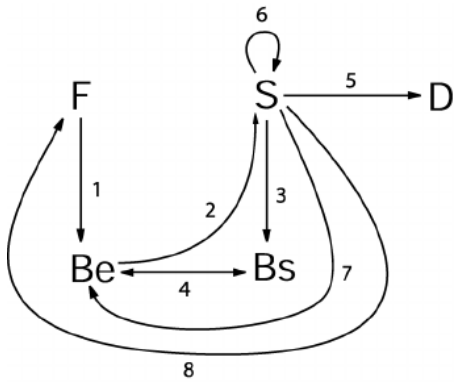

Figure 2-1 : The FBS framework [146].

Table 2-1: Definition of the six design issues [146].

Design Issue	Definition
Requirements (R)	All expressions of customer or market needs, demands, wishes and constraints that are explicitly provided to the designers at the outset of a design task
Function (F)	Teleological representations that can cover any expression related to potential purposes of the artefact
Expected Behavior (Be)	Attributes that describe the artefact's expected interaction with the environment
Structure Behavior (Bs) Or Behavior derived from structure	Attributes of the artefact that are measured, calculated or derived from the observation of a specific design solution and its interaction with the environment
Structure (S)	Components of an artefact and their relationships
Design description (D)	Any form of design-related representations produced by designers, at any stage of the design process

Table 2-2 : The eight fundamental design process synthetized from [146].

Fundamental process	Description
Formulation (1)	Transforms requirements into functions and functions into expected behavior
Synthesis (2)	Transforms expected behavior into structure
Analysis (3)	Transforms structure into structure behavior
Evaluation (4)	Compares expected behavior with structure behavior
Documentation (5)	Transforms structure into a description
Reformulation type 1 (6)	Transforms structure into a new structure
Reformulation type 2 (7)	Transforms structure into new expected behavior
Reformulation type 3 (8)	Transforms structure into new function

Over the years, some ambiguities and weaknesses have been revealed in the FBS model [147,148]; one of the main criticisms of the FBS framework is the lack of '*the dynamic character of the context in which designing takes place*'. In order to overcome this limitation, Gero and Kannengiesser [146] extended the FBS framework to the so-called situated FBS (sFBS) framework by reconstructing the eight fundamental processes to represent designing in a dynamic world. The sFBS framework introduces three different worlds in which the processes take place:

- The *external world* includes representations outside the designer;
- The *interpreted world* is built up inside the designer. It represents the interpreted representation of the external world by the designer;
- The *expected world* is predicted by the interpretation of the designer.

The basic processes that stem from the sFBS framework are shown in Figure 2-2 and summarized in Table 2-3.

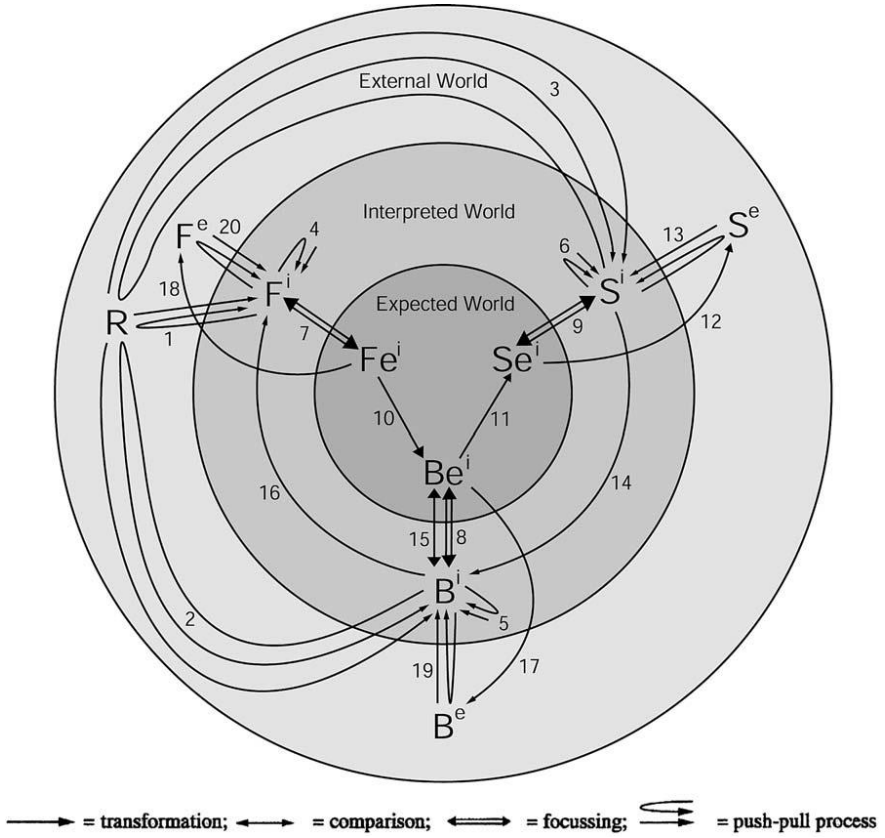

Figure 2-2: The situated FBS framework [146].

Table 2-3 : The twenty fundamental design process synthetized from [146].

Fundamental process	Description
Formulation (1-10)	Interpretation of the requirement to produce an interpreted representation and then focuses on the corresponding subsets that constitute the initial design state space.
Synthesis (11,12)	Defines the external representation of the structure starting from the expected behavior.
Analysis (13,14)	Derives the 'actual' behavior shown by the synthesized structure.
Evaluation (15)	Compares expected behavior with structure behavior.
Documentation (12,17,18)	Provides a design description for manufacturing the artefact.
Reformulation type 1 (6,9,13)	Addresses changes in the design task in terms of structure variables.
Reformulation type 2 (5,8,14,19)	Addresses changes in the behavior during designing.
Reformulation type 3 (4,7,16,20)	Addresses changes in the design state space in terms of modifications of the function variables.

2.2.2 Mapping building design into the FBS framework

To map energy efficient building design integrating occupants' thermal comfort onto the sFBS framework, we use the following set of variables:

- R variable: Energy efficient building integrating occupants' thermal comfort
- F variable: maintain a healthy and comfortable environment
- B variable: thermal comfort condition and energy consumption levels in accordance with standards recommendations
- S variable: opaque surface properties, windows properties, systems, etc.

First, the designer interprets the explicit requirements by producing the interpreted representations (such as enhancing thermal comfort) and, ultimately, interpreted behavior and structure (processes 1–3). These three interpreted variables are then improved by representations originating from the designer's own experience (processes 4–6). For instance, the designer uses his/her constructive memory to produce further Fi, Bi, and Si, such as improving visual comfort by increasing daylight allowance via improving the light transmission and as a result glazing properties. Then, the designer sets up an initial design state by focusing on subsets on these internalized requirements to produce an initial expected function, behavior, and structure (processes 7–9). In Process 10, the designer transforms the expected function, which is enhancing thermal comfort, of the building into an expected behavior, such as the consistent thermal environment. This expected behavior is then transformed into an external structure by synthesis (process 11 and 12). Here, for example, the designer transforms the consistent thermal environment, behavior, to a range of values of glazing system properties, such as reducing the glazing area to alleviate the variation in the radiant temperature. Later on, the synthesized structure is used to derive the actual behavior, energy consumption, and thermal comfort levels of the building (processes 13 and 14). Followed by evaluation criteria (process 15) to evaluate the synthesized structure, this could be performed by comparing the obtained data with the standards recommendations. If the evaluation results are satisfactory, this means that the desired objectives are met and a design description could be produced (processes 12, 17, and 18).

If the evaluation is not satisfactory, three types of reformulations are proposed in the sFBS framework, noted as reformulation of structure (processes 9, 13 and 6), reformulation of expected behavior (processes 8, 14 and 19) and reformulation of function (processes 7, 16, 20 and 4). In the case of building, in most cases, the designer reformulates the structure (changing wall insulation, glazing area and type, etc.) but not the function or expected behavior, because standards and regulations set up the recommended behavior of the buildings.

In this research work, it is assumed that the requirements, function and expected behavior are barely reformulated during the design phases of the building. This is because the requirements and function of the building are assumed to be predefined via the communicative interaction between the designer and customer, and the expected behavior could be obtained from the existing standards and regulations, such as the desired thermal comfort level. In addition, the designer using synthesis

transforms the expected behavior into a structure. So the main focus will be on analysis, evaluation and reformulation type 1. This last, as discussed in the sFBS framework, is intended to addresses changes in the design state space in terms of structure variables if the actual behavior is evaluated to be unsatisfactory, followed by re-evaluation criteria. The designer is suggested to keep the reformulation process until the desired design is achieved. This process could require an extensive amount of scenarios to achieve the required results. In addition, if the designer is dealing with a large number of design parameters and objectives, then identifying the interaction between parameters, to achieve the optimal design, requires a huge number of simulations. In order to overcome this limitation, statistical models could be used, which enables the designer to achieve a mathematical formulation that relates the studied variable, to design parameters. The obtained mathematical formulation allows the designer or engineer to evaluate the sensitivity of the studied variables to the deemed parameters. In addition, the developed function, or mathematical formulation, could be used to carry out an optimization process, so that the predefined expected behavior is implemented as an objective to achieve the desired design.

Indeed, the analysis process requires a suitable and adequate approach to predict the actual thermal behavior of the building. This last is influenced by many factors alongside the building structure, such as weather conditions, the operation of lighting and HVAC systems, occupancy and behavior. Thus, the prediction of building thermal performance requires models that accurately describe the physical phenomena. Numerous models were developed in the literature to predict the building performance including dynamic simulation methods [60], statistical methods [61] and artificial intelligence methods [62].

Each approach has its own advantages and drawbacks. Dynamic simulation is an elaborate and comprehensive model that outcomes accurate predictions, but it is difficult to perform in practice due to its high complexity and the lack of input information [63]. The statistical model is relatively easy to develop but its disadvantages are inaccuracy and lack of flexibility [63]. Artificial intelligence methods are good at solving non-linear problems, such as building energy prediction; they can give a highly accurate prediction as long as model selection and parameters setting are well performed. The drawbacks of these models are that they require sufficient historical performance data and are extremely complex [63].

In this consequence, in the context of this research work, the combined use of building simulation and statistical models is adopted. This is because, in one hand, building performance simulations has gained a big attention in this field as an alternative to the empirical approach due to their capability to provide adequate conclusions with less time and cost, as well as it enables the designer or engineer to analyze different scenarios during the design phase without the need of existing building. On the other hand, the statistical model combines the speed of simple models and

the precision of dynamic simulations if developed adequately [64]. The statistical models are developed by regression techniques from historical data or dynamic models [61], which means that before obtaining the model, we need to collect enough data. The principle of the statistical models is to propose a function which relates the studied variable, such as thermal comfort, to environmental parameters (e.g. temperatures, MRT) and design parameters (e.g. glazing type and glazing area), then to identify the coefficients of this function by a regression method [149]. The obtained function enables the designer or engineer to evaluate the sensitivity of the studied variables to the deemed parameters. In addition, the developed function, or mathematical formulation, facilitates the optimization process to achieve the desired design.

2.2.3 Building thermal performance modeling

The dynamic analysis of the buildings' thermal performance using computer modeling and simulation methods is called Thermal Building Simulation (TBS). TBS is a valuable and powerful tool for evaluating the effect of building envelope design, control strategies, and advanced technologies in the design phase of the building. In recent years, the use of TBS tools is increasing by all professions elaborated in the design of buildings. This increase is correlated to two main reasons; the first is that TBS tools become more advanced, integrated, and easy to use. And the latter is that TBS allows building designers and engineers to take early decisions that help in improving building performance, reducing its costs, and save time [150].

Building thermal behavior modeling is based on the so-called physical techniques, also known as the "white box", which are based on the solving of equations describing the physical behavior of the heat transfer [151]. Other techniques such as the statistical and machine learning formulations recognized as "black box" are based on the collected data inside the building. The black box models are mainly used to derive prediction models using an appropriate database. And the coupling between both white and black box techniques is called "grey box" or hybrid approaches.

2.2.3.1 Physical models

Physical modeling techniques are used to model and evaluate the thermal performance of different building types, including models for different aspects such as HVAC systems, hygro-thermal effects, occupants' behavior, etc. They can be divided into three main categories: Computational Fluid Dynamics (CFD), zonal, and multi-zone/nodal methods. Each method has its own principle, application field, advantages, and drawbacks, thus the choice of the physical model depends principally on the problem under investigation. Table 2-4 summarizes the specificity of each technique. A detailed description of each approach and a review of their applications in the buildings modeling is presented in [151].

The CFD method is disputably the most detailed and comprehensive method, it allows the fine description of each mechanism occurring in the building system. However, this approach requires significant computational resources and is highly complex, so that it requires highly skilled laborers. A huge number of CFD software are available such as FLUENT, COMSOL Multiphysics, MIT-CFD, PHOENICS-CFD, etc. Their application fields are very large and not always specific to building simulation [151].

Table 2-4: Summary of the specificity of each physical technique [151].

Physical technique	Specificity	Application field	Advantages	Limitations
CFD approach	One cell = a control volume (3-D); Local state variables	Contaminant distribution; Indoor air quality; HVAC systems	Detailed description of different fluid flows inside the building (airflow, pollutant particles, etc.). Allows studying very complex geometries.	Huge computation time. Complexity of the model implementation.
Zonal approach	One cell = a division of a room (2-D); Local state variables	Indoor thermal comfort; Artificial and natural ventilation	Spatial and time distribution of local state variables (temperature, concentration, pressure, airflow) in a large volume	Large computation time. Requirement of a detailed description of the flow field and flow profiles.
Nodal approach	One cell=a room (1-D); Uniform state variables	Determination of the total energy consumption/the average of the indoor temperature/the cooling or heating load; Time evolution of the global energy consumption/the space-averaged indoor temperature	Multiple zone buildings; Reasonable computation time; Easier implementation	Difficulty to study large volume systems. Unable to study local effects as heat or pollutant source

The zonal approach represents a simplification of the first degree of the CFD method. It divides the building into different zones and each zone into different cells. It solves the physical equations of each zone instead of each mesh element. The zonal approach is less comprehensive and accurate than the CFD approach but represents a faster way that gives good results related to the indoor environment parameters. It also represents a fast way to estimate thermal comfort within a studied zone. One of the frequently employed zonal modeling software to describe and to visualize indoor air flows is the so-

called SimSPARK software [52]. Additionally, some researchers implemented their own zonal software as with POMA (Pressurized zOnal Model with Air-diffuser) in [152].

The multi-zone or nodal approach is probably the simplest method compared to the zonal and CFD techniques. It assumes that each building zone is a homogeneous volume with uniform state variables. In addition, this technique simplifies the physical problem by linearizing the equations, when it is possible. This results in significantly reducing the technical complexity of the problem and thus the computation time. Thus, the advantage of the nodal approach is its ability to compute simulations for large periods with minimum computation time. The most popular tools that use the nodal approach for building simulations are TRNSYS, EnergyPlus, IDA-ICE, and ESP-r.

Based on the aforementioned discussion and information provided in Table 2-4 one can deduce that the nodal technique is most useful among others for the study of low energy consumption buildings. Since in these buildings, the modeling process focuses on thermal loads and energy consumptions and the detailed analysis resulting from the CFD approach is unnecessary [63]. Moreover, the long term studies, system comparison, and the estimation of energy consumption and environmental parameters, such as space temperature are well suited to the nodal approach.

Furthermore, the valuable benefits resulting from the use of building simulations have been highlighted by different authors. Hong et al. [153] stated that "*before the advent of computer-aided building simulation, building services engineers relied heavily on manual calculations using pre-selected design conditions and "rules of thumbs"* ". For example, parametric and sensitivity studies that aim at evaluating the influence of altering building envelope parameters can be simply examined using simulation software, rather than changing the parameters of the actual building, which leads to additional costs or inconvenience to building stakeholder. In addition, building simulations enhanced human safety, by avoiding people exposure to extreme conditions when studying the effects of such condition on human well-being [154].

It is obvious that building simulations has gained huge acceptance and are now approved as the best practice to demonstrate the real-life scenarios [155]. However, the complex dynamic principles of the real buildings require realistic simulations, rather than simple estimation coupled with uncertainties due to the transition from the real life to simulations [155]. These uncertainties may lead to disclosing the accuracy of the model, thus affecting the validity of the outcomes.

2.2.3.2 Uncertainty in building thermal performance modeling

Several factors contribute to the uncertainty of the building simulation models. For instance, the simulation software itself, software user's knowledge or simulation skills may be sources of uncertainty. In addition, the input parameters such as weather data and thermo-physical properties,

since these parameters are always expressed under a certain part of uncertainties [151]. This could be correlated to the lack of detailed information related to the occupant behavior, equipment scenario, sub-metering instruments, and the complete as-built drawings, which could help in developing a detailed and accurate model. The stochastic nature of occupant behavior often leads to the largest source of uncertainty in building simulation, in addition to its large influence on energy consumption [156,157]. And also, incomplete and fragmented weather data used for the creation of real weather files could lead to some uncertainties in the collected data and thus in the simulation results [158].

Moreover, poor maintenance of the building could also lead to modeling inaccuracies. For instance, if the operation scenarios or performance levels of the building is not in agreement with those suggested in the design phase, which usually assumed as acknowledged in the technical specifications, then, the simulations will not accurately imitate the reality. Additionally, some uncertainties are also prompted due to certain assumptions predicted by the user. These assumptions could be either to estimate the real thermo-physical properties of the building envelope due to alterations in the envelope and structural assemblies throughout their lives or to reduce the complexity of the thermal mechanisms occurring in the buildings. Thus, all these uncertainties lead to a real difficulty to evaluate the accuracy degree of the models [151]. Heo [159] classified the sources of uncertainty in building models into four main categories, as presented in Table 2-5.

Table 2-5: Source of uncertainty in building energy models [159].

Category	Factor
Scenario uncertainty	Outdoor weather conditions
	Building usage/occupancy schedule
Building physical/operational uncertainty	Building envelope properties
	Internal gains
	HVAC systems
	Operation and control settings
Model inadequacy	Modeling assumptions
	Simplification in the model algorithm
	Ignored phenomena in the algorithm
Observation error	Metered data accuracy

The discussed uncertainty in the model input leads to variations in the output, known as uncertainty in the output of a model, the process of quantifying the variability in the output is called uncertainty analysis [160]. The study of how the uncertainty in the model output can be apportioned to different sources of uncertainty in the model input is called the sensitivity analysis (SA) [161]. Thus, the SA can be considered as an ‘input-output analysis’ of the simulation model [162]. The following section presents, the purpose behind using sensitivity analysis in building thermal performance modeling, and the methods used to assess sensitivity measures.

2.2.3.3 Sensitivity analysis (SA)

Sensitivity analysis (SA) was considered and often defined as a local measure of the effect of a given input on a given output [161]. It is a valuable approach that can be used to identify the key parameters influencing building thermal performance for both observational and energy simulation studies [163]. In the recent years, SA has been extensively used to discover the characteristics of building thermal performance [163,164], a literature review of the application and used methods of SA in building thermal performance analysis is presented in [163].

To implement SA in building performance analysis, six typical steps are needed (Figure 2-3): i) determine input variations; ii) create building energy models; iii) run energy models; iv) collect simulation results; v) run sensitivity analysis; vi) presentation of sensitivity analysis results. Although these steps are the same for different types of applications in building behavior analysis, the main difference is the variations (uncertainty or probability distributions) of input factors [163].

There are numerous techniques to employ SA in building performance studies. These techniques are commonly grouped into local and global methods [165]. The local sensitivity analysis (LSA) is performed in a similar means to the differential analysis, where the uncertainty of outputs is evaluated by a slight increase in the value of one input variable. However, in the global sensitivity analysis (GSA), the influences of all the input variables are estimated on the uncertainty of outputs.

2.2.3.3.1 Local Sensitivity Analysis (LSA)

LSA, also known as differential sensitivity analysis, belongs to the class of the One-Factor-At-a-Time (OFAT) methods [163]. In this technique, in each simulation or observation, one design variable is altered within the studied range and all other design variables are held fixed. As a result, it could be easily employed and interpreted. In addition, it is very straightforward and often requires fewer simulation runs compared with the global sensitivity study. However, this technique studies the performance, sensitivity, of the outputs of the models resulting from the changes in one input parameter, and as a result, some limitations of this method are figured [166]:

- It only explores a reduced space of the input factor around a base-case.
- It cannot consider the interactions between different factors.
- It has no self-verification.

2.2.3.3.2 Global Sensitivity Analysis (GSA)

GSA techniques evaluate the variations of the output resulting from one input variable by varying all other parameters over their variation range at the same time [161,167]. Thus, GSA methods measure the interaction of factors and provide robust sensitivity measures. It is considered more

reliable than the LSA, but it requires higher computational time compared to LSA. The GSA includes regression, screening-based, variance-based, and meta-modeling methods. The characteristics of the mentioned methods are summarized in Table 2-6.

- ***Regression method*** is the most employed technique for SA in building performance analysis due to its fast to compute and easy to understand features [168–170]. In this approach, the uncertainty of output is assessed due to the overall uncertainty of input variables, regardless of the number of variables and interactions. In addition, regression analysis can be used in both early design stages and in post-construction stages [158]. The first aims at considering the impact of different design scenarios on building performance, and the latter aims at assisting the calibration of a building model.

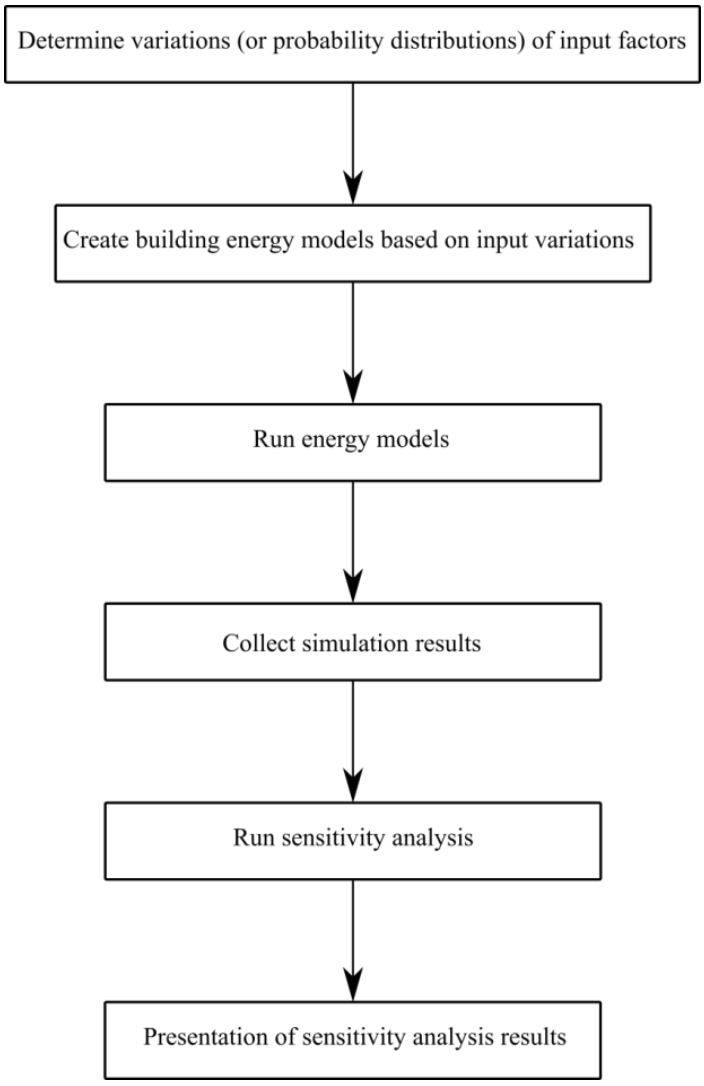

Figure 2-3: Typical schematic flow diagram for sensitivity analysis in building performance analysis [163].

Table 2-6 : Comparison of sensitivity analysis methods used in building performance analysis [163].

Method	Characteristics
Local	Explore a reduced space of the input factor around a base case; low computational cost; simple to implement; easy to interpret; not consider interactions between inputs; no self-verification
Regression	SRC and t-value, suitable for linear models; SRRC, suitable for non-linear but monotonic models; moderate computational cost for energy models; fast to compute; easy to implement and understand; high SRC means more important of the variable
Screen	Suitable for a larger number of inputs and computationally intensive models; model-free approach; qualitative measure to rank factors; no self-verification; not suitable for uncertainty analysis
ANOVA	Decompose the variance of the model output for every input; model-free approach; consider both main and interactions effects; quantitative measures; high computational cost; FAST is not suitable for discrete distributions
Meta-model	Suitable for complex and computationally intensive models; quantify output variance due to different inputs; the accuracy dependent on the meta-model

- ***Screening-based method*** often aims at fixing some input parameters from a large group of parameters without decreasing the output variance [163]. In fact, the method indicated by Morris is the widely used technique in the building behavior analysis field. This method is based on the elementary effects of parameters, but without any assumptions of the relationship between input parameters and outputs. The input parameters in this technique are taken as a discrete number of values. In addition, the screening-based method is a low computation cost approach that tends to provide qualitative measures by prioritizing input parameters, but it cannot quantify the influences of parameters, or recognize how much of the total variances of outputs have been taken into account in the analysis [163].

- ***Variance-based method or Analysis-Of-Variance (ANOVA)*** is a sampling method but also relied on the computations of conditional variance. The purpose of the variance-based method is to decompose the uncertainty of outputs for the corresponding input or group of inputs [161]. Specifically, this technique has two main sensitivity measures noted as the first order effects and the total effects. The first order effect signifies the main effect of the input parameter on the output variations. The total effects represent the total contributions of the input parameter on the output variance, which comprise both the first order and higher order effects due to the interactions between inputs. As a result, the interaction between factors could be determined by the difference between the total and the first order effects. Therefore, if the study aims at ranking the parameters, the first order effect should be used. However if the purpose is to fix the factors, the total sensitivity effects are the better choice. In addition, the variance-based method is considered as a model-free approach, which implies that it is an appropriate SA technique for complex nonlinear and non-additive models [163].

- ***Meta-model based method*** is a two-stage approach [171]. First, a meta-model is created using non-parametric regression methods, which do not have a predetermined form (such as linear or nonlinear regression) and consequently it can be suitable for complex models. Second, sensitivity measures are calculated using this meta-model based on the variance-based method. The main advantage of using this approach is that running meat-models needs much less computational time than comprehensive building simulation models. Hence, this method can provide a more efficient sensitivity index compared to the variance-based method. In addition, the meta-modeling method can also quantify the variance of the output for different input factors since it uses the variance-based method.

To sum up, although a wide range of uncertainties may occur in the development of building simulation models that lead to output uncertainties as a function of the sensitivity of the output, this technique is widely used to predict the thermal behavior of buildings. Thus, the prediction capability of these models is an influential factor in order to reflect the reliability of the results. These models must be suitable and provide significant contributions to reflect the ambiguity effects associated to the design parameters, construction quality, building uses and climatic conditions; therefore, the validation of the developed model is essential.

2.2.3.4 Model boundary conditions and validation

Since simulation tools are widely used to model buildings in order to predict their thermal behavior, the prediction capability of these models is an influential factor in order to reflect the reliability of the results. These models must be suitable and provide significant contributions to reflect the ambiguity effects associated to the design parameters, construction quality, building uses and climatic conditions; therefore, the validation of the developed model is essential. Indeed, to predict the thermal behavior of the building, all the contributing factors must be adequately defined in the model in order to outcome truthful results. Weather data is one of the main factors that contribute to the quantification of the thermal behavior of the buildings.

2.2.3.4.1 Weather data

Typical Meteorological Year (TMY), a year of hourly weather data collected from a dataset of several preceding years so that it exemplifies a typical annual data for a specified location, is recommended to be used in the building simulations [172]. However, extreme weather events are not included in the TMY data files, since these files are intended to best represent the building operation and performance when exposed to normal weather conditions. And also TMY data files are not suitable for the validation of the building models since they represent a typical prototype, but not the real data during a particular time. Thus, for validation, actual weather data occurring during the monitoring of the real building is recommended, so that the response of the model and that of the real

building are matched during a specified period. This yields to best tuning the building model by comparing actual and predicted parameters profiles using the same input factors, hence diminishing the uncertainty related to weather parameters.

Nevertheless, the real weather data should not be used for long term evaluations, since they only provide definite results for the location and over the studied period. Therefore, after the model validation is accomplished, the real weather data must be replaced by the TMY data file of the specified location to carry out simulations. So that the desired investigations using the building model could be performed, the objectives of the study could be achieved and the obtained results will be more representative. Noting that, the implementation of real weather data depends on the used simulation software.

2.2.3.4.2 Validation methodology

To validate a developed building model, several resulting parameters, called predicted or simulated results, should be compared to real measured data from the real building. This comparison should be performed by the application of metrics that aim at quantifying the discrepancies between predicted and actual data. Along with accurate geometrical data, thermo-physical properties of the building envelope, and historical weather data during the monitoring period, in addition to some other parameters such as occupancy and equipment scenario, uncertainties could be eliminated and valid comparison between the recognized parameters could be attained.

A comprehensive documentation for the calibration and validation of building thermal models was published by ASHRAE in 2002. This document, known as ASHRAE Guideline-14 (G-14) [74], is extensively used for the validation of models using energy data. Specifically, the document recommends the use of the so-called normalized mean bias error (NMBE) and the coefficient of variation of the root mean square error (CVRMSE) to evaluate the validity of the developed model. The procedures to calculate the NMBE and CVRMSE are presented hereafter, but first, the explanation of the Mean Bias Error (MBE) is introduced, due to its importance in the calculation of both coefficients [173].

MBE is the average of the residuals between the measured, m_i, and predicted or simulated, s_i, data. MBE is expressed as indicated in Equation (2.1), where n is the total number of measured data. A positive value signifies that the model under-predicts the measured data, and a negative value means an over-prediction. However, the main drawback with MBE is that it is subject to cancellation errors.

$$MBE = \frac{\sum_{i=1}^{n}(m_i - s_i)}{n} \tag{2.1}$$

NMBE is a measure of how close the predicted data fits the measured data and is expressed in percentage (%). It is a normalization of the MBE index, which is used to gauge the results of MBE. NMBE gives the global difference between the measured and predicted values since it quantifies the MBE by dividing it by the average of measured values ($\overline{m}$). Thus, it is the ratio of the sum of discrepancies between actual and predicted data to the mean of all measured data. Positive and negative values signify under- or over-prediction of the normalization, as in the MBE index.

$$NMBE = \frac{1}{\overline{m}} \times \frac{\sum_{i=1}^{n}(m_i - s_i)}{n} \times 100 \tag{2.2}$$

CVRMSE measures the dispersion (variability) of the residuals between measured and predicted data. In other words, it is a measure of the ability of the model to fit the measured data. A lower value indicated that the model is a better fit. This index is not subjected to the cancellation phenomenon.

$$CVRMSE = \frac{1}{\overline{m}} \times \sqrt{\frac{\sum_{i=1}^{n}(m_i - s_i)^2}{n}} \times 100 \tag{2.3}$$

The coefficient of determination ($\boldsymbol{R^2}$) shows how close the predicted values are to the regression line of the measured data. This index is ranged between 0, which means that the predicted and measured data do not fit, and 1, which means that the predicted values match perfectly the measured data. It is recommended that the value of this index is above 0.75 for calibrated models [74]. Table 2-7 summarizes the criteria of ASHRAE G-14 [74] to validate a model as calibrated.

$$\boldsymbol{R^2} = \left(\frac{\boldsymbol{n \times \sum_{i=1}^{n} m_i \times s_i - \sum_{i=1}^{n} m_i \times \sum_{i=1}^{n} s_i}}{\sqrt{\left(\boldsymbol{n \times \sum_{i=1}^{n} m_i^2 - \left(\sum_{i=1}^{n} m_i\right)^2}\right) \times \left(\boldsymbol{n \times \sum_{i=1}^{n} s_i^2 - \left(\sum_{i=1}^{n} s_i\right)^2}\right)}} \right)^{\boldsymbol{2}} \tag{2.4}$$

Table 2-7 : Threshold limits of statistical criteria for calibration in compliance with ASHRAE G-14 [74].

Statistical indices	Monthly Calibration	Hourly Calibration
NMBE (%)	± 5	± 10
CVRMSE (%)	15	30
R^2	> 0.75	> 0.75

2.3 Research Methodology

As previously discussed, in this research work the focus will be on deriving and evaluation thermal behavior of building from structure, and reformulate the structure of the building to achieve satisfactory results. To derive behavior from structure, a suitable and adequate approach to predict the actual behavior of the building is required. Here, we adopted the building performance simulation approach because of its capability to provide adequate results with less time and cost. So the first step will be selecting a simulation environment for modeling purposes. After modeling the structure, behavioral variables must be selected for the evaluation. Since the main intention of this research work is to integrate occupants' thermal comfort in the design for energy efficient building, the well-known thermal comfort indices, PMV and PPD, are used for the evaluation. If the evaluation results are satisfactory, then the structure is well suited with the intended behavior and no more investigations are required. However if the results are unsatisfactory, we need to identify the critical parameters that affect the actual behavior in order to reformulate the structure of the building. SA represents a worth approach for this aim, because it enables understanding the relationship between the studied variable and the design parameters. In this study, the use of meta-modeling approach based on the DoE technique is adopted, because it allows the designer to derive mathematical formulation, noted as meta-models, between the studied variable and design parameters. Indeed, the final step will be adopting an optimization approach that simultaneously optimizes building design for thermal comfort and energy consumption. Figure 2-4 shows the graphical representation of the proposed research methodology. The adopted simulation environment is presented in the next section, followed by a brief definition of the DoE technique, the determination and validation of the meta-models, and the used optimization processes, successively.

2.3.1 Define a reference case study

The importance of a case study is that it represents an instructive example to researchers who might encounter similar problems. Ideally, in buildings, a case study should detail a particular thermal behavior case, describing the background of the thermal problem and any clues the researchers picked up regarding the reasons for the problem. Thus, a case study should be an informative and useful part of the performed research work, both during investigations and on a continuing basis. In addition, as previously discussed, glass façades design has been the foundation of numerous research works in recent years due to its effect on both energy consumption and thermal comfort.

For all these reasons, a real case study, in particular, a highly glazed room representing a part of a low energy consumption building is adopted for this research work. This choice is based on the fact that existing buildings helps in acquiring real data using subjective and objective investigations. This

last allows the validation of the numerical models, hence, yielding more realistic and reliable results of the investigation.

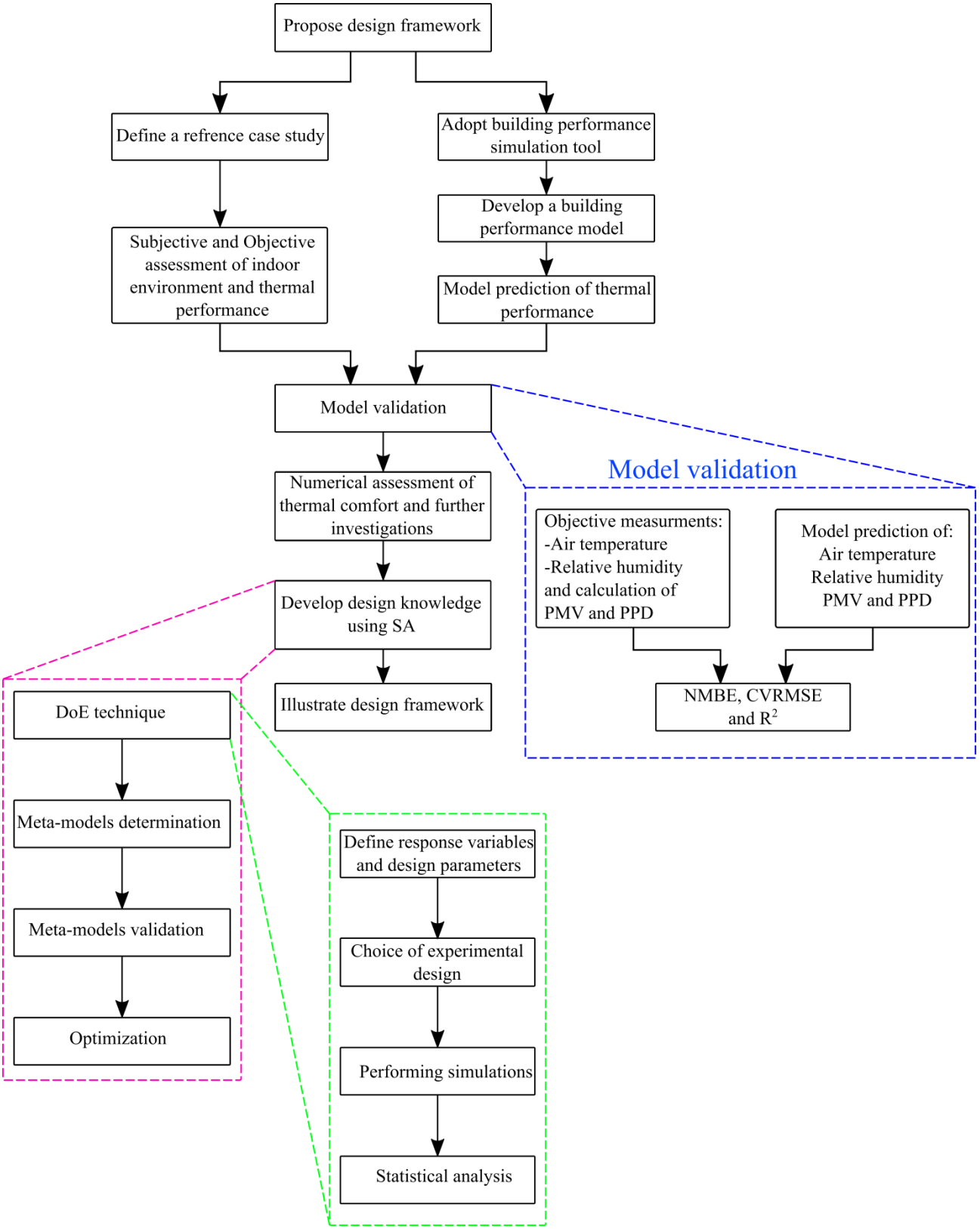

Figure 2-4: Research methodology.

2.3.2 Modelica for building simulations

The numerical modeling and simulations were performed using Modelica [65]; which is an open source object-oriented equation-based modelling language. Modelica allows the combined simulation and modelling of multi-physical systems. It differs from the other broadly used programming environments by using non-causal modelling. The modelling using Modelica can be done either through a graphical interface or by equations. The equation-based feature reduces faults compared to assignment-based modeling (e.g. TRNSYS, Matlab Simulink) [66]. A functional comparison was conducted in [67] indicating that Modelica is more suitable than TRNSYS® and Matlab Simulink® in terms of modularity, multi-domain modeling, realistic control behavior, and flexibility.

Models written in the Modelica language cannot be executed directly. A simulation environment, such as Dymola® (Dynamic Modeling Laboratory), OpenModelica® and JModelica®, is needed to translate a Modelica model into an executable program. OpenModelica® and JModelica® are open source tools, however, there are shortcomings regarding the adaptability of these tools with some developed libraries such as the Buildings Library [174]. Dymola® is a commercial tool developed by Dassault Systèmes AB [175]. The main features of Dymola® are its powerful graphical editor which facilitates the creation of models and Modelica equations symbolic translator that generates C-code for simulation. The former makes it ideal for modelling complex building models integrating several types of systems and the latter is crucial since the generated C-code can be exported and used in other systems.

Recently, numerous research teams have developed Modelica libraries for HVAC systems and building components, which lead to an increase in the usage of Modelica as an object-oriented building performance simulation program. Modelica Standard Library [176] has been the foundation of most developed building libraries. In the present work, Dymola® was chosen as the Modelica-based simulation tool since it is compatible with the libraries selected for the development of the building model.

2.3.3 DoE

An Experiment is defined as a test in which purposeful changes are made to the input parameters of a system/process so that the experimenter may observe and identify the reasons for changes in the response variable [68]. Poorly designed experiments can often lead to ineffective use of valuable resources and inconclusive results. Hence, experiments should be well-designed. One-factor-at-a-time is a popular approach, in which the influence of the tested parameters is measured by changing the level of one parameter while maintaining other parameters at their levels [163]. The major disadvantage of this method is that it fails to consider any possible interaction between the parameters [163]. Contrarily, in the DoE approach, the influence of each parameter on the studied

process is measured simultaneously on several levels of all other parameters, thus taking into consideration all the occurring interactions between parameters [68].

The DoE technique is a statistical method used to approximate the mathematical relationship between different factors affecting several response variables, and most often one response variable. It can be used to simplify parametric studies by significantly reducing the required number of experiments or simulations [58]. The obtained mathematical models, also known as meta-models, can be used instead of numerical simulation tools to simplify and accelerate the parametric studies to find optimal solutions. It is also utilized to analyze the effect of each factor on the response variable and the interaction between factors. To implement the DoE technique, the following steps should be followed [68,177]:

1. Recognition and statement of the problem.
2. Selection of the response variable.
3. Choice of factors, levels, and ranges.
4. Choice of experimental design.
5. Performing the experiment.
6. Statistical analysis of the data.
7. Conclusions and recommendations.

The Analysis of Variance (ANOVA) in combination with Fisher's statistical test (P-value < 0.05) can be used to test the significance of the model along with model terms. The significance of a factor or its effect is determined based on its P-value. If the P-value of a factor or its effect was less than 0.05, it is considered as significant [82]. Contrarily, factors with P-value greater than 0.05, are deemed as not significant [82]. Additionally, graphical illustrations, such as the Pareto charts and the Normal plots of standardized effects, can be used to identify the significant terms.

2.3.4 Meta-modeling and determination of meta-models coefficients

One of the main objectives of the DoE technique is to pursue a suitable mathematical model, called "meta-model" or "model of the model", which approximates the response variable as a function of predefined factors. The most common meta-models are the first-order linear model (Equation (2.5)), the linear model with interaction terms (Equation (2.6)), the pure quadratic model (Equation (2.7) and the complete quadratic model (Equation (2.8)) expressed as follow [68]:

$$Y_i = C_0 + \sum_{i=1}^{n} C_i X_i + \epsilon \tag{2.5}$$

$$Y_i = C_0 + \sum_{i=1}^{n} C_i X_i + \sum_{i=1}^{n-1} \sum_{j=1+1}^{n} C_{ij} X_i X_j + \epsilon \tag{2.6}$$

$$Y_i = C_0 + \sum_{i=1}^{n} C_{ii} X_i^2 + \epsilon \tag{2.7}$$

$$Y_i = C_0 + \sum_{i=1}^{n} C_i X_i + \sum_{i=1}^{n-1} \sum_{j=1+1}^{n} C_{ij} X_i X_j + \sum_{i=1}^{n} C_{ii} X_i^2 + \epsilon \tag{2.8}$$

where Y_i is the predicted response variable, X_i and X_j are the independent coded factors, $X_i X_j$ represents the two-factor interaction, C_0 and C_i represents the regression coefficients for intercept and linear terms, respectively, C_{ij} is the coefficients for interaction terms, C_{ii} is the coefficient of the quadratic terms, and ϵ is a random error term that accounts for the experimental error. Indeed, the transition from dimensional to coded factors must be made by applying the following formulation:

$$X_i = \frac{x_i - (x_{i,high} + x_{i,low})/2}{(x_{i,high} - x_{i,low})/2} \tag{2.9}$$

where X_i is the coded value of the variable x_i ranging between -1 and +1, and $x_{i,low}$ and $x_{i,high}$ are the values of the variable at low and high levels, respectively. Simple matrix multiplication could be used to determine the coefficients of the meta-model. Firstly, the meta-model is expressed in matrix notation as:

$$[Y] = [X].[A] + [e] \tag{2.10}$$

Where $[Y]$ is a vector consisting of the response observations, $[X]$ is design matrix of the considered factors, $[A]$ is the vector of regression coefficients $(C_0, C_i, C_{ij}, C_{ii})$, and $[e]$ is the residual vector. Then, the least squares method is used to calculate the coefficients vector $[A]$ as follow:

$$[A] = ([X]^t.[X])^{-1}.[X]^t.[Y] \tag{2.11}$$

After obtaining a meta-model that best describes the relationship between the response variable and the considered factors, its validity is vital to reflect the adequacy of the performed sensitivity analysis as well as apply an optimization procedure.

2.3.5 Validation of the obtained meta-models

The adequacy of the model, and as a result the performed analysis, can be done by graphical analysis of residuals [68]. The residual (e_i) is defined as the difference between the actual observation (y_i) and the corresponding fitted value $(\hat{y}_i)$:

$$e_i = y_i - \hat{y}_i \tag{2.12}$$

If the model is accurate, the residuals should be "structure-less"; in particular, they should be unrelated to any other variable including the predicted response [68]. A simple check is to plot the residuals versus the fitted values. This plot should not reveal any obvious pattern (in other words, there should be no relationship between the size of the residuals and the fitted values, such as tendency for negative or positive residuals to occur with low, intermediate or high fitted values.). In addition, a very useful method is "The Normality Assumption", which is to construct a normal probability plot of the residuals. If the underlying error distribution is normal, this plot resembles a straight line, and thus confirming the validity of the model [68].

Moreover, computer programs for supporting DoE display some other useful information. The coefficient of determination (R^2) is loosely interpreted as the proportion of the variability in the data "explained" by the ANOVA model. It ranges between zero and one, with larger values being more desirable. The "adjusted-R^2" is a variation of the ordinary R^2 that reflects the number of factors in the model. It can be a useful statistic for more complex experiments with several design factors when evaluating the impact of increasing or decreasing the number of model terms is desired. Prediction error sum of squares (PRESS) is a measure of how well the model is likely to predict the responses in a new experiment. Small values of PRESS are desirable. In addition, adequate precision statistic could be used to measure the ratio of the signal to noise [178]. The ratio compares the range of the predicted values at the design points to the average predicted error. Large values of this quantity are desirable; specifically, a ratio greater than 4 is an indicator of adequate model differentiation [68,179].

Up to this point, the use of DoE technique in order to identify the significant factors affecting a deemed response variable, the determination of regression meta-model, and the validation processes to check the adequacy of the obtained results is explained. The obtained meta-model is then used to find a desirable results, such as maximizing or minimizing the response variable. However, in many cases the term "desirable" is a function of more than one response. For instance, to achieve a trade-off

between energy-savings and thermal comfort a simultaneous optimization procedure is needed to minimize the energy consumption as well as maintain the PMV index in a desired range. Therefore, a simultaneous optimization procedure is needed to find a compromise solution [180].

2.3.6 Optimization methods

Simultaneous consideration of multiple-responses involves first building an appropriate mathematical model for each response and then trying to find a set of operating conditions, design factors, which in some sense optimizes all responses or at least keeps them in desired ranges.

A relatively straightforward approach is to overlay the contour plots for each response, then determine the appropriate conditions by examining visually the contour plot [180]. However, this approach works well when there are only few factors, because the contour plot is two-dimensional that means n-2 of the design factors must be held constant to construct the graph. The determination of these factors requires a lot of trial and error [180], which implies that the use of a formal optimization methods is of practical interest.

In this consequence, the simultaneous optimization technique, known as the desirability function approach, represents a useful approach to optimization of multiple responses. The desirability function approach proposed by Harrington [181] and then modified and popularized by Derringer and Suich [182] aims to simultaneously optimize multiple equations. Its basic idea is to convert a multiple response problem into a single one by converting each response y_i into an individual desirability function d_i that ranges from zero, if the response is outside the limits, to one if the response is at its target. The individual desirability functions have different formulations depending on the desired objective (maximize, minimize or target value). If the objective is a maximum, a minimum or a target value, the desirability functions are described, respectively, by the following equations:

$$d_i^{max} = \begin{cases} 0 & if \quad y_i < L \\ \left(\dfrac{y_i - L}{T - L}\right)^r & if \quad L \le y_i \le T \\ 1 & if \quad y_i > T \end{cases} \tag{2.13}$$

$$d_i^{min} = \begin{cases} 0 & if \quad y_i > U \\ \left(\dfrac{U - y_i}{U - T}\right)^r & if \quad T \le y_i \le U \\ 1 & if \quad y_i < T \end{cases} \tag{2.14}$$

$$d_i^{target} = \begin{cases} 0 & if \quad y_i < L \\ \left(\frac{y_i - L}{T - L}\right)^{r_1} & if \quad L \leq y_i \leq T \\ \left(\frac{U - y_i}{U - T}\right)^{r_2} & if \quad T \leq y_i \leq U \\ 1 & if \quad y_i > U \end{cases} \tag{2.15}$$

where, L, T and U are successively the lower, the target and the upper limits, and r_i is a weighting parameter used to assess the importance for the response to be close to the desired objective. Afterward, the individual desirability functions are combined in the so-called global desirability function (D) as expressed in Equation (2.16). Lastly, the algorithm searches for the set of input factors to maximize the overall desirability function D [69] using the Nelder-Mead simplex method [183].

$$D = (d_1 \times d_2 \times \ldots\ldots\ldots \times d_n)^{1/n} = \left(\prod_{i=1}^{n} d_i\right)^{1/n} \tag{2.16}$$

2.4 Conclusion

In this chapter, we summarized the FBS-framework concept. Building design was then mapped into the FBS-model to better understand the steps building designer could follow during the design stages of the building. Every step requires actions and activities to be performed, for this we introduced the prediction models proposed in the literature and adopted the required tools to perform our investigations. Finally, we proposed a research methodology that aims to simply and efficiently integrate occupants' thermal comfort in the design stages of the buildings.

As indicated above, a case study is required for modeling and investigations. A brief description of the characteristics of the considered case study is presented in the following chapter. Next, a qualitative study is carried out to assess the real thermal perception of occupants attending the deemed case study. A computer simulation model using Dymola® is then developed. Comparing model predictions with objective measurements enables the validation of the model. Numerical simulations are then performed using the validated model to assess thermal comfort levels.

Chapter 3: A numerical approach based on system modeling to assess thermal comfort

3.1 Introduction

Building simulation tools have been recognized as a broadly approved method of assessing indoor environment quality and energy consumption during the design process. Since constructing prototypes and carrying out experimentation is expensive and time-consuming, due to the complexity and high-performance requirements of new buildings. Thus, increasing the reliability of building simulation tools can make an essential contribution to the reduction of energy consumption while maintaining a comfortable indoor environment. The aim of this chapter is to develop a numerical model and validate it by comparing its predictions with experimental results.

As previously discussed, a case study should represent an informative and useful part of the research work to reflect the reliability and credibility of the obtained results. For this, a real case study, in particular, a highly glazed room representing a part of an energy-efficient building is adopted for the investigation. Since the considered room is a real case study, subjective evaluation of occupants' thermal comfort could be an influential approach to assess occupants' thermal comfort. In this regard, a survey questionnaire is used to evaluate the real occupants' perception of thermal environmental conditions. A computer simulation model using Dymola® is then developed and validated by comparing the predicted results with objective measurements. The model is then used to extend the investigation to a whole winter season and different scenarios with low additional costs and less time.

3.2 Case study

The building considered in this study was designed to be an exemplary engineering school building intended for graduate engineering students in the fields of buildings and smart cities. It was designed with the dual purpose of an educational environment and an experimental case study in order to analyze its energy consumption and Indoor Environment Quality (IEQ). It was designed to be a low energy consumption building to meet the French Standard requirements RT2012. The building, constructed in 2014 and located in Troyes, France, has a net surface area of 3200 m^2 spread over three levels (Figure 3-1). The ground floor contains an amphitheater, a café, students' open-work spaces, an atrium/exhibition area, association offices, computer teaching rooms, and a storage room containing the first Air Handler Unit (AHU). The first floor includes offices, teaching rooms, kitchen, meeting room, server room, and storage room containing the second AHU. The second floor comprises teaching rooms, offices, a meeting room, and a storage room containing the third AHU.

The building staff undertook several actions to implement an improving sustainable policy. Many facilities were integrated to reduce the building's energy consumption and favor the thermal comfort of students. The building is linked to an urban heating network, which provides hot water to the 8.8 MW biomass boiler using wood and straw. The building is heated by an underground floor heating system, radiators and dual-flow ventilation system which contains three AHUs integrating heating coils to enable heating and ventilation. The outdoor air, which is supplied to the building through a Canadian well, is naturally preheated in winter at 9-11 °C even if the outdoor temperature is a negative value. The preheated air flows through an enthalpy wheel that plays the role of a heat recovery system to reach the set-point air supply temperature of 20 °C. If necessary, the hydraulic heating coil turns-on to attain such set-point temperature. In summer, the outdoor air is naturally precooled at 16-18 °C through the Canadian well before it is supplied to the building. In addition, the AHUs are not equipped with cooling coils.

Both heating and ventilation systems are controlled by a Building Management System (BMS) which incorporates an array of air temperature and CO_2 sensors installed in various building locations. Such environmental data is collected in 1-min increments from sensors and is transmitted to the BMS, which enables the staff members to receive feedback on the building performance and occupancy rate. For example, for collecting data regarding the CO_2 concentration, the staff should be aware of whether the space is occupied. RT 2012 limits CO_2 concentrations of <400 ppm for unoccupied space, 400–1000 ppm for occupied space, and >1000 ppm for over-occupied space. In the case of over-occupied spaces, the air volume flow rate is increased by the action of the AHU fan rotation to maintain a CO_2 level less than 1000 ppm. The building was oriented to maximize daylight and winter solar access in the room spaces. A 20 kWc share of power is produced by the 128 m² photovoltaic panels, which are installed on the roof and are south-oriented. Further, rainwater is collected and filtered for sanitary water use.

(a) (b)

Figure 3-1 : EPF school building: (a) north-east view; (b) inside view.

Students occupying the area that includes the café and seating space, referred to as the foyer, reported a significant difference in temperature from that in other parts of the building and indicated dissatisfaction in the thermal conditions. The foyer, located in the south-eastern part of the ground floor (Figure 3-2), is a communal place of life in which students meet every day to eat, rest, and do activities. The foyer has a floor area of 58m^2 and south- and east-oriented glass façades of about 31m^2, including 13m^2 for the former and 18m^2 for the latter. Although these glass façades can improve visual comfort and reduce the lighting and heating energy consumption, it may result in large hot surface areas when exposed to intense solar radiation, thus affecting thermal environmental conditions and as a result the thermal comfort. Table 3-1 shows a brief description of the Foyer.

Figure 3-2 : The Foyer: (a) south-east view; (b) ground floor layout and Foyers' location; (c) inside view.

Table 3-1 : Brief description of the Foyer's characteristics.

Location	Troyes city, France (latitude 48.2° N, longitude 4.07 °E)
Net area	58.0 m²
Dimensions	L x l : 37.16 m x 37.16 m; floor-to-floor = 2.54 m
Ceiling height	2.54 m
Orientation	south- and east-oriented glass façades
Roof	U-value = 0.4 $W.m^{-2}.K^{-1}$
Internal wall	U-value = 4.1 $W.m^{-2}.K^{-1}$
Glass façade	Window Floor ratio = 0.6; double glazing with U = 2.8 $W.m^{-2}.K^{-1}$and SHGC = 0.6; equipped with internal shading.
Internal gains	Light = 3.6 $W.m^{-2}$, occupancy = 0.2 $person.m^{-2}$, appliance = 2 $W.m^{-2}$
Operating hours	Monday to Friday 08:00 to 20:00 (UTC +01:00);
HVAC system	
(a)Ventilation system	Supply air temperature 20°C, heat recovery system efficiency 66% Air volume flow rate 208 $m^3.h^{-1}$
(b)Radiators	Supply water temperature function of outdoor temperature Maximum water volume flow rate 0.1 $m^3.h^{-1}$

3.3 Survey questionnaire

Students' subjective sensations were determined by a survey questionnaire measuring thermal sensation vote (TSV), thermal preference, activity level, etc. The TSV was assessed using the ISO seven-level scale (Cold, Cool, Slightly cool, Neutral, Slightly warm, Warm, Hot) [20,22]. Thermal preference was assessed using a seven-point scale: 'a lot more cooler', 'more cooler', 'a bit more cooler', 'no change', 'a bit more warmer', 'more warmer' and 'a lot more warmer', which signifies that the subject wishes different thermal conditions. In addition, the thermal satisfaction rate was assessed using independent question using a two-point scale: 'satisfied' and 'dissatisfied'. Moreover, students' activity level was evaluated using a five-point scale: 'seated quiet', 'standing relaxed', 'light activity', 'medium activity' and 'high activity'.

The survey questionnaire was constructed using the *surveyplant* website [70]. Then a link was sent to the students in order to answer the questionnaire, the survey was entitled "Current Thermal comfort in the Foyer". The students' completed the questionnaires at the beginning of December 2016 (From 1st until 12th). Table 3-2 summarizes the survey questions and the proposed answers. In total, 53 questionnaires were collected and analyzed from students between the ages of 17-22 during December 2016 (From 1st until 12th). The collected responses are summarized in Table B-1. It is worth noting that the building was occupied by 281 students and staff members in 2016 [90]. Thus, the collected questionnaires represent a sample of 90% confidence interval and a 10% margin of error.

Table 3-2 : Survey questionnaire.

Question	Proposed answers
Do you spend time in the foyer?	(a) yes (b) No
How would you describe the weather outside today?	(a) Clear sky/ Sunny (b) overcast (c) Partly cloudy
How you feel inside the foyer?	(a) Hot (b) Warm (c) Slightly warm (d) Neutral (e) Slightly cool (f) Cool (g) Cold
How would you prefer the indoor condition of the foyer to be?	(a) a lot more cooler. (b) more cooler (c) a bit more cooler (d) no change (e) a bit more warmer (f) more warmer (g) a lot more warmer
Are you satisfied with the indoor conditions of the foyer?	(a) Yes (b) No
How would you describe your activity level in the foyer?	(a) Seated Quite (b) Standing Relaxed (c) Light Activity, standing (d) Medium Activity, Standing (e) High Activity

3.3.1 Thermal Sensation Vote (TSV) and thermal preference

Using the comfort survey questionnaire, TSV and thermal preference of the students were assessed using the questions “How do you feel inside the foyer?” and “How would you prefer the indoor condition of the foyer to be?” respectively. The distribution of collected subjects’ responses is shown in Figure 3-3. The results show that the distribution of students’ thermal sensations was skewed toward the warm side. The most frequently selected vote was “Warm”. More accurately, about 30 % of the students selected this option. In addition, 24.5% of the votes were for the “slightly warm” option. Further, the frequency for "cold" TSV is very small. To test the statistical significance of this response and the possibility to be considered an outlier, numerous types of possible statistical methods can be used [184,185]. In this study, two different methodologies, known as Tukey’s method and Grubbs' test, were employed to detect outliers in the data. Tukey’s method is based on box plots that identify the first (Q1) and third (Q3) quartiles of the data [184]. The difference between these values is known as the interquartile range (IQR). The range for outlier detection is then established by

identifying the inner and upper fences, located at a distance 1.5 IQR below Q1 and above Q3. If the value is less than the lower fence or higher than the upper fence, these values are considered as outliers. The Grubbs' test is a method that uses the approximate normal distribution to detect a single outlier in the dataset [185]. It detects outliers in the dataset through an established hypothesis with two statements – no outlier found or an outlier found in the dataset. In our case, the box plot of the TSV (Figure 3-3b) shows that the "cold" vote lays on the upper fence of the box plot, and the performed Grubbs' test indicated that the "cold" vote is far from the rest, but is not a significant outlier. Based on these results, the response is not considered as an outlier.

The distribution of thermal preference was broadly distributed but was mainly concentrated on the "a bit cooler" option (Figure 3-3c). More specifically, about 39% of the students selected the option "a bit cooler" and about 28% selected the "no change" option. Figure 3-3d shows the detailed relationship between thermal preference and thermal sensation. The first important inference is that the neutral thermal sensation was not preferred by the majority of students. About 80 % of the students who voted for 'Neutral' thermal sensation expressed an expectation to change the thermal conditions in the Foyer, by voting 'a bit warmer', 'a bit cooler', and 'more cooler'. The second important inference is that students tended to be more receptive to 'slightly warm' conditions. With about 50% of the students who voted 'slightly warm' did not vote to change the thermal conditions, and 56.25 % of the students who felt 'warm' preferred a bit cooler thermal conditions.

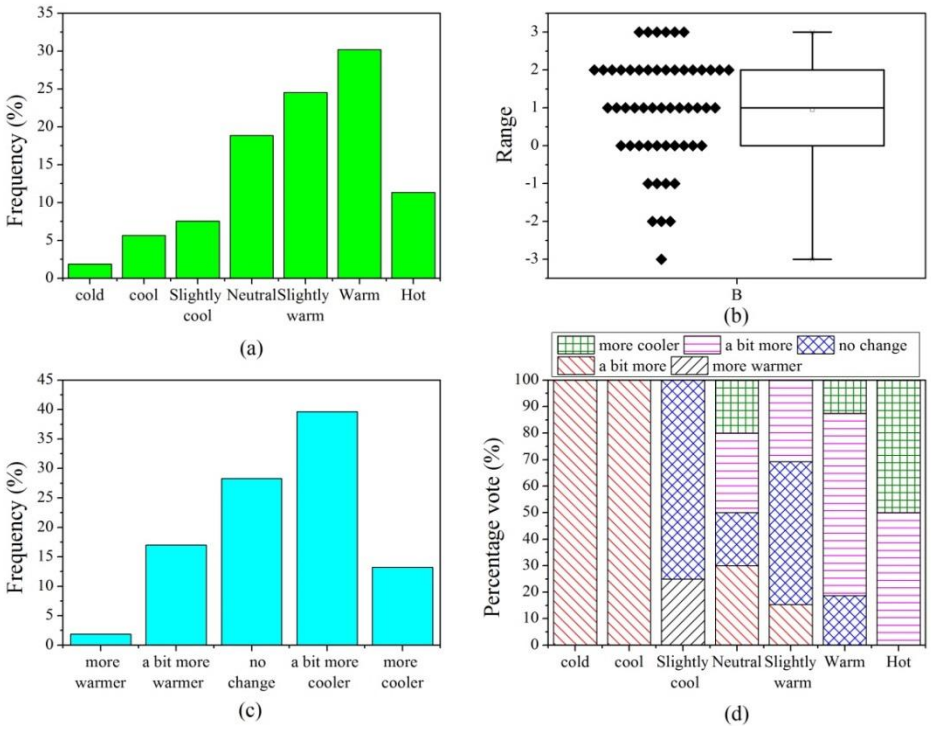

Figure 3-3 : Statistical summary of survey questions: (a) TSV, (b) box plot of TSV, (c) thermal preference and (d) relationship between thermal sensation and thermal preference.

3.3.2 Relationship between TSV and climate

In order to examine the relationship between thermal sensation and outdoor climatic conditions, the students were asked to answer the question "How would you describe the weather outside today?" and the three options were: "overcast", "partially cloudy", and "Sunny". These three options were based on weather data collected by a weather station in Barberey located 11.5km from the considered case study and are displayed online [186]. Figure 3-4 shows the distribution of collected responses and the detailed relationship between thermal sensation and outdoor climate. The results show that the majority of the students, nearly 70%, answered the survey questionnaire during a winter day with sunny sky. In addition, slightly warm, warm and hot were voted by the overwhelming majority of the respondent, nearly 80%, who answered sunny. On the other hand, the results show that during a partially cloud day, about 70% of the respondent voted between "slightly cool" and "slightly warm". Moreover, the "cold" and "hot" votes appeared only during "overcast" and "sunny" days, respectively. These results show a wide variation in thermal sensation during different climatic conditions. These results could be correlated to the presence of fully glazed facades because frequent changes in the outdoor climate affect the MRT, and eventually students' thermal comfort.

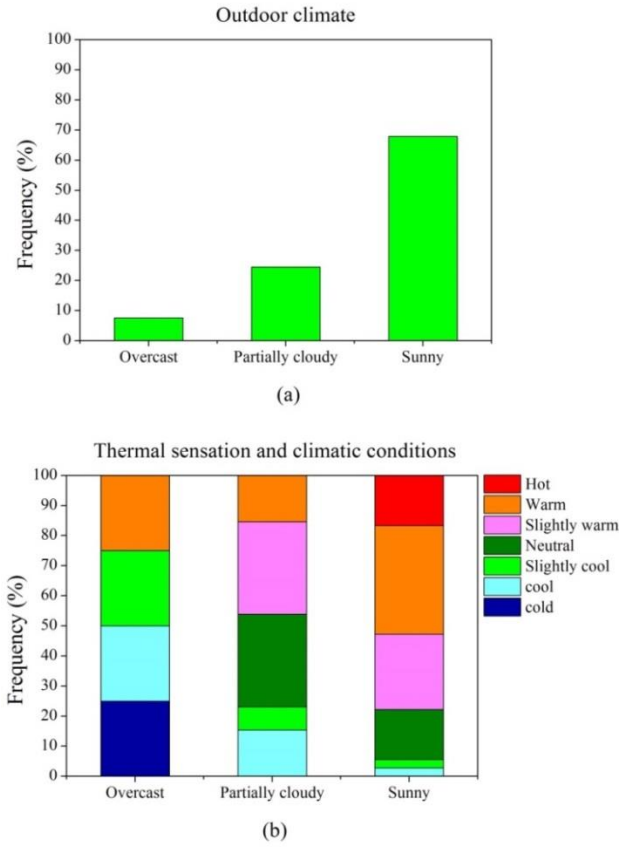

Figure 3-4: Statistical summary of survey questions: (a) outdoor climatic conditions during the questionnaire time and (b) relationship between thermal sensation and climatic conditions.

3.3.3 Effect of activity level on thermal sensation and preference

Activity level of the students attending the Foyer was evaluated using the question "How would you describe your activity level in the foyer?" Figure 3-5 shows the distribution of collected responses, the relationship between activity level and TSV, and the detailed relationship between activity level and thermal preference. The statistical results show that students' activity level was broadly distributed, but was centered around the three options 'standing relaxed', 'light activity' and 'medium activity'. The results show that about 60% of the students' respond with an activity level higher than 'standing relaxed', the assumed activity level during the design phase. This justifies why the 'warm' option appeared the most in the TSV.

Another important inference driven from the results is that neutral sensation appeared mainly with the standing relaxed votes and continued in descending order as we move away. Moreover, 46.6% of the respondents voted 'standing relaxed' preferred for no change in the thermal conditions. Furthermore, the majority of thermal preference for cooler thermal environment is distributed among the activity levels above the design value, while warmer thermal preference is concentrated mainly on the seated quiet option.

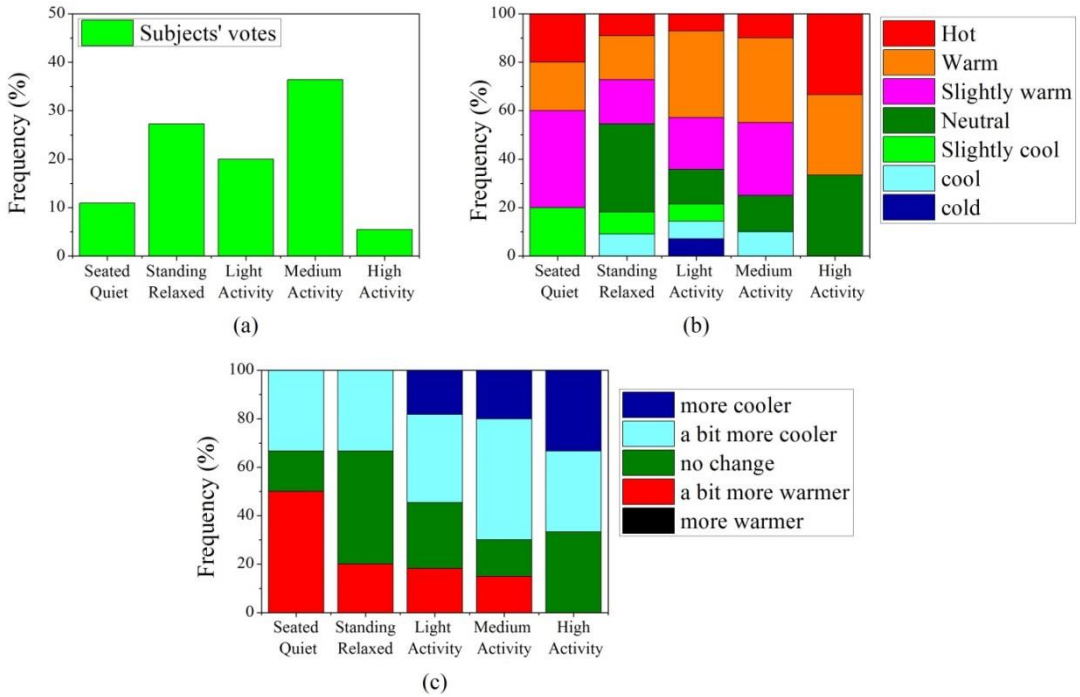

Figure 3-5: Statistical summary of survey questions: (a) students' activity level, (b) relationship between thermal sensation and activity level and (c) relationship between thermal preference and activity level.

3.3.4 Relationship between TSV and Satisfaction

Thermal satisfaction of the students was evaluated using the question "Are you satisfied with the indoor conditions of the foyer?" it was noted that 37% of the students' responses were dissatisfied. This value is above standards recommendations for the three different levels of acceptable classes of thermal comfort [20,27]. This means that the thermal comfort in the studied room is below expectations. Figure 3-6 illustrates the thermal satisfaction of the students as a function of TSV. One can observe that a neutral thermal sensation corresponds to the most satisfaction assessment, although 80% of students vote to change the thermal conditions (Figure 3-3). These results show that occupants may ask for cooler or warmer conditions even though they are satisfied with the indoor environment. In addition, when thermal sensation moves from neutral, more votes for dissatisfaction appear in the results. Another important inference is that the students expressed the least dissatisfaction when they felt slightly warm, while more dissatisfaction is expressed when they felt slightly cool. This may have occurred because the students became acclimatized to neutral or slightly warm thermal conditions in winter owing to the wide use of heating systems.

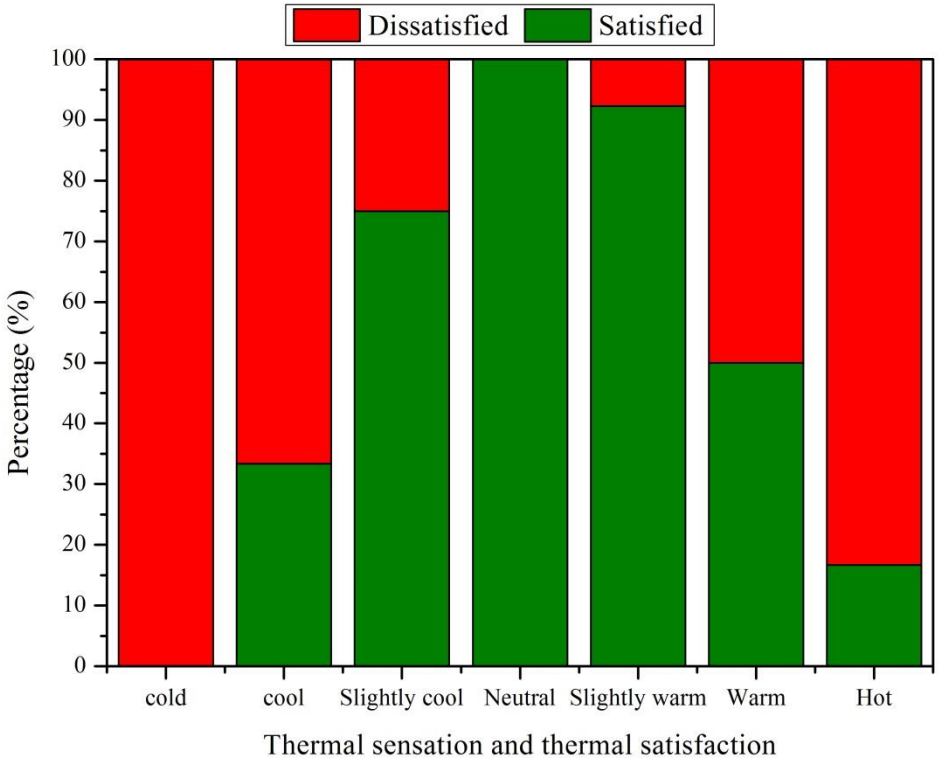

Figure 3-6: Relationship between thermal sensation and thermal satisfaction.

These results show that some students experience thermal discomfort in the foyer during winter. This could be correlated to the presence of the highly glazed envelope because frequent changes in the outdoor climate affect the mean radiant temperature. For instance, during sunny skies, a high-intensity of solar radiation may lead to high radiant temperature values, contrarily during cold days, low outdoor temperature with low solar radiation could lead to lower radiant temperature. Because the radiant temperature has a major influence on thermal comfort, this may have caused the aforementioned thermal discomfort.

In addition, occupants' thermal discomfort could be correlated to the heating system and occupants related parameters (such as activity level and clothing insulation), since from the survey results one can observe that different types of activity levels are occurring in the Foyer. Thus further investigations are required.

In this concern, the foyer was considered for investigation and analysis of the occupants' thermal comfort by means of in-situ measurements and numerical simulation. Measurements were fulfilled to confirm the students' complains and to understand the impact of physical and human parameters on thermal discomfort. The numerical study may be complementary to measurements and may be used as a fast and simple tool to predict occupants' thermal comfort by testing several scenarios such as a regulated heating system and a decreased area of glazing.

3.4 Dynamic numerical model

3.4.1 Model development

The dynamic numerical model of the deemed case study is developed using the Dymola® graphical interface. Figure 3-7 describes the interaction among the sub-models and Figure 3-8 shows the Dymola® model. Both Modelica Buildings Library and Modelica Standard Library have been used for this purpose. A detailed description of the model and the used components is presented below.

- ***Room model:*** `MixedAir` of the `Rooms` package [71] is the main component of the model. It is used to illustrate a single room with an unlimited number of opaque constructions. It implies that the air inside the room is completely mixed and simulates all the heat transfer processes (convection, conduction, solar radiation, and infrared radiation) within the room and through the building envelope. Hence, it takes into consideration the heat transfer through walls, ceiling, floor, and windows. The properties of the interior walls, ceiling, and floor are represented using the components `OpaqueConstructions` and `SingleLayer` of the `HeatTransfer` package. The thermal properties of the glazing façades were presented using the component `GlazingSystems` from the `HeatTransfer` package. The glazed

walls in the Foyer have no overhangs and side fins. However, it is equipped with roller blinds. Since our case study is a highly glazed room, it is important to understand the thermal performance of the transparent envelope. The heat transfer through the transparent envelope is completely represented by its thermal properties (first term of Equation (3.1)), or solar optical properties (second term of Equation (3.1)) [187],

$$Q = UA_{pf}(T_{ex} - T_{in}) + (SHGC)A_{pf}G_t \quad (3.1)$$

where Q is the total heat flow through the transparent envelope, U-value is the overall coefficient of heat transfer, T_{ex} and T_{in} are the exterior and the interior air temperatures, respectively, A_{pf} is the total projected area of fenestration, SHGC is solar heat gain coefficient, and G_t is the incident total irradiance. U-value or the thermal transmittance and the SHGC can be determined as illustrated in [187].

- ***Weather data model:*** The `ReaderTMY3` component of the `BoundaryConditions` package [73] was used to represent the outdoor weather conditions. The atmospheric pressure is a set parameter in the weather data reader, while the other parameters are obtained from the `TMY3` file. Another possibility is to use a constant value or an input connector for some parameters (dry bulb temperature, relative humidity, infrared horizontal radiation).
- ***Ventilation, heating and internal gains models:*** the mechanical ventilation system of the Foyer was implemented into our model by using the `FlowControlled_m_flow` of the `Fluid` package [72]. This component describes a fan with a prescribed mass flow rate. The prescribed mass flow rate and temperature of the ventilation systems were obtained from the BMS and implemented into our model using a `DaySchedule` of the `Rooms` package [71]. A `ConstantEffectiveness` heat exchanger of the `Fluid` package [72] is used to depict the heat recovery system. This component transfers the heat expressed as εQ_{max}, where ε is the constant effectiveness and Q_{max} is the maximum heat that can be transferred. The heating system was modeled using the `RadiatorEN442_2` of the `Fluid` package [72], It represents a radiator that can be used as a dynamic- or steady-state model. Moreover, `DaySchedule` was used to represent the occupancy profile in the Foyer. The `DaySchedule` was connected to the inlet connector `qGai` flow of the `MixedAir` model in order to add the internal radiative, convective and latent heat gains.

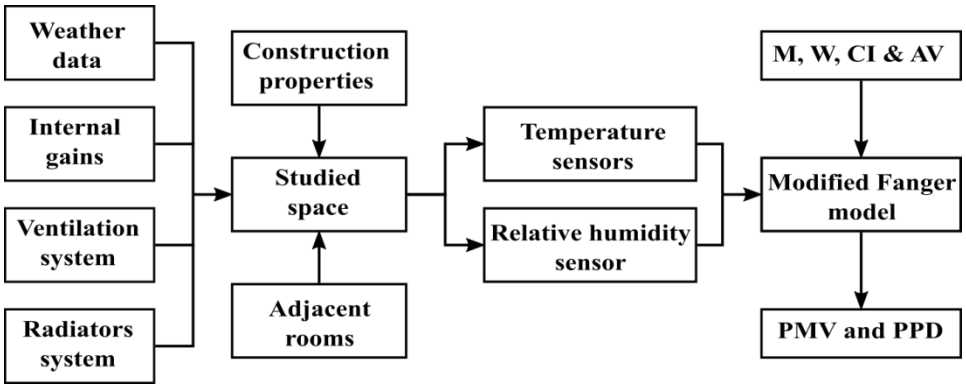

Figure 3-7 : Modelica model of the Foyer: Block diagram of sub-models

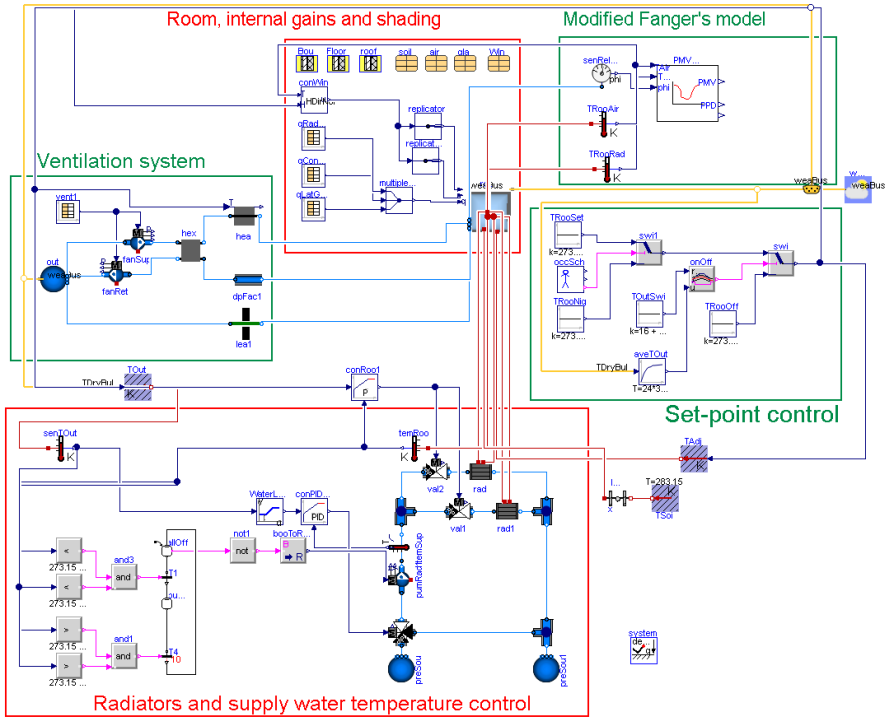

Figure 3-8 : Global Dymola® model of the Foyer

- ***Modified Fanger Model***: `Fanger` component of the `Utilities` package in the Modelica Buildings library was associated with the model to calculate the PMV and PPD values during simulation time. This model uses Equation (3.2) to calculate the clothing surface temperature. However, based on ISO 7730, ASHRAE and European standards [20,79,188], Equation (1.7) must be used for the calculation of the clothing surface temperature. In this context, the component was modified and Equation (3.2) was replaced by Equation (1.7). The six parameters that are used to calculate PMV and PPD could be implemented to the model as constant values or using input connectors.

$$T_{cl} = 35.7 - 0.0275(M - W) - 0.155I_{cl} \times [(M - W) - 3.05 \times 10^{-3}\{5733 - 6.99(M - W) - P_a\} - 0.42 \times \{(M - W) - 58.15\} - 1.7 \times 10^{-5}M(5867 - P_a) - 0.0014M(34 - T_a)] \quad (3.2)$$

In order to quantify the deviations between the existing and the modified `Fanger` models, the calculated values using both models were compared with the values calculated using ASHRAE-55 and EN-15251 [79,188]. Figure 3-9 shows the obtained PMV results as a function of the operative temperature. The results show that the modified model predicts better the PMV index, the maximum discrepancy between the obtained results from the modified model and the standards was 0.09, while the discrepancies reached 1.21 using the original model. These results could be considered sufficient to confirm the validation of the modified `Fanger` model. Based on these findings, the modified model was used in the later parts of this study for the calculation of the PMV index.

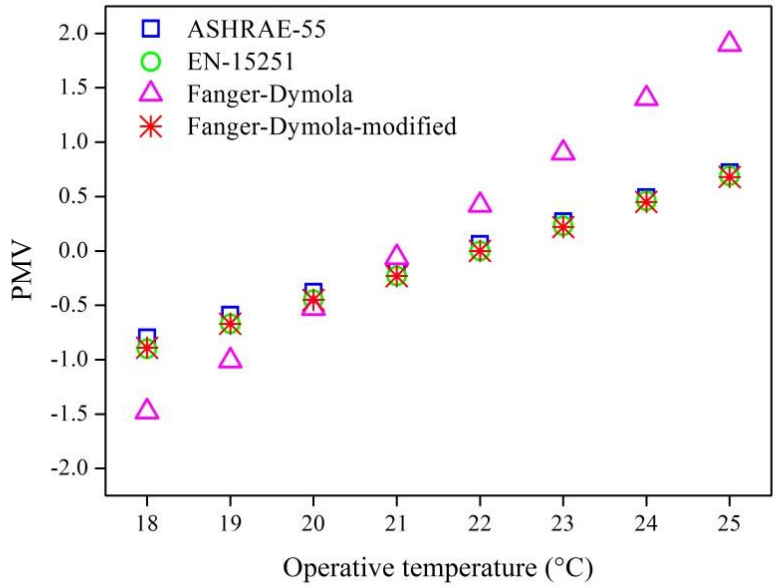

Figure 3-9: Modified Fanger model validation results.

3.4.2 Model validation

The validation of the developed model is essential since the prediction capability of the model is an influential factor in order to reflect the reliability of the results. To validate the developed model, predicted results are compared with real data taken from the building.

In a previous study [189], an in-situ measurement to monitor the environmental parameters within the foyer was conducted. The aim was to calculate and analyze the thermal comfort indices

PMV and PPD in order to assess the thermal comfort levels. The authors used a multifunctional sensor, shown in Figure 3-10, developed by l'Institut d'Electronique et des Systèmes (IES) (University of Montpellier) to monitor the environmental parameters of the foyer such as room temperature, mean radiant temperature, relative humidity, and air velocity and to calculate and visualize in real time the indices of thermal comfort (PMV and PPD). In such a system, a sensor transmits the data to a work station using Wi-Fi. During data collection, the measurements made by the sensor are recorded as data frames in text files that are directly used to plot the evolution of the different physical quantities during the series of measurements. This same interface also enables modification of complementary parameters such as metabolic rate and clothing insulation to calculate the PMV and PPD. The metabolic rate was assumed to be 70 $W.m^{-2}$ (1.2 met), representing sedentary activity. The clothing level was assumed to be 0.155 $K.m^2.W^{-1}$ (1 clo) for typical winter clothing. Table 3-3 summarizes the sensor characteristics and the five measurement cycles conducted from Wednesday, 12 November, until Friday, 14 November 2014.

Figure 3-10: Multifunctional sensor.

Table 3-3 : Multifunctional sensor characteristics and experimental cycles.

Parameters	Range of variation	Accuracy
Ambient temperature (°C)	[-40.0, 123.8]	± 0.4
Mean radiant temperature (°C)	[0, 100]	± 0.4
Relative humidity (%)	[0, 100]	± 3
Air velocity ($m.s^{-1}$)	[0.05, 5.00]	± 0.05 for [0.05, 1.00] ± 0.15 for [1.00, 5.00]

Experimental cycles					
	12/11		13/11	14/11	
	Cycle 1	Cycle 2	Cycle 3	Cycle 4	Cycle 5
Start hour	10:47 am	2:46 pm	8:21 am	10:01 am	2:31 pm
End hour	11:29 am	6:36 pm	8 :55 am (+1 day)	11:49 am	5:31 pm

For the validation, the predicted room temperature and relative humidity are compared with measured data. NMBE, CVRMSE and the coefficient of determination (R^2) were used to quantify the deviations between predicted and measured values. Figure 3-11 shows the discrepancies between the predicted results and the measured room temperature and relative humidity of the third cycle. The discrepancies averaged about -0.25 °C for the room temperature and 1.1% for the relative humidity. However, the discrepancies regarding the room temperature reached a maximum of 1.7°C during the presence of solar radiations and averaged about 0.4°C for the rest of the time. These results show that

the discrepancies were less than the uncertainty of the measurements (less than 0.4°C and 3% for the room temperature and relative humidity, respectively) for the overwhelming majority of the experimentation time as shown in Figure 3-11. It is suggested that this difference in experimentation time leads to more discrepancies between simulation and measurement data due to experimental errors, which are affected by the accuracy of the sensor. Another reason could be the lack of solar radiation data on the experimentation day, which affects the room temperature due to the presence of the two glazed external walls.

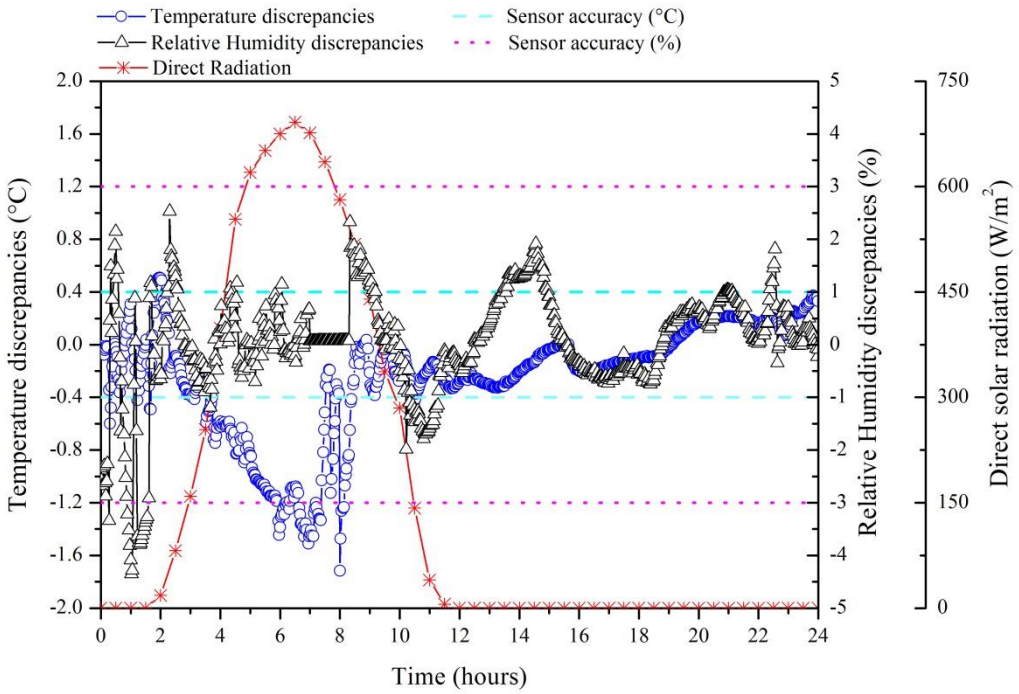

Figure 3-11: Discrepancies between the predicted and measured room temperature and relative humidity of the third cycle.

The NMBE and CVRMSE of both the room temperature and relative humidity for the five measurement cycles are calculated and reported in Table 3-4. The obtained values of both NMBE and CVRMSE are within the acceptable limits of $\pm 10\%$ and $\pm 30\%$, respectively [74]. The negative signs indicated that the model overpredicts the temperature and relative humidity on average.

Table 3-4 : NMBE and CVRMSE of the room temperature and relative humidity for the five cycles.

NMBE (%)	Cycle 1	Cycle 2	Cycle 3	Cycle 4	Cycle 5
Room Temperature	-2.12	-2.60	-0.29	-1.25	-4.68
Relative humidity	-2.21	1.55	-1.13	1.85	-3.10
CVRMSE (%)					
Room Temperature	2.20	5.00	6.38	2.40	4.73
Relative humidity	2.23	3.09	3.43	2.56	2.89

Moreover, the coefficient of determination that can give an indication of how the predicted values fit the measured data is obtained by plotting the predicted values on a scatter graph as a function of measured values. Figure 3-12 and Figure 3-13 give the obtained coefficient of determination. A good correlation is observed showing an R^2 value of 0.9751 and 0.9083 for the room temperature and relative humidity, respectively, meaning that 97.51% and 90.83% of the variance is explained by the model. In addition, the results show that the deviation of all the data is within a 10% deviation of the model.

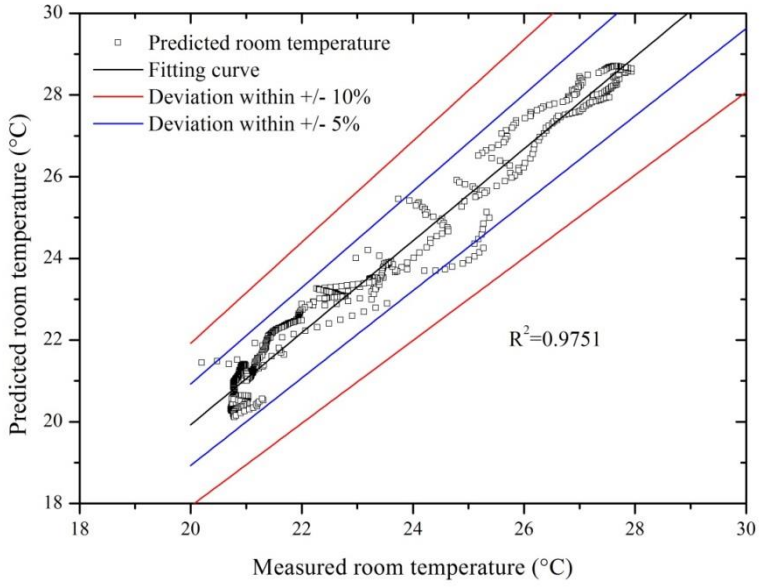

Figure 3-12 : Coefficient of determination of the room temperature for the five cycles and the relative deviation of the model prediction.

Furthermore, the average values of PMV and PPD obtained from both experimental and numerical studies for the five considered cycles are presented in Figure 3-14. The results show a good agreement between simulation and calculated results based on measured data. In general, all the obtained average values of PMV are negative and fall outside the acceptable comfort range [-0.5, +0.5]. Consequently, all the obtained average values of PPD are above the recommended comfort range of 10 %. These results indicate that the indoor thermal environment of the Foyer is cold. We note that the average outside temperatures have decreased gradually from 12th to 14th of November. These data are consistent with the measured PMV values which indicate that the indoor environment of the Foyer has become colder.

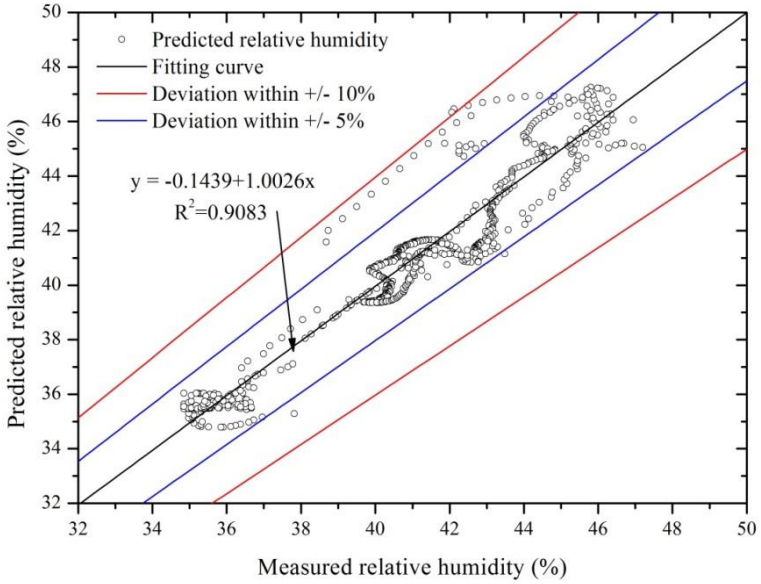

Figure 3-13: Coefficient of determination of relative humidity for the five cycles and the relative deviation of the model prediction.

Lastly, all the obtained results indicate that the model prediction is in good agreement with the measured data, although some discrepancies were noticed. These discrepancies could be attributed to experimental errors which are a function of the accuracy of the sensor. As well as the lack of exact occupancy profile at the time of experimentations and some weather data parameters, such as the solar radiation, outside relative humidity and wind speed and direction during the experimentation time could be the reason of much of the discrepancies observed at the beginning of the experimentation work and during the presence of intense direct solar radiations. On the other hand, the discrepancies can be reduced by monitoring occupancy profiles and matching simulation schedules with real data; however, this could result in increasing modelling time and complexity and outcomes robust results for specified periods.

Therefore, based on all these aforementioned discussions and bearing in mind that the main intention is to obtain a model that is able to represent the real building in general terms rather than out coming exact results for a specified time, the model is considered to be validated and deems it useful for further evaluations and investigations.

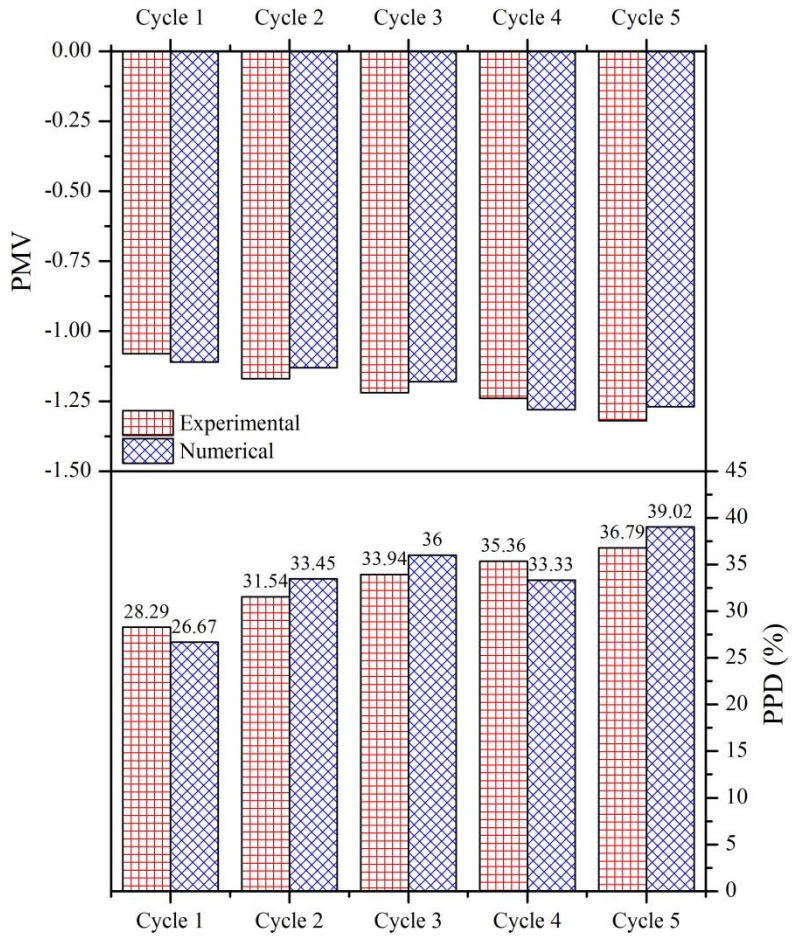

Figure 3-14: Average values of PMV and the corresponding PPD for the various cycles

3.5 Thermal comfort assessment

In order to evaluate and analyze the thermal comfort features of the foyer, the developed model was used to conduct simulations throughout representative winter days and the whole winter season. Using different time scale is important in the evaluation of building behavior because a building can have satisfactory behavior over a yearly or seasonally basis, while problems occur on a daily basis.

3.5.1 Daily basis

The thermal performance simulations highlighted the evolution of the PMV index and the MRT on four winter days corresponding to bright overcast, partly cloudy, dark overcast and sunny skies, noted as cases A, B, C and D, respectively. Outdoor temperatures, global solar radiations and solar

altitude angles are illustrated in Figure 3-15 and summarized in Table 3-5. Case A represents a typical winter day with no direct solar radiation due to overcast sky. Case B signifies a winter day with relatively high outdoor temperature and solar radiation. Case C designates a winter day with low outdoor temperature and weak solar radiation. Case D denotes a winter day with relatively high outdoor temperature and intense solar radiation.

Table 3-5: Outdoor climatic data of the different cases.

	Outdoor temperature (°C)		Global Solar radiation (W.m^{-2})
	min	max	max
Case A: Ordinary	2.23	6.32	124.11
Case B: Partly cloudy	-1.70	9.30	334.00
Case C: Cold	-4.40	-2.90	84.34
Case D: Sunny	1.30	11.40	594.63

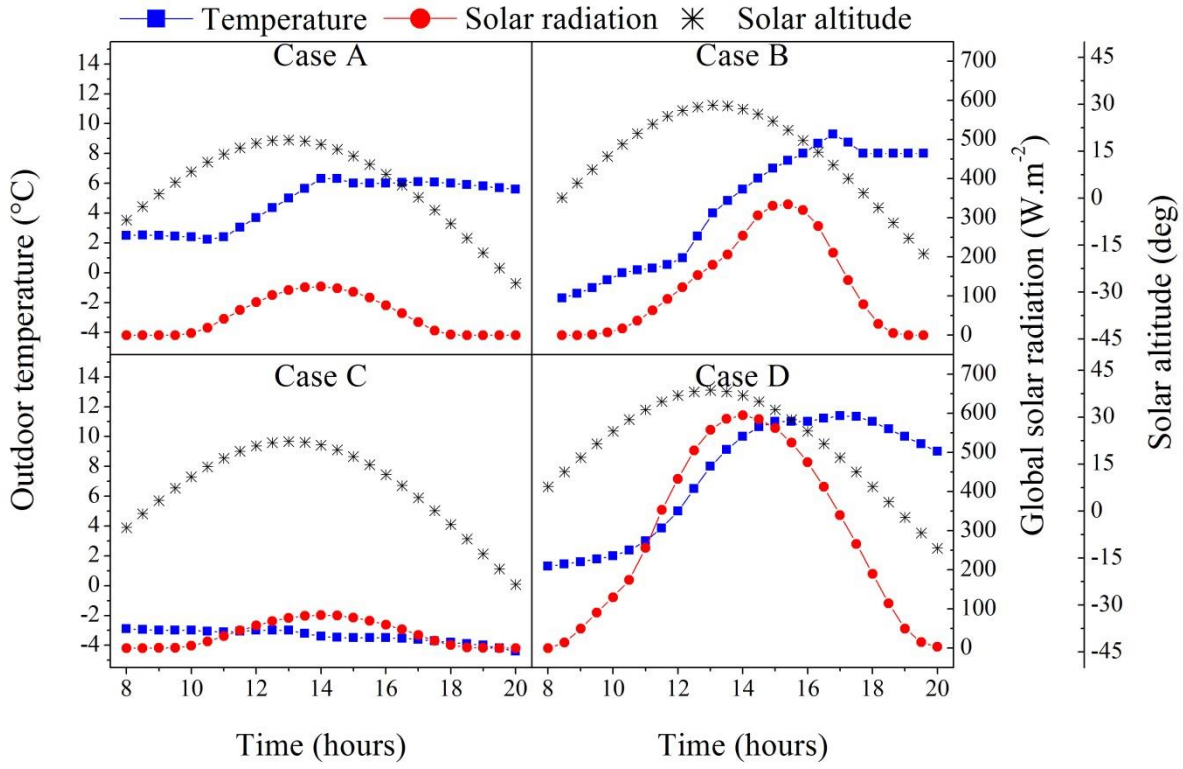

Figure 3-15: Outdoor climatic conditions of the four studied days.

PMV index and the mean radiant temperature of the four studied days are illustrated in Figure 3-16 (numerical data are reported in Table C-1). For cases A and B, the PMV index was stable until 10:00; it then started to increase to reach its maximum when the outdoor temperature and solar radiation reached their maximum at 14:30. The PMV index then decreased and maintained a stable value. For case C, the PMV index was below the acceptable comfort range throughout the entire occupied time. However, for case D, the PMV index exceeded the acceptable upper limit of PMV +0.5.

Figure 3-16 shows that the PMV index followed the same trend as the MRT, which also followed the same trend as the solar radiations. The obtained values of PMV were then correlated with MRT values to quantify the correlation between both parameters, as shown in Figure 3-17. A good correlation is observed showing an R^2 values greater than or equal to 0.95, meaning that more than 95% of the variance is explained by the variation of MRT. This indicates that PMV variations are correlated to the MRT variations due to the presence of extensive glass areas.

Moreover, simulation results are in good agreement with the survey results, and the obtained results justify why 75% of the votes in an overcast day were between "slightly cool" and "cold". In addition PMV index results of a day with relatively high outdoor temperature and strong solar radiation confirm the 80% appearance of the three votes, "slightly warm", "warm" and "hot".

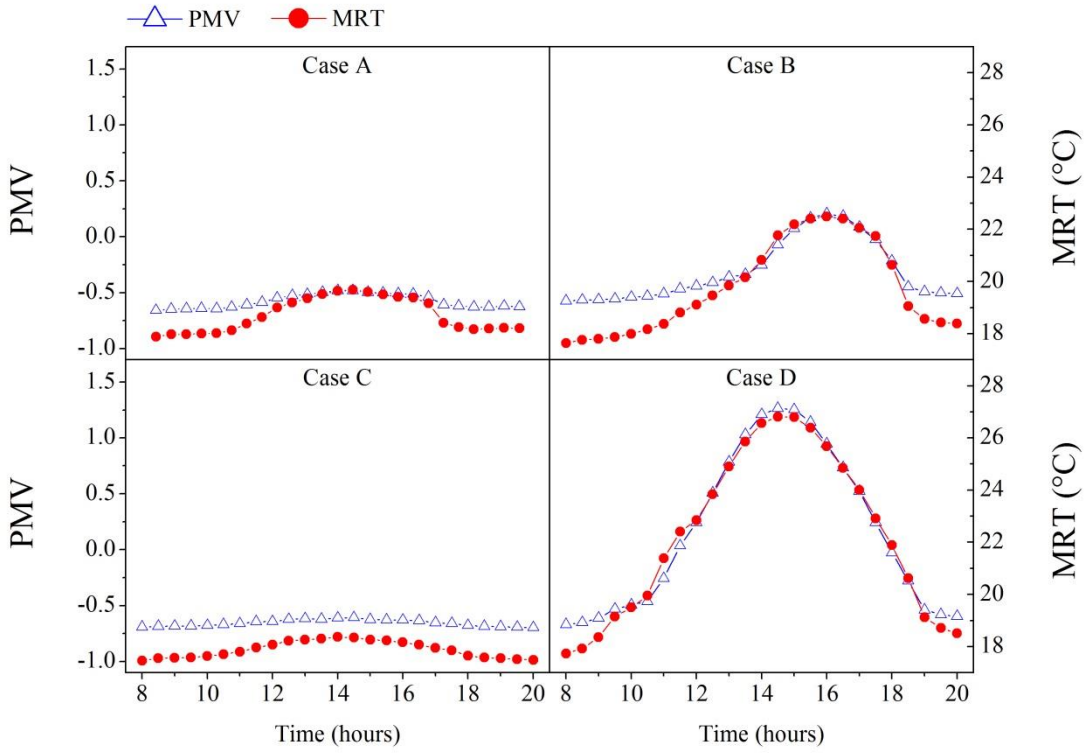

Figure 3-16 : PMV and MRT of the four studied days.

Furthermore, students' votes show a different activity level while spending time at the Foyer. In this regards, an investigation using the validated model was carried out to evaluate the effect of activity level on the PMV index during the four studied days. Figure 3-18 shows the PMV index for the different activity levels appeared in the students' votes (numerical data are reported in Table C-2). The results show that, for an ordinary or cold winter day, the PMV index falls below the acceptable comfort limits for a student with seated quiet or standing relaxed activity level. However, the PMV

index was maintained within the acceptable comfort range for a Light or Medium activity levels, and around the upper comfort limit for high activity level. Besides, on the day with intense solar radiation, the PMV index exceeded the upper comfort limit for all activity levels during the presence of the solar radiation.

These results explain the appearance of different votes and confirm the high variability of students' thermal sensation during the same period. For example, a student with low activity level present in the Foyer during the lack of solar radiation may experience a thermal sensation between "slightly cool" and "cold" depending on the other factors, such as clothing insulation. However, a student with the same activity level present in the Foyer during the occurrence of intense solar radiation may experience a "slightly warm", "warm" or "hot" thermal sensation depending on the other factors.

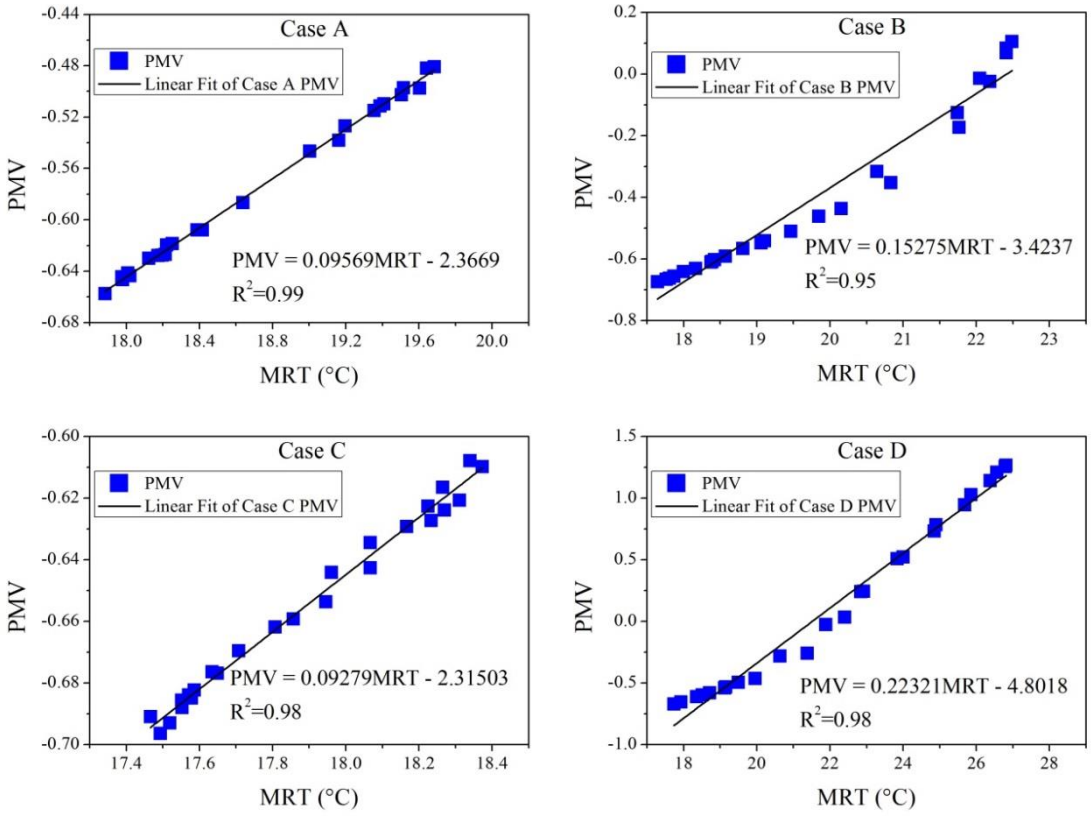

Figure 3-17 : Correlation between PMV and MRT.

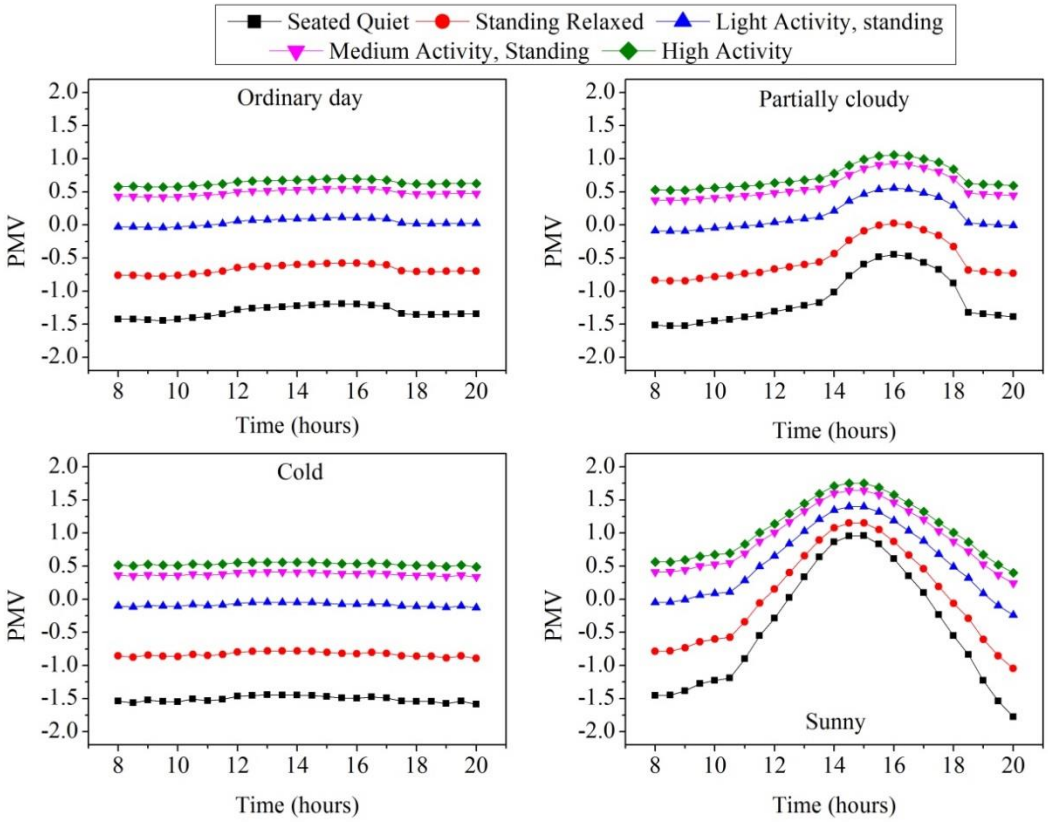

Figure 3-18: Effect of activity level on the PMV index in the four studied days.

3.5.2 Seasonal basis

In order to evaluate and analyze the thermal comfort features of the foyer, the developed model was used to conduct simulations throughout the heating period. The supply air temperature of the foyer was generally set at 20 °C during the heating season. However, the new French standards recommend that the room temperature set-point should be 19 °C. In this regard, the two cases with set-point room temperatures of 19 °C and 20 °C were studied.

Table 3-6 shows the frequency of the PMV index of both room temperature set-points of 19 °C and 20 °C for the entire heating period. The PMV index values at the two set-points varied at −1.5 to +3.0 and −0.7 to +3.0, respectively. The results indicate that 79.5% and 67.8% of the PMV indices at set-points of 19 °C and 20 °C, respectively, fell outside the acceptable comfort range of [-0.5, +0.5]; therefore, the recommended 10% PPD was not satisfied. At a set-point of 20 °C the thermal comfort was better maintained with 4.7% of the PMV indices outside the range of [-0.7, +0.7] compared with 64.5% at a set-point of 19 °C. This resulted in 15% PPD for 4.7% of the occupied time, which is slightly above the recommended 3% to satisfy the moderate expectation level.

Table 3-6 : Frequency (hours) of the PMV index during heating period.

PMV index	Set-point	
	19 °C	20 °C
-1.0 to -0.7	1442	0
-0.7 to -0.5	306	1427
-0.5 to -0.2	187	441
-0.2 to +0.2	199	214
+0.2 to +0.5	98	105
+0.5 to +0.7	49	68
+0.7 to +1.0	44	52
+1.0 to +1.5	34	49
+1.5 to +3.0	7	10
% outside category A, B, C and resultant comfort class		
A	91.58	90.95
B	79.54	67.87
C	64.53	4.69
Class	IV	IV

The results showed that occupants' thermal sensations of both hot and cold are expected. This relates to the fact that regular changes in the outdoor climate results in changes in ventilation and transmission heat loss. When the outdoor temperature and solar radiation reach maximum values, the external surface temperature of the glass façade increases, resulting in an increase in the internal wall surface temperature. This result is attributed to the thermal storage effect, which allows for an increased mean radiant temperature. On the contrary, low outdoor temperatures with low solar radiation could lead to a decrease in the mean radiant temperature. These frequent changes in mean radiant temperature affect the thermal comfort.

In addition, these results show that, PMV index, which designates the thermal sensation of a large group of people, is sensitive to the outdoor climatic condition, the activity level of the subjects and the set-point temperature. However, PMV index is directly and indirectly influenced by other main factors such as clothing insulation which directly affect the thermal sensation of occupants and glazing area which indirectly affect the PMV value by affecting the mean radiant temperature. Therefore, it is essential to investigate the sensitivity of the PMV index to some of these factors in order to evaluate the effect of each factor on the thermal comfort and to determine the most critical factors affecting the PMV value.

3.6 Conclusion

In this chapter, we adopted a highly glazed room within the European context for investigations. This case has been considered because it represents an informative and useful case study as well as because we had easy access to data, which allows for subjective and objective assessment of the thermal environment. A description of the case study is given followed by a subjective evaluation of thermal comfort conditions. Subjective thermal comfort was assessed using a survey questionnaire.

The collected responses show that 37% of the respondents were dissatisfied with the thermal environmental conditions. Then, a dynamic numerical model was developed and validated by comparing its predictions with objective measurement of room temperature and relative humidity. Additionally, model predictions were in agreement with the collected responses, which confirm the adequacy of the model. The validated model is then used to extend the investigation to the whole winter season.

The performed investigations indicated that the actual behavior of the selected case study is unsatisfactory, for both occupants and standards recommendations. In this case and to overcome this problem, we will focus now on reformulating the structure of the room. For this, we need to build knowledge on the relationship between design parameters and behaviors associated with functional requirements. This knowledge consists in identifying the critical parameters that affect thermal comfort in order to be able to regulate the design parameters of the room to achieve the desired thermal behavior. In this consequence, sensitivity analysis based on the DoE technique will be employed.

Chapter 4: Sensitivity study

4.1 Introduction

Sensitivity analysis (SA) is a local measure of the effect of a given input on a given output [161]. It is a valuable approach that can be used to identify the critical parameters influencing a response variable, such as building thermal performance. Applying such an approach to the deemed case study is important because the evaluation of the actual behavior, thermal performance, was unsatisfactory. Thus, identifying the key parameters affecting thermal comfort is a first step towards reformulating the structure; here structure stands for room envelope and systems, to achieve the desired thermal comfort levels.

The aim of this chapter is to build knowledge of the relationship between design parameters and occupants' thermal comfort. For this purpose, the DoE technique is used to develop the required plan of experiment. The use of DoE allows analyzing the sensitivity of thermal comfort index to the considered factors as well as the development of a meta-modeling relationship between the PMV index and deemed design parameters. The obtained meta-models are then used to integrate occupants' thermal comfort in the optimization process to achieve an optimal design. In order to implement the DoE technique, the steps presented in section 2.3.3 are followed.

4.2 Response variables and choice of factors and levels

The response variables are the average daily, maximum, and minimum PMV values. The reason behind the average daily value is that it makes no sense to have a weekly, monthly or yearly PMV value because it can frequently change during the day; in addition the average can be considered as a representative value to replace the hourly values. However, the average value alone, in the case of occupants' feeling, is not meaningful if not complemented by the maximum and minimum values. This helps in determining if the PMV value exceeded the upper or lower acceptable comfort limit.

PMV index is influenced by room temperature, MRT, relative humidity, air velocity, metabolic rate, and clothing insulation. Relative humidity and air velocity were excluded from the sensitivity study, since the PMV index was found to be less sensitive for both parameters compared to the four other parameters [76,77]. Additionally, since MRT is highly influenced by the outdoor climatic condition, as previously discussed, due to the presence of fully external glazed façades, it was replaced by the sol-air temperature. This last is a parameter defined as "the outside air temperature which, in the absence of solar radiation, would give the same temperature distribution and rate of heat transfer through a wall/roof as exists due to the combined effects of the actual outdoor temperature distribution

plus the incident solar radiation" [75]. The sol-air temperature was found to be a good illustration of the weather conditions [190]. The hourly and monthly sol-air temperature can be calculated using Equation (4.1) [75,191].

$$T_{sol-air} = \frac{\sum_{i=1}^{n}\left(T_{db,i} + \frac{\beta I_{h,i}}{h_{ex}}\right)}{n} \quad (4.1)$$

where T_{db} and I_h are the hourly outdoor dry-bulb temperature (°C), and global horizontal solar irradiance (W.m^{-2}), β is the solar radiation absorptivity of the surface exposed to solar radiation, h_{ex} is the external surface heat transfer coefficient (W.m^{-2}.K^{-1}), and n is the number of hours for a specific month. The values of T_o and I_h were obtained using Modelica TMY3 file. A default values of 0.6 and 17.78 W.m^{-2}.K^{-1} respectively for β and $h_{ex}$was assigned as stated in [190,191].

Lastly, the effect of the external glass façades on the PMV index was considered using both Window-to-Floor Ratio (WFR) and window type as two independent factors affecting the response variable.

Each considered parameter has a lower (-1) and higher (+1) level. The high level of the WFR (60%) and glazing type (double glazing with u-value = 2.8 W.m^{-2}.K^{-1} and SHGC = 0.77) represents the base case study, and the low level, 16% WFR and triple low-emissivity glazing (u-value = 0.7 W.m^{-2}.K^{-1} and SHGC = 0.3), has been selected with respect to the values that are recommended by the French and the European standards [7,79]. The daily average sol-air temperature was calculated and the minimum and maximum values were chosen to represent the lower and higher levels. While, the levels of the remaining factors were selected based on the questionnaire results and the recommended values by the standards [7,79]. Table 4-1 reports the considered parameters and their corresponding codes and levels.

Table 4-1: Investigated factors and their corresponding codes and levels.

Factor	Code	Unit	Level	
			-1	+1
Clothing insulation	*A*	clo	0.8	1.2
Metabolic rate	*B*	W.m^{-2}	58	125
Room temperature	*C*	°C	19	21
average daily sol-air temperature	*D*	°C	-2.2	17.2
glazing type (u-value)	*E*	W.m^{-2}.K^{-1}	0.7	2.8
(g-value)			0.3	0.77
WFR	*F*	%	16	60

4.3 Choice of design and performing the experiments

It is recommended to start any experimental design using a factorial plan of experiments [192]. This will yield developing a first order meta-model. If the meta-models are valid, then the metamodeling work is ended. Otherwise, the next step is to develop a second-order meta-model by using a face-centered composite design (CCD) [58]. This design consists of adding experimental points to the factorial design. In this study, DoE was performed using a two-level full factorial design. This design considers all possible factors combination. The full factorial design aims to identify the significant variables that influence the response variable, PMV index in our case. In addition, it helps to analyze the interaction between these factors [80], and also it offers more precise results compared to fractional factorial design and avoids specious conclusions [81]. The number of experiments, simulations in our case, is 2^k, where k is the number of factors. This design results in 64 simulations to investigate the main effect of factors and their interactions. Figure 4-1 shows the design matrix (64 runs) and the response variables resulting from the simulation results (numerical data are reported in Table D-1). Each run represents a unique combination of factors levels (e.g. first run represents all the factors at the lower level (-1), and last run all the factors at the higher level (+1)) and the resulting daily average, maximum, and minimum PMV values. Minitab® software, a statistical computer package, was used to analyze the data of Figure 4-1. Since runs at the center point do not impact the estimation of the effects, replicates of the center points were added to the design to examine the adequacy of the model for capturing the curvature expressed in the response.

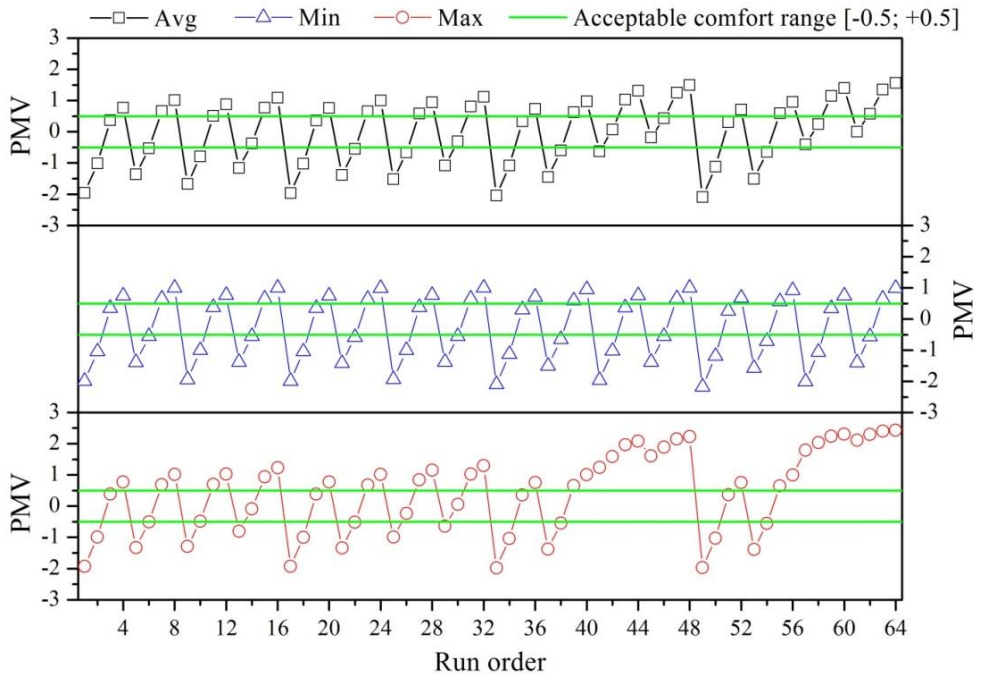

Figure 4-1: DoE simulation results (each run represnts a unique combination of factors levels).

4.4 Statistical analysis of the data

The Analysis of Variance (ANOVA) was carried out in order to identify the significant factors. The results of ANOVA reported in Table 4-2 (complete ANOVA results are reported in Table D-2, Table D-4 and Table D-6) indicate that the linear and 2-way interactions between factors are significant, while the remaining interactions and the curvature are not. As a result, the relationship between the investigated parameters and the response variable is deemed to follow a linear equation.

Table 4-2: ANOVA results for average, minimum and maximum PMV values.

Source	DF	Seq SS	Adj SS	Adj MS	F-Value	P-Value
Average PMV						
Model	63	68,4953	68,4953	1,0872	6166,54	0,01
Linear	6	63,4854	63,4854	10,5809	60012,77	0,003
2-Way Interactions	15	4,67	4,67	0,3113	1765,81	0,019
3-Way Interactions	20	0,3354	0,3354	0,0168	95,13	0,081
4-Way Interactions	14	0,0045	0,0045	0,0003	1,8	0,531
5-Way Interactions	6	0	0	0	0,03	0,999
6-Way Interactions	1	0	0	0	0	0,977
Curvature	1	0	0	0	3,29	0,321
Error	1	0,0002	0,0002	0,0002		
Total	64	68,4955	68,4955			
Minimum PMV						
Model	63	74,2413	74,2413	1,1784	4337,36	0,012
Linear	6	72,6844	72,6844	12,1141	44587,27	0,004
2-Way Interactions	15	1,5306	1,5306	0,102	375,56	0,04
3-Way Interactions	20	0,0255	0,0255	0,0013	4,69	0,351
4-Way Interactions	14	0,0008	0,0008	0,0001	0,2	0,957
5-Way Interactions	6	0	0	0	0,02	0,999
6-Way Interactions	1	0	0	0	0	0,982
Curvature	1	0	0	0	0,13	0,777
Error	1	0,0003	0,0003	0,0003		
Total	64	74,2416	74,2416			
Maximum PMV						
Model	63	104,256	104,256	1,6549	1394,38	0,021
Linear	6	82,704	82,704	13,784	11614,36	0,007
2-Way Interactions	15	19,791	19,791	1,3194	1111,74	0,024
3-Way Interactions	20	1,738	1,738	0,0869	73,2	0,092
4-Way Interactions	14	0,023	0,023	0,0016	1,37	0,593
5-Way Interactions	6	0	0	0	0,03	0,999
6-Way Interactions	1	0	0	0	0	0,978
Curvature	1	0	0	0	0,02	0,908
Error	1	0,001	0,001	0,0012		
Total	64	104,257	104,257			

The Pareto charts for standardized effects at p = 0.05 for the average daily, minimum and maximum PMV values are shown in Figure 4-2. The bars display the variables (A-F) and their interactions (e.g. AB, ADE), where all the bars that exceed the vertical dashed line are considered significant. The results reported in Figure 4-2 show that the metabolic rate (B) has the highest effect on the daily average, maximum and minimum PMV values. In addition, the daily average and maximum values were significantly influenced by the daily average sol-air temperature (D), clothing insulation (A), interaction between sol-air temperature and WFR (DF), set-point temperature (C) and WFR (F). However, the minimum PMV value was significantly influenced by clothing insulation (A), set-point temperature (C), interaction between clothing insulation and metabolic rate (AB) and WFR (F), respectively. Effects of other factors and their interactions are in descending order as shown in the Pareto charts. These results are in a good agreement with the previously discussed results regarding the effect of activity level and outdoor climates on the thermal sensation of the thermal sensation of the students.

Figure 4-3 illustrates the main effect plot of each of the studied factors. The effect of a factor is defined as the change in the response due to the change in the level of the factor. It can be clearly seen that the metabolic rate was the most significant parameter affecting the PMV values, while glazing type was the least significant. These results confirm that in the investigated Foyer, students' thermal comfort is highly affected by their activity and clothing levels. In addition, maximum PMV values are sensitive to climatic conditions and glazing area more than the set-point temperature, which confirms the effect of glass facades on the variations of PMV.

After identifying the main effects, it is important to study the interactions between them, since this was found to be significant using the Pareto charts, as described in Figure 4-2. Interactions occur when the effect of a factor is dependent on the level of another one. Figure 4-4 shows the interaction plot for the daily average, maximum and minimum PMV values. The interaction plot allows to easily identifying interactions between two factors. It plots the mean response of two factors for all occurring combinations. Non-parallel intersecting lines indicate that an interaction between factors occurs, while parallel lines signify no interaction between them.

The results reported in Figure 4-4 show that several lines are not parallel but the interaction between the sol-air temperature and the WFR has the most significant impact on the daily average and maximum PMV value. This interaction effect indicates that the relationship between PMV value and the outdoor climatic conditions depends on the external glazed surface. As the external glazed surface area decreases, the effect of outdoor climatic conditions become less important. Hence, decreasing glazing area results in more consistent thermal comfort conditions. The results also show that the interaction between metabolic rate and clothing insulation has the most significant impact on the minimum PMV value.

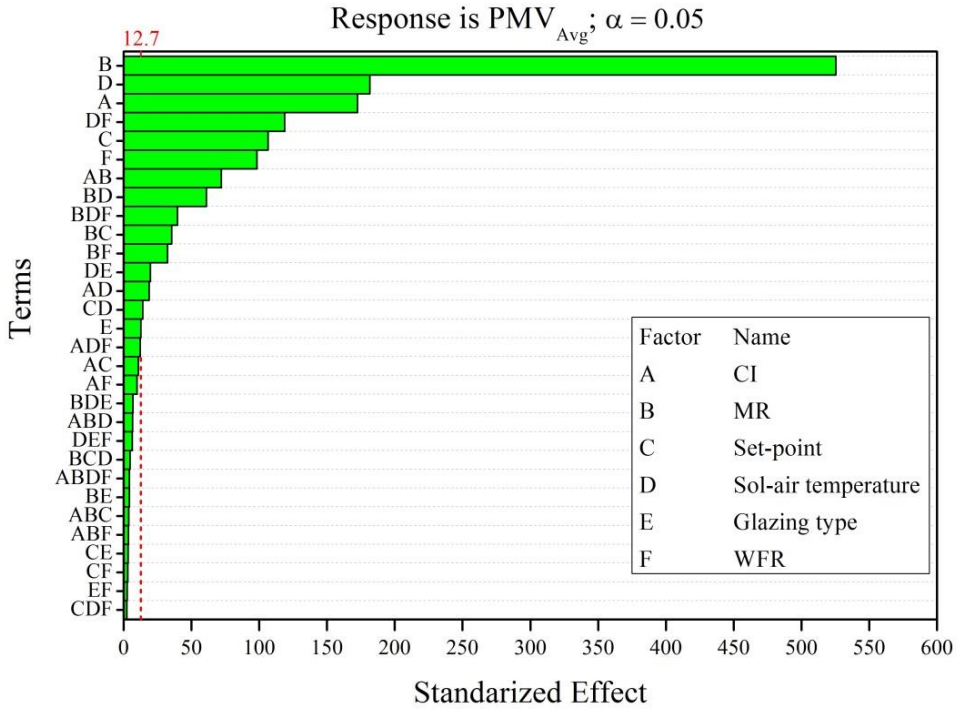
Response is PMV Avg; α = 0.05
12.7
Terms
B
D
A
DF
C
F
AB
BD
BDF
BC
BF
DE
AD
CD
E
ADF
AC
AF
BDE
ABD
DEF
BCD
ABDF
BE
ABC
ABF
CE
CF
EF
CDF
Factor Name
A CI
B MR
C Set-point
D Sol-air temperature
E Glazing type
F WFR
0 50 100 150 200 250 300 350 400 450 500 550 600
Standarized Effect

(a)

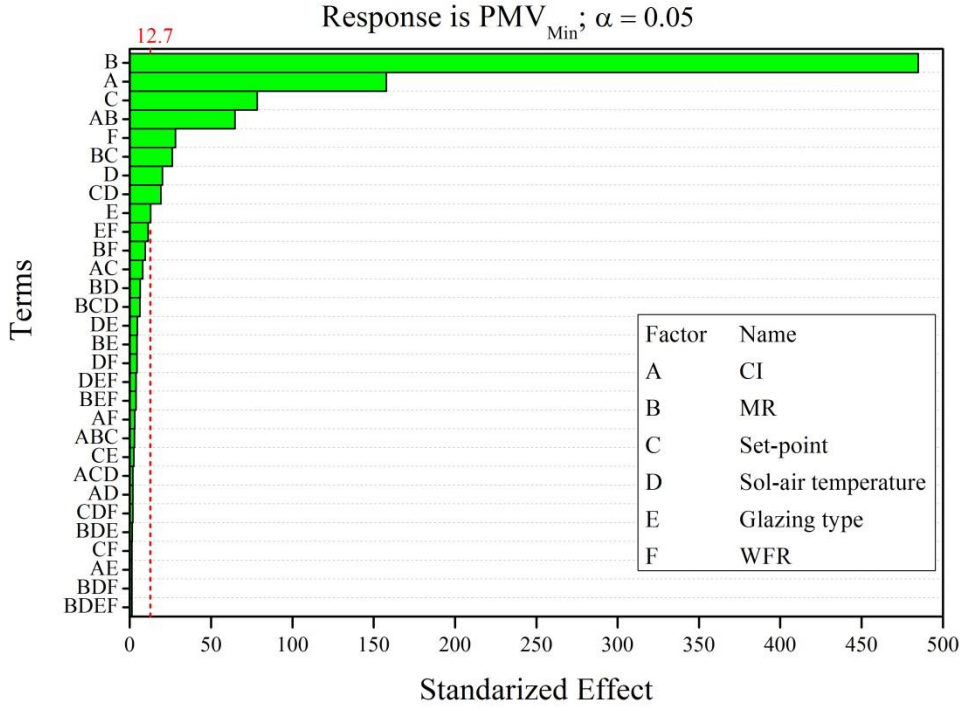
Response is PMV Min; α = 0.05
12.7
Terms
B
A
C
AB
F
BC
D
CD
E
EF
BF
AC
BD
BCD
DE
BE
DF
DEF
BEF
AF
ABC
CE
ACD
AD
CDF
BDE
CF
AE
BDF
BDEF
Factor Name
A CI
B MR
C Set-point
D Sol-air temperature
E Glazing type
F WFR
0 50 100 150 200 250 300 350 400 450 500
Standarized Effect

(b)

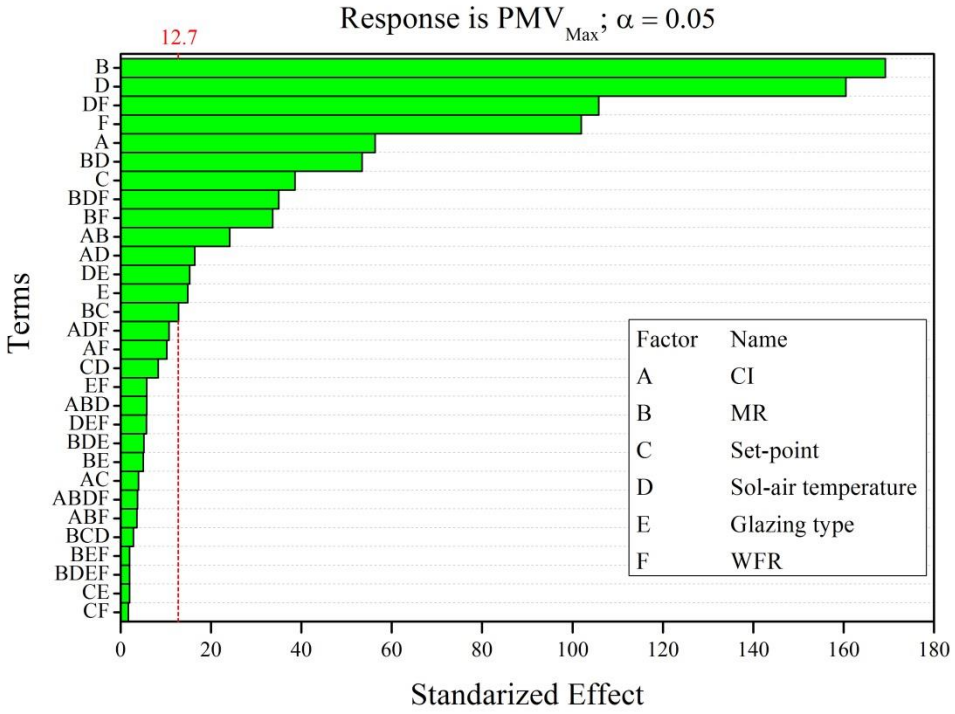

(c)

Figure 4-2 : Pareto plots of standardized effects at p = 0.05 for: (a) daily average PMV, (b) minimum PMV and (c) maximum PMV.

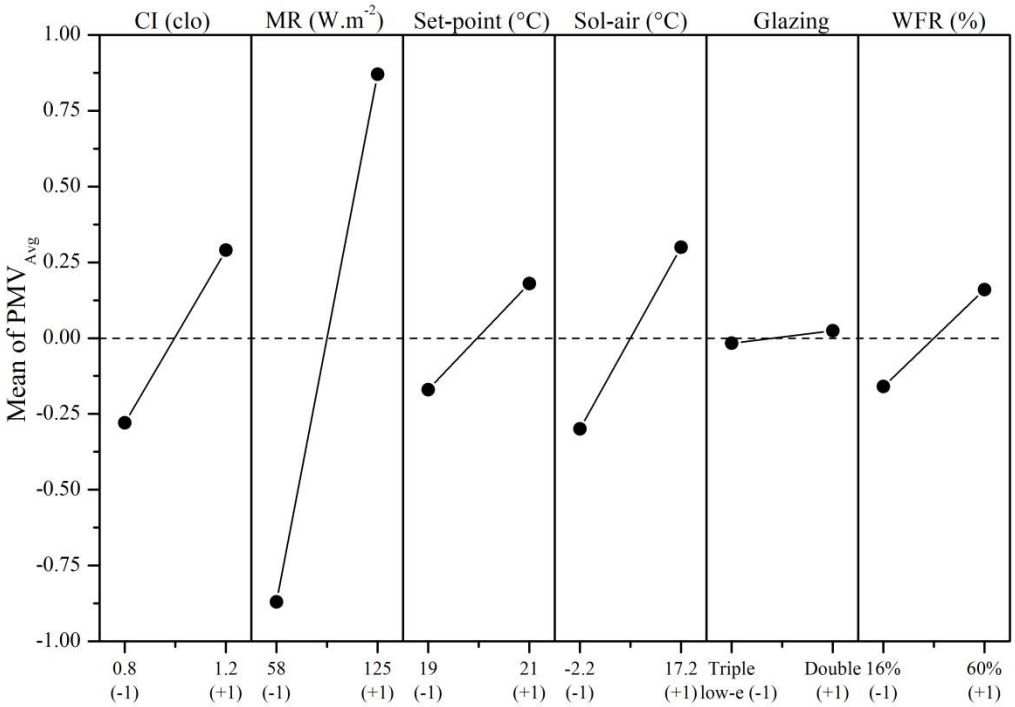

(a)

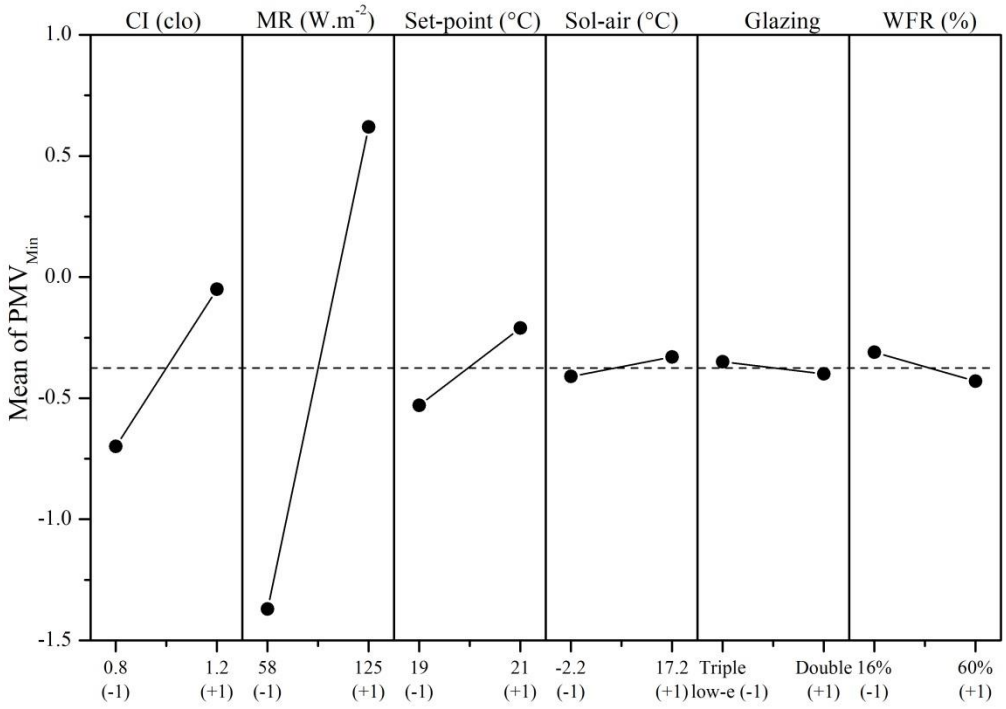

(b)

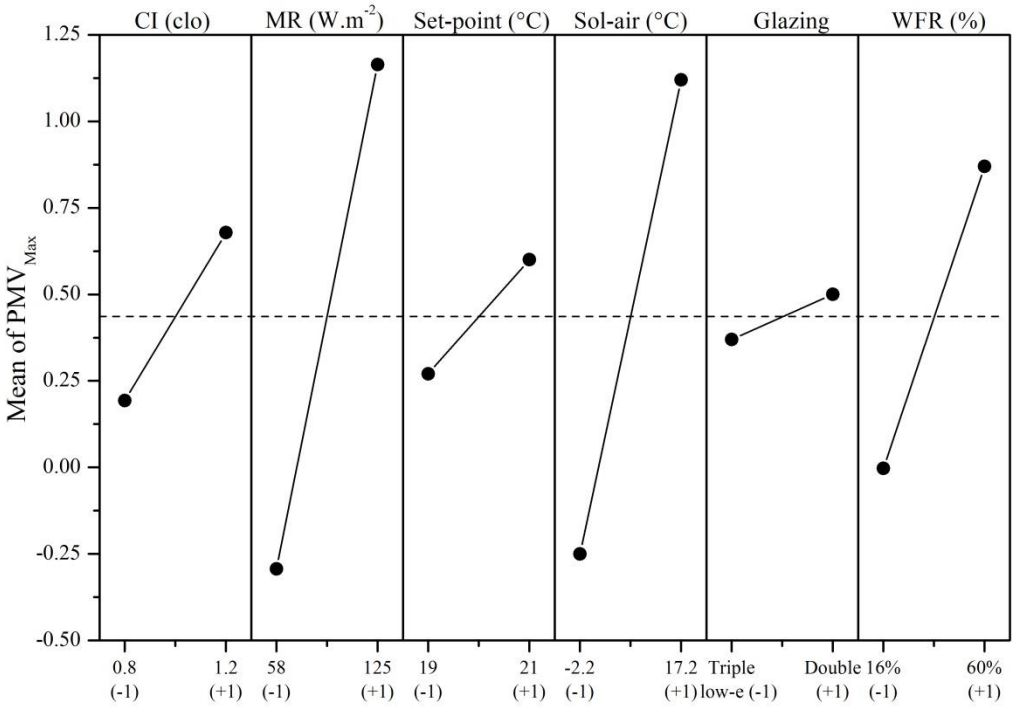

(c)

Figure 4-3: Main effect plot for: (a) daily average PMV, (b) minimum PMV and (c) maximum PMV.

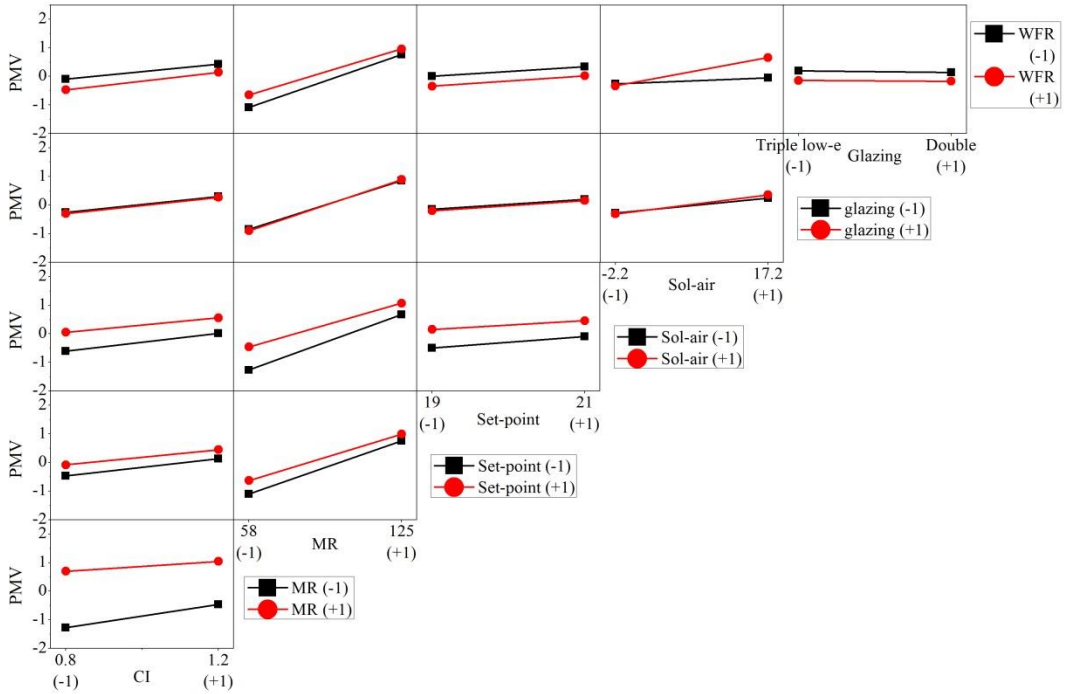
PMV
WFR (-1)
WFR (+1)
Triple low-e (-1)
Glazing
Double (+1)
glazing (-1)
glazing (+1)
-2.2 (-1)
Sol-air
17.2 (+1)
Sol-air (-1)
Sol-air (+1)
19 (-1)
Set-point
21 (+1)
Set-point (-1)
Set-point (+1)
58 (-1)
MR
125 (+1)
MR (-1)
MR (+1)
0.8 (-1)
CI
1.2 (+1)

(a)

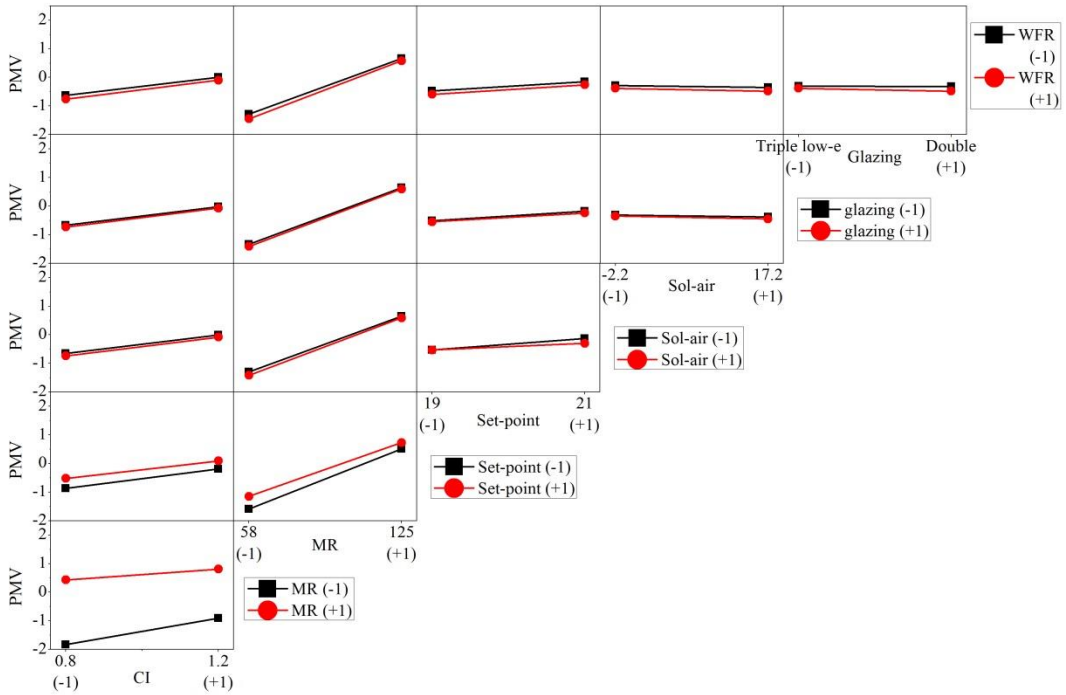
PMV
WFR (-1)
WFR (+1)
Triple low-e (-1)
Glazing
Double (+1)
glazing (-1)
glazing (+1)
-2.2 (-1)
Sol-air
17.2 (+1)
Sol-air (-1)
Sol-air (+1)
19 (-1)
Set-point
21 (+1)
Set-point (-1)
Set-point (+1)
58 (-1)
MR
125 (+1)
MR (-1)
MR (+1)
0.8 (-1)
CI
1.2 (+1)

(b)

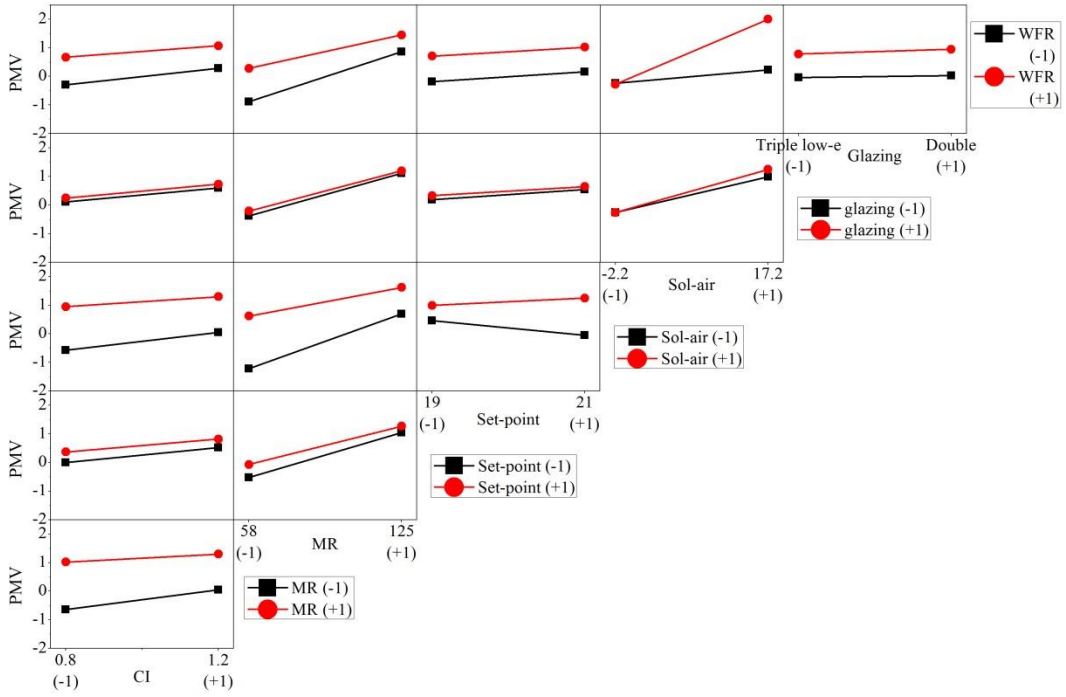

(c)

Figure 4-4: interaction plots for: (a) daily average PMV, (b) minimum PMV and (c) maximum PMV.

These results show that the PMV values are highly sensitive to students' activity level and clothing insulation and an underestimation of their values may lead to uncertainties in the results. In addition, the effect of outdoor climatic conditions on thermal comfort is correlated to the presence of the glass facades. Thus, an adequate design of the glass façades is required to ensure thermal comfort. Hence, meta-modeling the relationship between thermal comfort index and the considered design parameters is important to optimize the glass façades design for thermal comfort.

4.5 Development of meta-models for the prediction of the PMV values

Table D-3, Table D-5, and Table D-7 reports the coefficients of fitting polynomials to the simulation results by linear regression analysis. The ANOVA test shows that the meta-models for PMV values predictions are statistically significant at a 95% confidence level ($p < 0.05$). The obtained meta-models can be simplified by eliminating the non-significant factors ($p > 0.05$). The best fit meta-model equations that describe the average, the minimum and the maximum PMV values are given by Equations (4.2), (4.3) and (4.4), respectively.

$$PMV_{avg} = 0.00372 + 0.28635 \times A + 0.87226 \times B + 0.17675 \times C + 0.30146 \times D + 0.02108 \times E + 0.16296 \times F - 0.11939 \times AB - 0.03119 \times AD - 0.05882 \times BC - 0.10105 \times BD - 0.05360 \times BF - 0.02331 \times CD + 0.03271 \times DE + 0.19716 \times DF \quad (4.2)$$

$$PMV_{Min} = -0.37557 + 0.32530 \times A + 0.99898 \times B + 0.16164 \times C - 0.04150 \times D - 0.02642 \times E - 0.05801 \times F - 0.13309 \times AB - 0.05402 \times BC - 0.03939 \times CD \quad (4.3)$$

$$PMV_{Min} = 0.43566 + 0.24247 \times A + 0.72880 \times B + 0.16611 \times C + 0.69132 \times D + 0.06404 \times E + 0.43896 \times F - 0.10397 \times AB - 0.07044 \times AD - 0.05513 \times BC - 0.22996 \times BD - 0.14480 \times BF + 0.06577 \times DE + 0.45554 \times DF \quad (4.4)$$

The ANOVA results of the models indicate good performance with R^2 (> 0.98) and adjusted R^2 (0.97). The adjusted R^2 is an expressing form of degree of fit and it is more reliable than R^2 for comparing models with different numbers of independent variables [69]. The value of adjusted R^2 indicates that more than 97% of the total factors associated with the PMV are attributed to the selected parameters of the model. The Predicted R^2 is in reasonable agreement with the Adjusted R^2; i.e. the difference is less than 0.2.

Moreover, residuals versus predicted value plot and normal probability plot of residuals are two graphical approaches that are used to check the validity of a regression model [82]. The first shows the difference between the predicted and the observed values. If the residuals have a noticeable pattern, it will infer that the suggested model is not adequate [82]. The residual versus predicted response plots illustrated in Figure 4-5 show that less patterned structures are observed for the three deemed responses indicating that the proposed models are adequate. In addition, residuals in the normal probability plot should be positioned on a straight line [82]. The normal probability plots shown in Figure 4-5 indicate that the residuals followed a straight line, thus confirming the validity of the models.

Furthermore, 50 additional simulations were performed with different factors' levels using the numerical model and the results were compared to the meta-model predictions. The obtained results are shown in Figure 4-6. A good correlation is observed showing a R^2 value of 0.99, meaning that 99% of variance is explained by the obtained meta-model. Therefore, the meta-models are considered to be valid and adequate. These meta-models can be used instead of the numerical model as a fast and simple way to predict the thermal comfort condition within an indoor environment. However, the reliability of these meta-models is limited to a similar case study and the considered range of variation of the investigated factors.

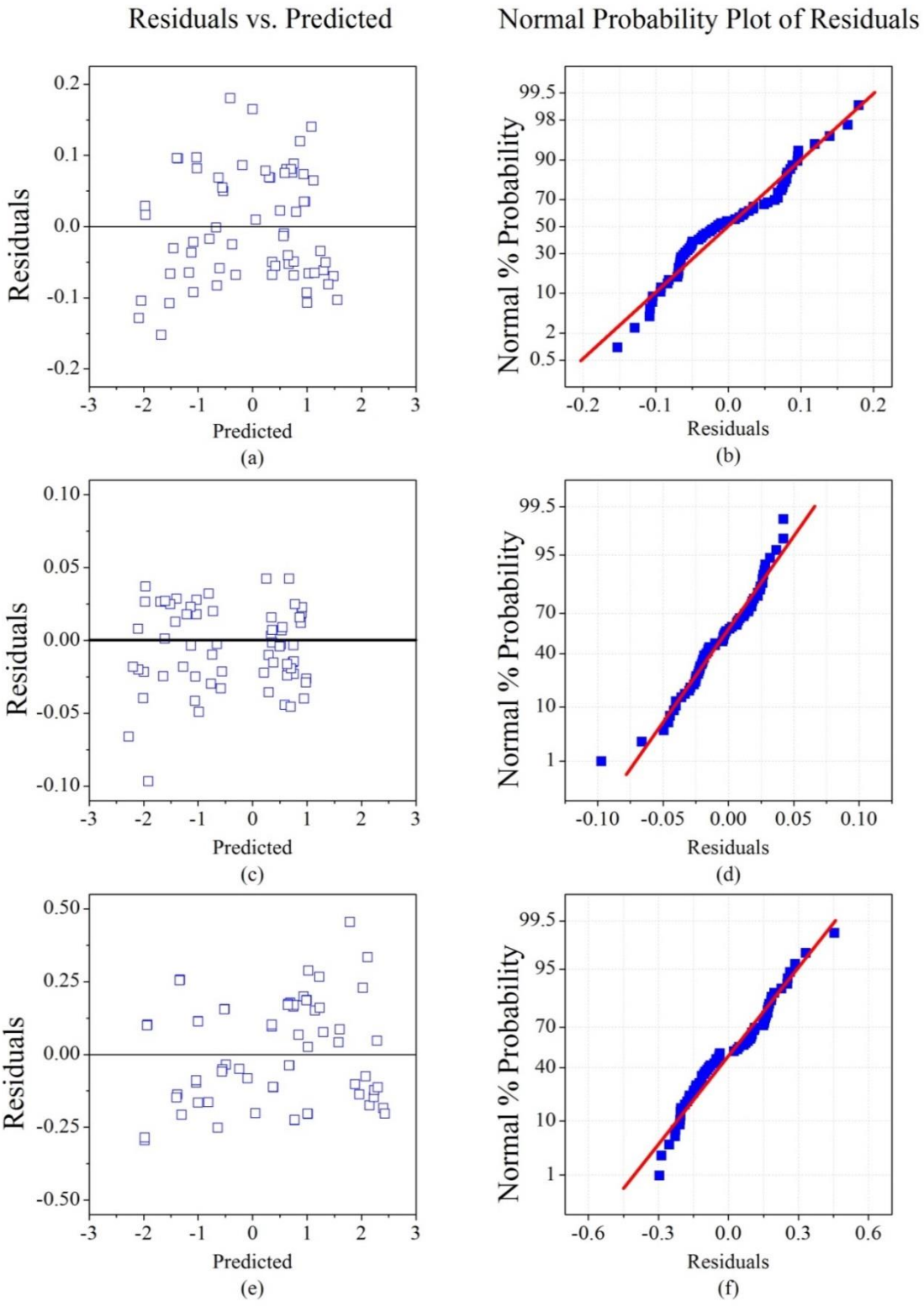

Figure 4-5: Residuals versus fitted values, (a), (c) and (e), and Normal probability of residuals, (b), (d) and (f), for average, minimum and maximum PMV values, respectively.

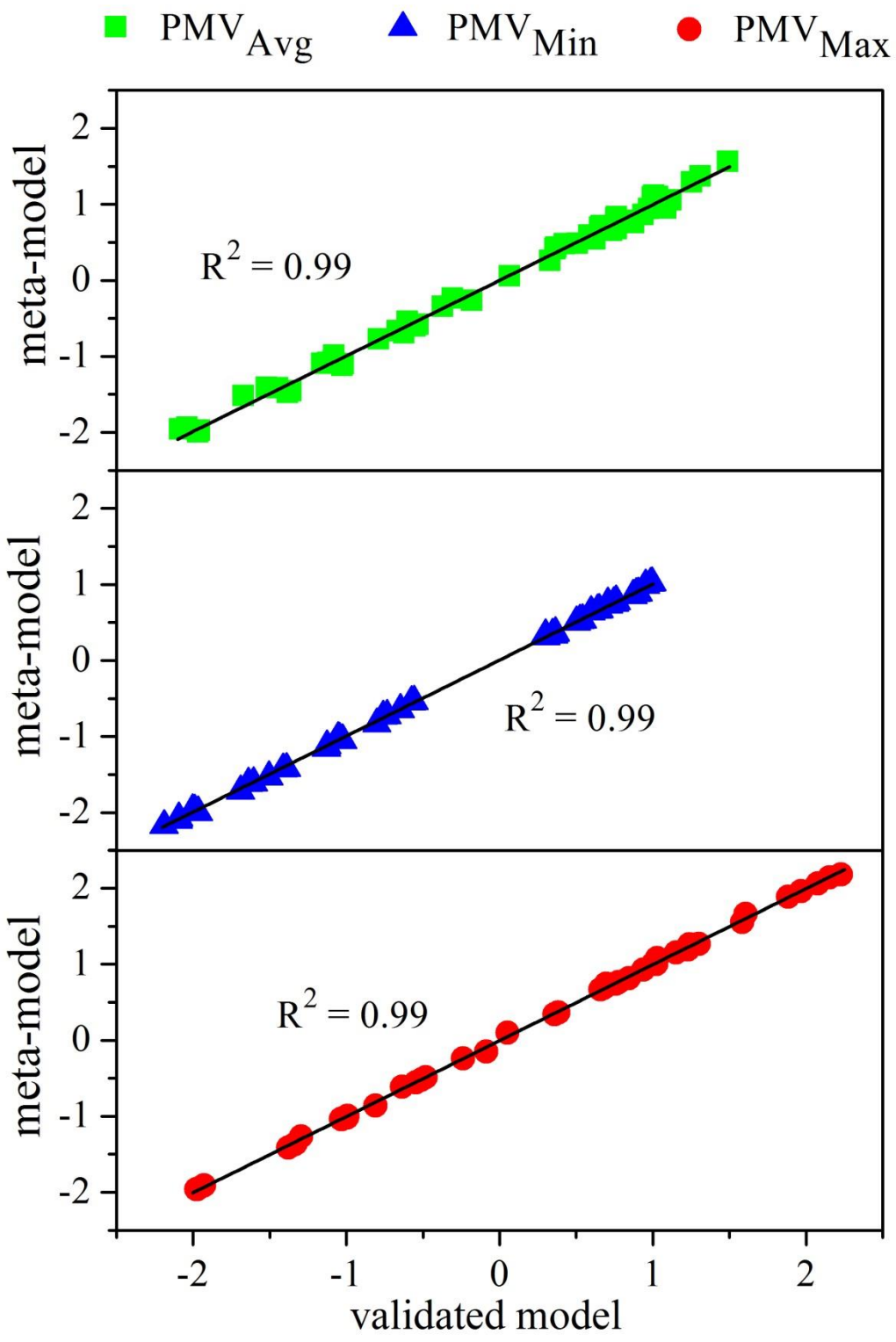

Figure 4-6: Coefficient of determination between simulation results and the meta-model predictions.

4.6 Determination and analysis of optimal solutions

Finally, an optimization is carried out using the obtained meta-models. The response variables are the average, minimum and maximum PMV values. The objective is to maximize the global desirability function so that PMV values are maintained within the acceptable thermal comfort range of [-0.5; +0.5]. The range of variation of the set-point temperature, glazing type and WFR is kept as indicated in Table 4-1, while the metabolic rate and clothing insulation are assumed to vary in the ranges of [66.5; 73.5] and [0.95; 1.05], respectively, representing sedentary activity and typical winter clothing with 5% variation [193].The sol-air temperature parameter is excluded from the optimization because it is an uncontrollable parameter.

The numerical optimization outcomes 51 solutions illustrated in Figure 4-7 and reported in Table E-1. According to the obtained results, the maximum D value, D=1, is provided when the set-point temperature, the glazing type and the WFR ranged between 20.8°C and 21°C, 0.7 $W.m^{-2}.K^{-1}$ and 2.8 $W.m^{-2}.K^{-1}$, and 16% and 28.9%, respectively. The results suggest that using this combination of parameters will outcome average, minimum and maximum PMV values of -0.381, -0.5 and 0.107, respectively.

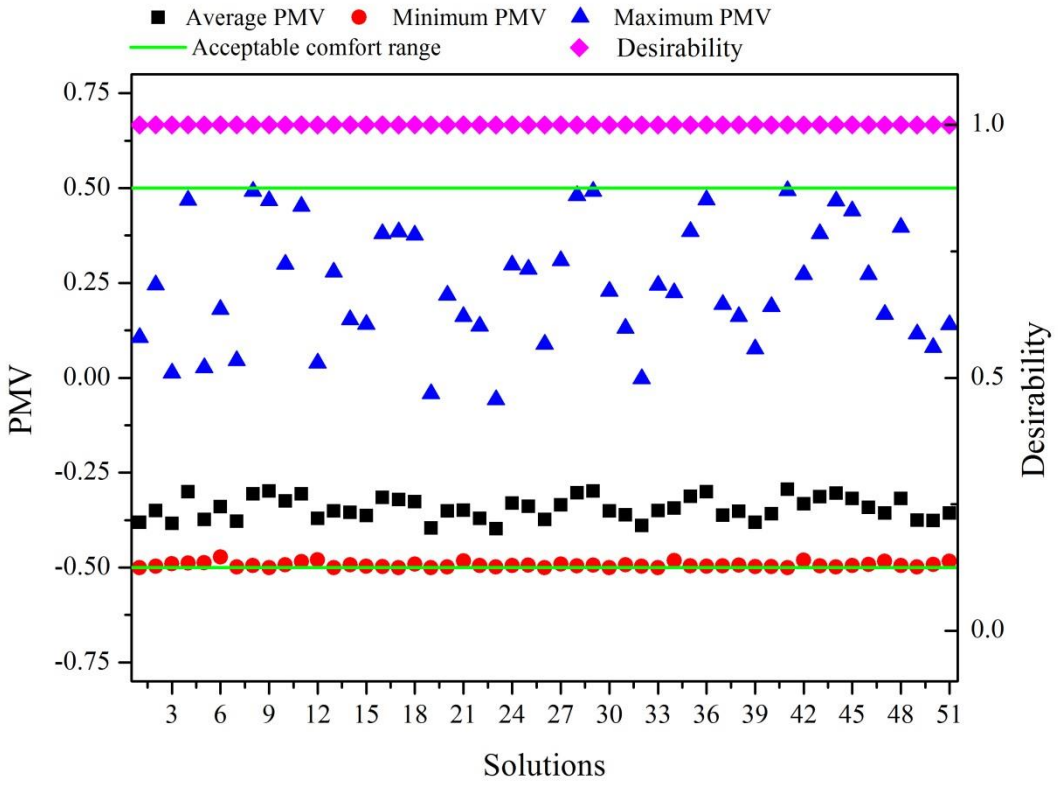

Figure 4-7: numerical optimization solutions to maintain acceptable thermal comfort condition.

The validated Dymola® model is used to simulate the optimized scenario in order to validate the adequacy of the obtained results. The first scenario of the 51 obtained solutions is used for the simulation; the obtained average, minimum and maximum PMV are -0.284, -0.41 and 0.124, respectively. These results are in a good agreement with the results predicted by optimizing the meta-models, thus confirming the validity of the obtained results.

In addition, the optimized case is compared to the base case and the obtained hourly numerical values of PMV and MRT are presented in Figure 4-8. The results show that the optimized design yields better thermal comfort condition within the studied room. More specifically, it leads to alleviate the high MRT values during high sol-air temperatures, thus preventing the PMV values from exceeding the upper acceptable limit. On the other hand, it reduces the heat loss through building envelope thus leading to increasing MRT during cold times, which means improved PMV values during low sol-air temperature values.

Furthermore, although the optimized case allows an increase in the set-point temperature to maintain acceptable thermal comfort condition, it results in reducing the heating energy consumption. An energy audit for the whole building comprising the Foyer is performed in [90]. One can refer to this study for a detailed description about the total number of days requiring heating and the outdoor climatic conditions. The total heating energy consumption of the base case, set-point 20°C, was 3034 kWh per year, while that of the optimized case was 2566 kWh per year. These results are correlated to the optimized glazing area that results in improved thermal resistance of the external walls, allowing the reduced transmission heat loss under low sol-air temperature, thus improving the heating energy consumption.

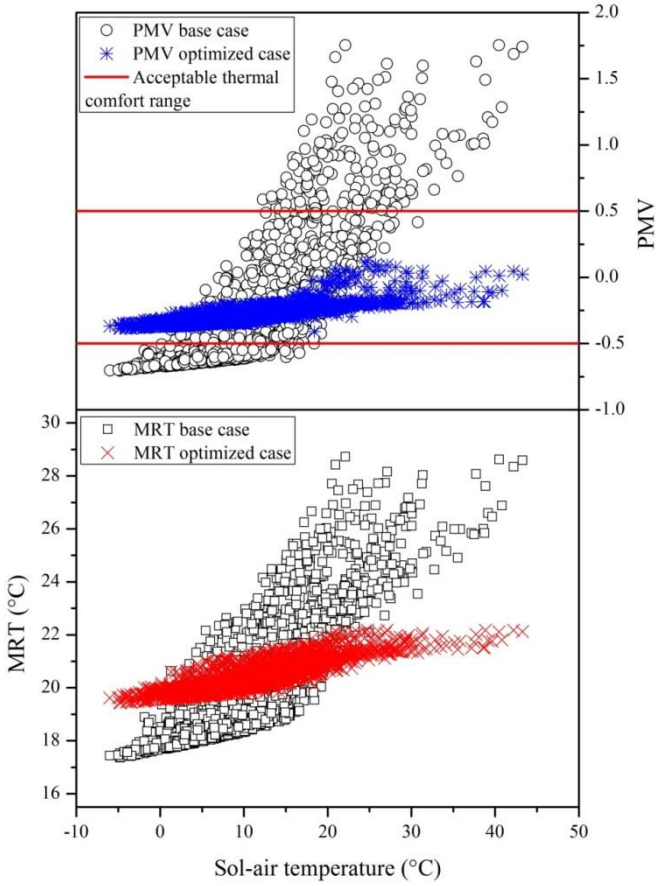

Figure 4-8: Numerical hourly values of (a) PMV index and (b) MRT obtained from the validated Dymola model for the two studied cases.

4.7 Conclusion

Adequate design of building envelope is essential to ensure a trade-off between several aspects, such as aesthetic appearance of the building, occupants' thermal and visual comfort and energy consumption. In this chapter, a sensitivity analysis based on the combined use of numerical simulation and DoE technique was performed. From this analysis, the most significant parameters and interactions affecting the response variables (average, minimum and maximum PMV value) were determined, as well as mathematical relationships, referred as meta-models, which approximate the response variables as a function of predefined factors were developed. The meta-models were validated using graphical analysis of residuals and the coefficient of determination R^2. The residual versus predicted response plots demonstrated less patterned structures; the normal probability plots indicated that the residuals followed a straight line and the coefficient of determination was greater than 0.98, thus confirming the validity of the meta-models. These meta-models are then used to integrate occupants' thermal comfort in the design of energy efficient buildings.

Lastly, an optimization procedure using the desirability function approach was carried out. The objective of the optimization was to maintain the PMV values within the acceptable comfort range of [-0.5; 0.5]. The results indicated that the optimized design yields better thermal comfort conditions, PMV values ranged from -0.381 to 0.107. In addition, it reduces heating energy consumption, even though it requires increased heating set-point. This indicates that an optimized design of building envelope is vital to achieve energy-saving and thermal comfort, rather than just reducing the set-point temperature.

Finally, in this chapter, we investigated the impact of integrating occupants' thermal comfort in the design of energy efficient buildings by modeling the relationship between thermal comfort and some design parameters and then optimizing building design using the obtained meta-models. In order to evaluate the added value of the proposed approach, a comparative study with another approach that integrates occupant thermal comfort in the control of the indoor environment is performed and presented in the next chapter.

Chapter 5: An analysis of the impact of applying PMV-based thermal comfort control

5.1 Introduction

We recall that the main objective of the present work is to integrate occupants' thermal comfort in the design of energy-efficient buildings. For this, we adopted a methodology based on the combined use of numerical simulations, the DoE technique and an optimization process. In the previous chapter, we developed meta-models to integrate occupants' thermal comfort in the design process using the proposed approach. The results show the benefits of using the proposed approach to achieving satisfactory thermal comfort. However, another solution could be the installation of PMV-based comfort control to regulate the indoor environment for thermal comfort. This approach adjusts the set-point room temperature according to a user-defined PMV and changes in the indoor environmental parameters [40].

In this chapter, the validated model is used to numerically investigate the energy-saving potential of a thermal comfort-control in the considered case study. For the analysis, a PMV-based control schema is implemented into the validated model followed by conducting a comparative simulation study between the thermal comfort control and conventional thermostatic control.

5.2 PMV-based thermal comfort control scheme

Of all the parameters affecting the thermal comfort within a space, the set-point temperature is the widely considered parameter that occupants try to adjust when perceiving thermal discomfort. Depending on this concept, Kang et al. [40] suggested a thermal comfort-control approach based on PMV inverse calculation, instead of a fixed temperature thermostatic-control. Such a control approach aims to maintain the user-defined PMV by adjusting the room temperature with respect to the changes in other parameters affecting the indoor thermal comfort, mainly the mean radiant temperature. This concept is briefly summarized and illustrated in Equation (5.1) and Figure 5-1, respectively.

$$T_a = f(PMV, T_{mr}, \mathrm{M}, \mathrm{T_{cl}}, RH, v_a) \tag{5.1}$$

To apply such a concept to our case study, the formula of PMV was inversed in the modified Fanger model. Then, the PMV, the metabolic rate, and the clothing insulation were implemented into the model as user-defined parameters assuming the following values: -0.5, 1.2 met (representing sedentary activity [193]), and 1.0 clo (representing a typical winter clothing [193]), respectively. The

relative humidity and the MRT were obtained from the developed model simulations. The air velocity (v_a) was assumed to be constant and has a value of 0.15 ms^{-1} since the model does not compute the real-time air velocity. Finally, the room temperature is calculated by iteratively computing the root of the nonlinear functions, and a control signal is sent to the heating system set-point controller to maintain the determined room temperature. Figure 5-2 illustrates the controller diagram implemented in the previously developed model.

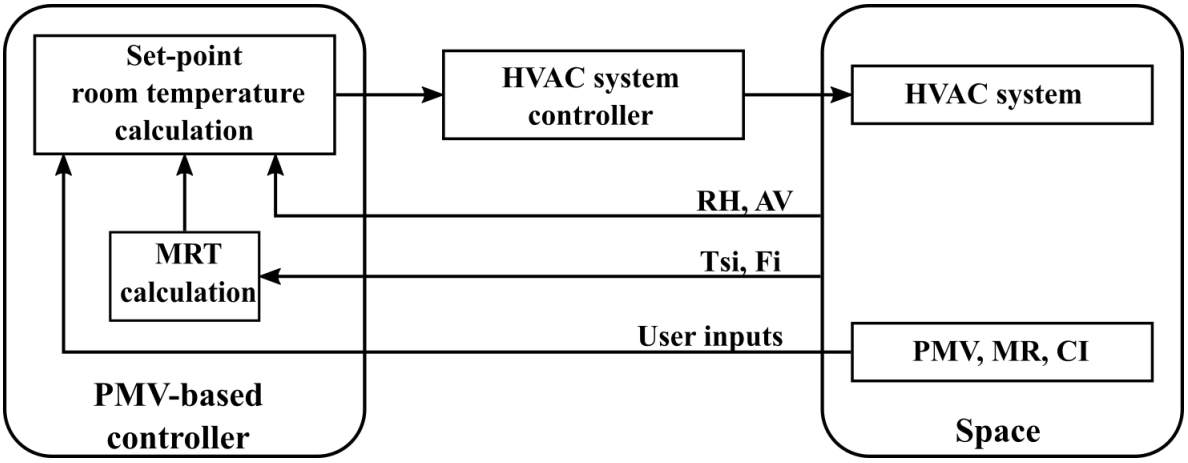

Figure 5-1: PMV-based thermal comfort scheme.

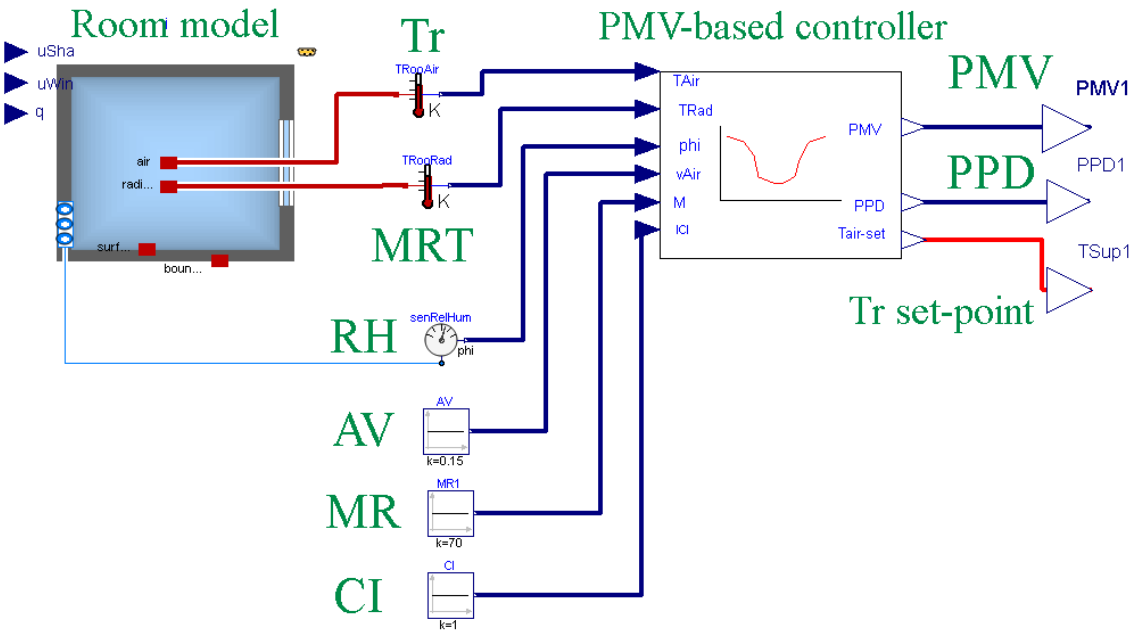

Figure 5-2: PMV-based thermal comfort control scheme implemented in the Dymola® model.

Although the fulfillment of a tradeoff between energy-saving potential and thermal comfort is the main objective of a PMV-based control, it is not sufficient to confirm its advantage over the

conventional thermostatic-control. The comfort-control must reduce energy consumption compared to conventional control while maintaining acceptable thermal comfort. Therefore, to confirm this advantage, a comparative study should be carried out between both control strategies.

5.3 Comparative study

A comparative study between the PMV-based comfort-control and conventional thermostatic-control is performed. Comparison criteria include heating energy consumption and the Environmental Quality Index (EQI) [83]. The latter is an index that is used for the long term assessment of the thermal environmental quality based on the four quality categories (I, II, III, and IV) outlined by the EN 15251 [79]. It is calculated using the following equation [83]:

$$EQI = 100 \times f_{PMV,I} + 70 \times f_{PMV,II} + 35 \times f_{PMV,III} \quad (5.2)$$

where $f_{PMV,j}$ is the occurrence frequency defined as the fraction of time during which the values of the PMV outcome within the range limits defining the j^{th} category of quality. This index varies between 0 and 100, obtained when all the assessed values fall in category IV and category I, respectively. Moreover, the value of 70 is considered for the case that all values fall in category II [83]. Besides, the sol-air temperature is used to investigate the reliability of the thermal comfort control under different climatic conditions.

For the simulations, the room temperature of the Foyer was generally set at 20 °C in the heating season following the regulation of low energy consumption buildings. However, the new French standards recommend the set-point of 19 °C [7]. On the other hand, the European standards [79] recommend the set-points of 19 °C, 20 °C or 21 °C to maintain moderate, normal or high expectation levels, respectively. In this regard, the room temperature set-point in the thermostatic-control was set to 19 °C, 20 °C, and 21 °C. As explained above, the PMV index was set to -0.5 in the PMV-based thermal comfort-control. This value represents the minimum in category II limits, the recommended category for new and renovated buildings [79], thus resulting in the least use of heating energy.

5.3.1 Results and discussion

This section presents and analyses the thermal comfort and heating energy consumption, where the PMV-based comfort-control and the thermostatic-control are applied, for the considered case study throughout the entire heating period. The section distinguished two evaluation criteria, short-term and long-term. The first aims to analyze the hourly thermal performance of both control strategies and their sensitivity to outdoor climatic conditions, thus evaluating the performance of both control strategies under extreme weather conditions. The second aims to investigate the energy-saving

potential and the indoor environmental conditions in a comfort-controlled case for a long evaluation period.

5.3.1.1 Short-term evaluation (hourly-base)

The obtained hourly PMV values using the validated model throughout the investigated heating period in both thermostatic-control and the comfort-control are shown in Figure 5-3 as a function of sol-air temperature and summarized in Table 5-1.

The PMV values in the thermostatic-control at the set-points of 19 °C (Figure 5-3a), 20 °C (Figure 5-3b) and 21°C (Figure 5-3c) varied in the range of [-1.0,+2.0], [-0.7,+2.0] and [-0.5,+2.0], resulting in 79.5%, 67.8% , and 9.17% of the occupied time, respectively, outside the acceptable comfort range of [-0.5,+0.5] throughout the investigated period. The PMV index values in the thermal comfort-control at a set-point of PMV -0.5 (Figure 5-3d) varied between [-0.5, +1.2] resulting in 3.25 % of the occupied time outside the acceptable comfort range throughout the studied winter season.

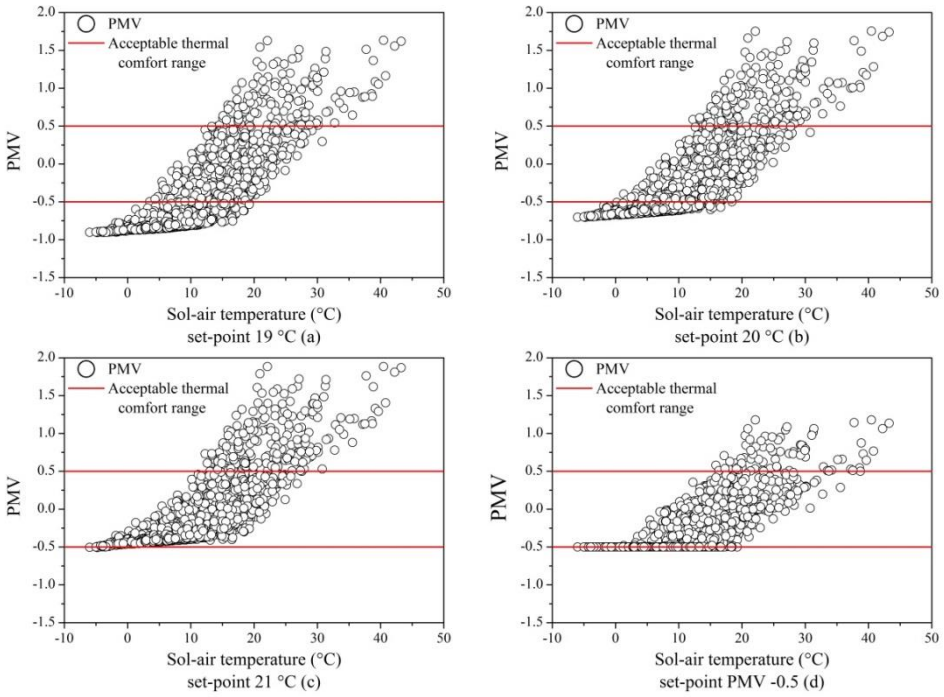

Figure 5-3: Numerical hourly PMV index values obtained from the validated Dymola® model for thermostatic-control at the set-points of 19°C (a), 20°C (b), and 21°C (c) and the comfort-control at a set-point of PMV -0.5 (d).

The results reported in Figure 5-3 show that, at low sol-air temperature (less than 10°C), the comfort-control has an apparent advantage of maintaining consistent thermal comfort, while the

thermostatic control at the set-points of 21°C and 19°C was found to have the best and worst thermal comfort, respectively. In addition, when sol-air temperature varies in the range of [10°C, 30°C], thermally comfortable conditions are maintained for the overwhelming majority of the time. However, the comfort-control still has an apparent advantage over the thermostatic-control by maintaining a thermally comfortable environment at higher sol-air temperature, for example at a sol-air temperature of 30°C the comfort-control could maintain the PMV values within the comfort range, while it exceeds the upper comfort limit in the thermostatic-control. Moreover, at high sol-air temperature (greater than 30°C), the PMV values in both thermostatic and comfort control exceeded the upper comfort limit of +0.5 but the comfort-control still has an apparent advantage by maintaining lesser PMV values than the thermostatic control.

Table 5-1: Frequency (hours) of the PMV index for the thermostatic controlled cases and for the thermal controlled case during heating period.

PMV index	Thermostatic control			Comfort control
	19 °C	20 °C	21 °C	PMV -0.5
-1.0 to -0.7	1442	0	0	0
-0.7 to -0.5	306	1427	0	0
-0.5 to -0.2	187	441	1721	1900
-0.2 to +0.2	199	214	299	305
+0.2 to +0.5	98	105	133	84
+0.5 to +0.7	49	68	67	37
+0.7 to +1.0	44	52	66	30
+1.0 to +1.5	34	49	63	10
+1.5 to +3.0	7	10	17	0
% outside category A, B, C and resultant comfort class				
A	91.58	90.95	87.36	87.10
B	79.54	67.87	9.00	3.25
C	64.53	4.69	6.17	1.69
Class	IV	IV	IV	III
Energy consumption (kWh)				
	2710	3034	3377	3078

Furthermore, the box plots of hourly PMV index values obtained from the validated Dymola® model for all the studied cases are illustrated in Figure 5-4. These plots provide a useful way to visualize the range and other characteristics of the obtained PMV values. The results illustrated in Figure 5-4 show that the box plot of the comfort-controlled case is comparatively shorter than that of thermostatic controlled cases. This signifies that thermal comfort is more stable in the comfort-controlled case than in the thermostatic-controlled cases.

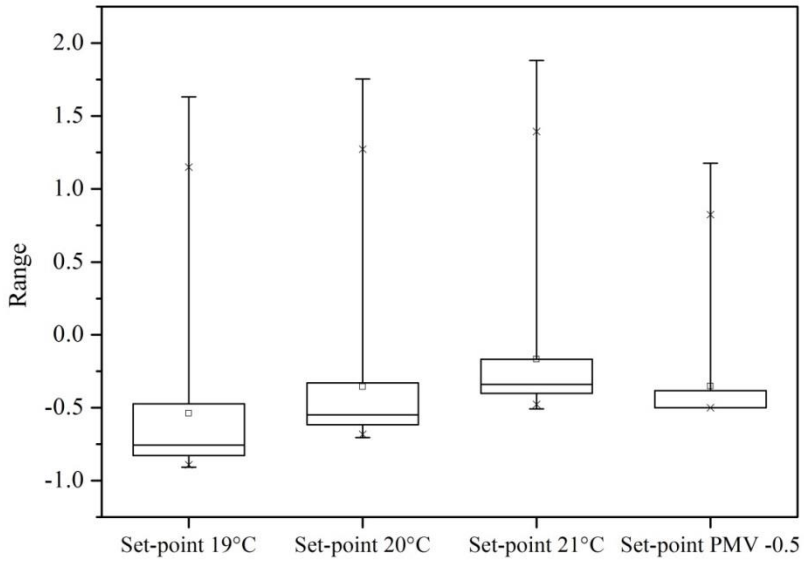

Figure 5-4: Box plots of hourly PMV index values obtained from the validated Dymola® model for all the studied cases. *(The quartiles represent the 25%-75% interval, and the intermediate line the median.)*

The hourly consumed power in both thermostatic-control and comfort-control is shown in Figure 5-5 as a function of sol-air temperature. The results show that at a low sol-air temperature, the thermostatic control at a set-point of 19°C has the best energy-saving potential, followed by the thermostatic control at a set-point of 20°C and then the comfort control at a set-point of PMV -0.5. For example, at a sol-air temperature equals to 0°C, the signature regression lines indicate that the thermostatic control at a set-point of 19°C has the lowest power consumption of 2.0971 kW, followed by the set-point of 20°C (2.29301 kW), then the comfort-control (2.40579 kW). These results show that the power consumption using the comfort control was about 15% and 5% more than the thermostatic control at a set-point of 19°C and 20°C, respectively. However, the comfort-control maintained a comfortable thermal environment while both set-points (19°C and 20°C) failed to maintain the PMV value within the acceptable comfort range. In addition, the comfort control allowed about 5% less than the thermostatic control at a set-point of 21°C, while maintaining equivalent thermal comfort.

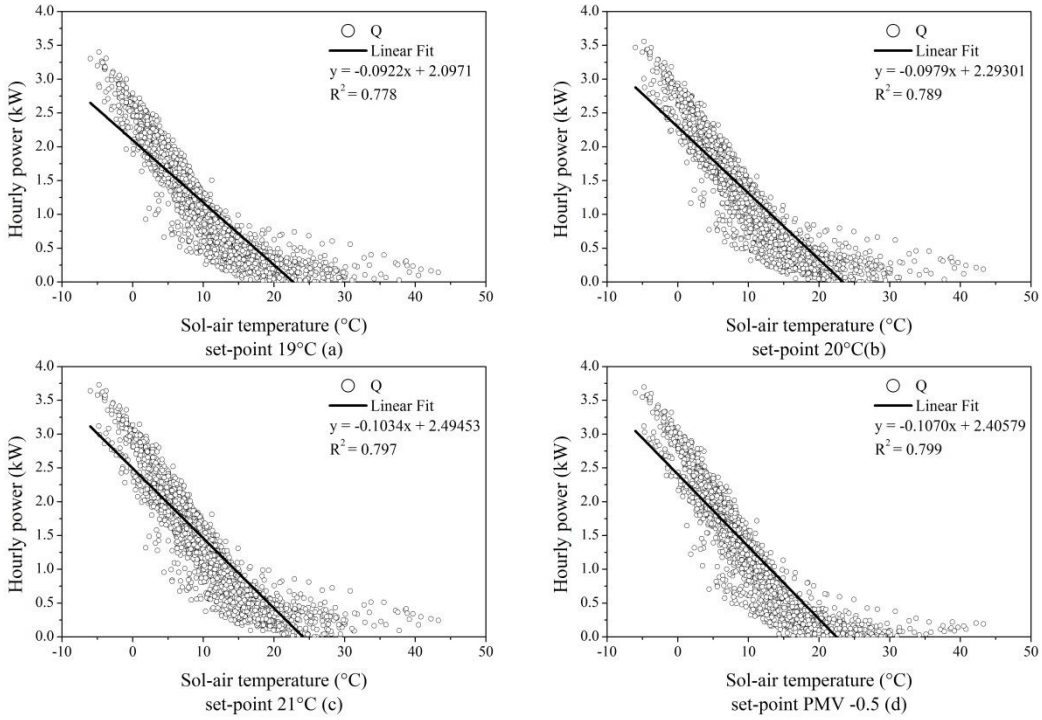

Figure 5-5: Hourly power consumption and energy signature regression lines relating power consumption to sol-air temperature: thermostatic-control at the set-points of 19°C (a), 20°C (b), and 21°C (c) and comfort-control at a set-point of PMV -0.5 (d).

Moreover, the slope constant absolute value of the comfort-control is higher than that of the thermostatic-control at the set-points of 19°C and 20°C, which means more sensitivity to outdoor climates, leading to reduced power consumption at high sol-air temperature, thus more energy-savings. This could be observed clearly using Figure 5-5, where the regression line of the comfort control intersect the sol-air temperature axis at a lower value (22.4°C) than the thermostatic control (22.75°C, 23.4°C and 24.11 at the set-points of 19°C, 20°C and 21°C, respectively). These results show that the PMV-based thermal comfort controller is a reasonable solution to neutralize the trade-off between thermal comfort and energy savings within all the covered sol-air temperature range.

To further analyze the occurrence of high PMV values, two winter days corresponding to cases A' and B' were selected to highlight the variation of the PMV index, mean radiant temperature, room temperature and energy consumption as a function of outdoor climatic conditions. Case A' represents a typical winter day with no direct solar radiation due to an overcast sky. Case B' designates a winter day with relatively high outdoor temperature and intense solar radiation. Outdoor temperature and solar radiations of the two selected days are illustrated in Figure 5-6.

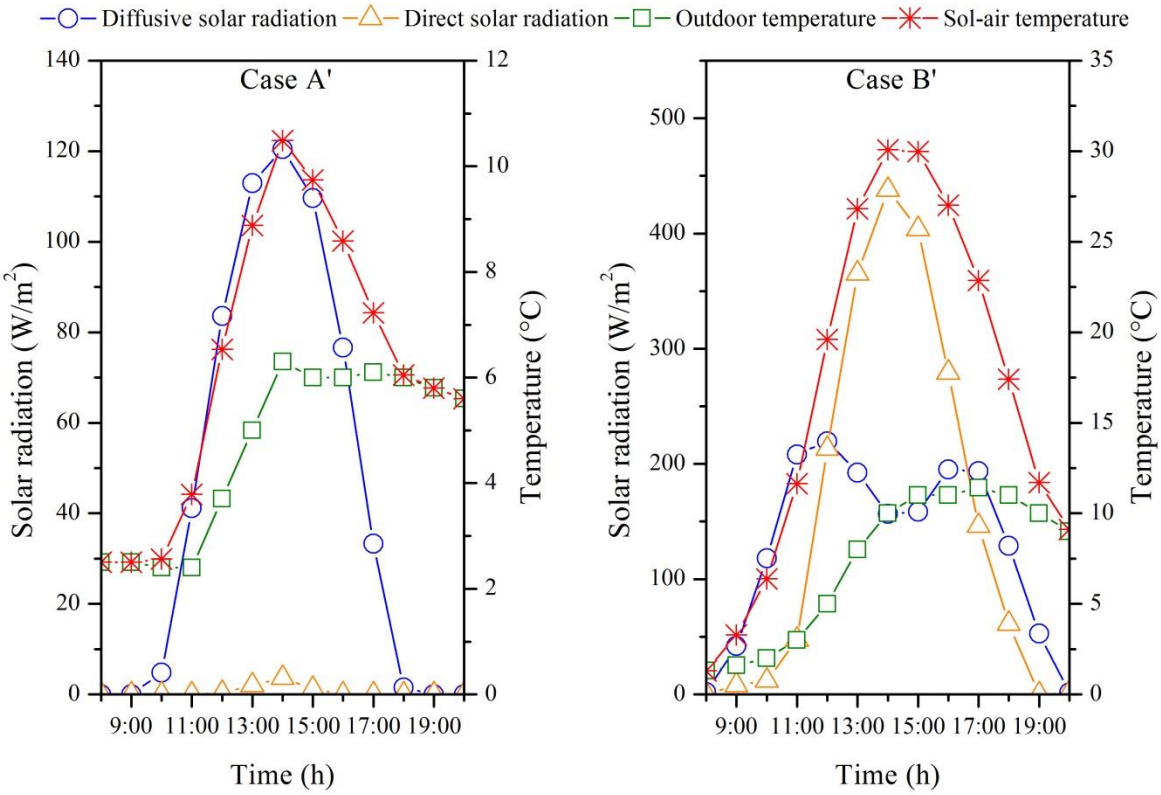

Figure 5-6: Outdoor climates of the two selected days.

5.3.1.1.1 Case A': Ordinary winter day

The PMV index, the mean radiant temperature, the room temperature and the energy consumption of all the studied cases for case A' are illustrated in Figure 5-7. The room temperature for the thermostatic controlled cases was stable at its set value throughout the entire occupied time of the day (Figure 5-7a). The PMV index and the MRT followed the same trend as the sol-air temperature, while the energy consumption presented an opposite trend against the sol-air temperature. The PMV index was stable until 10:00, and then it increased about 0.15 to reach its maximum when the sol-air temperature reached its maximum at 14:30, later the PMV index in all cases decreased and maintained a stable value.

However, in the thermal comfort controlled case, the PMV index was stable at -0.5 throughout the entire occupied time of the day (Figure 5-7b). The MRT followed the same trend as the sol-air temperature, while the room temperature and the energy consumption followed an opposite trend against the sol-air temperature, and thus MRT. These results illustrate the relationship between energy consumption and the MRT since the set-point temperature is principally determined by the MRT, thanks to the PMV-based controller that takes into consideration the changes in the MRT to control the set-point temperature in order to maintain a stable PMV value. For example, as the mean radiant

temperature increases, the set-point temperature decreases resulting in less heating energy. These results indicate that thermal comfort control has the apparent advantage of maintaining consistent thermal comfort.

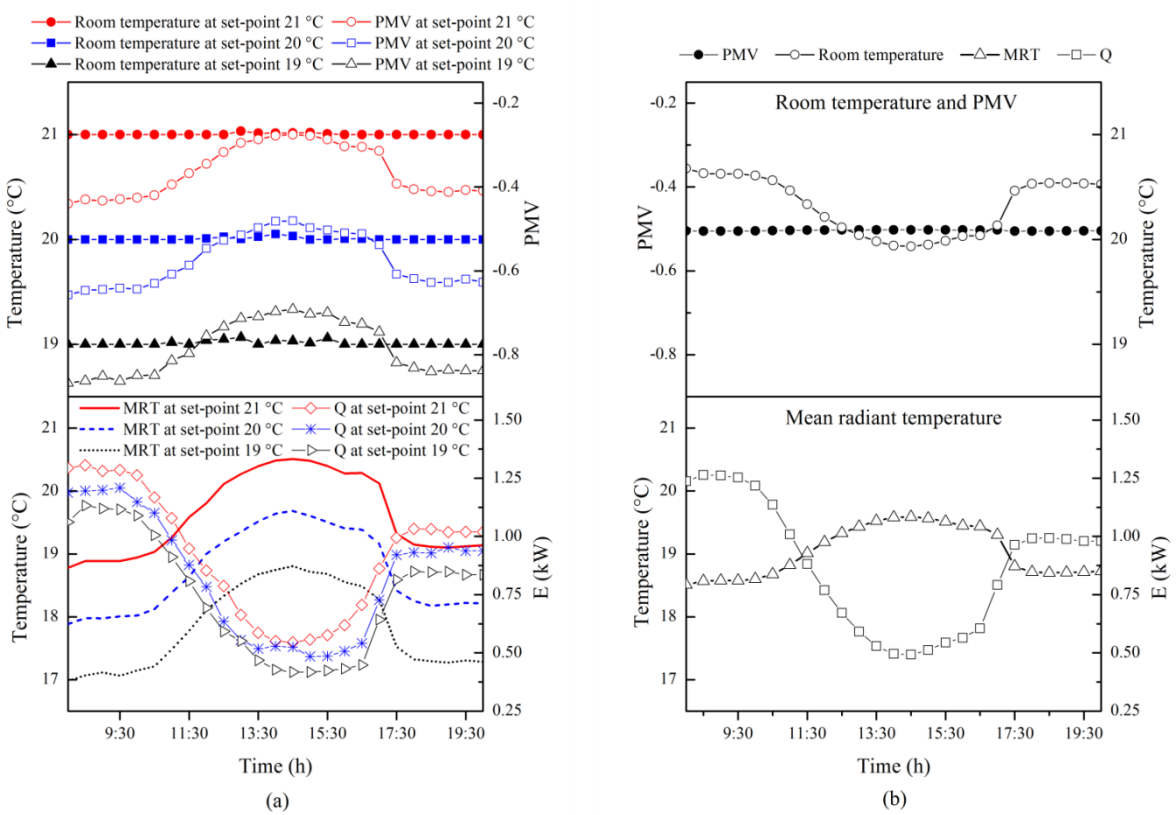

Figure 5-7: PMV, room temperature, mean radiant temperature and energy consumption for case A' in: (a) thermostatic control and (b) PMV-based control.

5.3.1.1.2 Case B': winter day with relatively high outdoor temperature and intense solar radiation.

The PMV index, the mean radiant temperature, the room temperature and the energy consumption of all the studied cases for case B' are illustrated in Figure 5-8. The PMV index, MRT, and room temperature for all the studied cases followed the same trend as the sol-air temperature. However, the energy consumption presented an opposite trend against the sol-air temperature. The results show that the PMV index exceeds the acceptable upper limit of PMV +0.5 for all the studied cases, although the heating system was turned off during the extreme outdoor climatic conditions, very high sol-air temperature. These results indicate that the risk of overheating could be correlated to the increasing of MRT under intense solar radiation, due to the presence of two fully glazed external walls, leading to higher PMV values. These results show that the risk of a hot environment and an overheating phenomenon can be alleviated by lowering the MRT values in the studied Foyer.

Therefore, a careful and appropriate treatment of the Foyer's glass façades configuration, such as reducing the glazing area, may offer improved thermal comfort.

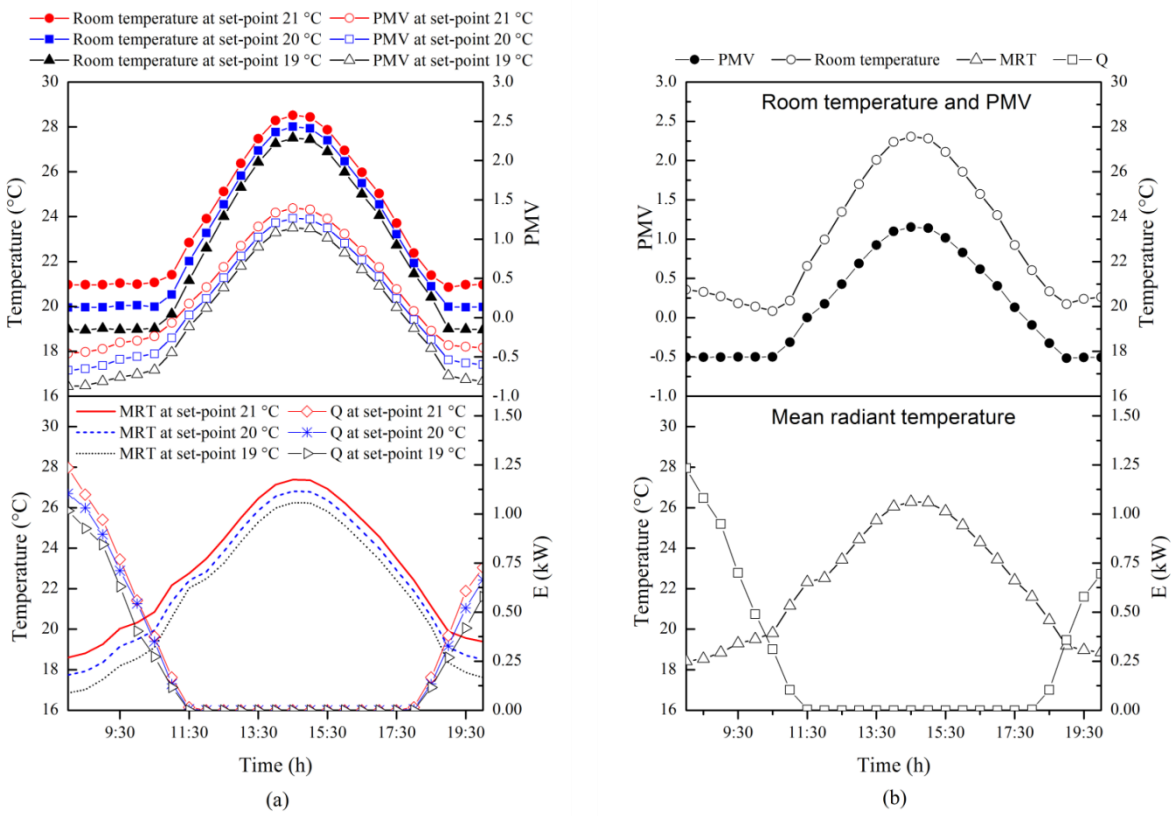

Figure 5-8: PMV, room temperature, mean radiant temperature and energy consumption for case B' in: (a) thermostatic control and (b) PMV-based control.

5.3.1.2 Long-term evaluation (monthly-base)

The monthly occurrence frequency of each comfort category and the monthly EQI are reported in Figure 5-9. The results show that category IV and category III appeared significantly in the thermostatic-control at set-points of 19°C (Figure 5-9a) and 20°C (Figure 5-9b), respectively, while, category II appeared considerably in the thermostatic-control at a set-point of 21°C (Figure 5-9c) and the comfort-control at a set-point of PMV -0.5 (Figure 5-9d) throughout the studied period. In addition, though the increase of monthly average sol-air temperature might improve the thermal comfort in the thermostatic-control at set-points of 19°C and 20°C (more appearance of categories I and II during March, April, and October), it leads to a slight decrease in the comfort quality at the set-point of 21°C and in the comfort-controlled case. These results show that the thermostatic-control at set-points of 19°C and 20°C is not sufficient to maintain the comfort quality within the limits of category II under the current design of the considered case study. Also, the set-point of 19°C recommended by the French standards failed to achieve the comfort quality of category III.

Furthermore, the results show that the monthly EQI in the thermostatic-control at a set-point of 19°C followed the same trend as the monthly average sol-air temperature, while at the set-points of 20°C and 21°C, a slight variation is observed, except at high monthly sol-air temperature (April), where a significant drop in the EQI is noticed at the set-point of 21°C. These results show that thermal comfort in the thermostatic-control is sensitive to climatic conditions, due to the presence of large glass surfaces, mainly at a high sol-air temperature, which leads to an increase in the internal surface temperature of the external glazed walls, allowing an increased mean radiant temperature, thus higher PMV values. On the other hand, the monthly EQI in the thermal comfort-control was maintained at about 70 throughout the studied period, and the results show less sensitivity to outdoor climatic conditions. This could be attributed to the fact that in the comfort-control the room temperature is mainly determined as a function of the MRT to maintain the predefined PMV value. These results suggest an apparent advantage of the thermal comfort-control to maintain consistent thermal comfort on a long term period.

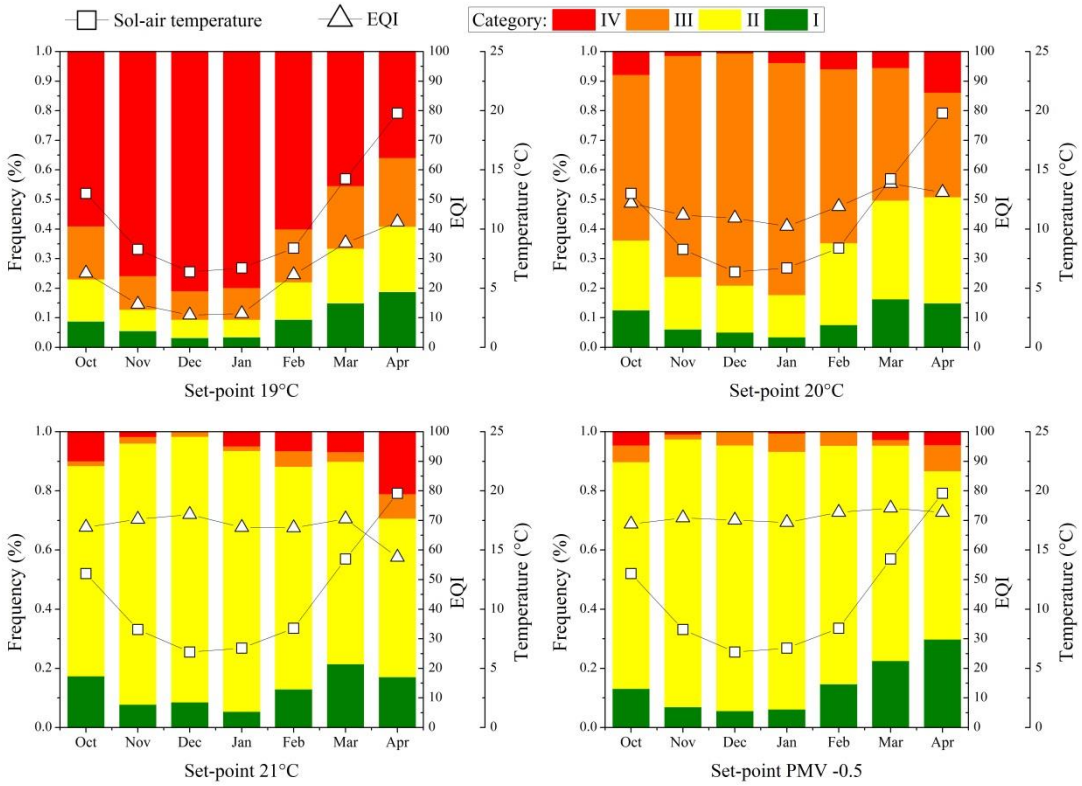

Figure 5-9: Occurrence frequency and the EQI for the thermostatic-control at a set-point of (19°C (a), 20°C (b), and 21°C (c)) and comfort-control at a set-point of PMV -0.5 (d).

Figure 5-10 shows the monthly heating energy consumption per meter square and the monthly EQI for all the studied cases. The results show that the thermostatic-control at set-points of 19°C and 21°C consumed the least and most amount of heating energy, respectively. In addition, the heating

energy consumption in the thermal comfort-controlled case was equivalent to that consumed at set-point of 20°C and allowed about a 10% reduction compared to the set-point of 21°C. On the other hand, the comfort-control at a set-point of PMV -0.5 offered better thermal comfort compared to the thermostatic-control at set-points of 19°C and 20°C (higher EQI throughout all the studied period), and equivalent to that offered at set-point of 21°C (almost equal EQI throughout all the studied period with an apparent advantage for the comfort-control during high monthly average sol-air temperature, such as in April). These results show that PMV-based thermal comfort controller is a reasonable solution to neutralize the trade-off between thermal comfort and energy savings.

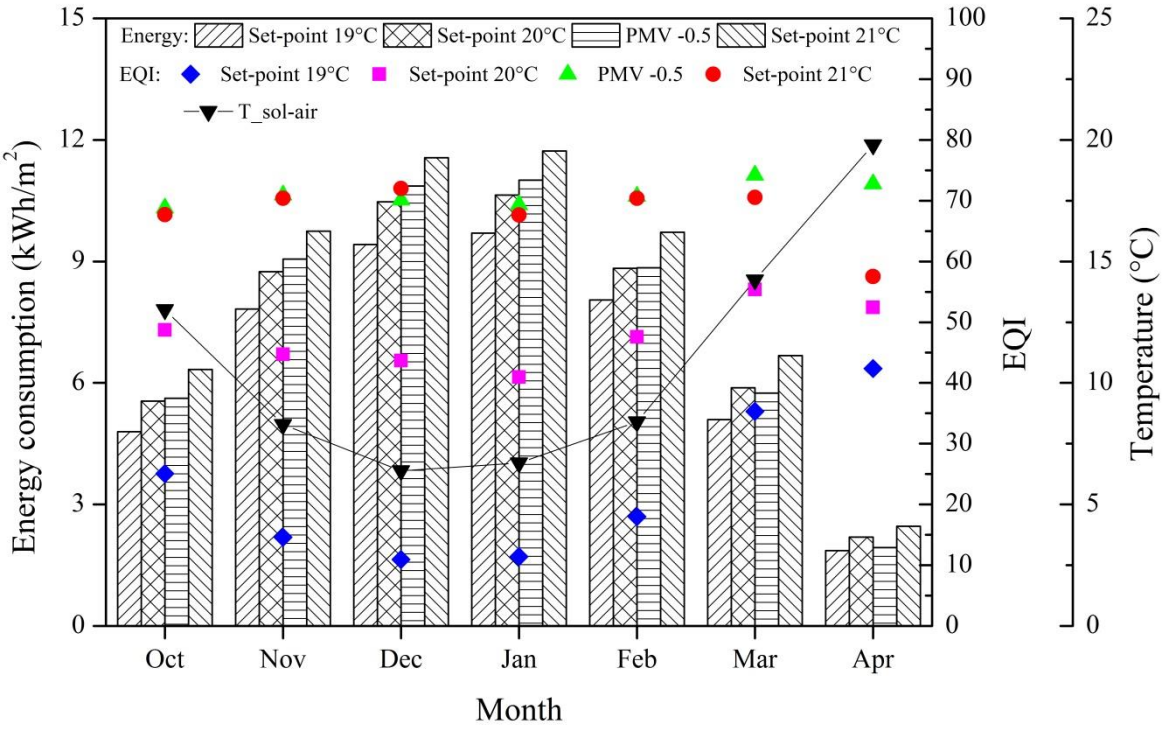

Figure 5-10: Monthly energy consumption per meter square and the monthly EQI of all the studied cases.

Furthermore, compared to the set-point of 20°C, thermal comfort-control allows a reduction in the heating energy consumption as sol-air temperature increases, such as in March and April; on the contrary, a decrease in the sol-air temperature leads to more energy consumption. These results are related to the presence of fully glazed external walls and their sensitivity to outdoor climatic conditions. In fact, a decrease in the sol-air temperature leads to an increase in transmission heat losses, resulting in decreasing the internal surface temperature of the external glass façades. This phenomenon leads to a decrease in the mean radiant temperature, and since the set-point temperature

in the comfort-control is predominantly determined by the mean radiant temperature, an increase in the set-point temperature is needed to maintain the PMV value, thus more heating energy consumption.

These results indicate that the PMV-based thermal comfort-control is a reasonable solution to neutralize the trade-off between thermal comfort and energy-savings. This could be attributed to the fact that the room temperature in a comfort controlled space is mainly determined as a function of the mean radiant temperature to maintain the predefined PMV value. However, under low sol-air temperature, the energy-saving potential is reduced using the thermal comfort-control, but consistent thermal comfort is maintained. Besides, the results designate that energy consumption using a comfort-control is more sensitive to outdoor climates than using a thermostatic-control, which results in more energy-savings under high sol-air temperature while maintaining better thermal comfort.

5.3.2 Comparison with optimized design conventional controlled case

In the following section, the thermal comfort controlled case is compared with the optimized conventional controlled case. The considered parameters are the PMV index, room temperature, MRT, the hourly power of the heating system and the total heating energy consumption. This comparative study aims to investigate if the PMV-based thermal comfort controller is a reasonable solution to neutralize the trade-off between thermal comfort and energy consumption. The obtained hourly numerical values of the considered parameters using the validated model throughout the investigated European winter are shown in Figure 5-11. The results show that applying the optimized design alleviated the high PMV and MRT values in the conventional controlled optimized case. In addition, the variations in all the studied parameters reduced drastically because of the adequate design of the glazed envelope, as a result of the optimization process. Moreover, the obtained results show that the optimized thermostatic case allowed about a 16.5% reduction of heating energy consumption compared to the comfort controlled case.

These results show that integrating thermal comfort in the design stage of the buildings leads to an optimized design for both thermal comfort and energy consumption. In addition, it suppresses the need for an advanced control strategy, which could require additional devices installations in order to keep continuous monitoring of the indoor environment, thus leading to additional installation and functional costs. Moreover, the results indicated that under the current design PMV-based thermal comfort-control is a reasonable solution to neutralize the trade-off between thermal comfort and energy-savings. This could be attributed to the fact that the room temperature in a comfort controlled space is mainly determined as a function of the mean radiant temperature to maintain the predefined PMV value. Furthermore, although the heating system is controlled to maintain a set-point of PMV -0.5, the PMV values exceeded this limit for a considerable amount of time, namely at high sol-air temperatures. This indicates that the PMV index and as a result heating energy consumption is

sensitive to the outdoor climatic conditions. This could be correlated to the presence of the two fully glazed façades. However, the set-point temperature in the thermal comfort-control is influenced by six main factors, as shown in Equation (5.1). Thus, investigating the sensitivity of energy consumption to these factors is essential to evaluate the impact of each factor on the final heating energy consumption, and as a consequence, to confirm if the problem is only related to the extensive glazing area or other contributing parameters.

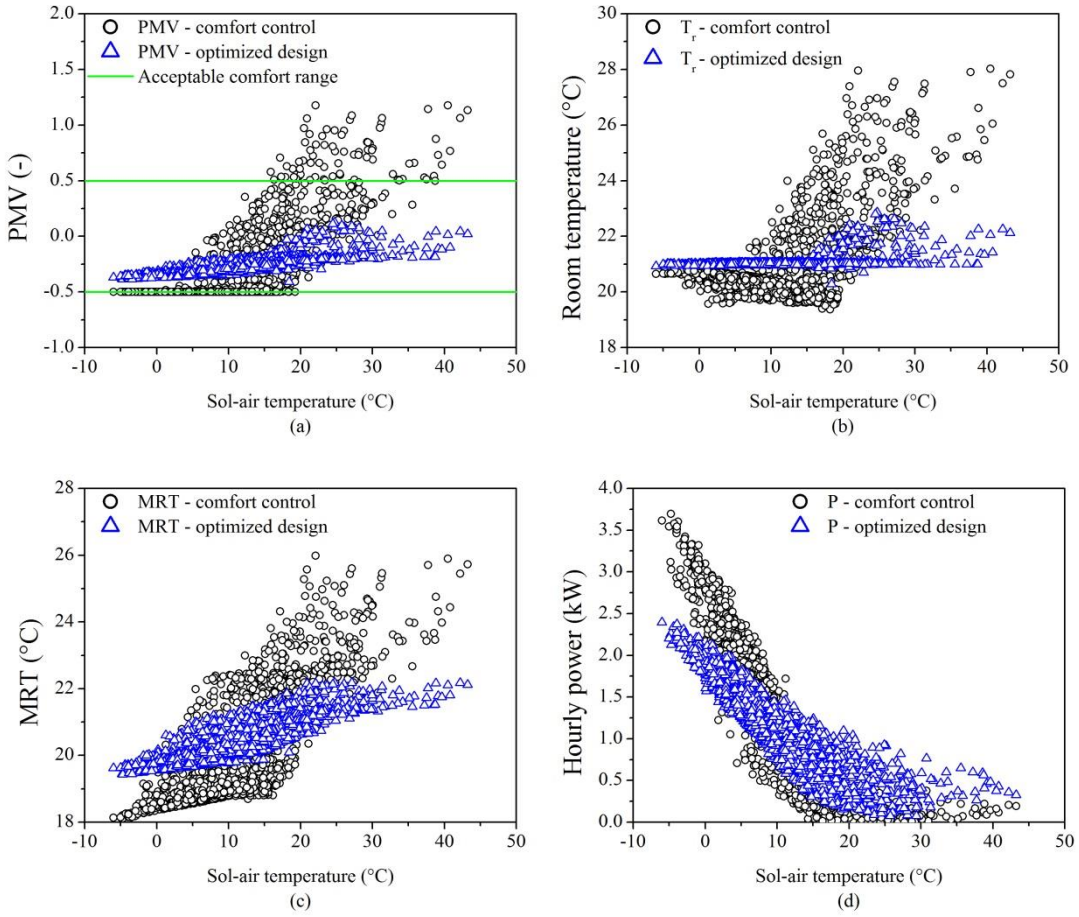

Figure 5-11 : Numerical hourly values of (a) PMV index, (b) room temperature, (c) MRT and (d) the hourly power of the heating energy obtained from the validated Dymola model for the two cases.

5.4 Sensitivity analysis

5.4.1 Heating energy consumption

Energy consumption of the heating system during one week is considered as the response variable. The investigated parameters are the mean radiant temperature, the relative humidity, the air velocity, the metabolic rate, and the clothing insulation. Each factor has two levels noted as high (+1) and low (-1). The higher and lower levels of each factor are based on the maximum and minimum values recommended by the European standards [79]. Table 5-2 reports the investigated factors and

their corresponding codes, units and higher and lower levels. The PMV was set as a fixed factor at -0.5.

Table 5-2 : Investigated factors and their corresponding codes and levels.

Factor	Code	Unit	Level	
			-1	+1
Mean radiant temperature	*A'*	°C	16	30
Relative humidity	*B'*	%	30	70
Air velocity	*C'*	$m.s^{-1}$	0.15	0.25
Metabolic rate	*D'*	$W.m^{-2}$	57	95
Clothing insulation	*E'*	clo	0.8	1.2

The full factorial design considering five factors, each at two levels results in 32 runs. Once the experimental plan was obtained, the experiments were carried out by running the simulation model for different combinations of factors' levels. The design matrix considering the further tests and the simulation results of the response variable is shown in Figure 5-12 and reported in Table D- 8. Each run represents a unique combination of factors' levels and the resulting weekly heating energy consumption. Minitab® software, a statistical computer package, was used to analyze the results.

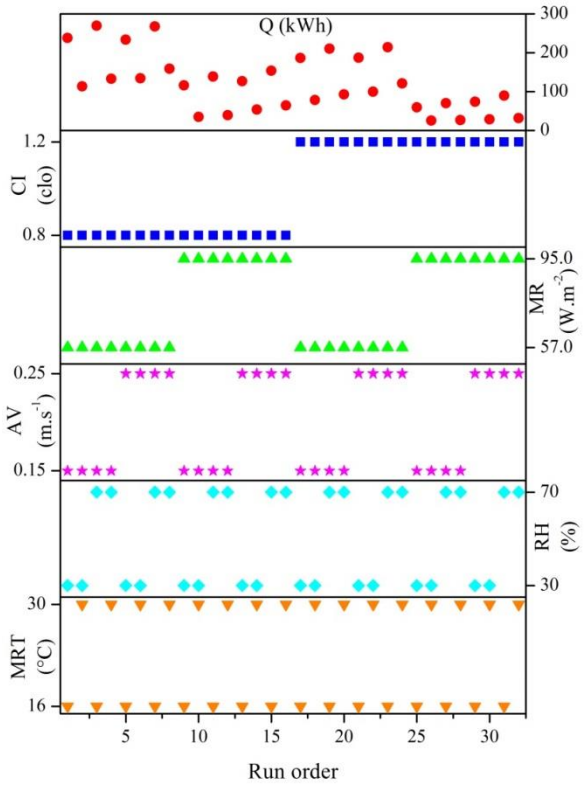

Figure 5-12: DoE simulation results.

The Analysis of Variance (ANOVA) was applied in order to identify the significant parameters affecting the heating demand. As mentioned in the previous chapter, factors of a small p-value, less than 0.05, are deemed as significant parameters [82]. The results of ANOVA are summarized in Table 5-3(complete results are reported in Table D-9).

Table 5-3: ANOVA table.

Source	DF	Seq SS	Adj SS	Adj MS	F-Value	P-Value	Remarks
Model	31	167343	167343	5398.1	4968.85	**0.011**	Significant
Main effects	5	159835	159835	31967.0	29424.73	**0.004**	Significant
2-Way Interactions	10	6502	6502	650.2	598.48	**0.032**	Significant
3-Way Interactions	10	838	838	83.8	77.13	0.088	Not significant
4-Way Interactions	5	49	49	9.9	9.11	0.246	Not significant
Curvature	1	118	118	118.4	108.96	0.061	Not significant
Error	1	1.09	1.09	1.09			
Total	32	167344					

The Pareto chart for standardized effects at p = 0.05 for the weekly heating demand is shown in Figure 5-13. The bars display the variables (A'-F') and their interactions, where all the bars that exceed the vertical dashed line are considered significant, which means that the variables and their interactions influence the heating demand response at a minimum statistically significant level of 95% confidence. The results reported in Figure 5-13 show that the metabolic rate (D'), the mean radiant temperature (A') and the clothing insulation (E') have the highest effect on the heating energy demand in a thermal comfort-controlled space. The effects of other factors are in descending order as shown in the Pareto chart.

The Pareto chart assists in determining which of the factors and interactions are most significant. However, it is important to consider the normal probability plot of standardized effects at p=0.05, to complement the analysis. Figure 5-14 shows the normal probability plot of standardized effects at p=0.05, for one week heating demand. The fit line specifies the values expected to be obtained if the variable has no effect. Significant effects are presented with their labels and positioned a certain distance to the left or right of the fit line indicating negative (when situated to the left) or positive (when situated to the right) values of the standardized effect. Negative values mean that an increase in their levels leads to a decrease in the heating demand; positive values mean that heating demand increase with increasing level. Metabolic rate, MRT, clothing insulation, the interaction between MRT and relative humidity, the interaction between metabolic rate and relative humidity, and the interaction between MRT, air velocity and metabolic rate are the parameters having a negative effect on the heating demand, while all the remaining significant parameters have a positive effect.

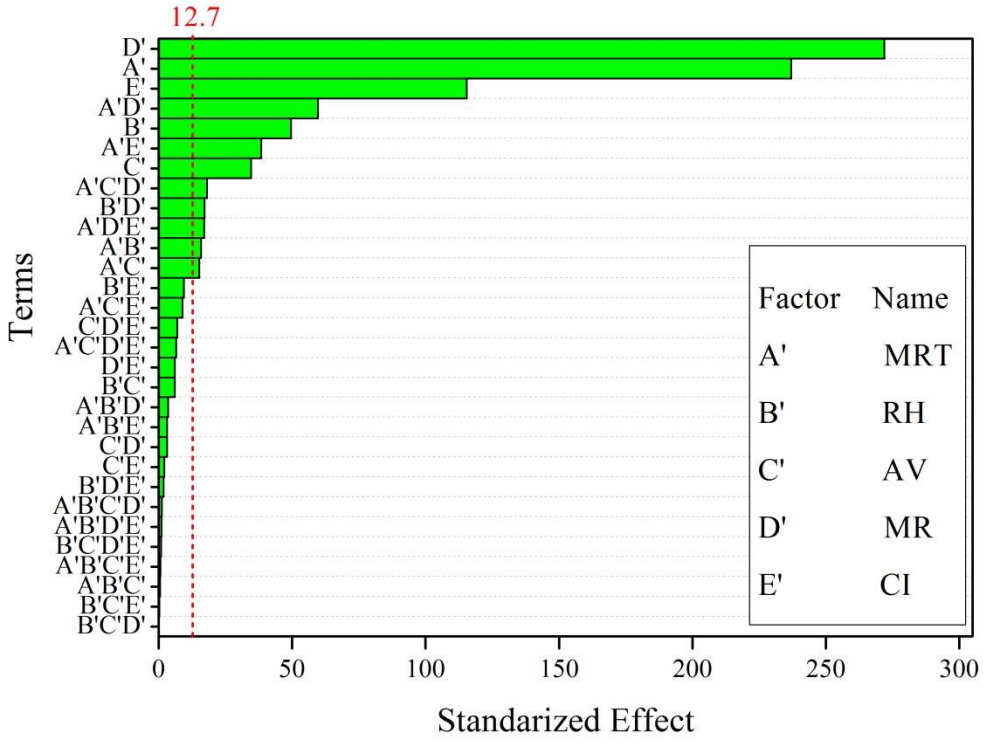

Figure 5-13 : Pareto chart of the standardized effects at p=0.05, for one week heating energy consumption.

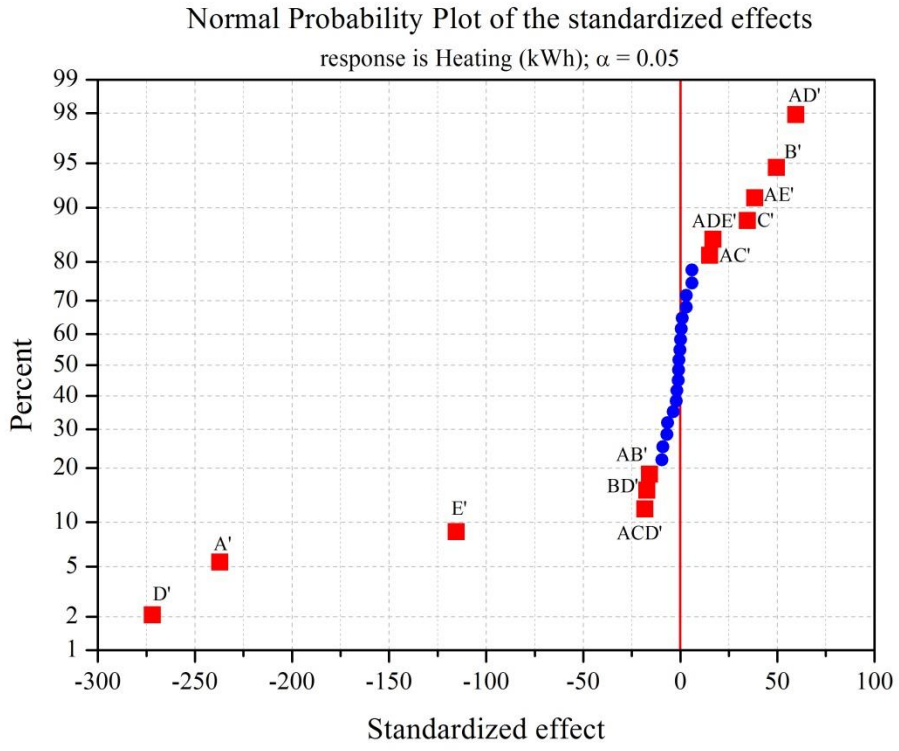

Figure 5-14: Normal plot of standardized effects at p=0.05, for one week heating energy consumption.

In addition, Figure 5-15 illustrates the main effect plot of each of the studied factors. The effect of a factor is defined as the change in the response due to the change in the level of the factor. It can be clearly seen that the slopes, which designate the influence, of the metabolic rate, the mean radiant temperature, and the clothing insulation, are the highest compared to those of the other parameters. These results indicate that the user-defined parameters, mainly occupants' behavior (clothing insulation and metabolic rate), must be accurately defined in a thermal comfort-controlled space due to their high effect on energy consumption.

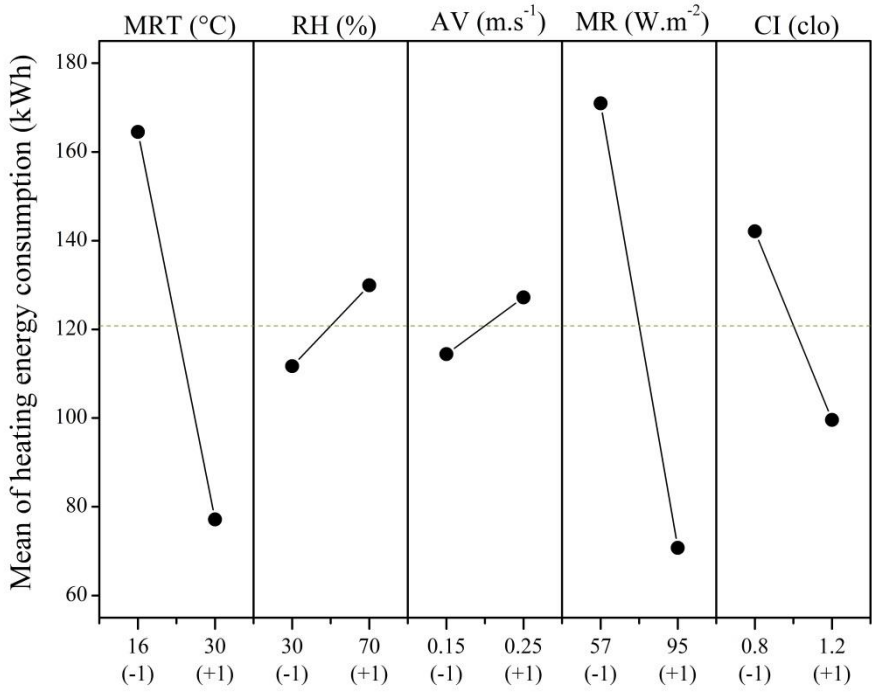

Figure 5-15: Main effect plot for one week heating energy consumption (kWh).

After identifying the main effects, the interactions between effects are essential, since these interactions were found to be significant using the Pareto charts (Figure 5-13). Figure 5-16 shows the interaction plot for the heating energy consumption noting that the significant interactions are only presented. The results reported in Figure 5-16 show that as the value of MRT increases the effects of MR, CI and RH decrease. For instance, at the low level of the MRT, changing the MR from its low to high level results in changing the response from 225.5 kWh to 103.5 kWh, while at the high level of MRT the change in the response is from 116.25 kWh to 38 kWh. The same trend is followed in the interaction between the MRT and the RH and CI, while the opposite is occurring between the MRT and AV.

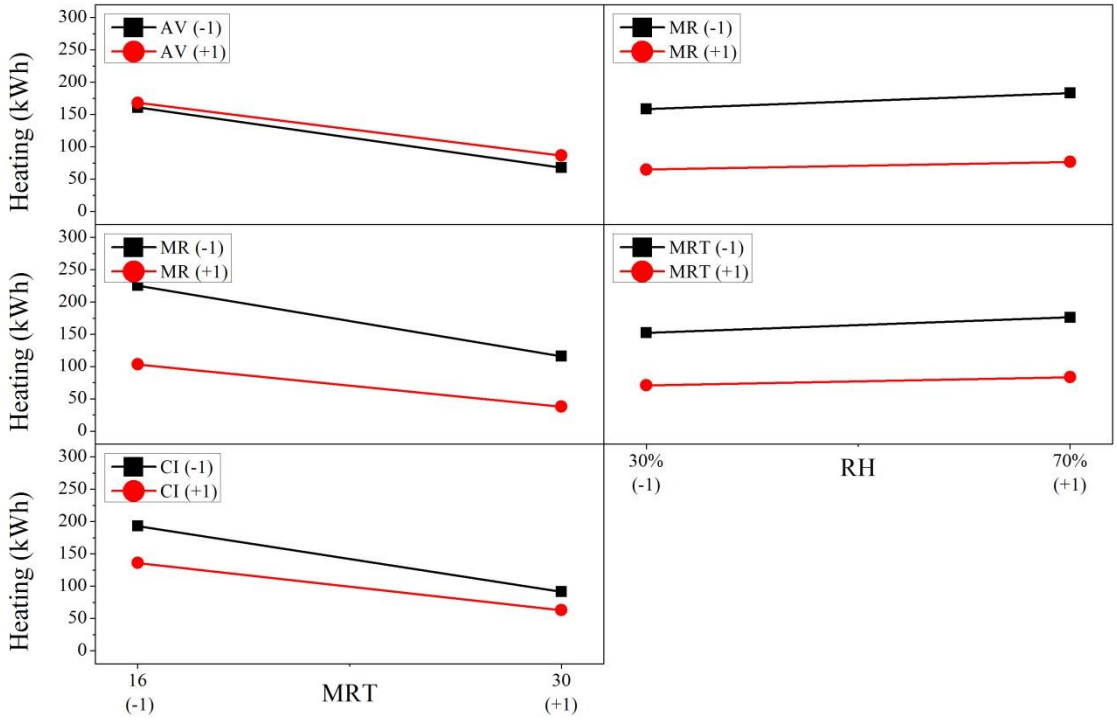

Figure 5-16: Significant interactions plot for one week heating energy consumption (kWh).

5.4.2 Development of meta-model for the prediction of heating energy consumption

The ANOVA test shows that the meta-model for heating energy consumption is statistically significant at a 95% confidence level ($p < 0.05$). The obtained meta-model can be simplified by eliminating the non-significant factors ($p > 0.05$), and the best fit meta-model equation that describes the weekly heating energy consumption is given by Equation (5.3):

$$Q = 120.83 - 43.68 \times MRT + 9.13 \times RH + 6.39 \times AV - 50.10 \times MR - 21.27 \times CI - 2.92 \times MRT \times RH + 2.8 \times MRT \times AV + 11.00 \times MRT \times MR + 7.07 \times MRT \times CI - 3.16 \times RH \times MR \quad (5.3)$$

The ANOVA results of the simplified meta-model indicated good performance with an R^2 value of 0.99 and adjusted R^2 value of 0.99. The R^2 of the model indicates that 99% of the total variations for the heating energy were attributed to the independent variables. The adjusted R^2 is an expressing form of degree of fit and it is more reliable than R^2 for comparing models with different numbers of independent variables [69]. The value of adjusted R^2 indicates that 99% of the total factors are attributed to the selected parameters of the model.

Furthermore, the validation of the obtained meta-model is essential to justify the adequacy of the performed analysis. Residual versus predicted value plot and normal probability plot of residuals are used to check the validity of the obtained model. The residual versus the predicted response plot illustrated in Figure 5-17 shows that there is a less patterned structure indicating that the proposed model is adequate. In addition, the normal probability plot shown in Figure 5-18 indicated that the residuals followed a straight line, thus confirming the validity of the model. Moreover, 15 additional simulations were performed with different factors' levels using the developed Modelica model and the results were compared to the meta-model predicted results. The obtained results are shown in Figure 5-19. A good correlation is observed showing an R^2 value of 0.98, meaning that 98% of the variance is explained by the obtained meta-model. In addition, the calculated NMBE and CVRMSE are -2.42 and 6.36, respectively, and are within the acceptable limits [74].

Therefore, the meta-model is considered to be validated and adequate. This meta-model can be used instead of the numerical model or any other building simulation model as a fast and simple way to predict the energy consumption of the studied room equipped with PMV-based thermal comfort-control at a set-point of PMV -0.5. As well as, it can be used to find the optimal solution in order to minimize the heating energy consumption, while maintaining acceptable thermal comfort conditions. However, the reliability of this meta-model is limited to a similar case study and the considered range of variation of the investigated factors.

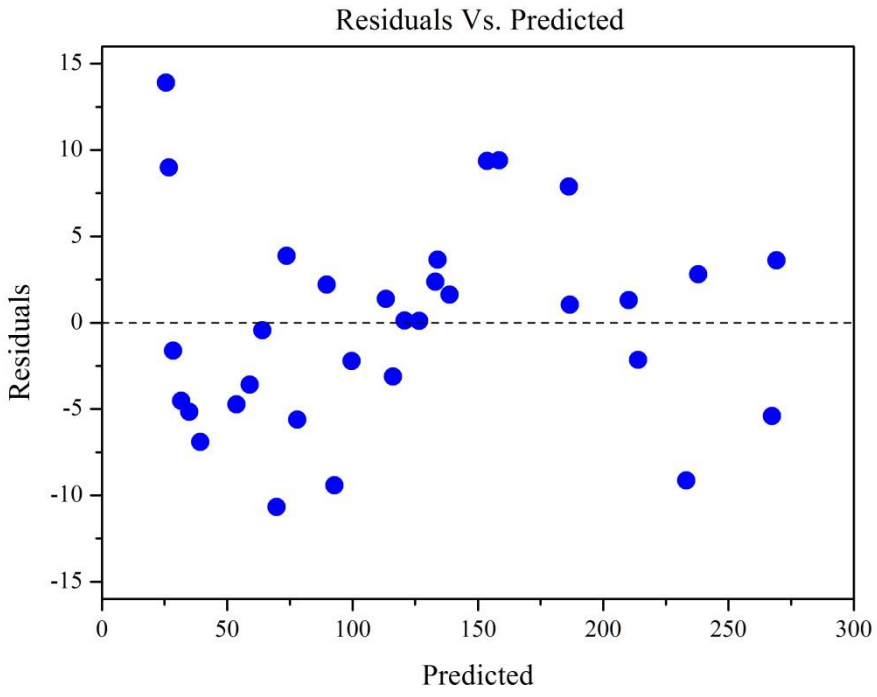

Figure 5-17 : Residuals versus fitted values for the heating energy consumption.

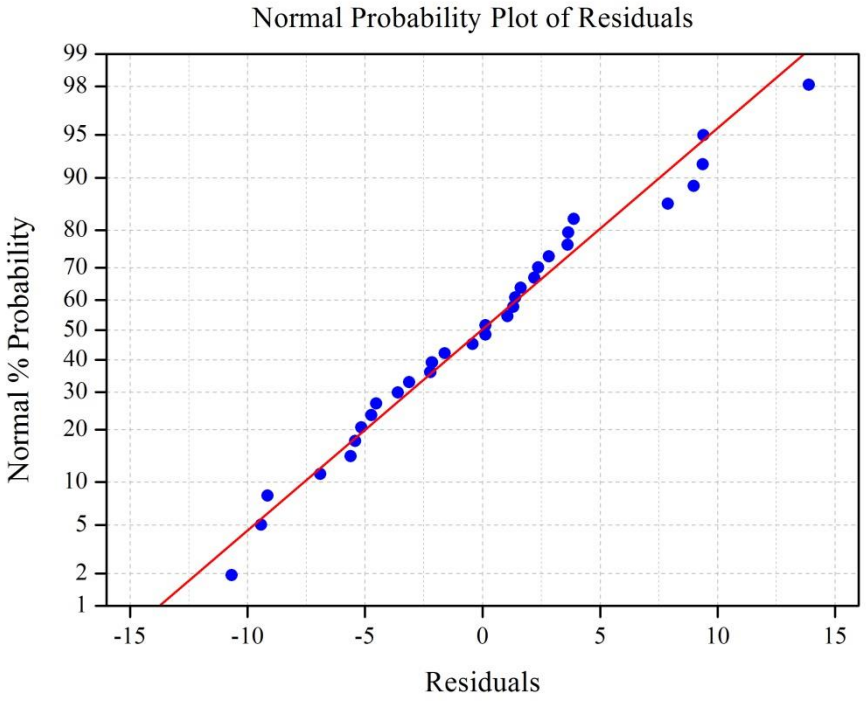

Figure 5-18 : Normal probability plot of residuals for the heating energy consumption.

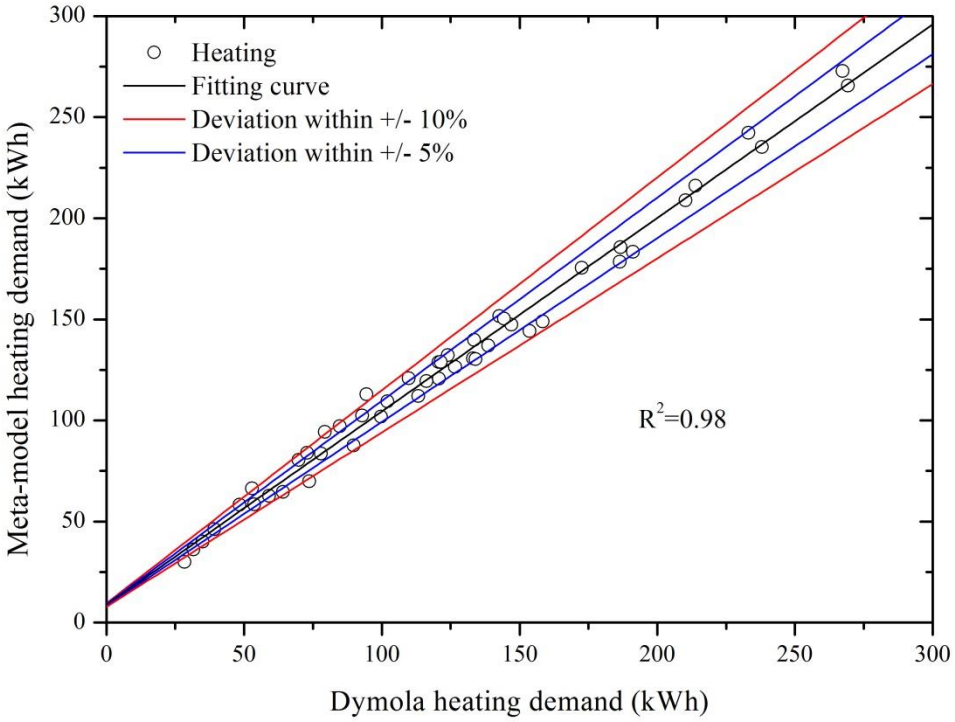

Figure 5-19 : Coefficient of determination between simulation results and the meta-model predictions.

To sum up, the performed sensitivity study indicates that the mean radiant temperature and personal parameters such as metabolic rate and clothing have the highest impact on the energy consumption in a comfort controlled highly glazed room. Thus, in order to achieve energy-savings, personal parameters must be adequately defined rather than just assuming them as default values. Regarding the metabolic rate, wearable devices could be used to provide continuous feedback for the averaged metabolism value of building occupants as discussed in [76]. However, more investigations are needed to confirm if such a solution is feasible in terms of acceptability by building occupants. In addition, in recent years, numerous models were developed to predict the clothing level and the change of indoor clothing insulation with outdoor temperature, based on different regression functions [84–86]. According to these models, a significant percentage of the variance in clothing insulation was explained by variations in an outdoor climatic index; such as outdoor temperature, mean daily outdoor temperature, mean monthly outdoor temperature and weighted outdoor temperature. These models can be applied in the buildings equipped with intelligent BEM systems for both thermostatic and comfort controlled spaces in order to predict the clothing insulation of the occupants based on the changes in outdoor climatic conditions.

Moreover, the results confirmed the findings presented in Figure 5-7 and Figure 5-8 that show the effect of continuous variation of the MRT on the PMV values and thus the heating energy consumption. On one hand, a low MRT leads to high heating energy consumption to maintain the predefined PMV value. On the other hand, a high MRT leads to reduced heating energy consumption, conversely, it leads to exceeding the upper comfort level when exposed to intense solar radiation. In addition, the aforementioned results show that in all cases, except with thermostatic control at a set point of 19 °C, the PMV value did not fall below -0.7, but exceeded the value of +0.7. These results indicate that, under the current design, the major problems targeting the thermal comfort in the studied space are the risk of a hot environment and an overheating phenomenon. Based on the aforementioned discussion, the risk of hot environment and overheating phenomenon can be alleviated by lowering the mean radiant temperature. Hence, a careful and appropriate treatment of the glass facades configuration could offer improved thermal comfort and energy consumption. In this consequence, it is essential to perform a sensitivity study where the response variable is the MRT to determine the critical parameters affecting the mean radiant temperature so that an optimal design could be achieved.

5.4.3 Mean radiant temperature

In this regard, the DoE technique was also used to perform another sensitivity study to determine the effect of glazed envelope configuration on the MRT and thus the heating energy consumption in a comfort controlled case. The parameters studied are the glass façades orientation, internal shading, glazing type, WFR, and the sol-air temperature. The DoE was based on full factorial design considering five parameters each at two levels, thus resulting in 32 runs. The higher and lower

levels of the orientation and shading are based on the simulation results which outcomes the minimum and maximum values of the MRT. For example, if the room is north-east oriented this will result in less exposure to solar radiation and thus decreasing the MRT values, so north-east oriented is set at -1 level; conversely south-west orientation is set at +1 level. In addition, The high level of the glazing area and glazing type represents the base case study, and the low level has been selected with respect to the values recommended by the low energy building and French standards [7,78]. Table 5-4 reports the investigated factors and their corresponding codes, units and higher and lower levels. The PMV was set as a fixed factor at -0.5. The average, maximum and minimum values of the MRT are considered as the response variables in the DoE. The design matrix considering the further tests and the simulation results of responses are shown in Table D-11. The results of ANOVA are summarized in Table 5-5 (Complete ANOVA results are reported in Table D-12, Table D-14, and Table D-16).

Table 5-4: Investigated factors and their corresponding codes and levels for the MRT.

Factor	Code	Unit	Level	
			-1	+1
Orientation	*U*	-	N-E	S-W
Shading	*V*	-	No shading	Internal shading
Glazing type (u-value)	*W*	$Wm^{-2}K^{1}$	0.7	2.8
(g-value)			0.3	0.77
Glazing area (WFR)	*X*	%	16	60 (base case)
Sol-air temperature	*Y*	°C	-2.2	17.2

The Pareto charts for standardized effects at p = 0.05 for the considered response variables shown in Figure 5-20 indicate that the sol-air temperature, the interaction between WFR and sol-air temperature, WFR, glass façades orientation, the interaction between orientation and sol-air and glazing area are the significant parameters affecting the average MRT values. The maximum MRT values are also affected by the same parameters in addition to the shading and the interaction between shading and sol-air temperature. However, WFR, sol-air temperature, glazing type and the interactions between them are the significant parameter affecting the minimum value of the MRT. Additionally, Figure 5-21 illustrates the main effect plot of each of the studied factors on the response variables. It can be clearly seen that the sol-air temperature, WFR, orientation, and shading affect the average and maximum MRT values, while the glazing type has no significant impact. However, sol-air temperature, WFR, and glazing type are the parameters affecting the minimum MRT.

Table 5-5: Analysis of variance for average, minimum and maximum MRT.

Source	DF	Seq SS	Adj SS	Adj MS	F-Value	P-Value
Average MRT						
Model	30	188,69	188,69	6,2897	497,27	0,035
Linear	5	119,819	119,819	23,9639	1894,63	0,017
2-Way Interactions	10	59,319	59,319	5,9319	468,98	0,036
3-Way Interactions	10	8,999	8,999	0,8999	71,14	0,092
4-Way Interactions	5	0,553	0,553	0,1107	8,75	0,251
Error	1	0,013	0,013	0,0126		
Total	31	188,702	188,702			
Minimum MRT						
Model	30	3,46122	3,46122	0,11537	656,35	0,031
Linear	5	2,89946	2,89946	0,57989	3298,94	0,013
2-Way Interactions	10	0,5393	0,5393	0,05393	306,8	0,044
3-Way Interactions	10	0,02156	0,02156	0,00216	12,26	0,219
4-Way Interactions	5	0,00091	0,00091	0,00018	1,03	0,63
Error	1	0,00018	0,00018	0,00018		
Total	31	3,4614	3,4614			
Maximum MRT						
Model	30	717,541	717,541	23,918	748,81	0,029
Linear	5	441,684	441,684	88,337	2765,6	0,014
2-Way Interactions	10	234,31	234,31	23,431	733,56	0,029
3-Way Interactions	10	39,728	39,728	3,973	124,38	0,07
4-Way Interactions	5	1,819	1,819	0,364	11,39	0,221
Error	1	0,032	0,032	0,032		
Total	31	717,572	717,572			

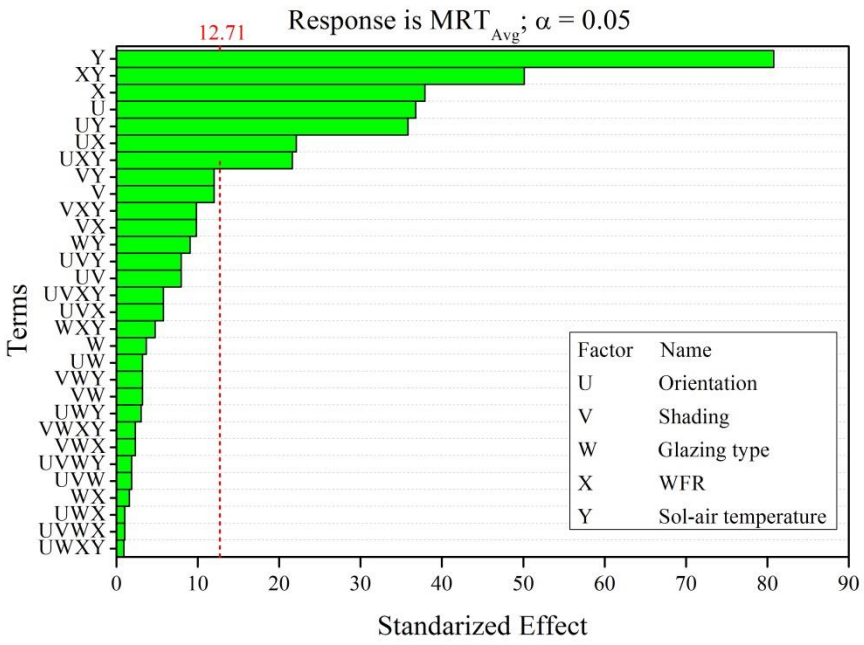
Response is MRT Avg; α = 0.05
12.71
Terms
Y
XY
X
U
UY
UX
UXY
VY
V
VXY
VX
WY
UVY
UV
UVXY
UVX
WXY
W
UW
VWY
VW
UWY
VWXY
VWX
UVWY
UVW
WX
UWX
UVWX
UWXY
0 10 20 30 40 50 60 70 80 90
Standarized Effect
Factor Name
U Orientation
V Shading
W Glazing type
X WFR
Y Sol-air temperature

(a)

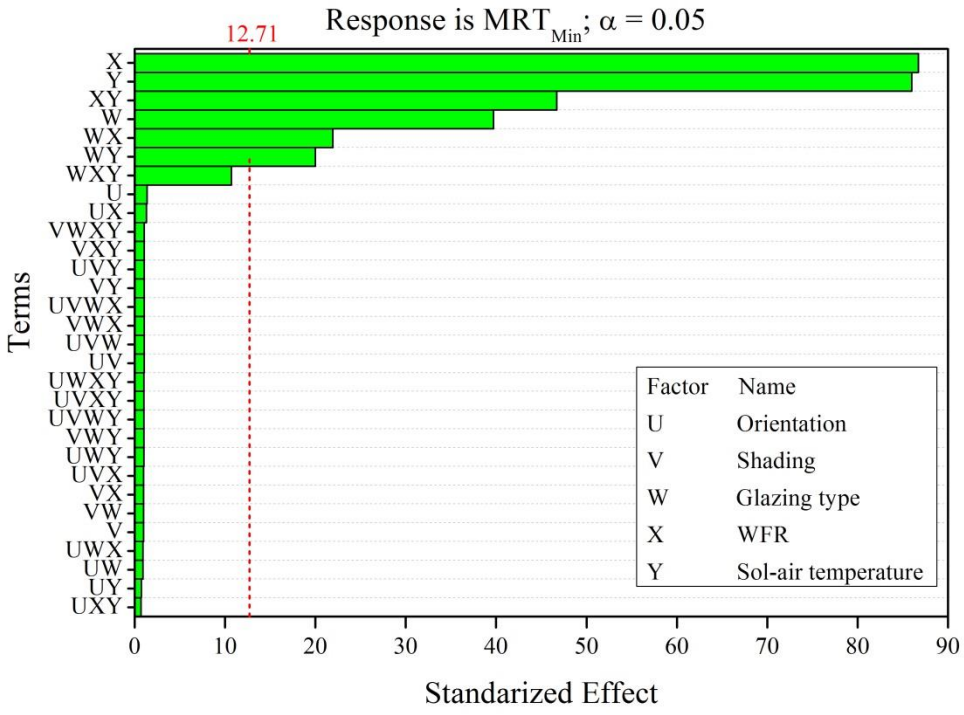
Response is MRT Min; α = 0.05
12.71
Terms
X
Y
XY
W
WX
WY
WXY
U
UX
VWXY
VXY
UVY
VY
UVWX
VWX
UVW
UV
UWXY
UVXY
UVWY
VWY
UWY
UVX
VX
VW
V
UWX
UW
UY
UXY
0 10 20 30 40 50 60 70 80 90
Standarized Effect
Factor Name
U Orientation
V Shading
W Glazing type
X WFR
Y Sol-air temperature

(b)

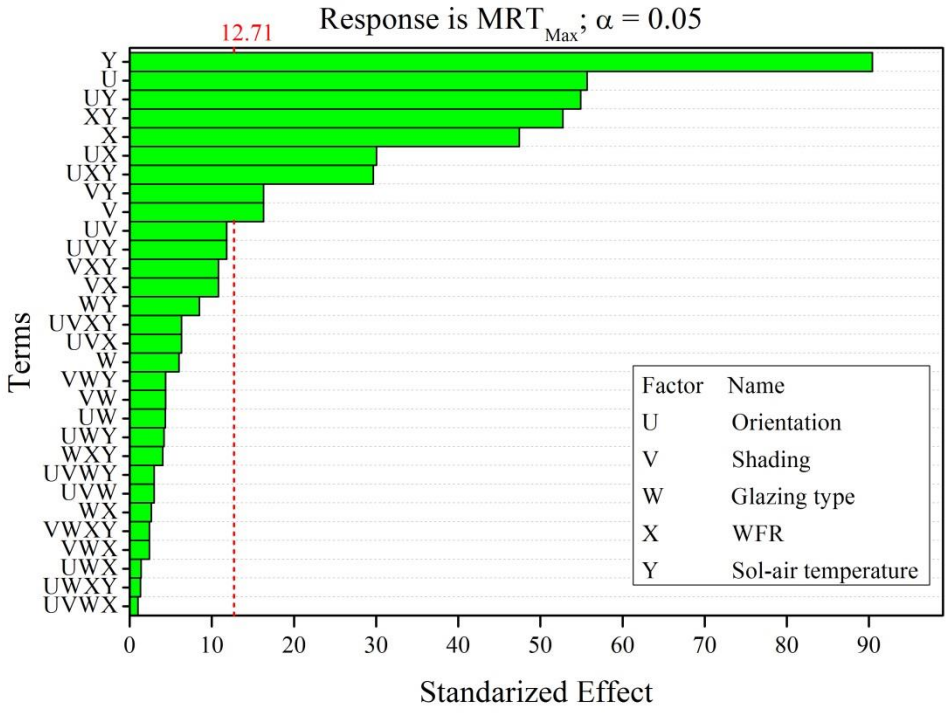

(c)

Figure 5-20: Pareto plots of standardized effects at p = 0.05 for: (a) average MRT, (b) minimum MRT and (c) maximum MRT.

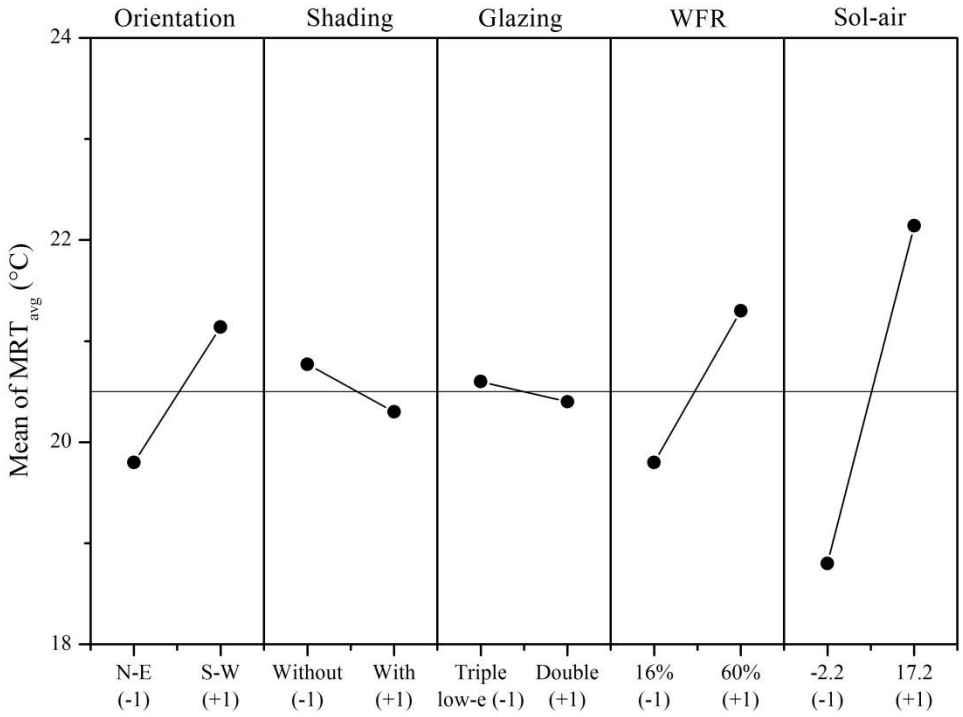

(a)

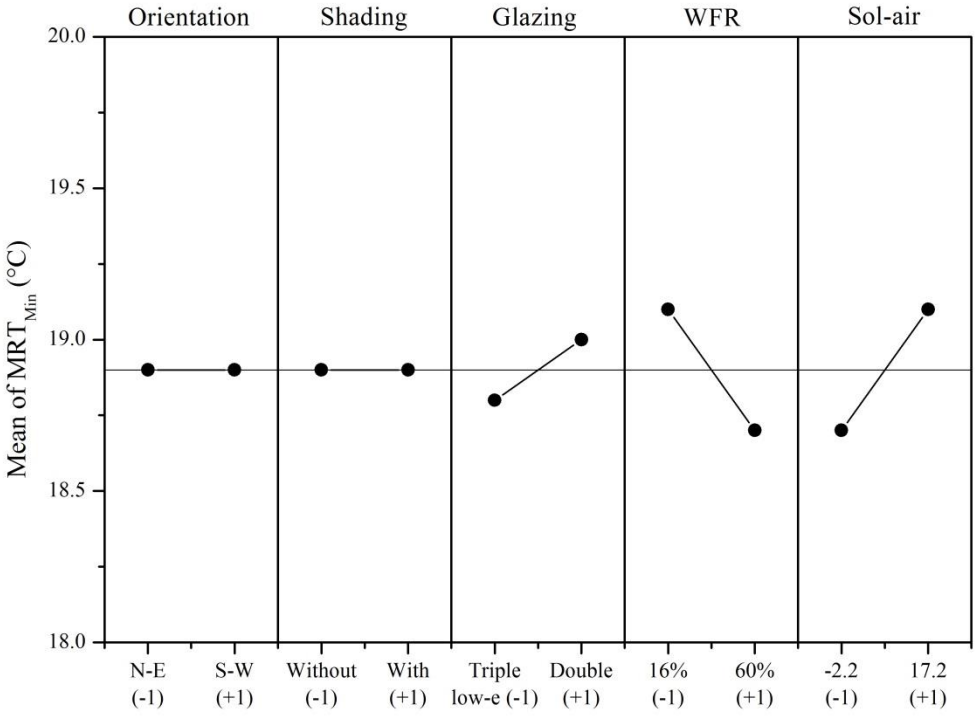

(b)

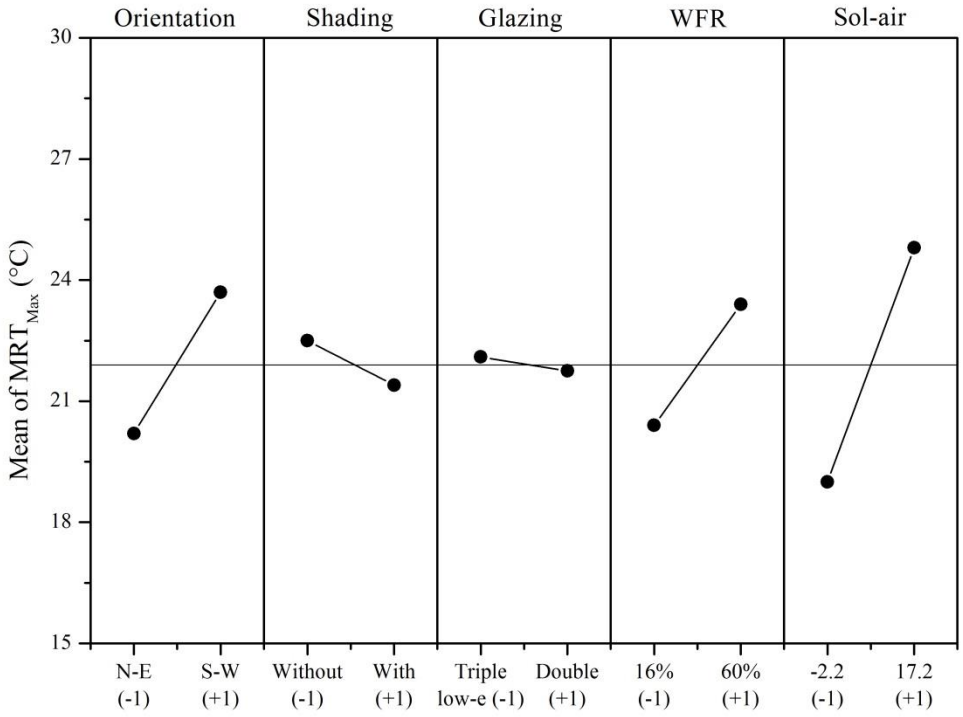

(c)

Figure 5-21: Main effect plot for: (a) average MRT, (b) minimum MRT and (c) maximum MRT.

Moreover, the interactions between some parameters were found to be significant, so it is essential to analyze these interactions. Figure 5-22 shows the significant interactions between parameters, while other interactions, which are not presented, were found to be insignificant. The interaction plot between WFR and sol-air temperature indicates that the effect of outdoor conditions on MRT is highly dependent on the glazing area. As the glazing area decreased the variation in the MRT as a function of sol-air temperature decreased. For instance, at 16% WFR the variation in the average and maximum values of MRT between a cold and hot day is 1.3 °C and 5.2 °C, respectively; while the variation reached 5.2 °C for the average and 9 °C for the maximum at 60% WFR. And also the interaction between orientation and sol-air temperature show that the effect of outdoor climatic conditions on the MRT is reduced significantly when the glazed facades of the room are north-east oriented. The interaction plot between WFR and Orientation indicates that the effect of orientation on the average and maximum MRT decreased as the WFR decreases. For instance, when the WFR is at its high level, average MRT increased from 19.8°C when the room is N-E oriented to 22.4°C when S-W oriented, however at the low level of WFR, the average MRT increased from 19.4°C to 20.1 °C. Conversely, the effect of the WFR increased as the orientation changes from the low to the high level. In addition, the interaction between WFR and shading indicates that the effect of the shading device could be eliminated if the area of the glazed envelope is reduced to 16% WFR (variation in the MRT is about 0.1°C if WFR is at its low level and shading varies between -1 and +1), or the glazed facades are north-east oriented. On the other hand, the interactions between glazing type and WFR and sol-air temperature appear to have a significant impact on the minimum MRT values. The results show that glazing type could have a significant impact as the glazing area increase or during low sol-air temperature because at high glazing areas and during a cold outdoor condition, improving the glazing u-value could reduce the heat loss through the glazed envelope, and thus preventing the decreased surface temperature of the glazed facades. These results indicate that the variations in the MRT values are hugely correlated to the WFR and glazed facades orientations, which with an adequate treatment could significantly offset the effects of shading, glazing type, and outdoor conditions.

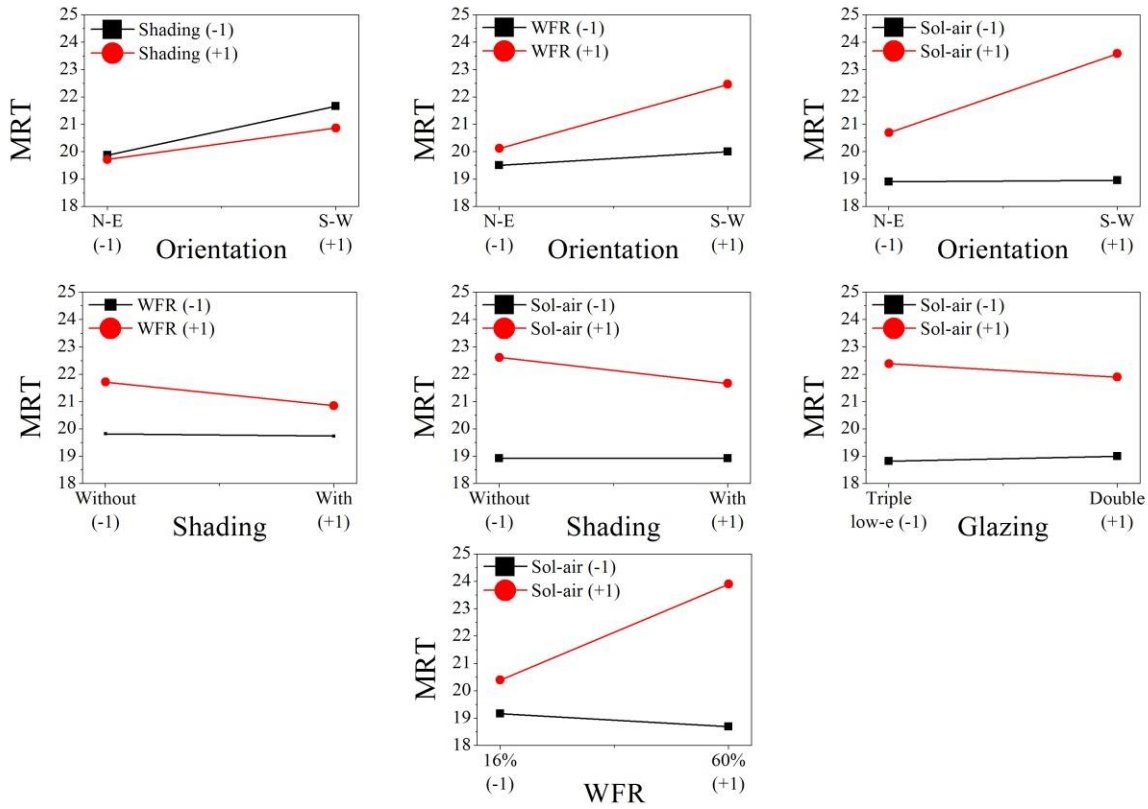
Shading (-1)
Shading (+1)
MRT
N-E
(-1)
Orientation
S-W
(+1)
WFR (-1)
WFR (+1)
Sol-air (-1)
Sol-air (+1)
Without
With
Shading
Triple
low-e (-1)
Double
Glazing
16%
60%
WFR

(a)

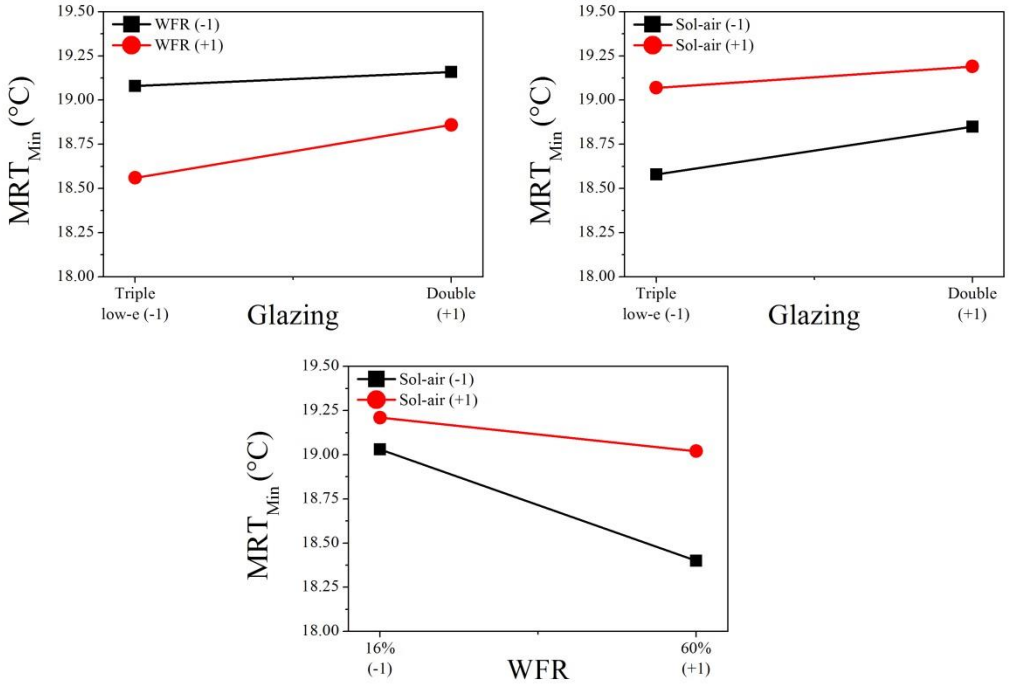
WFR (-1)
WFR (+1)
Sol-air (-1)
Sol-air (+1)
MRT$_{Min}$ (°C)
Triple
low-e (-1)
Glazing
Double
(+1)
16%
60%
WFR

(b)

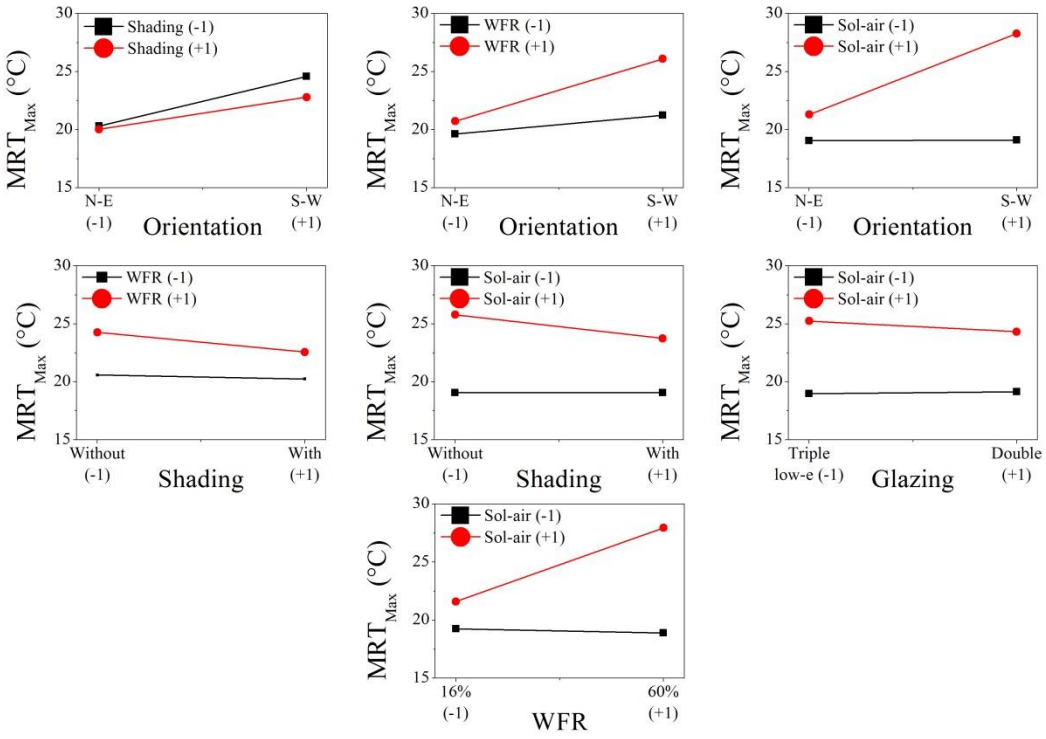

(c)

Figure 5-22 : interaction plots for: (a) average MRT, (b) minimum MRT and (c) maximum MRT.

The same previously used procedure is applied to obtain the fitting meta-models for the studied responses, and the best fit meta-model equations which describe the average, minimum and maximum MRT values as a function of the glass façades configuration and outdoor climatic conditions are given by Equations (5.4 to 5.6).

$$MRT_{Avg} = 20.54 + 0.7311 \times U - 0.2384 \times \mathrm{V} - 0.0725 \times \mathrm{W} + 0.7532 \times \mathrm{X} + 0.161 \times \mathrm{Y} - 0.1579\mathrm{UV} + 0.4392 \times \mathrm{UX} + 0.7123 \times \mathrm{UY} - 0.1949 \times \mathrm{VX} - 0.2384 \times \mathrm{VY} - 0.1797 \times \mathrm{WY} + 0.9962 \times \mathrm{XY} \quad (5.4)$$

$$MRT_{Min} = 18.92 + 0.0930 \times \mathrm{W} - 0.2033 \times \mathrm{X} + 0.2015 \times \mathrm{Y} + 0.0513 \times \mathrm{WX} - 0.0468 \times \mathrm{WY} + 0.1095 \times \mathrm{XY} \quad (5.5)$$

$$MRT_{Max} = 21.93 + 1.76 \times \mathrm{U} - 0.5143 \times \mathrm{V} - 0.1892 \times \mathrm{W} + 1.5 \times \mathrm{X} + 2.86 \times \mathrm{Y} - 0.3730 \times \mathrm{UV} + 0.9493 \times \mathrm{UX} + 1.73 \times \mathrm{UY} - 0.3406 \times \mathrm{VX} - 0.5142 \times \mathrm{VY} - 0.2677 \times \mathrm{XY} + 1.67 \times \mathrm{XY} \quad (5.6)$$

Furthermore, to justify the adequacy of the meta-models used in the analysis, the residual versus predicted plot is used to check the validity of the model [82]. The residual versus the predicted

response plot illustrated in Figure 5-23 shows that there is a less patterned structure indicating that the proposed models are adequate.

Eventually, the results show that even in the thermal comfort controlled case the PMV value may exceed the upper comfort range limit when exposed to high sol-air temperature (Figure 5-3). These results are associated with the increased MRT under high sol-air temperature due to the presence of extensive glazed area, as justified by the interaction plots (Figure 5-22). On the other hand, the sensitivity study regarding the heating energy consumption in the comfort controlled case shows that the MRT has a negative impact on the heating energy consumption, thus achieving energy-saving requires increased MRT. It can be seen from these results that the desired combination of the minimum energy consumption together with offsetting the high PMV values could not be obtained simultaneously. Thus an optimization is required to find an optimal condition simultaneously to offset the high PMV values and achieve energy-savings.

5.5 Optimization and validation

The response variables in our case are the heating energy consumption and the average and maximum PMV values. The objective is to minimize the energy consumption while maintaining the average and maximum PMV values within the acceptable comfort range of [-0.5; +0.5]. The range of variation of the optimized parameters is kept as indicated in the sensitivity study, except for the metabolic rate and clothing insulation they are assumed to vary in the ranges of [76.5; 73.5] and [0.95; 1.05], respectively, representing sedentary activity and typical winter clothing with 5% variation [193].

The numerical optimization outcomes 22 solutions illustrated in Figure 5-24 (numerical results are reported in Table E-2). According to the obtained results the maximum D value, of 0.718, is provided when the MRT is 18.268 °C, the RH is about 40%, the AV is 0.152 $m.s^{-1}$ and the metabolic rate and clothing insulation are 72.83 $W.m^{-2}$ and 1.05 clo, respectively. The optimum heating energy consumption to maintain the desired thermal comfort conditions is 143.44 kWh per the simulated week. Using the same parameters, the validated Dymola® model predicted the heating energy consumption to be 143.84 kWh. Thus, the predicted heating energy consumption by the optimized meta-model was similar to the simulation results.

Moreover, relative humidity and air velocity are HVAC related parameters and can be controlled by adjusting the settings of the system. However, metabolic rate and clothing insulation are uncontrollable parameters and it could be better to assume a range of variation rather than a fixed value. In addition, the MRT is a parameter that is highly affected by the room envelope, mainly the glazed parts, since it depends on the surface temperature of the opaque constructions.

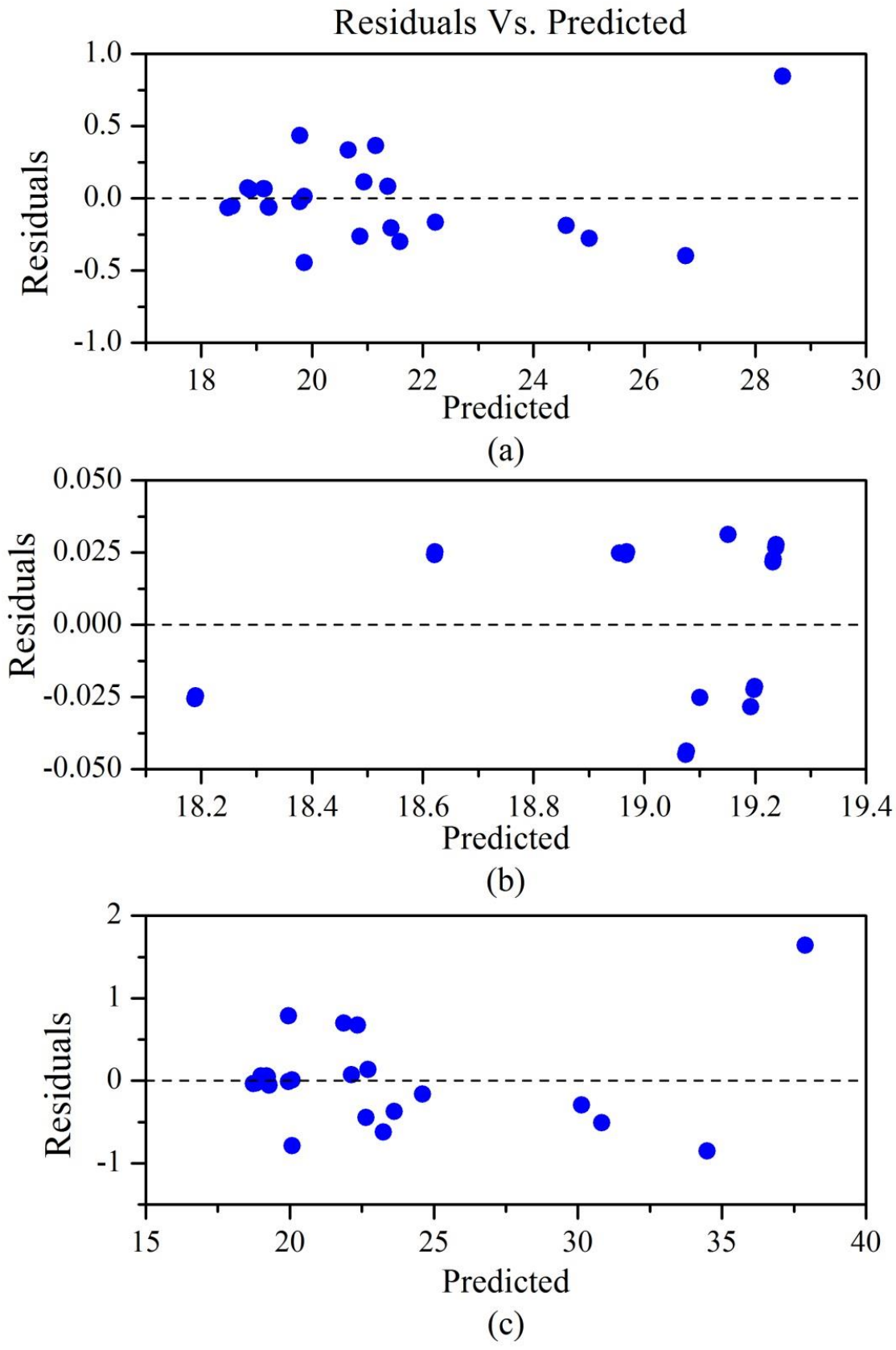

Figure 5-23: Residuals versus fitted values for: (a) average MRT, (b) minimum MRT and (c) maximum MRT.

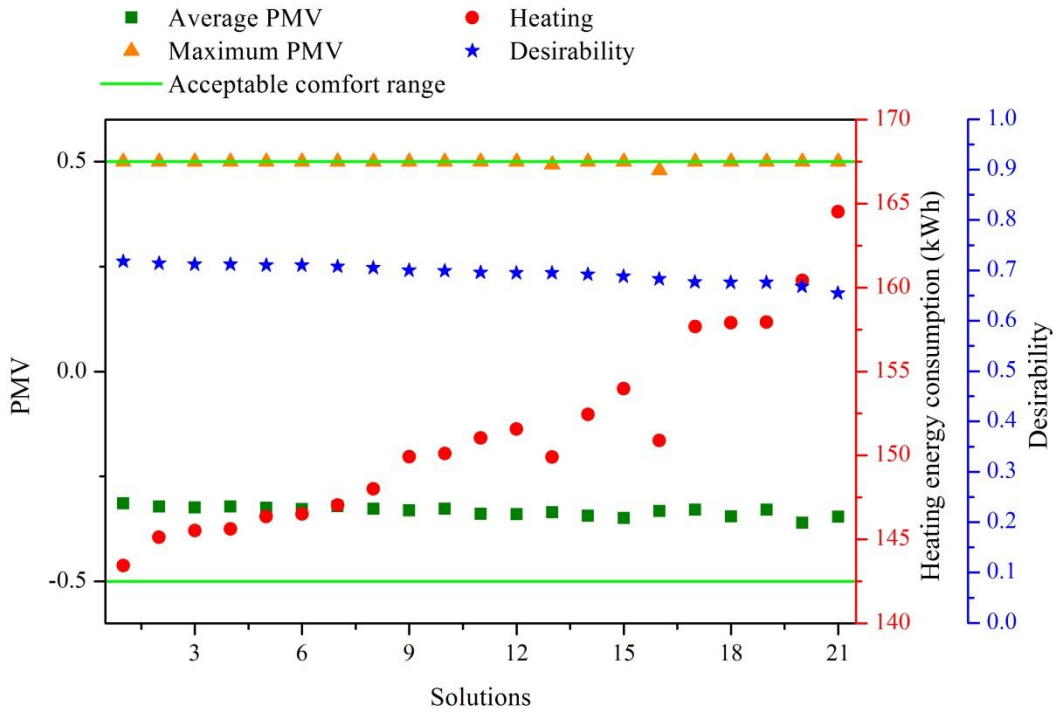

Figure 5-24 : numerical optimization solutions to minimize the heating energy consumption.

Therefore, based on numerical optimization results, in order to fulfil a trade-off between energy savings and thermal comfort in the considered case study, relative humidity, and air velocity must vary in the ranges of [40%, 55%] and [0.15 $m.s^{-1}$, 0.235 $m.s^{-1}$], respectively. In addition, the configuration of the room envelope must ensure that the MRT is within the range of [17.304 °C, 21.093 °C].

In this consequence, the meta-models of the average, minimum and maximum MRT are also optimized, and the objective is to maintain their values within the desired range of [17.304 °C, 21.093 °C]. The numerical optimization outcomes 29 solutions presented in Figure 5-25 (numerical results are reported in Table E-3). The results indicate that the maximum D value of 0.995 is provided when the room is south-east oriented, equipped with an internal shading system, the glazing system is triple low-e (u-value = 0.7, g-value = 0.3), and the WFR is minimized (16%). The obtained results suggest that applying these parameters to the case study will outcomes the MRT values with the range of [19.094 °C, 20.995 °C].

After identifying the critical parameters affecting the MRT and energy consumption in the deemed case study and finding the best solutions in order to reach a trade-off between energy-savings and thermal comfort, a comparative study is essential to confirm the advantages of these improvements. In this regard, a comparative study is performed among the optimized thermal comfort-controlled case, the base design comfort controlled case and the optimized conventional controlled case.

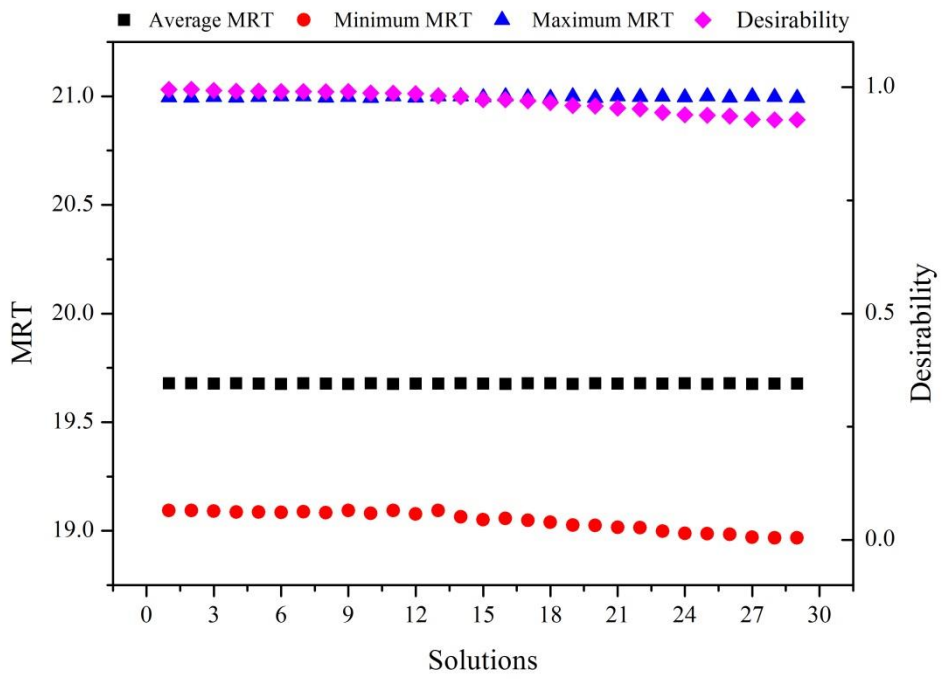

Figure 5-25 : Numerical optimization solutions to maintain MRT within the desired range.

5.6 Comparison between different scenarios

In the following section, the optimized thermal comfort controlled case is compared with the thermal comfort controlled case under the base design and the optimized conventional controlled case. The considered parameters are the PMV index, room temperature, MRT, the hourly power of the heating system and the total heating energy consumption. This comparative study aims to investigate if the PMV-based thermal comfort controller is still a reasonable solution to neutralize the trade-off between thermal comfort and energy consumption.

The obtained hourly numerical values of the considered parameters using the validated model throughout the investigated European winter are shown in Figure 5-26. The results show that applying the optimized design alleviated the high PMV and MRT values in both comfort and thermostatic controlled optimized cases. In addition, the results indicate that the optimized comfort-controlled case has an apparent advantage of maintaining consistent thermal comfort, while the optimized thermostatic controlled maintain consistent room temperature. The variations in the room temperature using the comfort control are correlated to the variation in the MRT. For instance, at high sol-air temperature, an increase in the MRT is observed and since the control variable is the PMV, this results in decreasing the set-point temperature and thus heating energy saving. Contrarily, when the MRT values increase in the conventional controlled case, the PMV values increase while the heating system

still in function until it reaches a predefined threshold. This justifies the appearance of greater PMV values at high sol-air temperature values. Moreover, the obtained results show that the optimized thermostatic and comfort controlled cases allowed about 16.5% and 26% reduction of heating energy consumption compared to the comfort controlled base case design.

These results indicated that an adequate treatment of the glazed envelope leads to improved thermal comfort conditions and reduce heating energy consumption. These findings are namely correlated to reducing glass facades area which implies less hot surfaces under high sol-air temperature, leading to decreased mean radiant temperature, thus alleviating the high PMV values. Besides, changing the glazing type and decreasing the glazing area, results in improved thermal resistance of the external walls, allowing the reduced transmission heat loss under low sol-air temperature, thus improving the heating energy consumption.

Furthermore, both optimized cases offered equivalent thermal comfort, with a slight advantage of the thermostatic controlled (PMV values skewed more toward zero, Figure 5-26), and better than all the studied cases using the base design. However, the optimized thermal-comfort controlled case allowed about 10 % reduction of heating energy consumption compared to the optimized thermostatic controlled case. Consequently, these results confirm the above findings that PMV-based thermal comfort control is a reasonable solution to neutralize the trade-off between thermal comfort and energy savings.

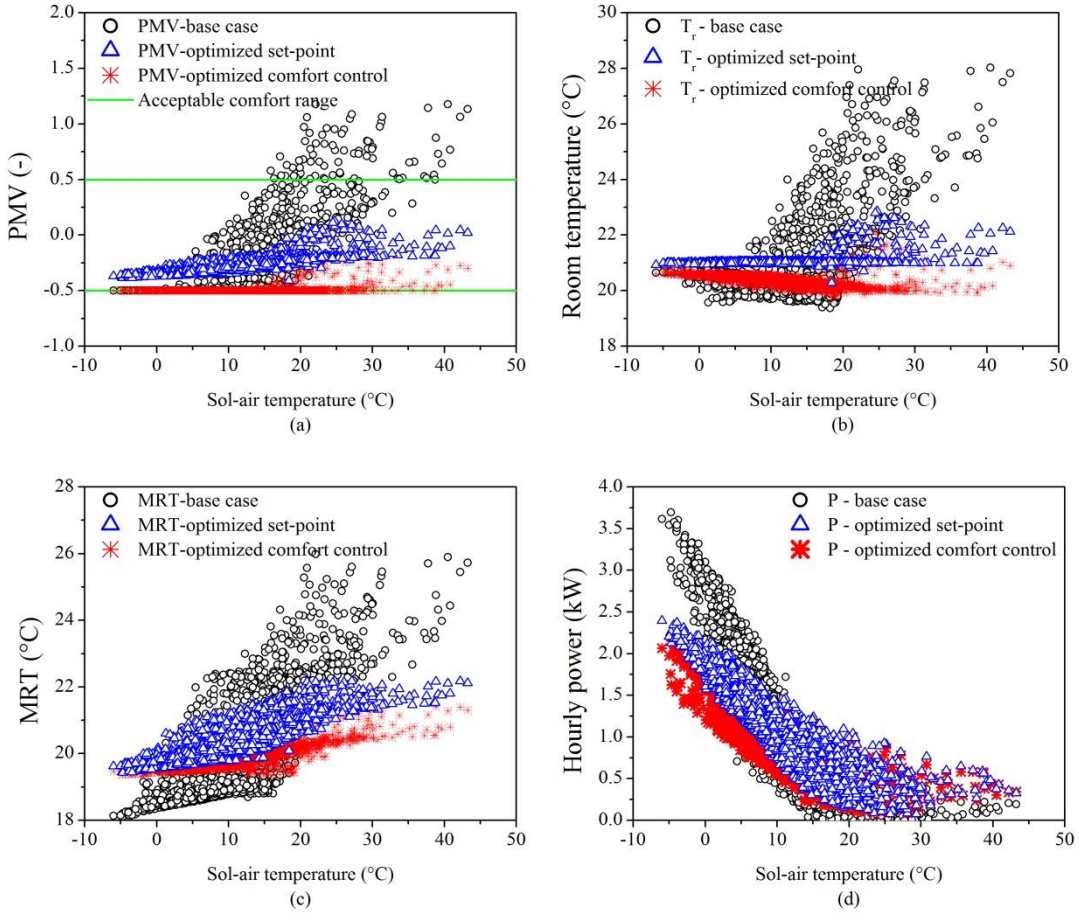

Figure 5-26 : Numerical hourly values of (a) PMV index, (b) room temperature, (c) MRT and (d) the hourly power of the heating energy obtained from the validated Dymola® model for the three cases.

5.7 Conclusion

The main conclusions of the chapter are as follow:

(i) Under the current design, PMV-based thermal comfort-control is a reasonable solution to neutralize the trade-off between thermal comfort and energy-savings. Besides, the metabolic rate, the mean radiant temperature, and the clothing insulation are the most influential factors affecting the heating energy consumption. These results indicate that this control approach could be suitable for spaces where occupants' activity and clothing levels are the same and could be assumed as fixed values, such as in office buildings and classrooms. In addition, they must be accurately defined due to their high effect on energy consumption.

(ii) An adequate treatment of the glazed envelope leads to improved thermal comfort conditions and reduce heating energy consumption. These findings are namely

correlated to reducing glass facades area which implies less hot surfaces under high sol-air temperature. Besides, changing the glazing type and decreasing the glazing area, results in improved thermal resistance of the external walls, allowing the reduced transmission heat loss under low sol-air temperature, thus improving the heating energy consumption.

(iii) Both optimized cases offered equivalent thermal comfort, with a slight advantage of the thermostatic controlled, PMV values skewed more toward zero. However, the optimized thermal-comfort controlled case allowed about 10 % reduction of heating energy consumption compared to the optimized thermostatic controlled case.

(iv) PMV-based comfort control requires continuous monitoring to calculate the set-point temperature and additional cost for the required devices. In addition, it is subject to measurement uncertainties and user-defined parameters errors. Taking these limitations into consideration, we can conclude that integrating occupants' thermal comfort in the design phase of energy-efficient buildings for the case of conventional control represents a significant step towards achieving a trade-off between energy-saving and thermal comfort without the need of advanced and complicated control strategies.

General conclusions

The general conclusions of this thesis are divided into three sections. The first section provides a summary of our scientific contributions along with the present dissertation. The second part of the conclusions summarizes the limitations of the present work. The third part exposes the perspectives issued out of this dissertation.

Contributions

In the present research work, we proposed that integrating occupants' thermal comfort in the design of energy-efficient buildings leads to a trade-off between energy-savings and thermal comfort. This act alongside the shift towards designing and constructing energy-efficient buildings, which leads to further requirements of performance and sustainability, causes the design process of buildings to be more and more complex. Adopting a method that is capable of, firstly integrating occupants' thermal comfort in a simple and efficient way, and secondly providing accurate predictions, is thus an essential need for building designers. In this regard, the situated Function-Behavior-Structure (sFBS) was used as a bridge to link design features and desired objectives throughout the design process. Mapping building design into the sFBS ontology allowed us to identify the critical steps that require the intervention of the design agent. This enabled then the selection of adequate tools and approaches to reduce the complexity of integrating occupants' thermal comfort in the design stages of building.

For this reason, in the present research work, we proposed the combined use of numerical building simulations, design of experiment technique and an optimization process based on the desirability function approach. Building performance simulations are capable of providing adequate results with less time and cost. The DoE technique enables the development of metamodeling relationships between studied variables and some design parameters. These meta-models allow the prediction of studied variables in a fast and simple way, as well as to identify the most influential parameters on the studied variables so that we can know where to extend the investigation in the design process. In addition, the meta-models allowed us to search for an optimal design of building in a multi-criterion dimension.

The adopted method was then applied to a real case study, particularly a highly glazed room, to investigate the impact of integrating occupants' thermal comfort in the design of energy efficient buildings. Firstly, a dynamic numerical model was developed and validated by comparing the model prediction to objective measurements as well as subjective responses regarding the real perception of the indoor environment. The DoE technique was then used to perform sensitivity analysis and to develop meta-models that approximate the PMV index as a function of predefined factors. Using the desirability function approach the meta-models are then used to integrate occupants' thermal comfort

in the optimization process of building design. The results indicated that integrating occupants' thermal comfort in the design of energy efficient buildings leads to optimized building design for both thermal comfort and heating energy consumption, even though it requires increased heating set-point.

A comparative study between the proposed approach and the use of comfort controlled approach was then performed. The results indicate that in the case of extensive glazing areas, thermal comfort in a thermostatic-controlled space competes with energy saving, while PMV-based thermal comfort-control is a reasonable solution to neutralize the trade-off between thermal comfort and energy-savings. This could be attributed to the fact that the room temperature in a comfort controlled space is mainly determined as a function of the mean radiant temperature to maintain the predefined PMV value. However, compared to the case of integrating occupants' thermal comfort in the design of building the results show that this last leads to suppress the need for an advanced control strategy, which could require additional devices installations in order to keep continuous monitoring of the indoor environment, thus leading to additional installation and functional costs.

Moreover, PMV-based comfort control could be suitable for spaces where occupants' activity and clothing levels are the same and could be assumed as fixed values, such as in office buildings and classrooms. Besides, occupants' behavior must be accurately defined due to their high effect on energy consumption. Also, an adequate treatment of the glazed envelope leads to improved thermal comfort conditions and reduce heating energy consumption.

Furthermore, integrating occupants' thermal comfort in the design phase of energy-efficient buildings for the case of conventional control represents a significant step towards achieving a trade-off between energy-saving and thermal comfort without the need of advanced and complicated control strategies.

Finally, we succeeded to achieve a trade-off between energy-savings and thermal comfort, by integrating this last in the design of buildings. For this reason, we now propose a generalized framework for the design of energy-efficient buildings taking account of occupants' thermal comfort. This includes the following stages:

1. The design agent defines the functional requirements of the building via communicative interaction with the customer or building owner. The expected behavior is then obtained from the existing standards and regulations, such as the desired thermal comfort level (categories of thermal comfort).
2. Adopt a building performance simulation tool and develop a reliable numerical model. Since the building does not exist in the early design process, the design agent could use data from similar buildings to validate the model or use previously validate numerical models.

3. Define the response variable, based on the functional requirements of the building (such as thermal comfort and energy consumption levels, economic and environmental impacts, etc.), and design parameters. Design parameters ranges could be obtained from standards recommendations (such as opaque construction u-values)
4. Choose an experimental design plan (full factorial, fractional, composite, etc.) depending on the number of design parameters and perform numerical simulation for each experiment.
5. Identify the critical parameters using statistical analysis (ANOVA).
6. Develop meta-modeling relationships between response variables and design parameters. Meta-models should then be validated using graphical methods or by comparing their predictions to additional random simulations.
7. Launch an optimization process to achieve the desired objectives. (Objectives and constraints for the optimization are obtained from building standards).
8. Apply the optimization results to the building design parameters and evaluate the obtained behavior by comparing with standards recommendations. In case the results are unsatisfactory, restart from step 3.

Limitations

The limitations of this research work are the following:

- The proposed approach is applied to a very specific case study.
- The generalized framework was derived based on the obtained results from the considered case study and was not validated in another case study with different response variables, such as cooling energy consumption.
- A few parameters and response variables are considered in the analysis.

Perspectives

To overcome the limitation of the present research work, some possible directions in which future work should be oriented are as follow:

- Extend the application of the proposed approach to other building typologies.
- Increase the number of parameters and response variables by simultaneously considering several issues (economic, environmental, etc.). DoE technique could help in reducing drastically the number of simulations, when increasing the number of parameters, by applying different types of experimental designs such as fractional factorial.
- Because of its impact on both energy consumption and thermal comfort, developing a model that predicts the clothing level based on outdoor climatic conditions may represent a step

forward in taking occupants based activity level in the design process of buildings, rather than assuming a fixed value throughout the investigations.

- Developing a tool that allows the combined use of dynamic simulation, DoE and desirability function approach would make the application of the proposed methodology very useful for designers and decision-makers of building construction projects.

References

[1] P. Nejat, F. Jomehzadeh, M.M. Taheri, M. Gohari, M.Z. Muhd, A global review of energy consumption, CO2 emissions and policy in the residential sector (with an overview of the top ten CO2 emitting countries), Renew. Sustain. Energy Rev. 43 (2015) 843–862. doi:10.1016/j.rser.2014.11.066.

[2] F. Belaïd, Untangling the complexity of the direct and indirect determinants of the residential energy consumption in France: Quantitative analysis using a structural equation modeling approach, Energy Policy. 110 (2017) 246–256. doi:10.1016/j.enpol.2017.08.027.

[3] European Parliament, Directive 2010/31/EU of the European Parliament and of the Council of 19 May 2010 on the energy performance of buildings, Off. J. Eur. Union. (2010) 13–35. doi:10.3000/17252555.L_2010.153.eng.

[4] C. Robinson, B. Dilkina, J. Hubbs, W. Zhang, S. Guhathakurta, M.A. Brown, R.M. Pendyala, Machine learning approaches for estimating commercial building energy consumption, Appl. Energy. 208 (2017) 889–904. doi:10.1016/j.apenergy.2017.09.060.

[5] A. Robert, M. Kummert, Designing net-zero energy buildings for the future climate, not for the past, Build. Environ. 55 (2012) 150–158. doi:10.1016/j.buildenv.2011.12.014.

[6] A.J. Marszal, P. Heiselberg, J.S. Bourrelle, E. Musall, K. Voss, I. Sartori, A. Napolitano, Zero Energy Building – A review of definitions and calculation methodologies, Energy Build. 43 (2011) 971–979. doi:10.1016/J.ENBUILD.2010.12.022.

[7] MEDDE, Réglementation thermique 2012 : un saut énergétique pour les bâtiments neufs, 2011.

[8] M.G. Alpuche, I. González, J.M. Ochoa, I. Marincic, A. Duarte, E. Valdenebro, Influence of Absorptance in the Building Envelope of Affordable Housing in Warm Dry Climates, Energy Procedia. 57 (2014) 1842–1850. doi:10.1016/j.egypro.2014.10.048.

[9] N. Aste, A. Angelotti, M. Buzzetti, The influence of the external walls thermal inertia on the energy performance of well insulated buildings, Energy Build. 41 (2009) 1181–1187. doi:10.1016/j.enbuild.2009.06.005.

[10] U.S Department of Labor, Bureau of Labor Statistics, Occup. Outlook Handbook, 2012-13 Ed. Med. Assist. (2012). http://www.bls.gov/ooh/healthcare/medical-assistants.htm.

[11] D. Kolokotsa, D. Tsiavos, G.S. Stavrakakis, K. Kalaitzakis, E. Antonidakis, Advanced fuzzy logic controllers design and evaluation for buildings' occupants thermal-visual comfort and indoor air quality satisfaction, Energy Build. 33 (2001) 531–543. doi:10.1016/S0378-7788(00)00098-0.

[12] M. Castilla, J.D. Álvarez, M.G. Ortega, M.R. Arahal, Neural network and polynomial approximated thermal comfort models for HVAC systems, Build. Environ. 59 (2013) 107–115. doi:10.1016/j.buildenv.2012.08.012.

[13] B. Givoni, Man, climate and architecture, 2nd ed., Applied Science Publishers, London, 1976. https://trove.nla.gov.au/version/31128462.

[14] N. Djongyang, R. Tchinda, D. Njomo, Thermal comfort: A review paper, Renew. Sustain. Energy Rev. 14 (2010) 2626–2640. doi:10.1016/j.rser.2010.07.040.

[15] P.O. Fanger, Thermal comfort: Analysis and applications in environmental engineering, 1970.

[16] ANSI/ASHRAE, Thermal Environmental Conditions for Human Occupancy Standard 55-2013,

Ashrae. (2013). doi:ISSN 1041-2336.

[17] A.K. Singh, H. Singh, S.P. Singh, R.L. Sawhney, Numerical calculation of psychrometric properties on a calculator, Build. Environ. 37 (2002) 415–419. doi:10.1016/S0360-1323(01)00032-4.

[18] D. Enescu, A review of thermal comfort models and indicators for indoor environments, Renew. Sustain. Energy Rev. 79 (2017) 1353–1379. doi:10.1016/j.rser.2017.05.175.

[19] ASHRAE, Thermal environmental conditions for human occupancy, ASHRAE Stand. (2010) 1–44. doi:1041-2336.

[20] ISO, ISO 7730: Ergonomics of the thermal environment Analytical determination and interpretation of thermal comfort using calculation of the PMV and PPD indices and local thermal comfort criteria, Management. 3 (2005) 605–615. doi:10.1016/j.soildyn.2004.11.005.

[21] R.J. de Dear, Global database of thermal comfort field experiments, in: ASHRAE Trans., 1998.

[22] ANSI/ ASHRAE Standard 55-2010, Thermal environmental conditions for human occupancy, 2010. doi:ISSN 1041-2336.

[23] M. Taleghani, M. Tenpierik, S. Kurvers, A. Van Den Dobbelsteen, A review into thermal comfort in buildings, Renew. Sustain. Energy Rev. 26 (2013) 201–215. doi:10.1016/j.rser.2013.05.050.

[24] P.O. Fanger, Thermal comfort. Analysis and applications in environmental engineering., New York Mcgraw-Hill. (1972).

[25] A. Sayigh, A.H. Marafia, Chapter 1—Thermal comfort and the development of bioclimatic concept in building design, Renew. Sustain. Energy Rev. 2 (1998) 3–24. doi:10.1016/S1364-0321(98)00009-4.

[26] R.A. Hoovestol, T.R. Mikuls, Environmental Exposures and Rheumatoid Arthritis Risk, Curr. Rheumatol. Rep. 13 (2011) 431–439. doi:10.1007/s11926-011-0203-9.

[27] J. Van Hoof, Forty years of Fanger's model of thermal comfort: Comfort for all?, Indoor Air. 18 (2008) 182–201. doi:10.1111/j.1600-0668.2007.00516.x.

[28] F. Nicol, Standards for thermal comfort : indoor air temperature standards for the 21st century, Chapman & Hall, 1995. https://books.google.fr/books?hl=fr&lr=&id=fxXS85SQqHcC&oi=fnd&pg=PA3&dq=Humphreys,+thermal+comfort&ots=7J8BlXeBYh&sig=se_J5LTQ6dMlHFt34NmA6M9RYpo#v=onepage&q=Humphreys%2C thermal comfort&f=false (accessed January 31, 2019).

[29] J. Široký, F. Oldewurtel, J. Cigler, S. Prívara, Experimental analysis of model predictive control for an energy efficient building heating system, Appl. Energy. 88 (2011) 3079–3087. doi:10.1016/j.apenergy.2011.03.009.

[30] M. Hamdi, G. Lachiver, A fuzzy control system based on the human sensation of thermal comfort, in: 1998 IEEE Int. Conf. Fuzzy Syst. Proceedings. IEEE World Congr. Comput. Intell. (Cat. No.98CH36228), IEEE, 1998: pp. 487–492. doi:10.1109/FUZZY.1998.687534.

[31] D. Kolokotsa, Comparison of the performance of fuzzy controllers for the management of the indoor environment, Build. Environ. 38 (2003) 1439–1450. doi:10.1016/S0360-1323(03)00130-6.

[32] F. Calvino, M. La Gennusa, G. Rizzo, G. Scaccianoce, The control of indoor thermal comfort conditions: introducing a fuzzy adaptive controller, Energy Build. 36 (2004) 97–102.

doi:10.1016/j.enbuild.2003.10.004.

[33] Jian Liang, Ruxu Du, Thermal comfort control based on neural network for HVAC application, in: Proc. 2005 IEEE Conf. Control Appl. 2005. CCA 2005., IEEE, 2005: pp. 819–824. doi:10.1109/CCA.2005.1507230.

[34] E. Donaisky, G.H.C. Oliveira, R.Z. Freire, N. Mendes, PMV-Based Predictive Algorithms for Controlling Thermal Comfort in Building Plants, in: 2007 IEEE Int. Conf. Control Appl., IEEE, 2007: pp. 182–187. doi:10.1109/CCA.2007.4389227.

[35] R.Z. Freire, G.H.C. Oliveira, N. Mendes, Predictive controllers for thermal comfort optimization and energy savings, Energy Build. 40 (2008) 1353–1365. doi:10.1016/j.enbuild.2007.12.007.

[36] M. Castilla, J.D. Alvarez, M. Berenguel, F. Rodriguez, J.L. Guzman, M. Perez, A comparison of thermal comfort predictive control strategies, ENERGY Build. 43 (2011) 2737–2746. doi:10.1016/j.enbuild.2011.06.030.

[37] P.M. Ferreira, A.E. Ruano, S. Silva, E.Z.E. Conceição, Neural networks based predictive control for thermal comfort and energy savings in public buildings, Energy Build. 55 (2012) 238–251. doi:10.1016/j.enbuild.2012.08.002.

[38] A. Ruano, S. Pesteh, S. Silva, H. Duarte, G. Mestre, P.M. Ferreira, H. Khosravani, R. Horta, PVM-based intelligent predictive control of HVAC systems, IFAC-PapersOnLine. 49 (2016) 371–376. doi:10.1016/j.ifacol.2016.07.141.

[39] Z. Xu, G. Hu, C.J. Spanos, S. Schiavon, PMV-based event-triggered mechanism for building energy management under uncertainties, Energy Build. 152 (2017) 73–85. doi:10.1016/j.enbuild.2017.07.008.

[40] D.H. Kang, P.H. Mo, D.H. Choi, S.Y. Song, M.S. Yeo, K.W. Kim, Effect of MRT variation on the energy consumption in a PMV-controlled office, Build. Environ. 45 (2010) 1914–1922. doi:10.1016/j.buildenv.2010.02.020.

[41] R.L. Hwang, S.Y. Shu, Building envelope regulations on thermal comfort in glass facade buildings and energy-saving potential for PMV-based comfort control, Build. Environ. 46 (2011) 824–834. doi:10.1016/j.buildenv.2010.10.009.

[42] L. Erakovic, B. Evans, Use of Pmv Control To Improve Energy Efficiency in Comfort Cooling Applications, in: 9th Int. Conf. CFD Miner. Process Ind., 2012: pp. 1–6.

[43] B. Bueno, J.M. Cejudo-López, A. Katsifaraki, H.R. Wilson, A systematic workflow for retrofitting office façades with large window-to-wall ratios based on automatic control and building simulations, Build. Environ. 132 (2018) 104–113. doi:10.1016/J.BUILDENV.2018.01.031.

[44] W. Sop Shin, The influence of forest view through a window on job satisfaction and job stress, Scand. J. For. Res. 22 (2007) 248–253. doi:10.1080/02827580701262733.

[45] C.-Y. Chang, P.-K. Chen, Human Response to Window Views and Indoor Plants in the Workplace, HortScience. 40 (2005) 1354–1359. doi:10.21273/HORTSCI.40.5.1354.

[46] M. Thalfeldt, E. Pikas, J. Kurnitski, H. Voll, Facade design principles for nearly zero energy buildings in a cold climate, Energy Build. 67 (2013) 309–321. doi:10.1016/j.enbuild.2013.08.027.

[47] H. Poirazis, Å. Blomsterberg, M. Wall, Energy simulations for glazed office buildings in Sweden, Energy Build. 40 (2008) 1161–1170. doi:10.1016/j.enbuild.2007.10.011.

[48] Q. Jin, M. Overend, A comparative study on high-performance glazing for office buildings, Intell. Build. Int. 9 (2017) 181–203. doi:10.1080/17508975.2015.1130681.

[49] J.W. Lee, H.J. Jung, J.Y. Park, J.B. Lee, Y. Yoon, Optimization of building window system in Asian regions by analyzing solar heat gain and daylighting elements, Renew. Energy. 50 (2013) 522–531. doi:10.1016/j.renene.2012.07.029.

[50] L. Vanhoutteghem, G.C.J. Skarning, C.A. Hviid, S. Svendsen, Impact of façade window design on energy, daylighting and thermal comfort in nearly zero-energy houses, Energy Build. 102 (2015) 149–156. doi:10.1016/j.enbuild.2015.05.018.

[51] A. Tzempelikos, M. Bessoudo, A.K. Athienitis, R. Zmeureanu, Indoor thermal environmental conditions near glazed facades with shading devices - Part II: Thermal comfort simulation and impact of glazing and shading properties, Build. Environ. 45 (2010) 2517–2525. doi:10.1016/j.buildenv.2010.05.014.

[52] T. Anderson, M. Luther, Designing for thermal comfort near a glazed exterior wall, Archit. Sci. Rev. 55 (2012) 186–195. doi:10.1080/00038628.2012.697863.

[53] G.M. Stavrakakis, P.L. Zervas, H. Sarimveis, N.C. Markatos, Optimization of window-openings design for thermal comfort in naturally ventilated buildings, Appl. Math. Model. 36 (2012) 193–211. doi:10.1016/j.apm.2011.05.052.

[54] Z.S. Zomorodian, M. Tahsildoost, Assessment of window performance in classrooms by long term spatial comfort metrics, Energy Build. 134 (2017) 80–93. doi:10.1016/j.enbuild.2016.10.018.

[55] M. Bessoudo, A. Tzempelikos, A.K. Athienitis, R. Zmeureanu, Indoor thermal environmental conditions near glazed facades with shading devices - Part I: Experiments and building thermal model, Build. Environ. 45 (2010) 2506–2516. doi:10.1016/j.buildenv.2010.05.013.

[56] F.V. Winther, P.K. Heiselberg, R.L. Jensen, Intelligent glazed facades for fulfilment of future energy regulations, Towar. 2020 - Sustain. Cities Build. (2010).

[57] R.A. Mangkuto, M. Rohmah, A.D. Asri, Design optimisation for window size, orientation, and wall reflectance with regard to various daylight metrics and lighting energy demand: A case study of buildings in the tropics, Appl. Energy. 164 (2016) 211–219. doi:10.1016/j.apenergy.2015.11.046.

[58] F. Chlela, A. Husaunndee, C. Inard, P. Riederer, A new methodology for the design of low energy buildings, Energy Build. 41 (2009) 982–990. doi:10.1016/j.enbuild.2009.05.001.

[59] J.S. Gero, H. Jiang, C.B. Williams, Design cognition differences when using unstructured, partially structured, and structured concept generation creativity techniques, Int. J. Des. Creat. Innov. 1 (2013) 196–214. doi:10.1080/21650349.2013.801760.

[60] V.S.K.V. Harish, A. Kumar, A review on modeling and simulation of building energy systems, Renew. Sustain. Energy Rev. 56 (2016) 1272–1292. doi:10.1016/J.RSER.2015.12.040.

[61] N. Fumo, M.A. Rafe Biswas, Regression analysis for prediction of residential energy consumption, Renew. Sustain. Energy Rev. 47 (2015) 332–343. doi:10.1016/j.rser.2015.03.035.

[62] Z. Wang, R.S. Srinivasan, A review of artificial intelligence based building energy use prediction: Contrasting the capabilities of single and ensemble prediction models, Renew. Sustain. Energy Rev. 75 (2017) 796–808. doi:10.1016/J.RSER.2016.10.079.

[63] H.X. Zhao, F. Magoulès, A review on the prediction of building energy consumption, Renew.

Sustain. Energy Rev. 16 (2012) 3586–3592. doi:10.1016/j.rser.2012.02.049.

[64] I. Jaffal, C. Inard, C. Ghiaus, Fast method to predict building heating demand based on the design of experiments, Energy Build. 41 (2009) 669–677. doi:10.1016/j.enbuild.2009.01.006.

[65] Modelica and the Modelica Association — Modelica Association, (n.d.). https://www.modelica.org/ (accessed January 8, 2019).

[66] J. Musić, B. Zupančič, Modeling, Simulation and Control of Inverted Pendulum on a Cart Using Object Oriented Approach with Modelica, Fifteenth Int. Electroteh. Comput. Sci. Conf. (ERK 2006). (2006). http://marjan.fesb.hr/~jmusic/josip_files/dymola_clanak_music.pdf.

[67] F.F.M. Soons, J.I. Torrens, J.L.M. Hensen, R.A.M. De Schrevel, A Modelica based computational model for evaluating a renewable district heating system, 9th Int. Conf. Syst. Simulations Build. 2 (2014) 1–16. https://pure.tue.nl/ws/files/3980938/899836577909065.pdf.

[68] D.C. Montgomery, Design and analysis of experiments, ninth, 2017. https://www.wiley.com/en-us/Design+and+Analysis+of+Experiments%2C+9th+Edition-p-9781119113478.

[69] G. Zhou, L. Fu, X. Li, Optimisation of ultrasound-assisted extraction conditions for maximal recovery of active monacolins and removal of toxic citrinin from red yeast rice by a full factorial design coupled with response surface methodology, Food Chem. 170 (2015) 186–192. doi:10.1016/j.foodchem.2014.08.080.

[70] SurveyPlanet, (n.d.). https://surveyplanet.com/ (accessed November 29, 2018).

[71] M. Wetter, W. Zuo, T.S. Nouidui, Modeling of Heat Transfer in Rooms in the Modelica "Buildings" Library, Proc. Build. Simul. 2011 12th Conf. Int. Build. Perform. Simul. Assoc. (2011) 1096–1103.

[72] M. Wetter, W. Zuo, T.S. Nouidui, Recent Developments of the Modelica "Buildings" Library for Building Energy and Control Systems, in: Model. Conf., 2011: pp. 266–275. doi:10.3384/ecp11063266.

[73] M. Wetter, W. Zuo, T.S. Nouidui, X. Pang, Modelica Buildings library, J. Build. Perform. Simul. 7 (2014) 253–270. doi:10.1080/19401493.2013.765506.

[74] ANSI/ASHRAE, Measurement of Energy and Demand Savings, in: ASHRAE Guidel. 14-2002, 2002. doi:10.1016/j.nima.2012.12.050.

[75] P.W. O'Callaghan, S.D. Probert, Sol-air temperature, Appl. Energy. 3 (1977) 307–311. doi:10.1016/0306-2619(77)90017-4.

[76] M.H. Hasan, F. Alsaleem, M. Rafaie, Sensitivity study for the PMV thermal comfort model and the use of wearable devices biometric data for metabolic rate estimation, Build. Environ. 110 (2016) 173–183. doi:10.1016/j.buildenv.2016.10.007.

[77] F.R. d'Ambrosio Alfano, B.I. Palella, G. Riccio, The role of measurement accuracy on the thermal environment assessment by means of PMV index, Build. Environ. 46 (2011) 1361–1369. doi:10.1016/j.buildenv.2011.01.001.

[78] W. Feist, J. Schnieders, V. Dorer, A. Haas, Re-inventing air heating: Convenient and comfortable within the frame of the Passive House concept, Energy Build. 37 (2005) 1186–1203. doi:10.1016/j.enbuild.2005.06.020.

[79] Cen, EN 15251: Indoor environmental input parameters for design and assessment of energy performance of buildings- addressing indoor air quality, thermal environment, lighting and

acoustics, Eur. Comm. Stand. 3 (2007) 1–52. doi:10.1520/E2019-03R13.Copyright.

[80] D.C. Montgomery, Design and Analysis of Experiments, Design. 2 (2001) 780 ST-Design and analysis of experiments. Adva. doi:10.1198/tech.2006.s372.

[81] S.J. Cheng, J.M. Miao, S.J. Wu, Investigating the effects of operational factors on PEMFC performance based on CFD simulations using a three-level full-factorial design, Renew. Energy. 39 (2012) 250–260. doi:10.1016/j.renene.2011.08.009.

[82] D. Montgomery, Introduction to statistical quality control, 2009. doi:10.1002/1521-3773(20010316)40:6<9823::AID-ANIE9823>3.3.CO;2-C.

[83] C. Marino, A. Nucara, M. Pietrafesa, Proposal of comfort classification indexes suitable for both single environments and whole buildings, Build. Environ. 57 (2012) 58–67. doi:10.1016/j.buildenv.2012.04.012.

[84] W. Liu, D. Yang, X. Shen, P. Yang, Indoor clothing insulation and thermal history: A clothing model based on logistic function and running mean outdoor temperature, Build. Environ. 135 (2018) 142–152. doi:10.1016/j.buildenv.2018.03.015.

[85] S. Schiavon, K.H. Lee, Dynamic predictive clothing insulation models based on outdoor air and indoor operative temperatures, Build. Environ. 59 (2013) 250–260. doi:10.1016/j.buildenv.2012.08.024.

[86] M. De Carli, B.W. Olesen, A. Zarrella, R. Zecchin, People's clothing behaviour according to external weather and indoor environment, Build. Environ. 42 (2007) 3965–3973. doi:10.1016/j.buildenv.2006.06.038.

[87] J. Williams, R. Mitchell, V. Raicic, M. Vellei, G. Mustard, A. Wismayer, X. Yin, S. Davey, M. Shakil, Y. Yang, A. Parkin, D. Coley, Less is more: A review of low energy standards and the urgent need for an international universal zero energy standard, J. Build. Eng. 6 (2016) 65–74. doi:10.1016/j.jobe.2016.02.007.

[88] A.A.W. Hawila, A. Merabtine, N. Troussier, R. Bennacer, Combined use of dynamic building simulation and metamodeling to optimize glass facades for thermal comfort, Build. Environ. 157 (2019) 47–63. doi:10.1016/J.BUILDENV.2019.04.027.

[89] A.A.W. Hawila, A. Merabtine, N. Troussier, Numerical and experimental investigation on the thermal behavior of the building integrating occupant thermal comfort, in: Int. Conf. Mater. Energy, Tianjin, China, 2017.

[90] A. Merabtine, C. Maalouf, A.A.W. Hawila, N. Martaj, G. Polidori, Building energy audit, thermal comfort, and IAQ assessment of a school building: A case study, Build. Environ. 145 (2018) 62–76. doi:10.1016/j.buildenv.2018.09.015.

[91] A.A.W. Hawila, A. Merabtine, M. Chemkhi, R. Bennacer, N. Troussier, An analysis of the impact of PMV-based thermal comfort control during heating period: A case study of highly glazed room, J. Build. Eng. 20 (2018) 353–366. doi:10.1016/j.jobe.2018.08.010.

[92] A.A.W. Hawila, A. Merabtine, M. Chemkhi, R. Bennacer, N. Troussier, Influence of PMV-based control on energy consumption and thermal comfort during heating period in a highly glazed room, in: Conférence IBPSA Fr., Bordeaux, 2018.

[93] International Energy Agency, Balances, (n.d.). http://www.iea.org/statistics/balances/ (accessed September 21, 2018).

[94] IBRD-IDA, The Worl Bank GDP (current US$) | Data, (n.d.). https://data.worldbank.org/indicator/NY.GDP.MKTP.CD (accessed September 20, 2018).

[95] IPCC, Climate change 2014: Impacts, Adaptaion, and Vulnerability. Part A: Global and Sectoral Aspects., Cambridge University Press, Cambridge, United Kingdom and New York, NY, USA, 2014. http://www.ipcc.ch/home_languages_main.shtml.

[96] SDES, SCEE, I4CE, Key figures on climate France, Europe and Worldwide, 2018. http://www.statistiques.developpement-durable.gouv.fr/fileadmin/documents/Produits_editoriaux/Publications/Datalab/2017/datalab-27-CC-climat-nov2017-GB-b.pdf.

[97] D. Ürge-Vorsatz, L.F. Cabeza, S. Serrano, C. Barreneche, K. Petrichenko, Heating and cooling energy trends and drivers in buildings, Renew. Sustain. Energy Rev. 41 (2015) 85–98. doi:10.1016/j.rser.2014.08.039.

[98] L. De Boeck, S. Verbeke, A. Audenaert, L. De Mesmaeker, Improving the energy performance of residential buildings: A literature review, Renew. Sustain. Energy Rev. 52 (2015) 960–975. doi:10.1016/j.rser.2015.07.037.

[99] R.M. Lazzarin, Condensing boilers in buildings and plants refurbishment, Energy Build. 47 (2012) 61–67. doi:10.1016/J.ENBUILD.2011.11.029.

[100] N. Kannan, D. Vakeesan, Solar energy for future world: - A review, Renew. Sustain. Energy Rev. 62 (2016) 1092–1105. doi:10.1016/J.RSER.2016.05.022.

[101] T.T. Chow, A review on photovoltaic/thermal hybrid solar technology, Appl. Energy. 87 (2010) 365–379. doi:10.1016/J.APENERGY.2009.06.037.

[102] P.M. Cuce, S. Riffat, A comprehensive review of heat recovery systems for building applications, Renew. Sustain. Energy Rev. 47 (2015) 665–682. doi:10.1016/J.RSER.2015.03.087.

[103] F. Nicol, M. Humphreys, S. Roaf, Adaptive thermal comfort: Principles and practice, 2012. doi:10.4324/9780203123010.

[104] K.C. Parsons, The effects of gender, acclimation state, the opportunity to adjust clothing and physical disability on requirements for thermal comfort, Energy Build. 34 (2002) 593–599. doi:10.1016/S0378-7788(02)00009-9.

[105] K. Cena, R. de Dear, Thermal comfort and behavioural strategies in office buildings located in a hot-arid climate, J. Therm. Biol. 26 (2001) 409–414. doi:10.1016/S0306-4565(01)00052-3.

[106] W. Liu, Z. Lian, Q. Deng, Y. Liu, Evaluation of calculation methods of mean skin temperature for use in thermal comfort study, Build. Environ. 46 (2011) 478–488. doi:10.1016/J.BUILDENV.2010.08.011.

[107] L. Lan, Z. Lian, W. Liu, Y. Liu, Investigation of gender difference in thermal comfort for Chinese people, Eur. J. Appl. Physiol. 102 (2008) 471–480. doi:10.1007/s00421-007-0609-2.

[108] N. Hashiguchi, Y. Feng, Y. Tochihara, Gender differences in thermal comfort and mental performance at different vertical air temperatures, Eur. J. Appl. Physiol. 109 (2010) 41–48. doi:10.1007/s00421-009-1158-7.

[109] J. Choi, A. Aziz, V. Loftness, Investigation on the impacts of different genders and ages on satisfaction with thermal environments in office buildings, Build. Environ. 45 (2010) 1529–1535. doi:10.1016/J.BUILDENV.2010.01.004.

[110] M. Indraganti, K.D. Rao, Effect of age, gender, economic group and tenure on thermal comfort: A field study in residential buildings in hot and dry climate with seasonal variations, Energy Build. 42 (2010) 273–281. doi:10.1016/J.ENBUILD.2009.09.003.

[111] S. Karjalainen, Thermal comfort and gender: a literature review, Indoor Air. 22 (2012) 96–109. doi:10.1111/j.1600-0668.2011.00747.x.

[112] G.S. Brager, R.J. de Dear, Thermal adaptation in the built environment: a literature review, Energy Build. 27 (1998) 83–96. doi:10.1016/S0378-7788(97)00053-4.

[113] M. Fountain, G. Brager, R. de Dear, Expectations of indoor climate control, Energy Build. 24 (1996) 179–182. doi:10.1016/S0378-7788(96)00988-7.

[114] Z. Lin, S. Deng, A study on the thermal comfort in sleeping environments in the subtropics—Developing a thermal comfort model for sleeping environments, Build. Environ. 43 (2008) 70–81. doi:10.1016/j.buildenv.2006.11.026.

[115] Ashrae Standard, ASHRAE Handbook 2001 Fundamentals, 2001. doi:10.1017/CBO9781107415324.004.

[116] L. Fang, G. Clausen, P. Fanger, Impact of temperature and humidity on perception of indoor air quality during immediate and longer whole-body exposures, Indoor Air. 8 (1998) 276–284. doi:10.1111/j.1600-0668.1998.00008.x.

[117] P. Wargocki, D. Wyon, Y. Baik, G. Clausen, P. Fanger, Perceived air quality, sick building syndrome (SBS) symptoms and productivity in an office with two different pollution loads, Indoor Air. 9 (1999) 165–179. doi:10.1111/j.1600-0668.1999.t01-1-00003.x.

[118] K. Parsons, Human Thermal Environments: The Effects of Hot, Moderate, and Cold Environments on Human Health, Comfort, and Performance, Third Edition, 2014. doi:10.4324/9780203302620.

[119] I. Standard, ISO 7726 Ergonomics of the thermal environment — Instruments for measuring physical quantities, ISO Stand. (1998). doi:ISO 7726:1998 (E).

[120] F.M. Butera, Chapter 3—Principles of thermal comfort, Renew. Sustain. Energy Rev. 2 (1998) 39–66. doi:10.1016/S1364-0321(98)00011-2.

[121] R. De Dear, G. Brager, Developing an adaptive model of thermal comfort and preference, ASHRAE Trans. 104 (1998).

[122] R.F. Rupp, N.G. Vásquez, R. Lamberts, A review of human thermal comfort in the built environment, Energy Build. 105 (2015) 178–205. doi:10.1016/j.enbuild.2015.07.047.

[123] R. de Dear, G.S. Brager, Developing an Adaptive Model of Thermal Comfort and Preference, ASHRAE Trans. 104 (1998) 145–167. doi:https://escholarship.org/uc/item/4qq2p9c6.

[124] M.A. Humphreys, M. Hancock, Do people like to feel "neutral"?. Exploring the variation of the desired thermal sensation on the ASHRAE scale, Energy Build. (2007). doi:10.1016/j.enbuild.2007.02.014.

[125] M.A. Humphreys, Standards for Thermal Comfort, Routledge, 2015. doi:10.4324/9780203860465.

[126] J. van Hoof, M. Mazej, J.L.M. Hensen, Thermal comfort: research and practice, Front. Biosci. 15 (2010) 765–788.

[127] W.L. Tse, A.T.P. So, W.L. Chan, I.K.Y. Mak, The validity of predicted mean vote for air-conditioned offices, Facilities. 23 (2005) 558–569. doi:10.1108/02632770510627543.

[128] N. Nasrollahi, I. Knight, P. Jones, Workplace Satisfaction and Thermal Comfort in Air Conditioned Office Buildings: Findings from a Summer Survey and Field Experiments in Iran,

Indoor Built Environ. 17 (2008) 69–79. doi:10.1177/1420326X07086945.

[129] N.A. Oseland, Predicted and reported thermal sensation in climate chambers, offices and homes, Energy Build. 23 (1995) 105–115. doi:10.1016/0378-7788(95)00934-5.

[130] J. Han, G. Zhang, Q. Zhang, J. Zhang, J. Liu, L. Tian, C. Zheng, J. Hao, J. Lin, Y. Liu, D.J. Moschandreas, Field study on occupants' thermal comfort and residential thermal environment in a hot-humid climate of China, Build. Environ. 42 (2007) 4043–4050. doi:10.1016/j.buildenv.2006.06.028.

[131] S.H. Hong, J. Gilbertson, T. Oreszczyn, G. Green, I. Ridley, A field study of thermal comfort in low-income dwellings in England before and after energy efficient refurbishment, Build. Environ. 44 (2009) 1228–1236. doi:10.1016/j.buildenv.2008.09.003.

[132] X. Yang, K. Zhong, Y. Kang, T. Tao, Numerical investigation on the airflow characteristics and thermal comfort in buoyancy-driven natural ventilation rooms, Energy Build. 109 (2015) 255–266. doi:10.1016/j.enbuild.2015.09.071.

[133] S.I.U.H. Gilani, M.H. Khan, W. Pao, Thermal Comfort Analysis of PMV Model Prediction in Air Conditioned and Naturally Ventilated Buildings, Energy Procedia. 75 (2015) 1373–1379. doi:10.1016/j.egypro.2015.07.218.

[134] R.-L. Hwang, M.-J. Cheng, T.-P. Lin, M.-C. Ho, Thermal perceptions, general adaptation methods and occupant's idea about the trade-off between thermal comfort and energy saving in hot–humid regions, Build. Environ. 44 (2009) 1128–1134. doi:10.1016/J.BUILDENV.2008.08.001.

[135] F.R. d'Ambrosio Alfano, B.W. Olesen, B.I. Palella, G. Riccio, Thermal comfort: Design and assessment for energy saving, Energy Build. 81 (2014) 326–336. doi:10.1016/j.enbuild.2014.06.033.

[136] E. Donaisky, G.H.C. Oliveira, R.Z. Freire, N. Mendes, PMV-based predictive algorithms for controlling thermal comfort in building plants, in: Proc. IEEE Int. Conf. Control Appl., 2007: pp. 182–187. doi:10.1109/CCA.2007.4389227.

[137] M. Saffari, A. De Gracia, S. Ushak, L.F. Cabeza, Economic impact of integrating PCM as passive system in buildings using Fanger comfort model, Energy Build. 112 (2016) 159–172. doi:10.1016/j.enbuild.2015.12.006.

[138] W.J. Hee, M.A. Alghoul, B. Bakhtyar, O. Elayeb, M.A. Shameri, M.S. Alrubaih, K. Sopian, The role of window glazing on daylighting and energy saving in buildings, Renew. Sustain. Energy Rev. 42 (2015) 323–343. doi:10.1016/j.rser.2014.09.020.

[139] C. Bouden, Influence of glass curtain walls on the building thermal energy consumption under Tunisian climatic conditions: The case of administrative buildings, Renew. Energy. 32 (2007) 141–156. doi:10.1016/j.renene.2006.01.007.

[140] E. Gratia, A. De Herde, Natural ventilation in a double-skin facade, Energy Build. 36 (2004) 137–146. doi:10.1016/j.enbuild.2003.10.008.

[141] D. Faggembauu, M. Costa, M. Soria, A. Oliva, Numerical analysis of the thermal behaviour of glazed ventilated facades in Mediterranean climates. Part II: applications and analysis of results, Sol. Energy. 75 (2003) 229–239. doi:10.1016/j.solener.2003.07.014.

[142] C.H. Cheong, T. Kim, S.B. Leigh, Thermal and daylighting performance of energy-efficient windows in highly glazed residential buildings: Case study in Korea, Sustain. 6 (2014) 7311–7333. doi:10.3390/su6107311.

[143] L. Li, S. Yu, J. Tao, L. Li, A FBS-based energy modelling method for energy efficiency-oriented design, J. Clean. Prod. 172 (2018) 1–13. doi:10.1016/J.JCLEPRO.2017.09.254.

[144] G. Cascini, G. Fantoni, F. Montagna, Situating needs and requirements in the FBS framework, Des. Stud. 34 (2013) 636–662. doi:10.1016/J.DESTUD.2012.12.001.

[145] J.S. Gero, Design Prototypes: A Knowledge Representation Schema for Design, AI Mag. 11 (1990) 26–26. doi:10.1609/AIMAG.V11I4.854.

[146] J.S. Gero, U. Kannengiesser, The situated function–behaviour–structure framework, Des. Stud. 25 (2004) 373–391. doi:10.1016/J.DESTUD.2003.10.010.

[147] P.E. Vermaas, K. Dorst, On the conceptual framework of John Gero's FBS-model and the prescriptive aims of design methodology, Des. Stud. 28 (2007) 133–157. doi:10.1016/J.DESTUD.2006.11.001.

[148] P. Galle, The ontology of Gero's FBS model of designing, Des. Stud. 30 (2009) 321–339. doi:10.1016/J.DESTUD.2009.02.002.

[149] D.C. Montgomery, E.A. Peck, G.G. Vining, Introduction to linear regression analysis, Wiley, 2012.

[150] M.S. Al-Homoud, Computer-aided building energy analysis techniques, Build. Environ. 36 (2001) 421–433. doi:10.1016/S0360-1323(00)00026-3.

[151] A. Foucquier, S. Robert, F. Suard, L. Stéphan, A. Jay, State of the art in building modelling and energy performances prediction: A review, Renew. Sustain. Energy Rev. 23 (2013) 272–288. doi:10.1016/j.rser.2013.03.004.

[152] F. Haghighat, Y. Li, A.C. Megri, Development and validation of a zonal model - POMA, Build. Environ. 36 (2001) 1039–1047. doi:10.1016/S0360-1323(00)00073-1.

[153] T. Hong, S.K. Chou, T.Y. Bong, Building simulation: An overview of developments and information sources, Build. Environ. 35 (2000) 347–361. doi:10.1016/S0360-1323(99)00023-2.

[154] M. Pidd, Computer Simulation in Mangement Science, 5th Edition, n.d.

[155] J.A. Clarke, Energy simulation in building design, 2nd edition, Butterworth-Heinemann, 2001. https://www.sciencedirect.com/book/9780750650823/energy-simulation-in-building-design (accessed October 16, 2018).

[156] O.T. Masoso, L.J. Grobler, The dark side of occupants' behaviour on building energy use, Energy Build. 42 (2010) 173–177. doi:10.1016/j.enbuild.2009.08.009.

[157] F. Haldi, D. Robinson, The impact of occupants' behaviour on building energy demand, J. Build. Perform. Simul. 4 (2011) 323–338. doi:10.1080/19401493.2011.558213.

[158] E. Fabrizio, V. Monetti, Methodologies and Advancements in the Calibration of Building Energy Models, Energies. 8 (2015) 2548–2574. doi:10.3390/en8042548.

[159] Y. Heo, Bayesian calibration of building energy models for energy retrofit decision-making under uncertainty., Georgia Institute of Technology, Atlanta, GA, USA, n.d.

[160] F. Campolongo, A. Saltelli, J. Cariboni, From screening to quantitative sensitivity analysis. A unified approach, Comput. Phys. Commun. 182 (2011) 978–988. doi:10.1016/j.cpc.2010.12.039.

[161] A. Saltelli, S. Tarantola, F. Campolongo, M. Ratto, Sensitivity analysis in preactice: A guide to assessing scientific models, John Wiley & Sons, Ltd, 2004.

[162] G.C. Corson, Input-output sensitivity of building energy simulations, ASHRAE Trans. 98 (1992) 618–626.

[163] W. Tian, A review of sensitivity analysis methods in building energy analysis, Renew. Sustain. Energy Rev. 20 (2013) 411–419. doi:10.1016/j.rser.2012.12.014.

[164] N. Delgarm, B. Sajadi, K. Azarbad, S. Delgarm, Sensitivity analysis of building energy performance: A simulation-based approach using OFAT and variance-based sensitivity analysis methods, J. Build. Eng. 15 (2018) 181–193. doi:10.1016/j.jobe.2017.11.020.

[165] K.J. Lomas, H. Eppel, Sensitivity analysis techniques for building thermal simulation programs, Energy Build. 19 (1992) 21–44. doi:10.1016/0378-7788(92)90033-D.

[166] A. Saltelli, Sensitivity analysis: Could better methods be used?, J. Geophys. Res. Atmos. 104 (1999) 3789–3793. doi:10.1029/1998JD100042.

[167] A. Ioannou, L.C.M. Itard, Energy performance and comfort in residential buildings: Sensitivity for building parameters and occupancy, Energy Build. 92 (2015) 216–233. doi:10.1016/j.enbuild.2015.01.055.

[168] J.S. Hygh, J.F. DeCarolis, D.B. Hill, S. Ranji Ranjithan, Multivariate regression as an energy assessment tool in early building design, Build. Environ. 57 (2012) 165–175. doi:10.1007/s13197-015-1935-8.

[169] P. de Wilde, W. Tian, Identification of key factors for uncertainty in the prediction of the thermal performance of an office building under climate change, Build. Simul. 2 (2009) 157–174. doi:10.1007/s12273-009-9116-1.

[170] Y. Yildiz, K. Korkmaz, T. Göksal özbalta, Z. Durmus Arsan, An approach for developing sensitive design parameter guidelines to reduce the energy requirements of low-rise apartment buildings, Appl. Energy. 93 (2012) 337–347. doi:10.1016/j.apenergy.2011.12.048.

[171] A. Saltelli, M. Ratto, S. Tarantola, F. Campolongo, Update 1 of: Sensitivity Analysis for Chemical Models, Chem. Rev. 112 (2012) PR1–PR21. doi:10.1021/cr200301u.

[172] D.B. Crawley, Which weather data should you use for energy simulations of commercial buildings?, ASHRAE Trans. 104 (1998) 498–515.

[173] G.R. Ruiz, C.F. Bandera, Validation of calibrated energy models: Common errors, Energies. 10 (2017) 1587. doi:10.3390/en10101587.

[174] D.W.U. Perera, D. Winkler, N.-O. Skeie, Multi-floor building heating models in MATLAB and Modelica environments, Appl. Energy. 171 (2016) 46–57. doi:10.1016/J.APENERGY.2016.02.143.

[175] 3D Design & Engineering Software - Dassault Systèmes®, (n.d.). https://www.3ds.com/ (accessed January 8, 2019).

[176] Modelica Standard Library 3.2.1 Released — Modelica Association, (n.d.). https://www.modelica.org/news_items/modelica-standard-library-3.2.1-released (accessed November 29, 2018).

[177] D.E. Coleman, D.C. Montgomery, A Systematic Approach to Planning for a Designed Industrial Experiment, Technometrics. 35 (1993) 1–12. doi:10.1080/00401706.1993.10484984.

[178] R.A. Brown, G.E.P. Box, N.R. Draper, Empirical Model-Building and Response Surfaces., Biometrics. 46 (1990) 283. doi:10.2307/2531659.

[179] S. Madani, R. Gheshlaghi, M.A. Mahdavi, M. Sobhani, A. Elkamel, Optimization of the performance of a double-chamber microbial fuel cell through factorial design of experiments and response surface methodology, Fuel. 150 (2015) 434–440. doi:10.1016/j.fuel.2015.02.039.

[180] R.H. Myers, D.C. Montgomery, C.M. Anderson-Cook, Response Surface Methodology : Process and Product Optimization Using Designed Experiments., Fourth edi, Wiley, 2016. https://www.wiley.com/en-us/Response+Surface+Methodology%3A+Process+and+Product+Optimization+Using+Designed+Experiments%2C+4th+Edition-p-9781118916032 (accessed December 11, 2018).

[181] E.C. Harrington, The desirability Function, Ind. Qual. Control. 21 (1965) 494–498.

[182] G. Derringer, R. Suich, Simultaneous Optimization of Several Response Variables, J. Qual. Technol. 12 (1980) 214–219. doi:10.1080/00224065.1980.11980968.

[183] J.A. Nelder, R. Mead, A Simplex Method for Function Minimization, Comput. J. 7 (1965) 308–313. doi:10.1093/comjnl/7.4.308.

[184] S. Seo, P.D. Gary M. Marsh, A review and comparison of methods for detecting outliers in univariate data sets, Grad. Sch. Public Heal. Univ. Pittsburgh. (2006). doi:10.1016/j.arth.2008.03.010.

[185] H. Do, K.S. Cetin, Evaluation of the causes and impact of outliers on residential building energy use prediction using inverse modeling, Build. Environ. 138 (2018) 194–206. doi:10.1016/j.buildenv.2018.04.039.

[186] Climatologie mensuelle en décembre 2016 à Troyes-Barberey | climatologie depuis 1900 - Infoclimat, (n.d.). https://www.infoclimat.fr/climatologie-mensuelle/07168/decembre/2016/troyes-barberey.html (accessed March 1, 2019).

[187] A. Sharda, S. Kumar, Heat Transfer through Glazing Systems with Inter-Pane Shading Devices: A Review, Energy Technol. Policy. 1 (2014) 23–34. doi:10.1080/23317000.2014.969451.

[188] ASHRAE, ASHRAE Standard 55-2013 Thermal Environmental Conditions for Human Occupancy, 2013. doi:ISSN 1041-2336.

[189] W. Makondo, A. Merabtine, S. Pincemin, J. Podlecki, R. Garcia, Capteur multifonctions pour l ' évaluation du confort thermique dans les bâtiments, in: Congrès Fr. Therm., La Rochelle, France, 2015.

[190] T. Catalina, V. Iordache, B. Caracaleanu, Multiple regression model for fast prediction of the heating energy demand, Energy Build. 57 (2013) 302–312. doi:10.1016/j.enbuild.2012.11.010.

[191] T. Catalina, V. Iordache, IEQ assessment on schools in the design stage, Build. Environ. 49 (2012) 129–140. doi:10.1016/j.buildenv.2011.09.014.

[192] J. Dhariwal, R. Banerjee, An approach for building design optimization using design of experiments, Build. Simul. 10 (2017) 323–336. doi:10.1007/s12273-016-0334-z.

[193] Ashrae, ASHRAE Handbook - Fundamentals (SI Edition), 2009.

[194] B.W. Olesen, K.C. Parsons, Introduction to thermal comfort standards and to the proposed new version of EN ISO 7730, Energy Build. 34 (2002) 537–548. doi:10.1016/S0378-7788(02)00004-X.

[195] B.W. Olesen, O. Seppanen, A. Boerstra, Criteria for the indoor environment for energy performance of buildings, Facilities. 24 (2006) 445–457. doi:10.1108/02632770610684927.

[196] B.W. Olesen, The philosophy behind EN15251: Indoor environmental criteria for design and calculation of energy performance of buildings, Energy Build. 39 (2007) 740–749. doi:10.1016/j.enbuild.2007.02.011.

[197] K.J. McCartney, J. Fergus Nicol, Developing an adaptive control algorithm for Europe, Energy Build. 34 (2002) 623–635. doi:10.1016/S0378-7788(02)00013-0.

Appendix A: Thermal comfort standards

Thermal comfort standards are regularly reviewed on a carful basis by organizations. In the European countries, ISO 7730 [20] is the current standard for evaluating occupants' thermal comfort, besides EN 15251 [79], which covers thermal comfort in addition to other indoor environmental parameters. In North America, ANSI/ASHRAE 55 [16] is the standard that deals with occupants' thermal comfort. These documents assign comfort zones such that a major percentage of occupants with certain individual parameters to consider the thermal environment as acceptable. In addition to the mentioned standards, the adaptive models have been presented in ANSI/ASHRAE Standard 55-2010 for the assessment of the indoor environment in non-air-conditioned (naturally ventilated) buildings as well as in EN 15251.

A.1 ISO 7730 standard

ISO 7730 is an international standard, which has been established to access thermal comfort of indoor environment. This standard offers methods for forecasting the thermal comfort and degree of thermal discomfort of occupants' in moderate thermal environment. For the design of new or existing buildings, this standard enables the determination of occupants' thermal comfort using calculation of the PMV and PPD indices and local thermal discomfort [194]. ISO 7730 also provides methods for the assessment of local discomfort caused by draught, asymmetric radiation and temperature gradients [194]. In addition, ISO 7730 recommends three different levels of acceptable classes for general thermal comfort and local thermal discomfort parameters as shown in Table A-1.

Table A-1 : Categories of thermal environment based on ISO 7730 [20].

Category	**General comfort**		**Local discomfort**			
	PPD (%)	PMV	Percentage of dissatisfied (PD) due to draught (%)	PD due to vertical air temperature difference (%)	PD due to cool or warm floor (%)	PD due to radiant temperature asymmetry (%)
A	<6	-0.2 to 0.2	<10	<3	<10	<5
B	<10	-0.5 to 0.5	<20	<5	<10	<5
C	<15	-0.7 to 0.7	<30	<10	<15	<10

A.2 ASHRAE Standards 55

ASHRAE standard 55 is developed and intended for use in design, commissioning, and testing of buildings and their HVAC systems and for the evaluation of thermal environmental conditions [22,26]. The main objective of this standard is to identify the combinations of four indoor thermal environmental factors, noted as air temperature, mean radiant temperature, relative humidity, and air velocity, and two personal parameters, noted as metabolic rate or occupant activity level and clothing

insulation, that will result the acceptable thermal environmental conditions to a majority of the occupants' within a space. The adaptation criteria and the calculation methods of thermal comfort indices, PMV and PPD, have been developed in this standard in a close agreement with ISO 7730 standard. In order to respect the existing necessity for sustainable buildings alongside with providing thermally comfortable environment, an incremental variety of design solutions was accommodated in the revised version of the standard [22].

In the 1990s, de Dear and Brager [121] conducted a research project, at the request of ASHRAE, aiming at collecting information from various field studies carried out in several countries. The results of the study show that, in free running building, subjects' thermal responses depend majorly on the outdoor temperature. In addition, the responses may differ from the responses of occupants' in buildings equipped with HVAC systems. These differences are primarily because of the different thermal experiences, availability of control, changes in clothing and changes in occupant expectations [22]. Based on these results, ASHRAE 55-2010 [22] proposed an optional method for determining acceptable thermal comfort conditions in naturally conditioned spaces. Noting that, ASHRAE standard 55 [22] defined these spaces as a space with no mechanical cooling system and must have operable windows that can be controlled by the occupants. In addition, it is acceptable for the space to be equipped with a heating system, but then the proposed method does not apply when it is in operation. This suggested method uses the derived equation from more than 21000 measurements taken mainly in office buildings. The equation is as follow:

$$T_{op} = 0.31T_{ref} + 17.8°C \ . \tag{A.1}$$

where T_{ref} is the prevailing mean outdoor air temperature for a time period between 7 and 30 days before the day in question [22], which can be determined using three ASHRAE 55 [16] methods:

1. A simple average of all means daily outdoor air temperatures, calculated with 7 and 30 sequential days prior to the day in question.
2. The weighting method using Equation (A.2), where α is the weighting factor ranged between 0.6 and 0.8, $T_{e(d-1)}$ is the mean outdoor temperature of the previous day, $T_{e(d-2)}$ is the mean outdoor temperature of the day before and so on.

$$T_{ref} = (1-\alpha)\left[T_{e(d-1)} + \alpha T_{e(d-2)} + \alpha^2 T_{e(d-3)} + \alpha^3 T_{e(d-4)} + \cdots\right] \tag{A.2}$$

3. The published meteorological monthly means for each calendar month.

The acceptable operative indoor temperature ranges for naturally conditioned spaces are shown in Figure A-1. It shows two relevant sets of operative temperature limits, 80% and 90% acceptability

ranges. The 80% acceptability limits corresponds to typical applications, while the 90% acceptability limits is recommended when a higher standard of thermal comfort is desired. In addition, the equation is only applicable between the end points (10°C and 33.5°C) of the curves shown in Figure A-1.

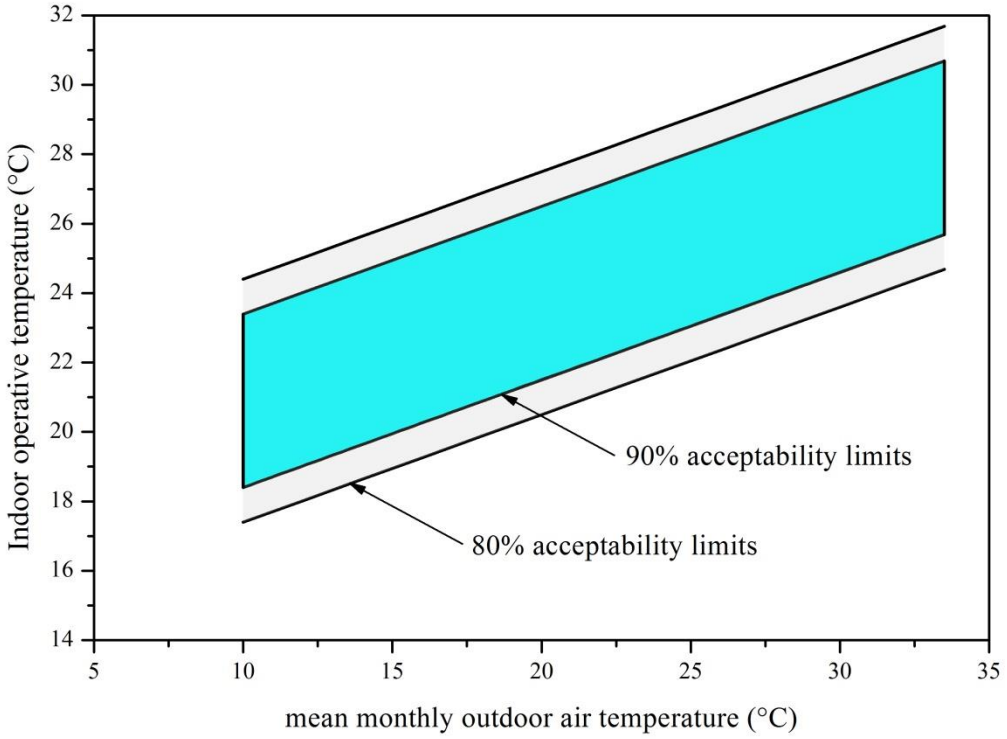

Figure A-1: Acceptable operative temperature ranges for naturally conditioned spaces [22].

A.3 EN15251

Olesen et al. [195] and Olesen [196] described briefly the European Standard EN 15251 and its contents. The majority content of EN 15251 standard is overlap with ISO 7730 and ANSI/ASHRAE 55 standards for thermal comfort. This standard specifies design values of indoor environmental factors for the non-industrial buildings, i.e. residential and educational buildings. The standard also specifies values to be used in energy performance calculations and presents methods to validate the specified indoor environments in buildings [79,196]. In addition, it includes methods for long-term evaluation of the indoor environment [196]. Thermal comfort guidelines in EN 15251 standard are based on the smart controls and thermal comfort (SCATs) research project. The project was authorized and funded by the European commission. In this project, 26 European buildings located in France, Greece, Sweden, Portugal, and the UK were surveyed for a period of three years. The survey covered conditioned, free running and mixed-mode buildings [197]. Based on the data collected from the survey, different adaptive algorithms for each participating country were developed. These adaptive

algorithms are an alternative to fixed temperature set-point controls within buildings. Table A-2 shows the developed ACA for the participated countries in the survey.

Table A-2 : Adaptive comfort algorithms for individual countries [197].

Country	Adaptive control algorithm	
	$T_{rm} \leq 10\ ^{\circ}C$	$T_{rm} > 10\ ^{\circ}C$
France	$0.049 \times T_{rm} + 22.85$	$0.206 \times T_{rm} + 21.42$
Greece	NA	$0.205 \times T_{rm} + 21.69$
Portugal	$0.381 \times T_{rm} + 18.12$	$0.381 \times T_{rm} + 18.12$
Sweden	$0.051 \times T_{rm} + 22.83$	$0.051 \times T_{rm} + 22.83$
UK	$0.104 \times T_{rm} + 22.85$	$0.168 \times T_{rm} + 21.63$
ALL	21.88	$0.302 \times T_{rm} + 19.39$

Regarding the naturally ventilated buildings, EN15251 standard recommends the use of the following equation:

$$T_{op} = 0.33T_{rm} + 18.8 \tag{A.3}$$

where $T_{op}\ (^{\circ}C)$ is the indoor operative comfort temperature, and $T_{rm}\ (^{\circ}C)$ is the exponentially weighted running mean of the daily outdoor temperature [196], which can be obtained from Equation (A.4):

$$T_{rm} = (1-\alpha)\left[T_{e(d-1)} + \alpha T_{e(d-2)} + \alpha^2 T_{e(d-3)} + \cdots\right] \tag{A.4}$$

But the standard recommends the use of the exponentially weighted running mean of the previous seven days, with 0.8 for the constantα, thus leading to:

$$T_{rm7} = \frac{T_{d-1} + 0.8T_{d-2} + 0.6T_{d-3} + 0.5T_{d-4} + 0.4T_{d-5} + 0.3T_{d-6} + 0.2T_{d-7}}{3.8} \tag{A.5}$$

In this standard, the accepted deviation of the indoor operative temperature from the comfort temperature is divided into four categories, as shown in Table A-3. Figure A-2 presents the comfort bandwidths based on the comfort algorithm and the range permitted for different percentages of acceptability.

Table A-3 : Suggested applicability for the categories and their associated acceptable temperature ranges [79].

Category	Explanation	Limit of deviation (°C)	Range of acceptability (%)
I	High level of expectation for very sensitive and fragile users (hospitals, …)	± 2	90
II	Normal expectation for new buildings	± 3	80
III	Moderate expectation (existing buildings)	± 4	65
IV	Values outside the criteria for the above categories (only in a limited period)	$> \pm 4$	< 65

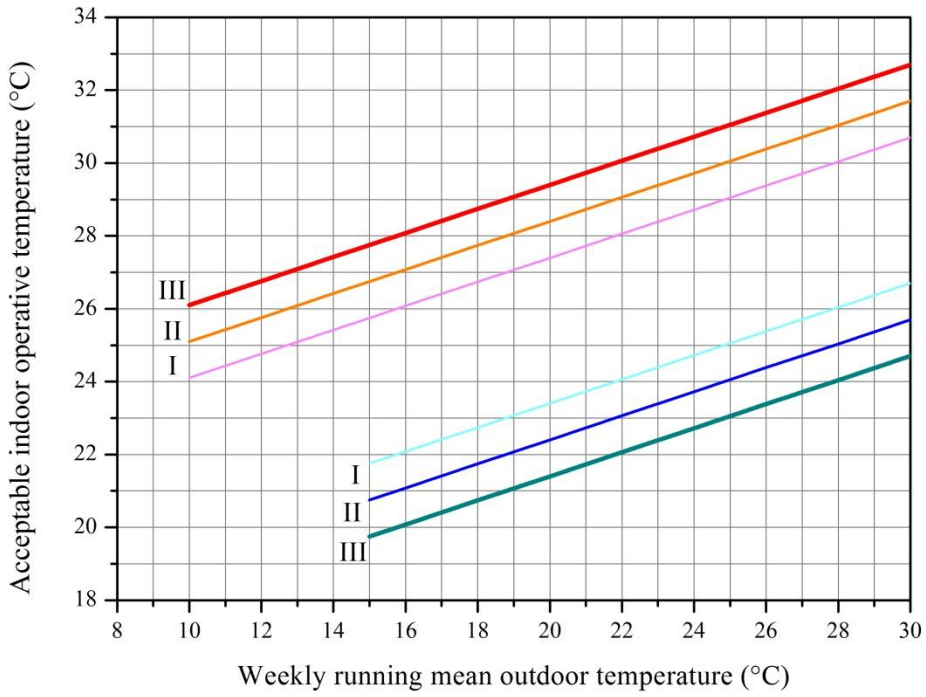

Figure A-2 : Design values for the indoor operative temperature for buildings without mechanical cooling systems as a function of the exponentially weighted running mean of the outdoor temperature [196].

Appendix B: Web-based survey questionnaire results for assessing thermal comfort in the Foyer

Table B-1: Survey questionnaire responses.

Response number	Questions					
	1	2	3	4	5	6
1	Yes	Partly cloudy	Cool	no change	Yes	Light activity, standing
2	Yes	Sunny	Cool	no change	Yes	standing relaxed
3	Yes	Partly cloudy	Cool	no change	Yes	Medium activity, standing
4	Yes	Overcast	Cool	more warmer	No	Medium activity, standing
5	Yes	Overcast	Cold	a bit more warmer	No	standing relaxed
6	Yes	Sunny	Hot	more cooler	No	Medium activity, standing
7	Yes	Sunny	Hot	more cooler	No	High activity
8	Yes	Sunny	Hot	a bit more cooler	No	Seated quite
9	Yes	Sunny	Hot	a bit more cooler	No	Medium activity, standing
10	Yes	Sunny	Hot	a bit more cooler	Yes	standing relaxed
11	Yes	Sunny	Hot	more cooler	No	Light activity, standing
12	Yes	Partly cloudy	Neutral	more cooler	Yes	Medium activity, standing
13	Yes	Sunny	Neutral	a bit more cooler	Yes	standing relaxed
14	Yes	Sunny	Neutral	no change	Yes	Light activity, standing
15	Yes	Partly cloudy	Neutral	a bit more warmer	Yes	Medium activity, standing
16	No					
17	No					
18	Yes	Sunny	Neutral	no change	Yes	High activity
19	Yes	Partly cloudy	Neutral	more cooler	Yes	Medium activity, standing
20	Yes	Sunny	Neutral	a bit more cooler	Yes	Light activity, standing
21	Yes	Sunny	Neutral	a bit more warmer	Yes	standing relaxed
22	Yes	Partly cloudy	Neutral	a bit more warmer	Yes	Light activity, standing
23	Yes	Sunny	Neutral	a bit more cooler	Yes	Light activity, standing
24	Yes	Overcast	Slightly Cool	a bit more warmer	No	Light activity, standing
25	Yes	Sunny	Slightly Cool	a bit more warmer	Yes	standing relaxed
26	Yes	Partly cloudy	Slightly Warm	no change	Yes	Medium activity, standing
27	Yes	Partly cloudy	Slightly Warm	a bit more cooler	Yes	Light activity, standing
28	Yes	Sunny	Slightly Warm	no change	Yes	standing relaxed
29	Yes	Sunny	Slightly Warm	no change	Yes	standing relaxed
30	Yes	Partly cloudy	Slightly Warm	no change	Yes	Seated quite
31	Yes	Sunny	Slightly Warm	a bit more cooler	Yes	Medium activity, standing
32	Yes	Sunny	Slightly Warm	no change	Yes	Light activity, standing
33	Yes	Partly cloudy	Slightly Warm	no change	Yes	Medium activity, standing
34	Yes	Sunny	Slightly Warm	no change	Yes	standing relaxed
35	Yes	Sunny	Slightly Warm	a bit more warmer	Yes	Seated quite
36	Yes	Sunny	Slightly Warm	a bit more cooler	No	Medium activity, standing
37	Yes	Sunny	Slightly Warm	a bit more warmer	Yes	Medium activity, standing
38	Yes	Sunny	Slightly Cool	a bit more warmer	No	Seated quite

39	Yes	Sunny	Slightly Warm	a bit more cooler	Yes	Medium activity, standing
40	Yes	Sunny	Warm	no change	Yes	standing relaxed
41	Yes	Sunny	Warm	more cooler	No	Light activity, standing
42	Yes	Sunny	Warm	a bit more cooler	No	Medium activity, standing
43	Yes	Sunny	Warm	a bit more cooler	No	Medium activity, standing
44	Yes	Sunny	Warm	a bit more cooler	No	Medium activity, standing
45	Yes	Sunny	Warm	no change	Yes	standing relaxed
46	Yes	Sunny	Warm	more cooler	Yes	Medium activity, standing
47	Yes	Sunny	Warm	a bit more cooler	No	Seated quite
48	Yes	Partly cloudy	Warm	a bit more cooler	No	High activity
49	Yes	Overcast	Warm	a bit more cooler	No	Light activity, standing
50	Yes	Sunny	Warm	no change	Yes	standing relaxed
51	Yes	Sunny	Warm	a bit more cooler	Yes	standing relaxed
52	Yes	Sunny	Warm	a bit more cooler	No	standing relaxed
53	Yes	Sunny	Warm	a bit more cooler	Yes	Medium activity, standing
54	Yes	Partly cloudy	Warm	a bit more cooler	Yes	Seated quite
55	Yes	Sunny	Warm	a bit more cooler	Yes	Medium activity, standing

Appendix C: Hourly numerical results

Table C-1 : Hourly numerical values of PMV index, air, mean radiant and operative temperatures and outdoor climatic conditions for ordinary, partly cloudy, cold, and sunny winter days.

Time (hours)	T_a (°C)	MRT (°C)	T_{op} (°C)	PMV	Outdoor temperature (°C)	Global solar radiation ($W.m^{-2}$)
Case A : Ordinary winter day						
8	19.95	17.88	19.02	-0.65	2.5	0.01
9	19.98	17.97	19.08	-0.64	2.5	0.01
10	19.95	18.01	19.09	-0.64	2.4	4.75
11	19.97	18.38	19.26	-0.60	2.4	41.14
12	20.00	19.00	19.56	-0.54	3.7	83.90
13	20.00	19.35	19.71	-0.51	5	114.94
14	20.05	19.64	19.86	-0.48	6.3	124.10
15	19.96	19.60	19.80	-0.49	6	110.85
16	20.00	19.40	19.73	-0.50	6	76.47
17	19.96	19.16	19.60	-0.53	6.1	33.33
18	19.98	18.25	19.21	-0.61	6	1.5
19	19.95	18.19	19.17	-0.62	5.8	0.01
20	19.95	18.21	19.17	-0.62	5.6	0.01
Case B : partly cloudy winter day						
8	19.99	18.94	19.58	-0.67	-1.7	0.01
9	19.95	19.00	19.59	-0.66	-1	1.99
10	19.99	19.10	19.65	-0.64	0	17.27
11	19.96	19.25	19.69	-0.61	0.3	63.28
12	19.98	19.59	19.84	-0.54	1	122.44
13	20.06	19.97	20.05	-0.46	4	179.80
14	20.19	20.48	20.36	-0.35	5.6	253.97
15	21.72	21.93	21.84	-0.02	7	330.56
16	22.49	22.49	22.52	0.105	8	319.95
17	21.90	21.97	21.98	-0.01	9.3	210.84
18	20.61	20.62	20.71	-0.31	8	78.46
19	19.97	19.35	19.76	-0.59	8	5.40
20	19.96	19.26	19.71	-0.60	8	0.01
Case C : Cold winter day						
8	19.98	17.46	18.86	-0.67	-2.9	0.01
9	19.96	17.57	18.89	-0.68	-3	0.23
10	19.97	17.63	18.93	-0.67	-3	6.09
11	19.96	17.80	19.00	-0.66	-3.1	30.94
12	19.93	18.06	19.10	-0.64	-3	57.58
13	19.99	18.26	19.22	-0.61	-3	77.19
14	19.96	18.37	19.25	-0.60	-3.4	84.34
15	19.93	18.27	19.19	-0.62	-3.5	78
16	19.96	18.16	19.16	-0.62	-3.5	59.77

17	19.93	17.94	19.04	-0.65	-3.6	33.52
18	19.96	17.64	18.93	-0.67	-3.8	7.87
19	19.94	17.55	18.87	-0.68	-4	0.48
20	19.91	17.49	18.83	-0.69	-4.4	0.01
Case D : Sunny winter day						
8	19.95	17.73	18.96	-0.66	1.3	0.01
9	19.96	18.35	19.25	-0.61	1.6	49.84
10	20.05	19.49	19.80	-0.49	2	129.86
11	20.53	21.38	20.91	-0.25	3	255.62
12	23.27	22.83	23.08	0.24	5	432.63
13	25.83	24.90	25.41	0.78	8	557.77
14	27.77	26.56	27.23	1.20	10	594.63
15	27.94	26.78	27.42	1.25	11	562.14
16	26.47	25.68	26.12	0.94	11	474.58
17	24.54	24.00	24.30	0.52	11.4	339.70
18	21.92	21.88	21.90	-0.02	11	190.02
19	19.98	19.12	19.60	-0.53	10	50.13
20	19.97	18.50	19.32	-0.59	9	3.30

Table C-2 : Hourly numerical values of PMV index for different activity levels.

Time (hours)	Seated Quiet	Standing Relaxed	Light Activity, standing	Medium Activity, Standing	High Activity
Case A : Ordinary winter day					
8	-1.42	-0.76	-0.02	0.42	0.57
9	-1.43	-0.77	-0.03	0.42	0.57
10	-1.42	-0.76	-0.02	0.42	0.57
11	-1.38	-0.72	0.00	0.44	0.60
12	-1.28	-0.64	0.05	0.49	0.64
13	-1.25	-0.62	0.07	0.51	0.66
14	-1.22	-0.59	0.09	0.53	0.67
15	-1.20	-0.58	0.10	0.54	0.69
16	-1.19	-0.57	0.10	0.54	0.69
17	-1.23	-0.60	0.09	0.52	0.67
18	-1.35	-0.70	0.01	0.46	0.61
19	-1.35	-0.70	0.02	0.47	0.62
20	-1.34	-0.69	0.02	0.47	0.62
Case B : partly cloudy winter day					
8	-1.51	-0.83	-0.08	0.37	0.52
9	-1.52	-0.84	-0.09	0.36	0.52
10	-1.44	-0.78	-0.04	0.40	0.56
11	-1.39	-0.73	-0.01	0.43	0.59
12	-1.30	-0.66	0.03	0.48	0.63
13	-1.21	-0.59	0.09	0.52	0.67
14	-1.01	-0.43	0.21	0.63	0.77
15	-0.59	-0.09	0.46	0.85	0.98

16	-0.44	0.02	0.55	0.92	1.05
17	-0.57	-0.07	0.48	0.86	0.99
18	-0.88	-0.32	0.29	0.70	0.84
19	-1.34	-0.70	0.01	0.46	0.61
20	-1.38	-0.73	0.00	0.44	0.59
Case C : Cold winter day					
8	-1.53	-0.85	-0.10	0.36	0.51
9	-1.52	-0.84	-0.09	0.37	0.52
10	-1.54	-0.86	-0.10	0.35	0.51
11	-1.53	-0.85	-0.09	0.36	0.51
12	-1.46	-0.79	-0.05	0.39	0.55
13	-1.44	-0.78	-0.04	0.40	0.56
14	-1.44	-0.78	-0.04	0.40	0.56
15	-1.46	-0.79	-0.05	0.39	0.54
16	-1.49	-0.82	-0.07	0.38	0.53
17	-1.48	-0.81	-0.07	0.38	0.53
18	-1.54	-0.86	-0.10	0.35	0.51
19	-1.57	-0.88	-0.12	0.34	0.49
20	-1.58	-0.89	-0.13	0.33	0.49
Case D : Sunny winter day					
8	-1.45	-0.78	-0.04	0.40	0.56
9	-1.38	-0.73	0.00	0.44	0.59
10	-1.22	-0.60	0.09	0.52	0.67
11	-0.89	-0.34	0.28	0.69	0.83
12	-0.28	0.15	0.65	1.00	1.13
13	0.33	0.65	1.02	1.32	1.44
14	0.86	1.07	1.34	1.59	1.70
15	0.96	1.15	1.39	1.64	1.75
16	0.60	0.87	1.18	1.46	1.57
17	0.10	0.46	0.88	1.20	1.32
18	-0.55	-0.06	0.49	0.86	1.00
19	-1.22	-0.60	0.08	0.52	0.67
20	-1.77	-1.04	-0.241	0.24	0.40

Appendix D: DoE matrices and results

Table D-1 : Result of running simulation experiment of PMV index.

Experiment Number	Factors						Response (PMV)		
	CI	MR	Set-point	sol-air temperature	Glazing type	WFR	Avg	Min	Max
1	-1	-1	-1	-1	-1	-1	-1.96	-2.00	-1.93
2	1	-1	-1	-1	-1	-1	-1.02	-1.05	-0.99
3	-1	1	-1	-1	-1	-1	0.37	0.35	0.38
4	1	1	-1	-1	-1	-1	0.76	0.75	0.78
5	-1	-1	1	-1	-1	-1	-1.36	-1.39	-1.33
6	1	-1	1	-1	-1	-1	-0.53	-0.56	-0.51
7	-1	1	1	-1	-1	-1	0.67	0.65	0.68
8	1	1	1	-1	-1	-1	1.01	1.00	1.02
9	-1	-1	-1	1	-1	-1	-1.67	-1.97	-1.30
10	1	-1	-1	1	-1	-1	-0.79	-1.03	-0.48
11	-1	1	-1	1	-1	-1	0.51	0.36	0.69
12	1	1	-1	1	-1	-1	0.88	0.76	1.03
13	-1	-1	1	1	-1	-1	-1.16	-1.61	-0.81
14	1	-1	1	1	-1	-1	-0.37	-0.73	-0.09
15	-1	1	1	1	-1	-1	0.76	0.54	0.94
16	1	1	1	1	-1	-1	1.09	0.90	1.23
17	-1	-1	-1	-1	1	-1	-1.97	-1.99	-1.93
18	1	-1	-1	-1	1	-1	-1.03	-1.04	-1.00
19	-1	1	-1	-1	1	-1	0.36	0.35	0.38
20	1	1	-1	-1	1	-1	0.76	0.75	0.77
21	-1	-1	1	-1	1	-1	-1.38	-1.41	-1.34
22	1	-1	1	-1	1	-1	-0.55	-0.58	-0.51
23	-1	1	1	-1	1	-1	0.65	0.64	0.68
24	1	1	1	-1	1	-1	1.00	0.99	1.02
25	-1	-1	-1	1	1	-1	-1.52	-1.96	-0.99
26	1	-1	-1	1	1	-1	-0.66	-1.02	-0.24
27	-1	1	-1	1	1	-1	0.58	0.37	0.84
28	1	1	-1	1	1	-1	0.94	0.76	1.15
29	-1	-1	1	1	1	-1	-1.08	-1.64	-0.64
30	1	-1	1	1	1	-1	-0.31	-0.76	0.05
31	-1	1	1	1	1	-1	0.80	0.53	1.02
32	1	1	1	1	1	-1	1.12	0.89	1.30
33	-1	-1	-1	-1	-1	1	-2.04	-2.09	-1.98
34	1	-1	-1	-1	-1	1	-1.08	-1.13	-1.04
35	-1	1	-1	-1	-1	1	0.33	0.30	0.36
36	1	1	-1	-1	-1	1	0.73	0.71	0.76
37	-1	-1	1	-1	-1	1	-1.45	-1.50	-1.38
38	1	-1	1	-1	-1	1	-0.60	-0.65	-0.55
39	-1	1	1	-1	-1	1	0.62	0.60	0.66

40	1	1	1	-1	-1	1	0.97	0.95	1.00
41	-1	-1	-1	1	-1	1	-0.62	-2.09	1.24
42	1	-1	-1	1	-1	1	0.07	-1.13	1.58
43	-1	1	-1	1	-1	1	1.03	0.30	1.97
44	1	1	-1	1	-1	1	1.31	0.71	2.08
45	-1	-1	1	1	-1	1	-0.18	-1.69	1.61
46	1	-1	1	1	-1	1	0.43	-0.80	1.88
47	-1	1	1	1	-1	1	1.25	0.50	2.15
48	1	1	1	1	-1	1	1.49	0.87	2.23
49	-1	-1	-1	-1	1	1	-2.09	-2.19	-1.97
50	1	-1	-1	-1	1	1	-1.12	-1.20	-1.03
51	-1	1	-1	-1	1	1	0.31	0.26	0.36
52	1	1	-1	-1	1	1	0.71	0.67	0.76
53	-1	-1	1	-1	1	1	-1.51	-1.60	-1.39
54	1	-1	1	-1	1	1	-0.65	-0.72	-0.56
55	-1	1	1	-1	1	1	0.60	0.55	0.65
56	1	1	1	-1	1	1	0.95	0.92	1.00
57	-1	-1	-1	1	1	1	-0.40	-2.27	1.79
58	1	-1	-1	1	1	1	0.24	-1.27	2.03
59	-1	1	-1	1	1	1	1.14	0.21	2.24
60	1	1	-1	1	1	1	1.40	0.64	2.30
61	-1	-1	1	1	1	1	0.00	-1.91	2.11
62	1	-1	1	1	1	1	0.58	-0.98	2.29
63	-1	1	1	1	1	1	1.35	0.39	2.40
64	1	1	1	1	1	1	1.56	0.78	2.43
65	0	0	0	0	0	0	0.00	-0.37	0.43

Table D-2 : ANOVA table for average PMV.

Source	DF	Adj SS	Adj MS	F-Value	P-Value	Remarks
Model	63	68.4953	1.0872	6166.54	0.01	significant
Linear	6	63.4854	10.5809	60012.77	0.003	significant
A-CI	1	5.2476	5.2476	29763.36	0.004	significant
B-MR	1	48.6941	48.6941	276182.99	0.001	significant
C-Set-point	1	1.9995	1.9995	11340.63	0.006	significant
D-Sol-air	1	5.8162	5.8162	32988.36	0.004	significant
E-Glazing type	1	0.0284	0.0284	161.35	0.05	
F-WFR	1	1.6996	1.6996	9639.91	0.006	significant
2-Way Interactions	15	4.67	0.3113	1765.81	0.019	significant
A*B	1	0.9123	0.9123	5174.38	0.009	significant
A*C	1	0.0207	0.0207	117.38	0.059	
A*D	1	0.0623	0.0623	353.18	0.034	significant
A*E	1	0.0003	0.0003	1.74	0.413	
A*F	1	0.0169	0.0169	95.7	0.065	
B*C	1	0.2214	0.2214	1255.94	0.018	significant
B*D	1	0.6535	0.6535	3706.45	0.01	significant
B*E	1	0.0032	0.0032	18.04	0.147	
B*F	1	0.1839	0.1839	1043.05	0.02	significant
C*D	1	0.0348	0.0348	197.23	0.045	significant
C*E	1	0.0019	0.0019	10.98	0.187	
C*F	1	0.0015	0.0015	8.3	0.213	
D*E	1	0.0685	0.0685	388.29	0.032	significant
D*F	1	2.4878	2.4878	14110.23	0.005	significant
E*F	1	0.0011	0.0011	6.31	0.241	
3-Way Interactions	20	0.3354	0.0168	95.13	0.081	
A*B*C	1	0.0026	0.0026	14.5	0.164	
A*B*D	1	0.0077	0.0077	43.62	0.096	
A*B*E	1	0	0	0.22	0.723	
A*B*F	1	0.0021	0.0021	11.82	0.18	
A*C*D	1	0.0004	0.0004	2.09	0.385	
A*C*E	1	0	0	0.11	0.794	
A*C*F	1	0	0	0.09	0.819	
A*D*E	1	0.0008	0.0008	4.46	0.282	
A*D*F	1	0.0258	0.0258	146.29	0.053	
A*E*F	1	0	0	0.08	0.827	
B*C*D	1	0.0039	0.0039	22.3	0.133	
B*C*E	1	0.0002	0.0002	1.21	0.47	
B*C*F	1	0.0002	0.0002	0.92	0.513	
B*D*E	1	0.0079	0.0079	44.94	0.094	
B*D*F	1	0.275	0.275	1559.99	0.016	significant
B*E*F	1	0.0001	0.0001	0.72	0.551	
C*D*E	1	0.0008	0.0008	4.36	0.284	

C*D*F	1	0.001	0.001	5.41	0.259
C*E*F	1	0.0002	0.0002	1.05	0.493
D*E*F	1	0.0068	0.0068	38.4	0.102
4-Way Interactions	14	0.0045	0.0003	1.8	0.531
A*B*C*D	1	0	0	0.26	0.701
A*B*C*E	1	0	0	0.01	0.925
A*B*C*F	1	0	0	0.01	0.935
A*B*D*E	1	0.0001	0.0001	0.55	0.594
A*B*D*F	1	0.0032	0.0032	18.07	0.147
A*B*E*F	1	0	0	0.01	0.938
A*C*D*E	1	0	0	0.04	0.87
A*C*D*F	1	0	0	0.05	0.864
A*C*E*F	1	0	0	0.01	0.935
A*D*E*F	1	0.0001	0.0001	0.48	0.613
B*C*D*E	1	0.0001	0.0001	0.47	0.616
B*C*D*F	1	0.0001	0.0001	0.57	0.589
B*C*E*F	1	0	0	0.11	0.793
B*D*E*F	1	0.0008	0.0008	4.6	0.278
5-Way Interactions	6	0	0	0.03	0.999
A*B*C*D*E	1	0	0	0.01	0.954
A*B*C*D*F	1	0	0	0.01	0.952
A*B*C*E*F	1	0	0	0	0.977
A*B*D*E*F	1	0	0	0.06	0.847
A*C*D*E*F	1	0	0	0.01	0.934
B*C*D*E*F	1	0	0	0.11	0.795
6-Way Interactions	1	0	0	0	0.977
A*B*C*D*E*F	1	0	0	0	0.977
Curvature	1	0	0	3.29	0.321
Error	1	0.0002	0.0002		
Total	64	68.4955			

Table D-3: Effects and coefficients of factors for average PMV.

Term	Effect	Coef	SE Coef	T-Value	P-Value
Constant		0.00372	0.00166	2.24	0.267
A	0.57269	0.28635	0.00166	172.52	0.004
B	1.74453	0.87226	0.00166	525.53	0.001
C	0.35351	0.17675	0.00166	106.49	0.006
D	0.60292	0.30146	0.00166	181.63	0.004
E	0.04217	0.02108	0.00166	12.7	0.05
F	0.32592	0.16296	0.00166	98.18	0.006
A*B	-0.23879	-0.11939	0.00166	-71.93	0.009
A*C	-0.03597	-0.01798	0.00166	-10.83	0.059
A*D	-0.06238	-0.03119	0.00166	-18.79	0.034
A*E	-0.00438	-0.00219	0.00166	-1.32	0.413
A*F	-0.03247	-0.01624	0.00166	-9.78	0.065
B*C	-0.11764	-0.05882	0.00166	-35.44	0.018
B*D	-0.2021	-0.10105	0.00166	-60.88	0.01
B*E	-0.0141	-0.00705	0.00166	-4.25	0.147
B*F	-0.10721	-0.0536	0.00166	-32.3	0.02
C*D	-0.04662	-0.02331	0.00166	-14.04	0.045
C*E	-0.011	-0.0055	0.00166	-3.31	0.187
C*F	-0.00957	-0.00478	0.00166	-2.88	0.213
D*E	0.06541	0.03271	0.00166	19.71	0.032
D*F	0.39432	0.19716	0.00166	118.79	0.005
E*F	0.00834	0.00417	0.00166	2.51	0.241
A*B*C	0.01264	0.00632	0.00166	3.81	0.164
A*B*D	0.02192	0.01096	0.00166	6.6	0.096
A*B*E	0.00154	0.00077	0.00166	0.46	0.723
A*B*F	0.01141	0.00571	0.00166	3.44	0.18
A*C*D	0.0048	0.0024	0.00166	1.45	0.385
A*C*E	0.00111	0.00056	0.00166	0.34	0.794
A*C*F	0.00097	0.00048	0.00166	0.29	0.819
A*D*E	-0.00701	-0.00351	0.00166	-2.11	0.282
A*D*F	-0.04015	-0.02007	0.00166	-12.09	0.053
A*E*F	-0.00092	-0.00046	0.00166	-0.28	0.827
B*C*D	0.01568	0.00784	0.00166	4.72	0.133
B*C*E	0.00365	0.00183	0.00166	1.1	0.47
B*C*F	0.00318	0.00159	0.00166	0.96	0.513
B*D*E	-0.02225	-0.01113	0.00166	-6.7	0.094
B*D*F	-0.13111	-0.06556	0.00166	-39.5	0.016
B*E*F	-0.00283	-0.00141	0.00166	-0.85	0.551
C*D*E	-0.00693	-0.00346	0.00166	-2.09	0.284
C*D*F	-0.00772	-0.00386	0.00166	-2.32	0.259
C*E*F	0.0034	0.0017	0.00166	1.02	0.493
D*E*F	0.02057	0.01029	0.00166	6.2	0.102
A*B*C*D	-0.00169	-0.00084	0.00166	-0.51	0.701
A*B*C*E	-0.00039	-0.0002	0.00166	-0.12	0.925

A*B*C*F	-0.00034	-0.00017	0.00166	-0.1	0.935
A*B*D*E	0.00246	0.00123	0.00166	0.74	0.594
A*B*D*F	0.01411	0.00706	0.00166	4.25	0.147
A*B*E*F	0.00032	0.00016	0.00166	0.1	0.938
A*C*D*E	0.00069	0.00034	0.00166	0.21	0.87
A*C*D*F	0.00072	0.00036	0.00166	0.22	0.864
A*C*E*F	-0.00034	-0.00017	0.00166	-0.1	0.935
A*D*E*F	-0.00231	-0.00115	0.00166	-0.7	0.613
B*C*D*E	0.00229	0.00114	0.00166	0.69	0.616
B*C*D*F	0.0025	0.00125	0.00166	0.75	0.589
B*C*E*F	-0.00112	-0.00056	0.00166	-0.34	0.793
B*D*E*F	-0.00712	-0.00356	0.00166	-2.15	0.278
A*B*C*D*E	-0.00024	-0.00012	0.00166	-0.07	0.954
A*B*C*D*F	-0.00025	-0.00013	0.00166	-0.08	0.952
A*B*C*E*F	0.00012	0.00006	0.00166	0.04	0.977
A*B*D*E*F	0.00081	0.00041	0.00166	0.24	0.847
A*C*D*E*F	-0.00034	-0.00017	0.00166	-0.1	0.934
B*C*D*E*F	-0.00111	-0.00055	0.00166	-0.33	0.795
A*B*C*D*E*F	0.00012	0.00006	0.00166	0.04	0.977
Ct Pt		0.0009	0.0134	0.07	0.958

Table D-4: ANOVA table for minimum PMV.

Source	DF	Adj SS	Adj MS	F-Value	P-Value	Remarks
Model	63	74.2413	1.1784	4337.36	0.012	significant
Linear	6	72.6844	12.1141	44587.27	0.004	significant
A	1	6.7725	6.7725	24927.03	0.004	significant
B	1	63.8693	63.8693	235078.76	0.001	significant
C	1	1.6723	1.6723	6154.94	0.008	significant
D	1	0.1102	0.1102	405.68	0.032	significant
E	1	0.0447	0.0447	164.46	0.05	
F	1	0.2154	0.2154	792.73	0.023	significant
2-Way Interactions	15	1.5306	0.102	375.56	0.04	significant
A*B	1	1.1337	1.1337	4172.56	0.01	significant
A*C	1	0.0176	0.0176	64.66	0.079	
A*D	1	0.0009	0.0009	3.45	0.315	
A*E	1	0.0005	0.0005	1.9	0.4	
A*F	1	0.0025	0.0025	9.12	0.204	
B*C	1	0.1868	0.1868	687.42	0.024	significant
B*D	1	0.0111	0.0111	40.96	0.099	
B*E	1	0.0052	0.0052	19.24	0.143	
B*F	1	0.0251	0.0251	92.53	0.066	
C*D	1	0.0993	0.0993	365.51	0.033	significant
C*E	1	0.0016	0.0016	6.04	0.246	
C*F	1	0.0005	0.0005	1.91	0.399	
D*E	1	0.0058	0.0058	21.17	0.136	
D*F	1	0.0052	0.0052	19.1	0.143	
E*F	1	0.0347	0.0347	127.9	0.056	
3-Way Interactions	20	0.0255	0.0013	4.69	0.351	
A*B*C	1	0.0022	0.0022	8.01	0.216	
A*B*D	1	0.0001	0.0001	0.42	0.634	
A*B*E	1	0.0001	0.0001	0.24	0.711	
A*B*F	1	0.0003	0.0003	1.12	0.482	
A*C*D	1	0.001	0.001	3.59	0.309	
A*C*E	1	0	0	0.06	0.842	
A*C*F	1	0	0	0.01	0.943	
A*D*E	1	0.0001	0.0001	0.19	0.739	
A*D*F	1	0	0	0.12	0.791	
A*E*F	1	0.0004	0.0004	1.44	0.443	
B*C*D	1	0.0107	0.0107	39.57	0.1	
B*C*E	1	0.0002	0.0002	0.67	0.563	
B*C*F	1	0	0	0.15	0.766	
B*D*E	1	0.0006	0.0006	2.19	0.379	
B*D*F	1	0.0005	0.0005	1.67	0.419	

B*E*F	1	0.004	0.004	14.76	0.162
C*D*E	1	0.0003	0.0003	1.17	0.474
C*D*F	1	0.0009	0.0009	3.41	0.316
C*E*F	1	0.0001	0.0001	0.22	0.721
D*E*F	1	0.004	0.004	14.86	0.162
4-Way Interactions	14	0.0008	0.0001	0.2	0.957
A*B*C*D	1	0.0001	0.0001	0.45	0.624
A*B*C*E	1	0	0	0.01	0.946
A*B*C*F	1	0	0	0	0.982
A*B*D*E	1	0	0	0.02	0.906
A*B*D*F	1	0	0	0.02	0.921
A*B*E*F	1	0	0	0.17	0.748
A*C*D*E	1	0	0	0.01	0.935
A*C*D*F	1	0	0	0.03	0.896
A*C*E*F	1	0	0	0	0.979
A*D*E*F	1	0	0	0.13	0.782
B*C*D*E	1	0	0	0.12	0.786
B*C*D*F	1	0.0001	0.0001	0.33	0.667
B*C*E*F	1	0	0	0.02	0.915
B*D*E*F	1	0.0004	0.0004	1.51	0.435
5-Way Interactions	6	0	0	0.02	0.999
A*B*C*D*E	1	0	0	0	0.975
A*B*C*D*F	1	0	0	0	0.96
A*B*C*E*F	1	0	0	0	0.995
A*B*D*E*F	1	0	0	0.02	0.918
A*C*D*E*F	1	0	0	0.01	0.941
B*C*D*E*F	1	0	0	0.1	0.803
6-Way Interactions	1	0	0	0	0.982
A*B*C*D*E*F	1	0	0	0	0.982
Curvature	1	0	0	0.13	0.777
Error	1	0.0003	0.0003		
Total	64	74.2416			

Table D-5 : Effects and coefficients of factors for minimum PMV.

Term	Effect	Coef	SE Coef	T-Value	P-Value
Constant		-0.37557	0.00206	-182.28	0.003
A	0.6506	0.3253	0.00206	157.88	0.004
B	1.99796	0.99898	0.00206	484.85	0.001
C	0.32329	0.16164	0.00206	78.45	0.008
D	-0.083	-0.0415	0.00206	-20.14	0.032
E	-0.05285	-0.02642	0.00206	-12.82	0.05
F	-0.11602	-0.05801	0.00206	-28.16	0.023
A*B	-0.26618	-0.13309	0.00206	-64.6	0.01
A*C	-0.03313	-0.01657	0.00206	-8.04	0.079
A*D	0.00765	0.00383	0.00206	1.86	0.315
A*E	0.00568	0.00284	0.00206	1.38	0.4
A*F	0.01244	0.00622	0.00206	3.02	0.204
B*C	-0.10804	-0.05402	0.00206	-26.22	0.024
B*D	0.02637	0.01319	0.00206	6.4	0.099
B*E	0.01807	0.00904	0.00206	4.39	0.143
B*F	0.03964	0.01982	0.00206	9.62	0.066
C*D	-0.07878	-0.03939	0.00206	-19.12	0.033
C*E	-0.01013	-0.00507	0.00206	-2.46	0.246
C*F	0.00569	0.00285	0.00206	1.38	0.399
D*E	-0.01896	-0.00948	0.00206	-4.6	0.136
D*F	-0.01801	-0.009	0.00206	-4.37	0.143
E*F	-0.0466	-0.0233	0.00206	-11.31	0.056
A*B*C	0.01166	0.00583	0.00206	2.83	0.216
A*B*D	-0.00267	-0.00134	0.00206	-0.65	0.634
A*B*E	-0.00201	-0.00101	0.00206	-0.49	0.711
A*B*F	-0.00436	-0.00218	0.00206	-1.06	0.482
A*C*D	0.00781	0.00391	0.00206	1.9	0.309
A*C*E	0.00104	0.00052	0.00206	0.25	0.842
A*C*F	-0.00037	-0.00019	0.00206	-0.09	0.943
A*D*E	0.00179	0.0009	0.00206	0.43	0.739
A*D*F	0.00141	0.0007	0.00206	0.34	0.791
A*E*F	0.00494	0.00247	0.00206	1.2	0.443
B*C*D	0.02592	0.01296	0.00206	6.29	0.1
B*C*E	0.00338	0.00169	0.00206	0.82	0.563
B*C*F	-0.00159	-0.0008	0.00206	-0.39	0.766
B*D*E	0.00609	0.00305	0.00206	1.48	0.379
B*D*F	0.00533	0.00266	0.00206	1.29	0.419
B*E*F	0.01583	0.00792	0.00206	3.84	0.162
C*D*E	-0.00447	-0.00223	0.00206	-1.08	0.474
C*D*F	0.00761	0.00381	0.00206	1.85	0.316
C*E*F	0.00193	0.00097	0.00206	0.47	0.721
D*E*F	-0.01588	-0.00794	0.00206	-3.85	0.162
A*B*C*D	-0.00276	-0.00138	0.00206	-0.67	0.624
A*B*C*E	-0.00035	-0.00018	0.00206	-0.09	0.946

A*B*C*F	0.00011	0.00006	0.00206	0.03	0.982
A*B*D*E	-0.00061	-0.00031	0.00206	-0.15	0.906
A*B*D*F	-0.00051	-0.00026	0.00206	-0.12	0.921
A*B*E*F	-0.00172	-0.00086	0.00206	-0.42	0.748
A*C*D*E	0.00042	0.00021	0.00206	0.1	0.935
A*C*D*F	-0.00068	-0.00034	0.00206	-0.17	0.896
A*C*E*F	-0.00014	-0.00007	0.00206	-0.03	0.979
A*D*E*F	0.00147	0.00074	0.00206	0.36	0.782
B*C*D*E	0.00144	0.00072	0.00206	0.35	0.786
B*C*D*F	-0.00238	-0.00119	0.00206	-0.58	0.667
B*C*E*F	-0.00056	-0.00028	0.00206	-0.13	0.915
B*D*E*F	0.00507	0.00253	0.00206	1.23	0.435
A*B*C*D*E	-0.00016	-0.00008	0.00206	-0.04	0.975
A*B*C*D*F	0.00026	0.00013	0.00206	0.06	0.96
A*B*C*E*F	0.00003	0.00002	0.00206	0.01	0.995
A*B*D*E*F	-0.00053	-0.00027	0.00206	-0.13	0.918
A*C*D*E*F	0.00038	0.00019	0.00206	0.09	0.941
B*C*D*E*F	0.00131	0.00066	0.00206	0.32	0.803
A*B*C*D*E*F	-0.00012	-0.00006	0.00206	-0.03	0.982
Ct Pt		0.0061	0.0166	0.37	0.777

Table D-6: ANOVA table for maximum PMV.

Source	DF	Adj SS	Adj MS	F-Value	P-Value	Remarks
Model	63	104.256	1.6549	1394.38	0.021	significant
Linear	6	82.704	13.784	11614.36	0.007	significant
A	1	3.763	3.7628	3170.49	0.011	significant
B	1	33.994	33.9937	28643.05	0.004	significant
C	1	1.766	1.7659	1487.94	0.017	significant
D	1	30.587	30.587	25772.52	0.004	significant
E	1	0.262	0.2625	221.14	0.043	significant
F	1	12.332	12.3321	10390.99	0.006	significant
2-Way Interactions	15	19.791	1.3194	1111.74	0.024	significant
A*B	1	0.692	0.6919	582.98	0.026	significant
A*C	1	0.018	0.0181	15.26	0.16	
A*D	1	0.318	0.3176	267.58	0.039	significant
A*E	1	0.003	0.0029	2.43	0.363	
A*F	1	0.124	0.1238	104.36	0.062	
B*C	1	0.195	0.1945	163.89	0.05	
B*D	1	3.384	3.3844	2851.67	0.012	significant
B*E	1	0.03	0.0297	24.99	0.126	
B*F	1	1.342	1.3419	1130.65	0.019	significant
C*D	1	0.081	0.0811	68.36	0.077	
C*E	1	0.005	0.0045	3.82	0.301	
C*F	1	0.003	0.0032	2.72	0.347	
D*E	1	0.277	0.2769	233.3	0.042	significant
D*F	1	13.281	13.2813	11190.77	0.006	significant
E*F	1	0.04	0.0396	33.39	0.109	
3-Way Interactions	20	1.738	0.0869	73.2	0.092	
A*B*C	1	0.002	0.0022	1.88	0.401	
A*B*D	1	0.039	0.0392	33.05	0.11	
A*B*E	1	0	0.0004	0.3	0.681	
A*B*F	1	0.015	0.0153	12.89	0.173	
A*C*D	1	0.001	0.0009	0.75	0.545	
A*C*E	1	0	0	0.04	0.878	
A*C*F	1	0	0	0.02	0.9	
A*D*E	1	0.003	0.0031	2.58	0.354	
A*D*F	1	0.134	0.1345	113.32	0.06	
A*E*F	1	0	0.0005	0.39	0.644	
B*C*D	1	0.009	0.0093	7.86	0.218	
B*C*E	1	0	0.0005	0.41	0.636	
B*C*F	1	0	0.0003	0.29	0.686	
B*D*E	1	0.031	0.0314	26.45	0.122	
B*D*F	1	1.451	1.4511	1222.66	0.018	significant
B*E*F	1	0.005	0.0046	3.85	0.3	
C*D*E	1	0.003	0.0028	2.37	0.367	
C*D*F	1	0.002	0.0024	2.01	0.391	
C*E*F	1	0	0.0004	0.36	0.655	

D*E*F	1	0.039	0.0387	32.59	0.11
4-Way Interactions	14	0.023	0.0016	1.37	0.593
A*B*C*D	1	0	0.0001	0.09	0.812
A*B*C*E	1	0	0	0	0.957
A*B*C*F	1	0	0	0	0.965
A*B*D*E	1	0	0.0004	0.32	0.673
A*B*D*F	1	0.017	0.0166	14	0.166
A*B*E*F	1	0	0.0001	0.05	0.862
A*C*D*E	1	0	0	0.02	0.902
A*C*D*F	1	0	0	0.02	0.92
A*C*E*F	1	0	0	0	0.96
A*D*E*F	1	0	0.0005	0.39	0.644
B*C*D*E	1	0	0.0003	0.26	0.699
B*C*D*F	1	0	0.0002	0.2	0.731
B*C*E*F	1	0	0	0.04	0.874
B*D*E*F	1	0.005	0.0045	3.79	0.302
5-Way Interactions	6	0	0	0.03	0.999
A*B*C*D*E	1	0	0	0	0.965
A*B*C*D*F	1	0	0	0	0.972
A*B*C*E*F	1	0	0	0	0.986
A*B*D*E*F	1	0	0.0001	0.05	0.862
A*C*D*E*F	1	0	0	0.01	0.936
B*C*D*E*F	1	0	0.0001	0.11	0.797
6-Way Interactions	1	0	0	0	0.978
A*B*C*D*E*F	1	0	0	0	0.978
Curvature	1	0	0	0.02	0.908
Error	1	0.001	0.0012		
Total	64	104.257			

Table D-7 : Effects and coefficients of factors for maximum PMV.

Term	Effect	Coef	SE Coef	T-Value	P-Value
Constant		0.43566	0.00431	101.17	0.006
A	0.48495	0.24247	0.00431	56.31	0.011
B	1.4576	0.7288	0.00431	169.24	0.004
C	0.33222	0.16611	0.00431	38.57	0.017
D	1.38264	0.69132	0.00431	160.54	0.004
E	0.12808	0.06404	0.00431	14.87	0.043
F	0.87793	0.43896	0.00431	101.94	0.006
A*B	-0.20795	-0.10397	0.00431	-24.14	0.026
A*C	-0.03364	-0.01682	0.00431	-3.91	0.16
A*D	-0.14088	-0.07044	0.00431	-16.36	0.039
A*E	-0.01344	-0.00672	0.00431	-1.56	0.363
A*F	-0.08798	-0.04399	0.00431	-10.22	0.062
B*C	-0.11026	-0.05513	0.00431	-12.8	0.05
B*D	-0.45992	-0.22996	0.00431	-53.4	0.012
B*E	-0.04305	-0.02153	0.00431	-5	0.126
B*F	-0.2896	-0.1448	0.00431	-33.63	0.019
C*D	-0.07121	-0.0356	0.00431	-8.27	0.077
C*E	-0.01682	-0.00841	0.00431	-1.95	0.301
C*F	-0.0142	-0.0071	0.00431	-1.65	0.347
D*E	0.13155	0.06577	0.00431	15.27	0.042
D*F	0.91109	0.45554	0.00431	105.79	0.006
E*F	0.04977	0.02488	0.00431	5.78	0.109
A*B*C	0.01182	0.00591	0.00431	1.37	0.401
A*B*D	0.04951	0.02476	0.00431	5.75	0.11
A*B*E	0.00472	0.00236	0.00431	0.55	0.681
A*B*F	0.03092	0.01546	0.00431	3.59	0.173
A*C*D	0.00747	0.00373	0.00431	0.87	0.545
A*C*E	0.00167	0.00083	0.00431	0.19	0.878
A*C*F	0.00136	0.00068	0.00431	0.16	0.9
A*D*E	-0.01385	-0.00692	0.00431	-1.61	0.354
A*D*F	-0.09168	-0.04584	0.00431	-10.65	0.06
A*E*F	-0.00539	-0.00269	0.00431	-0.63	0.644
B*C*D	0.02414	0.01207	0.00431	2.8	0.218
B*C*E	0.00554	0.00277	0.00431	0.64	0.636
B*C*F	0.00463	0.00232	0.00431	0.54	0.686
B*D*E	-0.04429	-0.02215	0.00431	-5.14	0.122
B*D*F	-0.30115	-0.15057	0.00431	-34.97	0.018
B*E*F	-0.01689	-0.00845	0.00431	-1.96	0.3
C*D*E	-0.01327	-0.00663	0.00431	-1.54	0.367
C*D*F	-0.0122	-0.0061	0.00431	-1.42	0.391
C*E*F	0.00518	0.00259	0.00431	0.6	0.655
D*E*F	0.04917	0.02458	0.00431	5.71	0.11
A*B*C*D	-0.00262	-0.00131	0.00431	-0.3	0.812
A*B*C*E	-0.00059	-0.00029	0.00431	-0.07	0.957

A*B*C*F	-0.00048	-0.00024	0.00431	-0.06	0.965
A*B*D*E	0.00487	0.00243	0.00431	0.57	0.673
A*B*D*F	0.03222	0.01611	0.00431	3.74	0.166
A*B*E*F	0.00189	0.00095	0.00431	0.22	0.862
A*C*D*E	0.00134	0.00067	0.00431	0.16	0.902
A*C*D*F	0.00109	0.00054	0.00431	0.13	0.92
A*C*E*F	-0.00054	-0.00027	0.00431	-0.06	0.96
A*D*E*F	-0.00538	-0.00269	0.00431	-0.62	0.644
B*C*D*E	0.0044	0.0022	0.00431	0.51	0.699
B*C*D*F	0.00387	0.00194	0.00431	0.45	0.731
B*C*E*F	-0.00173	-0.00086	0.00431	-0.2	0.874
B*D*E*F	-0.01678	-0.00839	0.00431	-1.95	0.302
A*B*C*D*E	-0.00047	-0.00024	0.00431	-0.05	0.965
A*B*C*D*F	-0.00038	-0.00019	0.00431	-0.04	0.972
A*B*C*E*F	0.00019	0.00009	0.00431	0.02	0.986
A*B*D*E*F	0.00189	0.00095	0.00431	0.22	0.862
A*C*D*E*F	-0.00087	-0.00044	0.00431	-0.1	0.936
B*C*D*E*F	-0.00285	-0.00142	0.00431	-0.33	0.797
A*B*C*D*E*F	0.0003	0.00015	0.00431	0.04	0.978
Ct Pt		-0.0051	0.0347	-0.15	0.908

Table D- 8: Result of running simulation experiment of weakly heating energy consumption for the comfort controlled case.

Experiment Number	Factors					Response
	MRT	RH	AV	MR	CI	Heating (kWh)
1	-1	-1	-1	-1	-1	237.98
2	+1	-1	-1	-1	-1	113.32
3	-1	+1	-1	-1	-1	269.20
4	+1	+1	-1	-1	-1	133.06
5	-1	-1	+1	-1	-1	233.18
6	+1	-1	+1	-1	-1	133.94
7	-1	+1	+1	-1	-1	267.33
8	+1	+1	+1	-1	-1	158.44
9	-1	-1	-1	+1	-1	116.19
10	+1	-1	-1	+1	-1	34.91
11	-1	+1	-1	+1	-1	138.71
12	+1	+1	-1	+1	-1	39.27
13	-1	-1	+1	+1	-1	126.59
14	+1	-1	+1	+1	-1	53.69
15	-1	+1	+1	+1	-1	153.62
16	+1	+1	+1	+1	-1	64.10
17	-1	-1	-1	-1	+1	186.36
18	+1	-1	-1	-1	+1	77.92
19	-1	+1	-1	-1	+1	210.21
20	+1	+1	-1	-1	+1	92.86
21	-1	-1	+1	-1	+1	186.70
22	+1	-1	+1	-1	+1	99.67
23	-1	+1	+1	-1	+1	213.91
24	+1	+1	+1	-1	+1	120.77
25	-1	-1	-1	+1	+1	59.03
26	+1	-1	-1	+1	+1	25.56
27	-1	+1	-1	+1	+1	69.73
28	+1	+1	-1	+1	+1	26.76
29	-1	-1	+1	+1	+1	73.67
30	+1	-1	+1	+1	+1	28.41
31	-1	+1	+1	+1	+1	89.77
32	+1	+1	+1	+1	+1	31.61

Table D-9: ANOVA table for heating energy consumption.

Source	DF	Adj SS	Adj MS	F-Value	P-Value	Remarks
Model	31	167343	5398.1	4968.85	0.011	Significant
Linear	5	159835	31967.0	29424.73	0.004	Significant
A'- MRT	1	61063	61062.9	56206.71	0.003	Significant
B'- RH	1	2668	2668.4	2456.18	0.013	Significant
C'- AV	1	1+15	1+14.9	1201.17	0.018	Significant
D'- MR	1	80324	80324.4	73936.44	0.002	Significant
E'- CI	1	14474	14474.3	13323.17	0.006	Significant
2-Way Interactions	10	6502	650.2	598.48	0.032	Significant
A'*B'	1	272	272.2	250.51	0.040	Significant
A'*C'	1	251	251.1	231.15	0.042	Significant
A'*D'	1	3869	3869.2	3561.52	0.011	Significant
A'*E'	1	1600	1599.5	1472.32	0.017	Significant
B'*C'	1	39	38.7	35.65	0.106	
B'*D'	1	320	320.0	294.53	0.037	Significant
B'*E'	1	97	96.6	88.96	0.067	
C'*D'	1	10	10.4	9.60	0.199	
C'*E'	1	5	4.6	4.27	0.287	
D'*E'	1	39	39.4	36.23	0.105	
3-Way Interactions	10	838	83.8	77.13	0.088	
A'*B'*C'	1	0	0.2	0.22	0.720	
A'*B'*D'	1	14	13.8	12.72	0.174	
A'*B'*E'	1	11	10.7	9.84	0.196	
A'*C'*D'	1	357	357.4	328.99	0.035	Significant
A'*C'*E'	1	86	85.6	78.76	0.071	
A'*D'*E'	1	314	314.4	289.38	0.037	Significant
B'*C'*D'	1	0	0.0	0.02	0.919	
B'*C'*E'	1	0	0.1	0.05	0.859	
B'*D'*E'	1	4	3.5	3.23	0.323	
C'*D'*E'	1	52	52.3	48.15	0.091	
4-Way Interactions	5	49	9.9	9.11	0.246	
A'*B'*C'*D'	1	1	1.3	1.21	0.470	
A'*B'*C'*E'	1	0	0.5	0.46	0.622	
A'*B'*D'*E'	1	1	1.2	1.13	0.480	
A'*C'*D'*E'	1	46	45.6	42.01	0.097	
B'*C'*D'*E'	1	1	0.8	0.72	0.553	
Curvature	1	118	118.4	108.96	0.061	
Error	1	1	1.1			
Total	32	167344				

Table D-10: Effects and coefficients of factors for heating energy consumption.

Term	Effect	Coef	SE Coef	P-value
Intercept		120.83	0.1843	
A’	-87.36	-43.68	0.1843	0.0027
B’	18.26	9.13	0.1843	0.0128
C’	12.77	6.39	0.1843	0.0184
D’	-100.20	-50.10	0.1843	0.0023
E’	-42.53	-21.27	0.1843	0.0055
A’*B’	-5.83	-2.92	0.1843	0.0402
A’*C’	5.60	2.80	0.1843	0.0418
A’*D’	21.99	11.00	0.1843	0.0107
A’*E’	14.14	7.07	0.1843	0.0166
B’*C’	2.20	1.10	0.1843	0.1056
B’*D’	-6.32	-3.16	0.1843	0.0371
B’*E’	-3.47	-1.74	0.1843	0.0672
C’*D’	1.14	0.5710	0.1843	0.1987
C’*E’	-0.76	-0.3809	0.1843	0.2868
D’*E’	2.21	1.11	0.1843	0.1048
A’*B’*C’	0.17	0.0865	0.1843	0.7205
A’*B’*D’	-1.31	-0.6571	0.1843	0.1740
A’*B’*E’	1.15	0.5779	0.1843	0.1965
A’*C’*D’	-6.68	-3.34	0.1843	0.0351
A’*C’*E’	-3.27	-1.64	0.1843	0.0714
A’*D’*E’	6.26	3.13	0.1843	0.0374
B’*C’*D’	0.04	0.0234	0.1843	0.9194
B’*C’*E’	-0.08	-0.0415	0.1843	0.8591
B’*D’*E’	-0.66	-0.3313	0.1843	0.3231
C’*D’*E’	-2.55	-1.28	0.1843	0.0911
A’*B’*C’*D’	-0.40	-0.2025	0.1843	0.4700
A’*B’*C’*E’	-0.25	-0.1245	0.1843	0.6218
A’*B’*D’*E’	0.39	0.1961	0.1843	0.4802
A’*C’*D’*E’	-2.38	-1.19	0.1843	0.0974
B’*C’*D’*E’	-0.31	-0.1559	0.1843	0.5529

Table D-11: Result of running simulation experiment of MRT.

Simulation Number	Factors					Responses		
	Orientation	Shading	Glazing type	WFR	Sol-air temperature	Min MRT	Avg MRT	Max MRT
1	-1	-1	-1	-1	-1	18.97	19.12	19.19
2	+1	-1	-1	-1	-1	18.97	19.14	19.22
3	-1	+1	-1	-1	-1	18.97	19.12	19.19
4	+1	+1	-1	-1	-1	18.97	19.14	19.22

5	-1	-1	+1	-1	-1	19.15	19.21	19.26
6	+1	-1	+1	-1	-1	19.07	19.22	19.28
7	-1	+1	+1	-1	-1	19.07	19.21	19.26
8	+1	+1	+1	-1	-1	19.07	19.22	19.28
9	-1	-1	-1	+1	-1	18.20	18.50	18.75
10	+1	-1	-1	+1	-1	18.20	18.55	18.82
11	-1	+1	-1	+1	-1	18.20	18.50	18.75
12	+1	+1	-1	+1	-1	18.20	18.55	18.82
13	-1	-1	+1	+1	-1	18.60	18.83	19.00
14	+1	-1	+1	+1	-1	18.62	18.88	19.06
15	-1	+1	+1	+1	-1	18.62	18.83	18.99
16	+1	+1	+1	+1	-1	18.62	18.88	19.05
17	-1	-1	-1	-1	+1	19.19	19.86	20.07
18	+1	-1	-1	-1	+1	19.19	21.42	24.60
19	-1	+1	-1	-1	+1	19.20	19.86	20.07
20	+1	+1	-1	-1	+1	19.19	20.93	22.72
21	-1	-1	+1	-1	+1	19.25	19.78	19.95
22	+1	-1	+1	-1	+1	19.25	20.86	23.24
23	-1	+1	+1	-1	+1	19.25	19.78	19.95
24	+1	+1	+1	-1	+1	19.25	20.65	22.35
25	-1	-1	-1	+1	+1	19.00	22.22	23.62
26	+1	-1	-1	+1	+1	19.00	28.49	37.88
27	-1	+1	-1	+1	+1	19.00	21.37	22.14
28	+1	+1	-1	+1	+1	19.00	25.00	30.82
29	-1	-1	+1	+1	+1	19.1	21.58	22.65
30	+1	-1	+1	+1	+1	19.1	26.75	34.50
31	-1	+1	+1	+1	+1	19.1	21.15	21.86
32	+1	+1	+1	+1	+1	19.1	24.59	30.13

Table D-12: ANOVA table for average MRT.

Source	DF	Adj SS	Adj MS	F-Value	P-Value	Remarks
Model	30	188.69	6.2897	497.27	0.035	significant
Linear	5	119.819	23.9639	1894.63	0.017	significant
U-Orientation	1	17.103	17.103	1352.19	0.017	significant
V-Shading	1	1.819	1.8194	143.85	0.053	
W-Glazing type	1	0.168	0.1683	13.31	0.17	
X-WFR	1	18.155	18.1555	1435.41	0.017	significant
Y-Sol-air	1	82.573	82.5732	6528.39	0.008	significant
2-Way Interactions	10	59.319	5.9319	468.98	0.036	significant
U*V	1	0.798	0.7977	63.07	0.08	
U*W	1	0.129	0.1292	10.22	0.193	
U*X	1	6.174	6.1738	488.12	0.029	significant
U*Y	1	16.236	16.2358	1283.63	0.018	significant
V*W	1	0.128	0.1283	10.15	0.194	
V*X	1	1.215	1.2149	96.06	0.065	
V*Y	1	1.819	1.8193	143.84	0.053	
W*X	1	0.031	0.031	2.45	0.362	
W*Y	1	1.034	1.0335	81.71	0.07	
X*Y	1	31.755	31.7547	2510.59	0.013	significant
3-Way Interactions	10	8.999	0.8999	71.14	0.092	
U*V*W	1	0.044	0.0444	3.51	0.312	
U*V*X	1	0.418	0.418	33.05	0.11	
U*V*Y	1	0.798	0.7977	63.07	0.08	
U*W*X	1	0.013	0.0131	1.04	0.494	
U*W*Y	1	0.116	0.1163	9.2	0.203	
U*X*Y	1	5.913	5.9134	467.52	0.029	significant
V*W*X	1	0.068	0.0676	5.35	0.26	
V*W*Y	1	0.128	0.1284	10.15	0.194	
V*X*Y	1	1.215	1.2148	96.05	0.065	
W*X*Y	1	0.285	0.2848	22.51	0.132	
4-Way Interactions	5	0.553	0.1107	8.75	0.251	
U*V*W*X	1	0.013	0.0126	1	0.5	
U*V*W*Y	1	0.044	0.0444	3.51	0.312	
U*V*X*Y	1	0.418	0.418	33.05	0.11	
U*W*X*Y	1	0.011	0.0107	0.85	0.527	
V*W*X*Y	1	0.068	0.0676	5.35	0.26	
Error	1	0.013	0.0126			significant
Total	31	188.702				significant

Table D-13: Effects and coefficients of factors for average MRT.

Term	Effect	Coef	SE Coef	T-Value	P-Value
Constant		20.5395	0.0199	1033.11	0.001
U	1.4621	0.7311	0.0199	36.77	0.017
V	-0.4769	-0.2384	0.0199	-11.99	0.053
W	-0.145	-0.0725	0.0199	-3.65	0.17
X	1.5065	0.7532	0.0199	37.89	0.017
Y	3.2127	1.6064	0.0199	80.8	0.008
U*V	-0.3158	-0.1579	0.0199	-7.94	0.08
U*W	-0.1271	-0.0636	0.0199	-3.2	0.193
U*X	0.8785	0.4392	0.0199	22.09	0.029
U*Y	1.4246	0.7123	0.0199	35.83	0.018
V*W	0.1267	0.0633	0.0199	3.19	0.194
V*X	-0.3897	-0.1949	0.0199	-9.8	0.065
V*Y	-0.4769	-0.2384	0.0199	-11.99	0.053
W*X	-0.0622	-0.0311	0.0199	-1.57	0.362
W*Y	-0.3594	-0.1797	0.0199	-9.04	0.07
X*Y	1.9923	0.9962	0.0199	50.11	0.013
U*V*W	0.0745	0.0373	0.0199	1.87	0.312
U*V*X	-0.2286	-0.1143	0.0199	-5.75	0.11
U*V*Y	-0.3158	-0.1579	0.0199	-7.94	0.08
U*W*X	-0.0405	-0.0203	0.0199	-1.02	0.494
U*W*Y	-0.1206	-0.0603	0.0199	-3.03	0.203
U*X*Y	0.8598	0.4299	0.0199	21.62	0.029
V*W*X	0.0919	0.046	0.0199	2.31	0.26
V*W*Y	0.1267	0.0633	0.0199	3.19	0.194
V*X*Y	-0.3897	-0.1948	0.0199	-9.8	0.065
W*X*Y	-0.1887	-0.0943	0.0199	-4.74	0.132
U*V*W*X	0.0398	0.0199	0.0199	1	0.5
U*V*W*Y	0.0745	0.0373	0.0199	1.87	0.312
U*V*X*Y	-0.2286	-0.1143	0.0199	-5.75	0.11
U*W*X*Y	-0.0366	-0.0183	0.0199	-0.92	0.527
V*W*X*Y	0.0919	0.046	0.0199	2.31	0.26

Table D-14: ANOVA table for minimum MRT.

Source	DF	Adj SS	Adj MS	F-Value	P-Value	Remarks
Model	30	3.46122	0.11537	656.35	0.031	significant
Linear	5	2.89946	0.57989	3298.94	0.013	significant
U	1	0.00032	0.00032	1.81	0.407	
V	1	0.00017	0.00017	0.95	0.509	
W	1	0.27695	0.27695	1575.56	0.016	significant
X	1	1.32234	1.32234	7522.67	0.007	significant
Y	1	1.29968	1.29968	7393.71	0.007	significant
2-Way Interactions	10	0.5393	0.05393	306.8	0.044	significant
U*V	1	0.00019	0.00019	1.05	0.492	
U*W	1	0.00015	0.00015	0.85	0.527	
U*X	1	0.00029	0.00029	1.67	0.419	
U*Y	1	0.00009	0.00009	0.54	0.597	
V*W	1	0.00017	0.00017	0.95	0.509	
V*X	1	0.00017	0.00017	0.95	0.509	
V*Y	1	0.0002	0.0002	1.11	0.483	
W*X	1	0.08436	0.08436	479.9	0.029	significant
W*Y	1	0.07022	0.07022	399.47	0.032	significant
X*Y	1	0.38347	0.38347	2181.51	0.014	significant
3-Way Interactions	10	0.02156	0.00216	12.26	0.219	
U*V*W	1	0.00019	0.00019	1.05	0.492	
U*V*X	1	0.00017	0.00017	0.95	0.509	
U*V*Y	1	0.0002	0.0002	1.11	0.483	
U*W*X	1	0.00015	0.00015	0.85	0.527	
U*W*Y	1	0.00018	0.00018	1	0.5	
U*X*Y	1	0.00008	0.00008	0.46	0.62	
V*W*X	1	0.00019	0.00019	1.05	0.492	
V*W*Y	1	0.00018	0.00018	1	0.5	
V*X*Y	1	0.0002	0.0002	1.11	0.483	
W*X*Y	1	0.02005	0.02005	114.06	0.059	
4-Way Interactions	5	0.00091	0.00018	1.03	0.63	
U*V*W*X	1	0.00019	0.00019	1.05	0.492	
U*V*W*Y	1	0.00018	0.00018	1	0.5	
U*V*X*Y	1	0.00018	0.00018	1	0.5	
U*W*X*Y	1	0.00018	0.00018	1	0.5	
V*W*X*Y	1	0.0002	0.0002	1.11	0.483	
Error	1	0.00018	0.00018			significant
Total	31	3.4614				significant

Table D-15: Effects and coefficients of factors for minimum MRT.

Term	Effect	Coef	SE Coef	T-Value	P-Value
Constant		18.9198	0.0023	8072.44	0
U	-0.00631	-0.00316	0.00234	-1.35	0.407
V	-0.00456	-0.00228	0.00234	-0.97	0.509
W	0.18606	0.09303	0.00234	39.69	0.016
X	-0.40656	-0.20328	0.00234	-86.73	0.007
Y	0.40306	0.20153	0.00234	85.99	0.007
U*V	0.00481	0.00241	0.00234	1.03	0.492
U*W	-0.00431	-0.00216	0.00234	-0.92	0.527
U*X	0.00606	0.00303	0.00234	1.29	0.419
U*Y	0.00344	0.00172	0.00234	0.73	0.597
V*W	-0.00456	-0.00228	0.00234	-0.97	0.509
V*X	0.00456	0.00228	0.00234	0.97	0.509
V*Y	0.00494	0.00247	0.00234	1.05	0.483
W*X	0.10269	0.05134	0.00234	21.91	0.029
W*Y	-0.09369	-0.04684	0.00234	-19.99	0.032
X*Y	0.21894	0.10947	0.00234	46.71	0.014
U*V*W	0.00481	0.00241	0.00234	1.03	0.492
U*V*X	-0.00456	-0.00228	0.00234	-0.97	0.509
U*V*Y	-0.00494	-0.00247	0.00234	-1.05	0.483
U*W*X	0.00431	0.00216	0.00234	0.92	0.527
U*W*Y	0.00469	0.00234	0.00234	1	0.5
U*X*Y	-0.00319	-0.00159	0.00234	-0.68	0.62
V*W*X	0.00481	0.00241	0.00234	1.03	0.492
V*W*Y	0.00469	0.00234	0.00234	1	0.5
V*X*Y	-0.00494	-0.00247	0.00234	-1.05	0.483
W*X*Y	-0.05006	-0.02503	0.00234	-10.68	0.059
U*V*W*X	-0.00481	-0.00241	0.00234	-1.03	0.492
U*V*W*Y	-0.00469	-0.00234	0.00234	-1	0.5
U*V*X*Y	0.00469	0.00234	0.00234	1	0.5
U*W*X*Y	-0.00469	-0.00234	0.00234	-1	0.5
V*W*X*Y	-0.00494	-0.00247	0.00234	-1.05	0.483

Table D-16: ANOVA table for maximum MRT.

Source	DF	Adj SS	Adj MS	F-Value	P-Value	Remarks
Model	30	717.541	23.918	748.81	0.029	significant
Linear	5	441.684	88.337	2765.6	0.014	significant
U	1	99.077	99.077	3101.86	0.011	significant
V	1	8.464	8.464	264.97	0.039	significant
W	1	1.145	1.145	35.85	0.105	
X	1	71.805	71.805	2248.04	0.013	significant
Y	1	261.193	261.193	8177.28	0.007	significant
2-Way Interactions	10	234.31	23.431	733.56	0.029	significant
U*V	1	4.451	4.451	139.36	0.054	
U*W	1	0.595	0.595	18.62	0.145	
U*X	1	28.836	28.836	902.79	0.021	significant
U*Y	1	96.275	96.275	3014.13	0.012	significant
V*W	1	0.604	0.604	18.92	0.144	
V*X	1	3.712	3.712	116.22	0.059	
V*Y	1	8.461	8.461	264.91	0.039	significant
W*X	1	0.22	0.22	6.88	0.232	
W*Y	1	2.294	2.294	71.81	0.075	
X*Y	1	88.861	88.861	2782.01	0.012	significant
3-Way Interactions	10	39.728	3.973	124.38	0.07	
U*V*W	1	0.281	0.281	8.8	0.207	
U*V*X	1	1.271	1.271	39.79	0.1	
U*V*Y	1	4.45	4.45	139.31	0.054	
U*W*X	1	0.061	0.061	1.9	0.4	
U*W*Y	1	0.559	0.559	17.5	0.149	
U*X*Y	1	28.093	28.093	879.52	0.021	significant
V*W*X	1	0.181	0.181	5.67	0.253	
V*W*Y	1	0.605	0.605	18.93	0.144	
V*X*Y	1	3.711	3.711	116.17	0.059	
W*X*Y	1	0.517	0.517	16.2	0.155	
4-Way Interactions	5	1.819	0.364	11.39	0.221	
U*V*W*X	1	0.032	0.032	1	0.501	
U*V*W*Y	1	0.281	0.281	8.81	0.207	
U*V*X*Y	1	1.27	1.27	39.76	0.1	
U*W*X*Y	1	0.054	0.054	1.69	0.417	
V*W*X*Y	1	0.181	0.181	5.68	0.253	
Error	1	0.032	0.032			
Total	31	717.572				

Table D-17: Effects and coefficients of factors for maximum MRT.

Term	Effect	Coef	SE Coef	T-Value	P-Value
Constant		21.9313	0.0316	694.17	0.001
U	3.5192	1.7596	0.0316	55.69	0.011
V	-1.0286	-0.5143	0.0316	-16.28	0.039
W	-0.3783	-0.1892	0.0316	-5.99	0.105
X	2.9959	1.498	0.0316	47.41	0.013
Y	5.7139	2.857	0.0316	90.43	0.007
U*V	-0.7459	-0.373	0.0316	-11.81	0.054
U*W	-0.2727	-0.1363	0.0316	-4.32	0.145
U*X	1.8986	0.9493	0.0316	30.05	0.021
U*Y	3.4691	1.7345	0.0316	54.9	0.012
V*W	0.2748	0.1374	0.0316	4.35	0.144
V*X	-0.6812	-0.3406	0.0316	-10.78	0.059
V*Y	-1.0284	-0.5142	0.0316	-16.28	0.039
W*X	-0.1657	-0.0828	0.0316	-2.62	0.232
W*Y	-0.5354	-0.2677	0.0316	-8.47	0.075
X*Y	3.3328	1.6664	0.0316	52.74	0.012
U*V*W	0.1874	0.0937	0.0316	2.97	0.207
U*V*X	-0.3986	-0.1993	0.0316	-6.31	0.1
U*V*Y	-0.7458	-0.3729	0.0316	-11.8	0.054
U*W*X	-0.0871	-0.0435	0.0316	-1.38	0.4
U*W*Y	-0.2643	-0.1322	0.0316	-4.18	0.149
U*X*Y	1.8739	0.937	0.0316	29.66	0.021
V*W*X	0.1504	0.0752	0.0316	2.38	0.253
V*W*Y	0.2749	0.1375	0.0316	4.35	0.144
V*X*Y	-0.6811	-0.3405	0.0316	-10.78	0.059
W*X*Y	-0.2543	-0.1272	0.0316	-4.02	0.155
U*V*W*X	0.0631	0.0315	0.0316	1	0.501
U*V*W*Y	0.1876	0.0938	0.0316	2.97	0.207
U*V*X*Y	-0.3984	-0.1992	0.0316	-6.31	0.1
U*W*X*Y	-0.0822	-0.0411	0.0316	-1.3	0.417
V*W*X*Y	0.1506	0.0753	0.0316	2.38	0.253

Appendix E: Numerical optimization results

Table E-1: Numerical optimization results to maintain acceptable thermal comfort conditions in the conventional controlled case.

Number	CI	MR	Set-point	Glazing	WFR	Avg	Min	Max	D
1	1.05	71.965	20.996	2.786	0.16	-0.381	-0.5	0.107	1
2	1.044	73.138	20.94	2.285	0.198	-0.35	-0.497	0.245	1
3	1.038	73.498	20.998	1.676	0.161	-0.384	-0.49	0.013	1
4	1.049	72.812	20.995	1.77	0.255	-0.3	-0.488	0.468	1
5	1.048	73.143	20.998	0.954	0.178	-0.374	-0.487	0.027	1
6	1.049	73.49	20.977	2.011	0.186	-0.34	-0.472	0.181	1
7	1.047	72.934	20.978	0.744	0.189	-0.378	-0.499	0.046	1
8	1.032	73.484	21	2.325	0.248	-0.306	-0.495	0.492	1
9	1.048	72.977	20.966	0.733	0.283	-0.299	-0.5	0.467	1
10	1.041	73.472	20.996	0.747	0.244	-0.325	-0.493	0.3	1
11	1.049	73.335	20.915	2.615	0.231	-0.306	-0.485	0.452	1
12	1.05	73.303	20.966	1.744	0.163	-0.371	-0.48	0.039	1
13	1.049	72.025	20.998	2.795	0.195	-0.351	-0.5	0.279	1
14	1.045	73.144	20.996	0.902	0.208	-0.355	-0.493	0.153	1
15	1.05	72.973	20.943	1.289	0.197	-0.363	-0.497	0.141	1
16	1.045	73.306	20.956	0.809	0.261	-0.315	-0.498	0.38	1
17	1.048	72.766	20.967	1.38	0.248	-0.321	-0.5	0.385	1
18	1.037	73.316	20.986	2.788	0.213	-0.327	-0.491	0.376	1
19	1.036	73.493	20.998	0.867	0.167	-0.396	-0.5	-0.041	1
20	1.046	72.894	20.969	1.342	0.213	-0.351	-0.499	0.218	1
21	1.045	73.432	20.988	1.327	0.199	-0.349	-0.483	0.162	1
22	1.033	73.362	20.998	2.726	0.167	-0.371	-0.495	0.137	1
23	1.045	73.009	20.987	0.806	0.165	-0.398	-0.499	-0.057	1
24	1.05	73.314	20.923	1.033	0.237	-0.33	-0.495	0.298	1
25	1.042	73.203	20.971	1.956	0.213	-0.339	-0.494	0.286	1
26	1.034	73.497	20.999	1.154	0.19	-0.374	-0.5	0.089	1
27	1.047	73.447	20.9	2.351	0.209	-0.335	-0.491	0.309	1
28	1.045	72.959	20.975	1.627	0.262	-0.303	-0.496	0.48	1
29	1.043	73.444	20.947	1.645	0.264	-0.299	-0.494	0.492	1
30	1.047	73.398	20.893	1.632	0.209	-0.351	-0.5	0.228	1
31	1.05	72.705	20.993	1.2	0.197	-0.361	-0.493	0.131	1
32	1.047	72.737	20.999	1.226	0.168	-0.389	-0.497	-0.002	1
33	1.04	73.492	20.928	1.874	0.207	-0.35	-0.5	0.244	1
34	1.05	72.908	20.976	2.607	0.185	-0.344	-0.482	0.225	1
35	1.045	73.392	20.954	0.932	0.259	-0.313	-0.496	0.386	1
36	1.041	73.159	20.999	1.058	0.275	-0.3	-0.497	0.469	1
37	1.032	73.444	20.994	2.689	0.18	-0.362	-0.496	0.194	1
38	1.046	73.253	20.976	0.718	0.214	-0.352	-0.494	0.162	1

39	1.034	73.383	20.993	2.184	0.165	-0.381	-0.498	0.077	1
40	1.05	72.604	20.965	1.726	0.198	-0.359	-0.498	0.188	1
41	1.05	72.516	21	0.743	0.289	-0.294	-0.5	0.493	1
42	1.047	73.171	20.989	2.1	0.205	-0.332	-0.481	0.272	1
43	1.039	73.426	20.995	0.871	0.26	-0.314	-0.496	0.38	1
44	1.048	72.528	20.997	1.335	0.267	-0.304	-0.499	0.466	1
45	1.044	73.494	20.888	2.799	0.227	-0.318	-0.495	0.44	1
46	1.048	72.863	20.962	2.253	0.203	-0.342	-0.492	0.272	1
47	1.043	73.31	20.97	2.712	0.171	-0.357	-0.484	0.167	1
48	1.04	73.465	20.965	1.711	0.242	-0.318	-0.495	0.397	1
49	1.041	73.105	20.959	2.199	0.173	-0.375	-0.499	0.116	1
50	1.049	72.795	20.966	2.06	0.167	-0.376	-0.492	0.08	1
51	1.048	73.307	20.954	1.965	0.181	-0.357	-0.484	0.14	1

Table E-2: Numerical optimization results to minimize heating energy consumption in the comfort controlled case.

Number	MRT	RH	AV	MR	CI	heating	PMV	Max PMV	Desirability
1	18.268	0.402	0.152	72.830	1.050	143.444	-0.314	0.500	0.718
2	18.696	0.401	0.150	73.500	0.998	145.133	-0.322	0.500	0.714
3	18.843	0.400	0.150	73.499	0.987	145.533	-0.324	0.500	0.712
4	18.595	0.411	0.150	73.488	1.004	145.614	-0.322	0.500	0.712
5	19.072	0.400	0.150	72.857	0.983	146.358	-0.325	0.500	0.710
6	18.363	0.400	0.171	73.500	1.019	146.514	-0.328	0.500	0.710
7	19.078	0.402	0.150	71.194	1.016	147.040	-0.321	0.500	0.708
8	19.529	0.400	0.150	71.201	0.982	148.013	-0.327	0.500	0.705
9	20.079	0.400	0.150	69.152	0.983	149.924	-0.331	0.500	0.700
10	18.454	0.466	0.151	73.500	1.001	150.119	-0.327	0.500	0.699
11	20.874	0.400	0.152	67.974	0.954	151.038	-0.339	0.500	0.696
12	20.216	0.408	0.165	70.328	0.950	151.574	-0.340	0.500	0.695
13	18.339	0.400	0.186	71.477	1.050	149.909	-0.335	0.493	0.695
14	18.486	0.400	0.207	71.026	1.049	152.442	-0.344	0.500	0.692
15	20.132	0.400	0.190	70.390	0.952	153.982	-0.349	0.500	0.688
16	19.188	0.400	0.150	69.783	1.011	150.891	-0.332	0.480	0.683
17	19.180	0.495	0.150	67.716	1.050	157.688	-0.329	0.500	0.677
18	19.980	0.494	0.163	70.345	0.950	157.908	-0.345	0.500	0.676
19	18.955	0.510	0.150	68.462	1.050	157.946	-0.329	0.500	0.676
20	17.304	0.520	0.222	73.500	1.050	160.428	-0.360	0.500	0.668
21	20.371	0.555	0.150	66.510	0.981	164.524	-0.346	0.500	0.655
22	21.093	0.440	0.234	66.675	0.950	164.944	-0.370	0.500	0.654

Table E-3: Numerical optimization results regarding MRT values.

Number	Orientation	Shading	Glazing type	Glazing area	Avg MRT	Min MRT	Max MRT	Desirability
1	S-E	Yes	-1.000	-0.999	19.678	19.094	20.995	0.995
2	S-E	Yes	-0.992	-1.000	19.678	19.094	20.993	0.995
3	S-E	Yes	-0.951	-1.000	19.677	19.091	20.997	0.993
4	S-E	Yes	-0.873	-1.000	19.678	19.086	20.993	0.991
5	S-E	Yes	-0.868	-1.000	19.677	19.086	20.997	0.991
6	S-E	Yes	-0.859	-1.000	19.676	19.085	21.000	0.990
7	S-E	Yes	-0.919	-0.994	19.679	19.088	21.000	0.990
8	S-E	Yes	-0.838	-1.000	19.677	19.084	20.993	0.990
9	S-E	Yes	-1.000	-1.000	19.675	19.094	20.996	0.990
10	S-E	Yes	-0.773	-1.000	19.678	19.080	20.992	0.987
11	S-E	Yes	-1.000	-0.997	19.675	19.094	21.000	0.987
12	S-E	Yes	-0.738	-1.000	19.677	19.078	20.993	0.986
13	S-E	Yes	-1.000	-0.991	19.677	19.093	20.999	0.981
14	S-E	Yes	-0.527	-0.996	19.679	19.064	20.999	0.979
15	S-E	Yes	-0.319	-1.000	19.677	19.051	20.995	0.972
16	S-E	Yes	-0.402	-1.000	19.675	19.057	21.000	0.972
17	S-E	Yes	-0.270	-0.998	19.678	19.048	20.995	0.970
18	S-E	Yes	-0.140	-1.000	19.678	19.040	20.992	0.966
19	S-E	Yes	0.076	-1.000	19.676	19.026	20.999	0.959
20	S-E	Yes	0.095	-1.000	19.678	19.025	20.992	0.958
21	S-E	Yes	0.229	-0.999	19.677	19.016	21.000	0.954
22	S-E	Yes	0.262	-0.998	19.678	19.014	20.997	0.952
23	S-E	Yes	0.505	-1.000	19.677	18.999	20.998	0.944
24	S-E	Yes	0.663	-0.999	19.678	18.988	20.995	0.939
25	S-E	Yes	0.695	-1.000	19.676	18.987	21.000	0.938
26	S-E	Yes	0.741	-1.000	19.678	18.984	20.993	0.936
27	S-E	Yes	0.950	-1.000	19.676	18.971	20.999	0.929
28	S-E	Yes	0.985	-1.000	19.677	18.968	20.996	0.928
29	S-E	Yes	0.990	-1.000	19.677	18.968	20.992	0.928

Abed Al Waheed HAWILA

Doctorat : Systèmes SocioTechniques

Année 2019

L'intégration du confort thermique des occupants dans la conception des bâtiments performants

Le secteur du bâtiment est l'un des plus grands consommateurs d'énergie parmi les secteurs économiques. Il est important alors de promouvoir la conception selon les critères de la basse consommation et du bien-être afin qu'un compromis entre le confort thermique et la performance énergétique puisse être trouvé. L'amélioration de l'efficacité énergétique des bâtiments a fait l'objet de nombreux travaux de recherche. Récemment, les systèmes des façades hautement vitrées ont gagné en popularité grâce à leur aspect esthétique. Cependant, si elles ne sont bien conçues, elles mènent à un inconfort thermique et à une surconsommation d'énergie. L'objectif de cette thèse est de comprendre et formaliser la relation entre les paramètres de conception, le confort thermique et la consommation d'énergie. En conséquence, nous adoptons une approche basée sur l'utilisation des plans d'expérience basée sur les simulations numériques. Ceci a permis le développement des méta-modèles afin d'évaluer le confort thermique et la consommation énergétique des bâtiments hautement vitrés. Ces modèles ont ensuite été déployés pour intégrer le confort thermique dans le processus d'optimisation de la conception des bâtiments. Une fonction de désirabilité a été considérée pour optimiser aussi bien le confort thermique et la consommation énergétique. La méthode proposée a été appliquée sur un bâtiment réel. Les résultats obtenus ont montré l'intérêt de l'intégration du confort thermique dans la conception des bâtiments.

Mots clés : plan d'expérience – simulation par ordinateur – consommation d'énergie – bien-être.

Integrating Occupants' Thermal Comfort in the Design of Energy-efficient Buildings

The building sector is one of the largest energy end-use sectors in the world and reducing energy consumption has been the foundation of numerous research works. However, the primary objective of buildings must be to provide a comfortable environment for its occupants. Thus, it is necessary to design energy-efficient buildings so that a trade-off between energy-savings and occupants' thermal comfort is fulfilled. Recently, glass façades have gained popularity due to their aesthetic appearance. However, they often cause occupants thermal discomfort, in addition to consuming considerable amounts of energy. In light of these conflict characteristics, the main purpose of this thesis is to understand the relationship between design parameters, thermal comfort and heating energy, in order to integrate thermal comfort in the design of energy efficient buildings. Consequently, we adopted a methodology based on the combined use of numerical simulations, Design of Experiments (DoE) technique and an optimization method. This allowed the development of meta-models of thermal comfort and heating energy. These models are then used to integrate thermal comfort in the process of building design. A desirability function was considered in order to simultaneously optimize both thermal comfort and heating energy. This trade-off helps in developing an optimal design of buildings at both energy consumption and thermal comfort levels. The proposed method is applied in a real case study. The obtained results show the added value of integrating thermal comfort in building design.

Keywords: experimental design – computer simulation – energy consumption – human comfort.

Thèse réalisée en partenariat entre :

Région ALSACE CHAMPAGNE-ARDENNE LORRAINE

UNION EUROPÉENNE Fonds Européen de Développement Régional

l'Europe s'engage en Champagne-Ardenne avec le FEDER

utt UNIVERSITÉ DE TECHNOLOGIE TROYES

Ecole Doctorale "Sciences pour l'Ingénieur"